AD_____

Award Number: DAMD17-98-1-8619

TITLE: Oxidative Damage in Parkinson's Disease

PRINCIPAL INVESTIGATOR: M. Flint Beal, M.D.

CONTRACTING ORGANIZATION: Massachusetts General Hospital
Boston, Massachusetts 02114

REPORT DATE: January 2005

TYPE OF REPORT: Final Addendum

PREPARED FOR: U.S. Army Medical Research and Materiel Command
Fort Detrick, Maryland 21702-5012

DISTRIBUTION STATEMENT: Approved for Public Release;
Distribution Unlimited

# REPORT DOCUMENTATION PAGE

Form Approved
OMB No. 074-0188



| 1. AGENCY USE ONLY (Leave blank) | 2. REPORT DATE | 3. REPORT TYPE AND DATES COVERED |
|---|---|---|
| | January 2005 | Final Addendum (1 Jan 203 - 31 Dec 2004) |

**4. TITLE AND SUBTITLE**
Oxidative Damage in Parkinson's Disease

**5. FUNDING NUMBERS**
DAMD17-98-1-8619

**6. AUTHOR(S)**
M. Flint Beal, M.D.

**7. PERFORMING ORGANIZATION NAME(S) AND ADDRESS(ES)**
Massachusetts General Hospital
Boston, Massachusetts 02114

*E-Mail:* fbeal@med.cornell.edu

**8. PERFORMING ORGANIZATION REPORT NUMBER**

**9. SPONSORING / MONITORING AGENCY NAME(S) AND ADDRESS(ES)**
U.S. Army Medical Research and Materiel Command
Fort Detrick, Maryland 21702-5012

**10. SPONSORING / MONITORING AGENCY REPORT NUMBER**

**11. SUPPLEMENTARY NOTES**

**12a. DISTRIBUTION / AVAILABILITY STATEMENT**
Approved for Public Release; Distribution Unlimited

**12b. DISTRIBUTION CODE**

**13. ABSTRACT (Maximum 200 Words)**

The overall goal of the proposal was to provide a detailed assessment of the role of oxidative damage in Parkinson's disease (PD) and the MPTP model of PD. During our one year addendum, we carried out studies which showed the anti-inflammatory agent minocycline exacerbated MPTP neurotoxicity. The anti-inflammatory compound rolipram produced dose-dependent neuroprotective effects against MPTP. Administration of the iron chelator clioquinol was neuroprotective against MPTP and this was associated with reduced oxidative stress. Systemic administration of a broad spectrum caspase inhibitor produced neuroprotection against MPTP toxicity as assessed by loss of both dopamingeric neurons and dopamine levels. We demonstrated for the first time that MMP-9 is increased after administration of MPTP. MMP-9 may be activated by oxidative stress. We found that a broad spectrum inhibitor MMP inhibitor protected against dopamine depletion and loss of tyrosine hydroxylase neurons. We carried out studies showing that a deficiency of DJ-1, which is linked to autosomal recessive PD, results in cells being more vulnerable to oxidative damage. We found that novel azulenyl nitrone was markedly neuroprotective against MPTP and prevented increases in malondialdehyde *in vivo*. These studies, therefore, have provided further evidence for oxidative damage in the pathogenesis of PD.

**14. SUBJECT TERMS**
Oxidative damage, MPTP, spintraps, matrix metalloprotease

**15. NUMBER OF PAGES**
86

**16. PRICE CODE**

| 17. SECURITY CLASSIFICATION OF REPORT | 18. SECURITY CLASSIFICATION OF THIS PAGE | 19. SECURITY CLASSIFICATION OF ABSTRACT | 20. LIMITATION OF ABSTRACT |
|---|---|---|---|
| Unclassified | Unclassified | Unclassified | Unlimited |

# FOREWORD

Opinions, interpretations, conclusions and recommendations are those of the author and are not necessarily endorsed by the U.S. Army.

____ Where copyrighted material is quoted, permission has been obtained to use such material.

____ Where material from documents designated for limited distribution is quoted, permission has been obtained to use the material.

____ Citations of commercial organizations and trade names in this report do not constitute an official Department of Army endorsement or approval of the products or services of these organizations.

__X__ In conducting research using animals, the investigator(s) adhered to the "Guide for the Care and Use of Laboratory Animals," prepared by the Committee on Care and Use of Laboratory Animals of the Institute of Laboratory Resources, National Research Council (NIH Publication No. 86-23, Revised 1985).

__X__ For the protection of human subjects, the investigator(s) adhered to policies of applicable Federal Law 45 CFR 46.

____ In conducting research utilizing recombinant DNA technology, the investigator(s) adhered to current guidelines promulgated by the National Institutes of Health.

____ In the conduct of research utilizing recombinant DNA, the investigator(s) adhered to the NIH Guidelines for research Involving Recombinant DNA Molecules.

____ In the conduct of research involving hazardous organisms, the investigator(s) adhered to the CDC-NIH guide for Biosafety in Microbiological and Biomedical laboratories

M J Lent Beal 1/03/05

PI-Signature Date

## 4. TABLE OF CONTENTS

## 5. INTRODUCTION

The overall goal of the original proposal was to provide a detailed assessment of the role of oxidative damage in Parkinson's Disease (PD). These studies were previously completed and a detailed report was filed. We then extended the grant with an addendum. The grant then was to carry out studies, which would look particularly at therapeutic agents which have both anti-inflammatory activity as well as antioxidative activity. We also proposed to determine whether anti-inflammatory drugs exert additive neuroprotective effects with either creatine or coenzyme $Q_{10}$ ($COQ_{10}$) against MPTP neurotoxicity. We have accomplished most of these objectives during the past year. We have a considerable number of publications as a consequence of these studies.

## 6. BODY

We initially carried out studies of the anti-inflammatory compound minocycline. Minocycline had previously been shown to have beneficial effects against ischemia in rats as well as against excitotoxic damage *in vitro*, nigral cell loss induced by 6-hydroxy-dopamine and in transgenic mouse models of Huntington's Disease (HD) and amyotrophic lateral sclerosis (ALS). We examined whether minocycline would protect against the toxic effects of 1-methyl-4-phenyl-1,2,3,6-tetrahydropyridine (MPTP), a toxin that selectively destroys the nigral striatal dopaminergic neurons. It produces clinical findings similar to those, which occur in PD in both rodent and primates. To our surprise, we found that minocycline exacerbated MPTP induced damage to dopamine neurons (Yang et al., 2003). It resulted in a significant decrease in the number of dopaminergic neurons as well as in dopamine levels. This occurred with a large number of different dosing paradigms. We found that minocycline did block microglial activation, yet the damage persisted. Minocycline when administered with MPTP exacerbated the damage by more than 50%. The number of neurons surviving in the minoclycline with MPTP treated mice was half of that than those treated with MPTP alone. We also examined old mice at 8 months of age, yet, even in these mice, we did not see any neuroprotective effects. We examined these mice since they have a more robust microglial reaction. We examined the effects of creatine in combination with minocycline. Creatine alone showed neuroprotection against the loss of dopaminergic neurons. The combination of creatine with minocycline however, showed no protection. We examined both minocycline and tetracycline brain levels before and after MPTP administration and showed that this led to significant increases in brain concentrations. Minocycline brain levels were approximately ten-fold greater than those seen with tetracycline. We examined the effects of minocycline on tritiated dopamine and tritiated $MPP^+$ uptake in the vesicular preparations. We found that uptake of tritiated dopamine into vesicles isolated from the mouse striata was inhibited by the addition of minocycline in a dose-dependent manner as compared to controls. We, therefore, believe that this inhibition of $MPP^+$ uptake into the striatal vesicles may contribute to the neurotoxic effects of minocycline. These findings are of importance, since minocycline has been proposed as an agent to test in PD patients.

We also carried out studies in collaboration with Julie Andersen at the Buck Institute for Age Research (Kaur et al., 2003). There is substantial evidence that there is increased iron in the substantia nigra of PD patients. It is possible that this increased iron contributes to cell death. This however, has been controversial. We, therefore, examined whether transgenic overexpression of the iron binding protein ferritin or oral administration of the bioavailable metal chelator clioquinol could protect against MPTP neurotoxicity. We found that reduction reactive iron by either genetic or pharmacologic means produced excellent protection against MPTP neurotoxicity. This was demonstrated using both

dopamine levels as well as cell counts. It, therefore, appears that oxidative stress may be exacerbated by the accumulation of iron within the substantia nigra.

We examined the effects of rolipram (unpublished data). We carried out two dose response studies. In the first, we examined the effects of rolipram at 1.25 and 2.5 mg/kg. We found that there was significant protection at the dose of 1.25 mg/kg. This approximately doubled the remaining levels of dopamine in the striatum; 2.5 mg also exerted neuroprotective effects. However, they were less robust than those seen at 1.25 mg. Similarly, in a follow-up experiment, 2.5 mg/kg exerted neuroprotective effects. However, 5 mg/kg was less efficacious.

We examined whether a cyclooxygenase inhibitor could exert protection in the MPTP mouse model of PD either alone or in combination with creatine (Klivenyi et al., 2003). We found that mice treated with 0.005% rofecoxib had significant protection against dopamine depletion in the striatum. Similarly, creatine produced a comparable degree of protection. The combination produced additive significant neuroprotective effects. This was confirmed with counts of tyrosine hydroxylase neurons in the substantia nigra.

We also utilized another novel strategy to see if we could protect against MPTP toxicity. We used a new caspase inhibitor, which is systemically active. A number of previous caspase inhibitors exerted significant toxicity since they have a fluoromethylketone group; zVAD-fmk is one of these. In the studies which we carried out, we utilized a new peptidyl broad spectrum caspase inhibitor, Q-VD-OPH (Yang et al., 2004). It offered significant improvements and potency, stability and toxicity over zVAD-fmk. It produced significant protection against MPTP toxicity as assessed both by dopamine levels and loss of dopaminergic neurons in the substantia nigra. The latter showed almost complete protection. Western blots performed on the midbrain following administration of MPTP, showed significant increases in the active forms of caspase-9 and caspase-8, as well as caspase-8-mediated proapoptotic protein Bid. These were inhibited by administration of Q-VD-OPH. This is the first study to show that systemic administration of caspase inhibitor can exert neuroprotective effects.

We carried out further studies of the mechanism of creatine neuroprotective effects against MPTP (Kivenyi e al., 2004). We examined whether it could exert neuroprotective effect in mice deficient in the ubiquitous mitochondrial creatine kinase. It has been hypothesized that creatine causes an alteration of this into an octomer which then inhibits the activity of the mitochondrial permeability transition. We found that the ubiquitous mitochondrial creatine kinase deficient mice showed increased sensitivity to MPTP induced dopamine depletion and loss of tyrosine hydroxylase stained neurons. Isolated mitochondria from these mice however, showed no alterations in any mitochondrial parameters such as calcium retention, oxygen utilization or membrane

potential. Creatine administration significantly increased brain concentrations of both creatine and phosphocreatine in the mitochondrial creatine kinase deficient mice. Creatine administration also exerted significant neuroprotective effects in these mice against MPTP. They were comparable in magnitude to those seen in wild-type mice. These results suggests that the neuroprotective effects of creatine are not mediated by an effect on the ubiquitous form of mitochondrial creatine kinase to inhibit the mitochondrial permeability transition and are more likely to be mediated by maintenance of appropriate ATP/ADP and PCr/Cr levels.

We examined whether matrix metalloprotease-9 (MMP-9) was increased after administration of MPTP (Lorenzl et al., 2004). We examined this using zymography, immunohistochemistry and Western blot analysis. We examined this, since MMP-9 can be activated by oxidative stress. The activity of MMP-9 was upregulated at 3 hours after MPTP injection in the striatum and 24 hours in the substantia nigra. It remained elevated in the substantia nigra as compared to controls for up to 7 days after MPTP administration. In contrast, MMP-9 expression was decreased in the striatum by 72 hours. Immunohistochemistry showed that neurons and microglia were the source of MMP-9 expression after MPTP administration to mice. We treated the mice with a hydroxamate-based MMP inhibitor which significantly decreased the dopamine depletion and loss of tyrosine hydroxylase immunoreactive neurons. This was accompanied by a decrease in MMP-9 expression as measured by zymography in the substantia nigra. These findings indicated that MMP-9 is induced after MPTP application of mice and the pharmacologic inhibition of MMPs protects against MPTP toxicity.

We carried out studies in collaboration with Asa Abeliovich on a new genetic form of PD, which results in increased sensitivity to oxidative stress (Martinat et al., 2004). We utilized ES-derived dopaminergic stem cells, which were made deficient in DJ-1 using RNAi. These were shown to display increased sensitivity to oxidative stress and proteosomal inhibition. The accumulation of reactive oxygen species in toxin-treated DJ-1 deficient cells appear to be initially normal but they were then no longer able to cope with this leading to apoptotic cell death. The dopaminergic neurons showed decreased survival and increased sensitivity to oxidative stress induced by hydrogen peroxide or 6-hydroxydopamine. These findings suggest that the DJ-1 protects against oxidative damage. This further links oxidative damage to PD pathogenesis.

Lastly, we have carried out studies with a novel antioxidant (Yang et al., 2005). This is a nitrone azulenyl antioxidant. It is a spin-trapping compound, which can form stable adducts with free radicals. Previous studies had shown that a number of free radical scavengers including spin-trapping compounds were protective in animal models of brain ischemia and neurodegenerative diseases. We administered a new nitrone antioxidant, stilbazulenyl nitrone (STAZN) with either MPTP or 3-nitropropionic acid (3-NP). STAZN significantly attenuated MPTP-induced striatal dopamine depletion by 40% and produced a tendency to dose-dependent neuroprotection. It dose-dependently

protected against loss of tyrosine hydroxylase immunoreactive neurons in the substantia nigra pars compacta. STAZN reduced striatal lesion volumes caused by 3-NP. It significantly reduced the lipid peroxidation marker malondialdehyde in the striatum and cortex after administration of 3-NP. These findings suggest that the development of free radical spin-traps might be useful for developing novel therapies for treating neurodegenerative diseases such as PD.

In summary, our studies have provided further evidence for both oxidative damage and inflammation as playing a critical role in PD pathogenesis. In the present studies, we examined this predominantly utilizing the MPTP model of PD. We found that there is increased activation of MMP-9 as well as increased inflammation in the substantia nigra following the administration of MPTP. Surprisingly, different anti-inflammatory agents exert different degrees of protection or exacerbation of MPTP. We have also demonstrated that systemic administration of caspase inhibitors and a novel free radical spin-trap exert potent or protective effects.

## 7. KEY RESEARCH ACCOMPLISHMENTS

1. The finding that minocycline exacerbates MPTP-induced parkinsonism, both in young and old mice.

2. The finding that minocycline blocks MPTP-induced activation of microglial cells despite its lack of neuroprotective effects.

3. The finding that the oral iron chelator clioquinol produces significant protection against neurotoxicity.

4. The finding that rolipram produces dose-dependent neuroprotective effects against MPTP showing an u-shaped neuroprotective curve.

5. The finding that both creatine and the COX-2 inhibitor rofecoxib exert significant neuroprotective effects against MPTP when administered alone and additive neuroprotective effects when administered in combination.

6. The finding for the first time that a novel systemically active caspase inhibitor significantly attenuates the toxicity of MPTP and also protects against activation of caspases.

7. The finding that the neuroprotective effects of creatine occur in the absence of mitochondrial creatine kinase suggesting that they are not mediated by effects on mitochondrial permeability transition.

8. The finding that MMP-9 is elevated in the substantia nigra following administration of MPTP and the finding that a matrix metalloprotease inhibitor can block MPTP toxicity.

9. The finding that DJ-1 is a protective agent against oxidative damage in dopaminergic neurons derived from ES cells.

10. The finding that a novel azulenyl nitrone antioxidant exerts significant protection against MPTP neurotoxicity and blocks oxidative damage in the substantia nigra produced by MPTP.

## 8. REPORTABLE OUTCOMES

Kaur D, Yantiri F, Rajagopalan S, Kumar J, Mo JQ, Boonplueang R, Viswanath V, Jacobs R, Yang L, Beal MF, DiMonte D, Volitaskis I, Ellerby L, Cherny RA, Bush AI, Andersen JK. Genetic or pharmacological iron chelation prevents MPTP-induced neurotoxicity in vivo: a novel therapy for Parkinson's disease. Neuron 2003; 37:899-909.

Klivenyi P, Calingasan NY, Starkov A, Stavrovskaya IG, Kristal BS, Yang L, Wieringa B, Beal MF. Neuroprotective mechanisms of creatine occur in the absence of mitochondrial creatine kinase. Neurobiol Dis 2004; 15:610-617.

Klivenyi P, Gardian G, Calingasan NY, Yang L, Beal MF. Additive neuroprotective effects of creatine and a cyclooxygenase 2 inhibitor against dopamine depletion in the 1-methyl-4-phenyl-1,2,3,6-tetrahydropyridine (MPTP) mouse model of Parkinson's disease. J Mol Neurosci 2003; 21:191-198.

Lorenzl S, Albers DS, Chirichigno JW, Augood SJ, Beal MF. Elevated levels of matrix metalloproteinases-9 and -1 and of tissue inhibitors of MMPs, TIMP-1 and TIMP-2 in postmortem brain tissue of progressive supranuclear palsy. J Neurol Sci 2004; 218:39-45.

Martinat C, Shendelman S, Jonason A, Leete T, Beal MF, Yang L, Floss T, Abeliovich A. Sensitivity to oxidative stress in DJ-1-deficient dopamine neurons: an ES-derived cell model of primary parkinsonism. PLoS Biol 2004; 2:1754-1763.

Yang L, Calingasan NY, Chen J, Ley JJ, Becker DA, Beal, MF. A novel azulenyl nitrone antioxidant protects against MPTP and 3-nitropropionic acid neurotoxicities. Exp Neurol 2005; 191;86-93.

Yang L, Sugama S, Mischak RP, Kiaei M, Bizat N, Brouillet E, Joh TH, Beal, MF. A novel systemically active caspase inhibitor attenuates the toxicities of MPTP, malonate , and 3NP in vivo. Neurobiol Dis 2004;17:250-259.

Yang L, Sugama S, Chirichingo JW, Gregorio J, Lorenzl S, Shin DH, Browne SE, Shimizu Y, Joh TH, Beal, MF, Albers DS. Minocycline enhances MPTP toxicity to dopaminergic neurons. J Neurosci Res 2003:15;278-285.

## 9. CONCLUSIONS

We carried out a number of studies examining the effects of therapeutic agents on both inflammation and oxidative damage in the MPTP model of Parkinson's Disease. We found that the anti-inflammatory agent minocycline did block activation of microglial cells, but to our surprise, it exacerbated MPTP neurotoxicity. This is of importance since this agent has been proposed for clinical trials in PD. Caution should be warranted in usng minocycline due to our findings. We found that the anti-inflammatory phosphodiestrase-4 inhibitor rolipram dose-dependent neuroprotective effects against MPTP. However, the effects were more robust at lower concentrations and there was an inverted dose response curve. We found that both creatine and a cyclooxygenase-2 inhibitor protect against dopamine depletion induced by MPTP and the two agents administered together produced additive neuroprotective effects. This is of interest, since this may lead to clinical trials using combinations of neuroprotective agents in PD.

We showed for the first time that a novel systemically active caspase inhibitor which has improvements in potency, stability and toxicity, significantly protected against dopamine depletion in striatum produced by MPTP administration. Furthermore, we demonstrated that it does indeed prevent activation of caspases and the production of the proapoptotic protein Bid. This provides the first evidence that therapy with antiapoptotic agents might have usefulness for the treatment of PD. We also further examined the mechanism by which creatine exerts its neuroprotective effects. We found that creatine was still protective in agents in mice deficient in ubiquitous mitochondrial creatine kinase suggesting that its effects were not mediated by inhibition of the mitochondrial permeability transition.

We carried out the first studies examining MMP-9 after administration of MPTP. These were done using both zymography, immunohistochemistry and Western blot analysis. We found that the activity of MMP-9 was significantly increased and remained increased in the substantia nigra for up to seven days after MPTP administration. This appeared to occur in both neurons and microglia. We also found for the first time, that treatment with an MMP inhibitor significantly protected against dopamine depletion and loss of tyrosine hydroxylase neurons. We found further evidence linking oxidative damage to the mechanisms by which deficiency of DJ-1 may lead to autosomal recessive PD. We found that a depletion of DJ-1 in dopaminergic neurons made these neurons much more sensitive to oxidative stress. This provides further evidence linking oxidative damage to PD pathogenesis.

Lastly, we carried out studies with a novel azulenyl nitrone antioxidant. This agent exerts markedly improved abilities to scavenge free radicals. We found that it was neuroprotective against MPTP and significantly protected against the increase in

malondialdehyde produced by 3-NP. This suggests that the development of further novel antioxidants might be useful for treating PD.

In summary, our studies have provided further evidence linking oxidative damage to both experimental models of PD as well as human genetic mutations, which cause autosomal recessive PD. We have also discovered a number of novel therapies, which may be useful in the treatment of PD. Lastly, we have demonstrated for the first time, that administration of two agents acting on different pathways can exert additive neuroprotective effects in a mouse model of PD.

## 10. REFERENCES

None

## 11. APPENDICES

Kaur D, Yantiri F, Rajagopalan S, Kumar J, Mo JQ, Boonplueang R, Viswanath V, Jacobs R, Yang L, Beal MF, DiMonte D, Volitaskis I, Ellerby L, Cherny RA, Bush AI, Andersen JK. Genetic or pharmacological iron chelation prevents MPTP-induced neurotoxicity in vivo: a novel therapy for Parkinson's disease. Neuron 2003; 37:899-909.

Klivenyi P, Calingasan NY, Starkov A, Stavrovskaya IG, Kristal BS, Yang L, Wieringa B, Beal MF. Neuroprotective mechanisms of creatine occur in the absence of mitochondrial creatine kinase. Neurobiol Dis 2004; 15:610-617.

Klivenyi P, Gardian G, Calingasan NY, Yang L, Beal MF. Additive neuroprotective effects of creatine and a cyclooxygenase 2 inhibitor against dopamine depletion in the 1-methyl-4-phenyl-1,2,3,6-tetrahydropyridine (MPTP) mouse model of Parkinson's disease. J Mol Neurosci 2003; 21:191-198.

Lorenzl S, Albers DS, Chirichigno JW, Augood SJ, Beal MF. Elevated levels of matrix metalloproteinases-9 and -1 and of tissue inhibitors of MMPs, TIMP-1 and TIMP-2 in postmortem brain tissue of progressive supranuclear palsy. J Neurol Sci 2004; 218:39-45.

Martinat C, Shendelman S, Jonason A, Leete T, Beal MF, Yang L, Floss T, Abeliovich A. Sensitivity to oxidative stress in DJ-1-deficient dopamine neurons: an ES-derived cell model of primary parkinsonism. PLoS Biol 2004; 2:1754-1763.

Yang L, Calingasan NY, Chen J, Ley JJ, Becker DA, Beal, MF. A novel azulenyl nitrone antioxidant protects against MPTP and 3-nitropropionic acid neurotoxicities. Exp Neurol 2005; 191;86-93.

Yang L, Sugama S, Mischak RP, Kiaei M, Bizat N, Brouillet E, Joh TH, Beal, MF. A novel systemically active caspase inhibitor attenuates the toxicities of MPTP, malonate , and 3NP in vivo. Neurobiol Dis 2004;17:250-259.

Yang L, Sugama S, Chirichingo JW, Gregorio J, Lorenzl S, Shin DH, Browne SE, Shimizu Y, Joh TH, Beal, MF, Albers DS. Minocycline enhances MPTP toxicity to dopaminergic neurons. J Neurosci Res 2003:15;278-285.

**11. PERSONNEL**

M. Flint Beal

Carine Cleren

Noel Y. Calingasan

Lichuan Yang

Peter Klivenyi

Stefan Lorenzl

Neuron, Vol. 37, 899–909, March 27, 2003, Copyright ©2003 by Cell Press

# Genetic or Pharmacological Iron Chelation Prevents MPTP-Induced Neurotoxicity In Vivo: A Novel Therapy for Parkinson's Disease

Deepinder Kaur,[1,8] Ferda Yantiri,[2,8]
Subramanian Rajagopalan,[1] Jyothi Kumar,[1]
Jun Qin Mo,[2] Rapee Boonplueang,[2]
Veena Viswanath,[2] Russell Jacobs,[3]
Lichuan Yang,[4] M. Flint Beal,[4] Dino DiMonte,[5]
Irene Volitaskis,[6] Lisa Ellerby,[1] Robert A. Cherny,[6]
Ashley I. Bush,[6,7] and Julie K. Andersen[1,2,*]
[1]Buck Institute for Age Research
Novato, California 94945
[2]Division of Neurogerontology
Andrus Gerontology Center
University of Southern California
Los Angeles, California 90089
[3]Biological Imaging Center
California Institute of Technology
Pasadena, California 91125
[4]Department of Neurology and Neuroscience
Weill Medical College of Cornell University
New York, New York 10021
[5]The Parkinson's Institute
Sunnyvale, California 94089
[6]Department of Pathology
The University of Melbourne
The Mental Health Research Institute of Victoria
Parkville 3052
Australia
[7]Laboratory of Oxidation Biology
Genetics and Aging Research Unit
Department of Psychiatry
Harvard Medical School
Massachusetts General Hospital
Charlestown, Massachusetts 02129

## Summary

**Studies on postmortem brains from Parkinson's patients reveal elevated iron in the substantia nigra (SN). Selective cell death in this brain region is associated with oxidative stress, which may be exacerbated by the presence of excess iron. Whether iron plays a causative role in cell death, however, is controversial. Here, we explore the effects of iron chelation via either transgenic expression of the iron binding protein ferritin or oral administration of the bioavailable metal chelator clioquinol (CQ) on susceptibility to the Parkinson's-inducing agent 1-methyl-4-phenyl-1,2,3,6-tetrapyridine (MPTP). Reduction in reactive iron by either genetic or pharmacological means was found to be well tolerated in animals in our studies and to result in protection against the toxin, suggesting that iron chelation may be an effective therapy for prevention and treatment of the disease.**

*Correspondence: jandersen@buckinstitute.org
[8]These authors contributed equally to this work.

## Introduction

Iron levels in the substantia nigra (SN), the dopamine-containing region of the brain that undergoes selective degeneration in Parkinson's disease (PD), have been reported to be elevated in patients with the disorder (Sofic et al., 1988, 1991; Dexter et al., 1987, 1989; Youdim et al., 1993; Gerlach et al., 1994; Yantiri and Andersen, 1999; Griffiths et al., 1999; Andersen, 2001). Accessible ferrous iron ($Fe^{2+}$) can react with hydrogen peroxide ($H_2O_2$) produced during oxidative deamination of dopamine to generate hydroxyl radicals (·OH) that can damage proteins, nucleic acids, and membrane phospholipids, leading to cellular degeneration (Beal, 1992; Gutteridge, 1992). However, whether the increase in SN iron is a causal factor in the disease or a consequence itself of neuronal degeneration is controversial (Adams and Odunze, 1991; Berg et al., 2001; Thompson et al., 2001). Experiments were therefore undertaken to test whether iron is causally involved in cellular degeneration associated with toxin-induced parkinsonism by assessing whether iron chelation can act to protect against dopaminergic cell loss.

In the first set of experiments, susceptibility of transgenic mice expressing the ferritin heavy subunit (H ferritin) within dopaminergic SN neurons to the PD-inducing neurotoxin 1-methyl-4-phenyl-1,2,3,6-tetrahydropyridine (MPTP) was assessed. Ferritin, the primary nonheme iron storage molecule in the body, can sequester up to 4500 atoms of ferric ($Fe^{3+}$) iron as an oxyhydroxide (Harrison and Arosio, 1996). Ferritin is believed to keep iron in a nonreactive form where it cannot promote redox reactions and therefore could be a key component for protecting tissues against iron-catalyzed oxidative damage (Jellinger, 1999). The ferroxidase activity of H ferritin converts harmful labile ferrous iron to less soluble, unreactive ferric iron, while the light subunit (L ferritin) stablizes the ferritin-iron complex, promoting long-term iron storage (Harrison and Arosio, 1996; Rucker et al., 1996). In the second set of experiments, mice were orally pretreated for 8 weeks with the antibiotic 5-chloro-7-iodo-8-hydroxyquinoline (clioquinol or CQ) and assessed for the ability of the compound to protect against MPTP-induced toxicity. Another antibiotic compound, minocycline, has previously been demonstrated to protect against MPTP toxicity, likely due to its ability to decrease nitric oxide-mediated apoptosis (Du et al., 2001). CQ's mechanism of action, however, is likely different. It has been shown to chelate both ferrous and ferric iron (Kidani et al., 1974) and to decrease brain iron levels in normal mice (Yassin et al., 2000). Its oral administration was reported to inhibit β-amyloid accumulation in an Alzheimer's disease (AD) transgenic mouse model via its actions as a metal chelator (Huang et al., 1999; Bush, 2000; Cherny et al., 2001). In addition, in a recently reported small two-year double-blind human phase II clinical trial, it has been reported to be well tolerated in patients and to delay the course of the disease by 9 months (Masters, 2002). Neither ferritin expression nor oral CQ treatment appear to elicit any

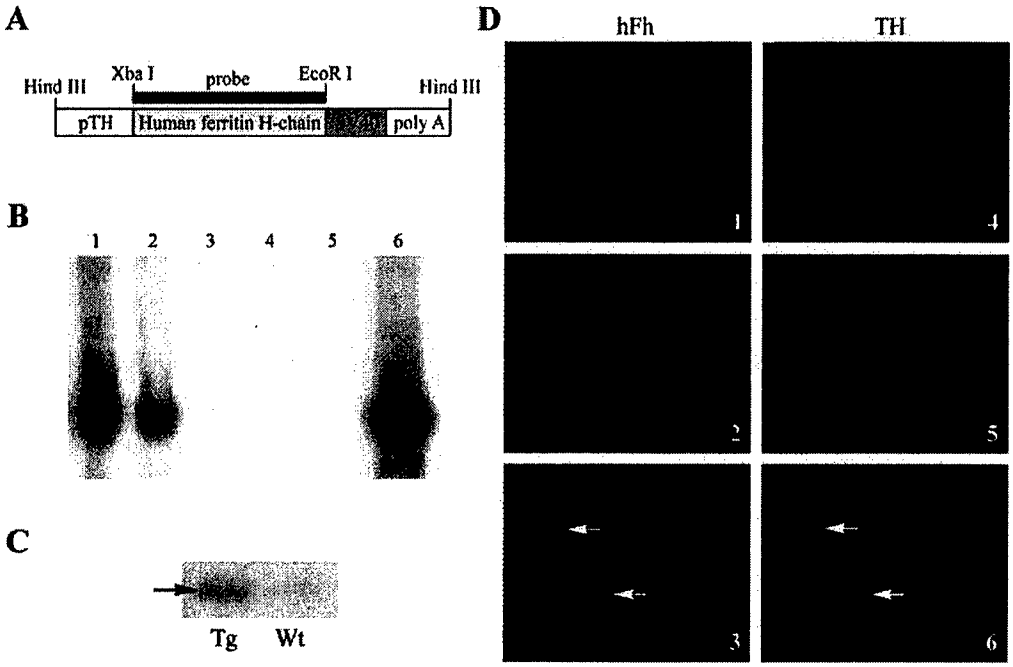


Figure 1. Creation of pTH-Ferritin Transgenics

(A) Schematic of pTH-ferritin construct used for creation of ferritin transgenics and Xba I-EcoRI probe used for Southern analysis. Abbreviations: pTH, 4.8 kb 5′ rat tyrosine hydroxylase promoter region; human ferritin H-chain, human ferritin heavy chain 2.6 kb genomic fragment; SV40/poly A, 900 bp 3′ large T antigen SV40 splice/polyadenylation sequences; probe, $^{32}$P-labeled Xba I/EcoRI cDNA fragment of ferritin H-chain.
(B) Representative Southern blot analysis of genomic tail DNA isolated from pTH-ferritin founders. Lanes 1 and 2, transgenics; lanes 3–5, nontransgenics; lane 6, 2.6 kb Xba I/EcoRI ferritin probe.
(C) Representative Western blot using monoclonal antibody directed against human H ferritin. Abbreviations: Tg, ferritin transgenic; wt, wild-type littermate. Arrow shows expected position of the 21 kDa human ferritin H-chain protein.
(D) Expression of human ferritin protein product in dopaminergic SN neurons verified by representative double immunocytochemistry (ICC) using H ferritin and TH antibodies. Images 1–3, ICC with monoclonal antibody against human H ferritin (hFh dilution, 1:500); images 4–6, ICC with TH antibody (dilution, 1:500). 1 and 4, 10× magnification; 2, 3, 5 and 6, 20× magnification.

apparent adverse general health or behavioral effects, unlike chelators currently used as therapy for iron overload conditions, which can have severe side effects (Porter and Huehns, 1989; Marciani et al., 1991). Results from our studies demonstrate that such in vivo iron chelation protects mice against the toxic effects of the parkinsonian-inducing agent MPTP and suggest that this may be a novel avenue of therapy for the disease.

## Results

Transgenic ferritin lines were generated by injection of an 8.3 kb DNA fragment into fertilized mouse embryos containing the rat tyrosine hydroxylase promoter (pTH) driving expression of the human H ferritin gene (Figure 1A). Human ferritin binds iron more tightly than the mouse isoforms, making it a superior iron chelating agent, and monoclonal antibodies are also available that are specific to the human protein (Rucker et al., 1996). In order to prevent iron-induced downregulation of transgenic ferritin RNA translation, the 5′ noncoding region of the gene containing an iron-response element (IRE) was excluded from the construct (Caughman et al., 1988).

Integration of the pTH-ferritin transgene in founder animals was verified by Southern blot analysis (Figure 1B). Expression of the human H ferritin protein in the SN of resulting lines was verified by both Western blot analysis (Figure 1C) and immunocytochemistry (ICC; Figure 1D, 1–3). No changes were observed in endogenous ferritin levels in these animals (data not shown). Double labeling of H ferritin-expressing cells with tyrosine hydroxylase (TH) antibody demonstrated that the transgenic ferritin protein is localized within dopaminergic SN neurons (Figure 1D, 4–6). Adult ferritin transgenics exhibited no overt phenotype, reproduced normally, and displayed no gross alterations in brain size or anatomical features in histologically stained brain sections (data not shown).

Increased iron binding to ferritin would be expected to result in increased conversion of ferrous to ferric iron as it enters the ferritin core and is oxidized to ferrihydrite. Ferric iron's paramagnetic characteristics allow for its visualization by high-field magnetic resonance imaging (MRI); the signal is intensified when iron is bound to ferritin and thereby can be used as a measure of ferritin bound iron (Gilissen et al., 1998; Griffiths et al., 1999). MRI was performed on brains from ferritin transgenics versus nontransgenic littermates and the signal intensity quantified using frontal cortex as an internal control. A 33.7% ± 8.5% increase in signal intensity was observed in transgenic animals versus wild-type controls (Figure 2A; $n = 4$ animals per parameter, $p < 0.01$). Conversely, bioavailable SN ferrous iron levels were found to be

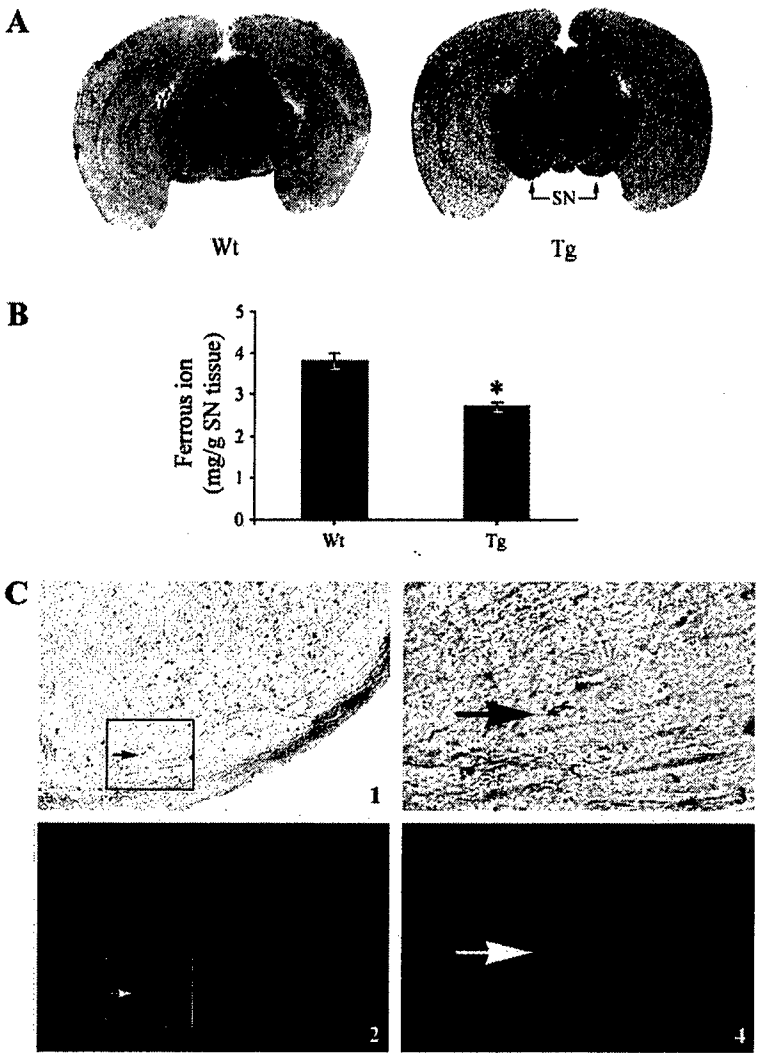


Figure 2. Levels and Localization of Ferric/Ferrous Iron in the SN of pTH-Ferritin Transgenics versus Wild-Type Littermates

(A) Representative MRI analysis of brains from ferritin transgenics versus wild-type animals demonstrating levels of ferritin bound ferric iron; n = 4 for each group. Abbreviations: SN, substantia nigra; wt, wild-type; Tg, transgenic.

(B) Bioavailable SN ferrous iron levels, n = 5 for each group. *$p < 0.01$ versus wild-type.

(C) Localization of SN ferric iron within dopaminergic neurons in the ferritin transgenics as verified by double staining of Perls-positive SN cells with TH antibody. 1, 4× magnification of Perls staining in a representative section of the SN region of a ferritin transgenic mouse; 2, 10× magnification of boxed region in panel 1 highlighting position of a $TH^+$ dopaminergic SN neuron in this brain area (arrow); 3, Perls staining of the dopaminergic neuron highlighted in panel 2; 4, 40× magnification of the dopaminergic neuron shown in panel 2 demonstrating TH positivity.

decreased by 22% ± 9.8% in the ferritin transgenic SN (Figure 2B; wt = 3.8 ± 0.20 μg/g SN tissue, Tg = 2.7 ± 0.13 μg/g SN tissue, n = 4 animals per parameter, *$p <$ 0.01), presumably due to its conversion to ferric during oxidation and storage in ferritin. To assess whether the increased ferric iron colocalized with dopaminergic SN neurons, Perls staining was performed in conjunction with immunocytochemistry using an antibody specific for TH (Figure 2C). Perls staining revealed that, in agreement with previous reports (Benkovic and Connor, 1993; Connor et al., 1994; Cheepsunthorn et al., 1998), ferric iron is predominantly localized within SN cells with the appearance of oligodendrocytes in wild-type animals (data not shown). The numbers of ferric iron-positive cells were increased in the transgenic SN and were found to be localized within cell bodies and neuritic processes of TH-positive SN cells (Figure 2C). Estimation of numbers of Perls-positive SN cells demonstrated a 22.4% ± 4.7% increase in the transgenic animals ($p <$ 0.01); these cells displayed the correct size, morphology, and TH-positive expression of dopaminergic neurons.

Systemic administration of the neurotoxin MPTP produces a clinical syndrome strikingly similar to PD (Tetrud and Langston, 1989; Chiueh and Rauhala, 1998). Animals treated with MPTP exhibit several of the major hallmarks of PD, including a substantial decrease in numbers of dopaminergic SN neurons. The damaging effect of MPTP administration also mirrors the disease in that oxidative stress appears to play a major role in ensuing neurodegeneration (Yong et al., 1986; Cassarino et al., 1999), including a decrease in glutathione (GSH) levels, as has been reported to occur early in the course of PD (Perry et al., 1982; Sian et al., 1994; Hung and Lee, 1998; Desole et al., 1993; Lan and Jiang, 1997). Both MPTP-induced increases in reactive oxygen species (ROS) and decreases in GSH levels were both found to be prevented in the ferritin transgenics (Figures 3A and 3B). Acute MPTP administration (4 × 20 mg/kg body weight, every 2 hr) resulted in a 56% ± 4% increase in ROS levels in wild-type SN (n = 6 animals, *$p < 0.01$), while no significant change was detected in transgenic animals (95% ± 4.0%, n = 8 animals, **$p > 0.05$). A 2.4% ± 0.3% decrease in SN GSH was observed at 2 hr and a 10.0% ± 0.05% at 8 hr, respectively, after the final MPTP injection in wild-type mice (n = 6, *$p < 0.01$), while no significant change was observed in the ferritin

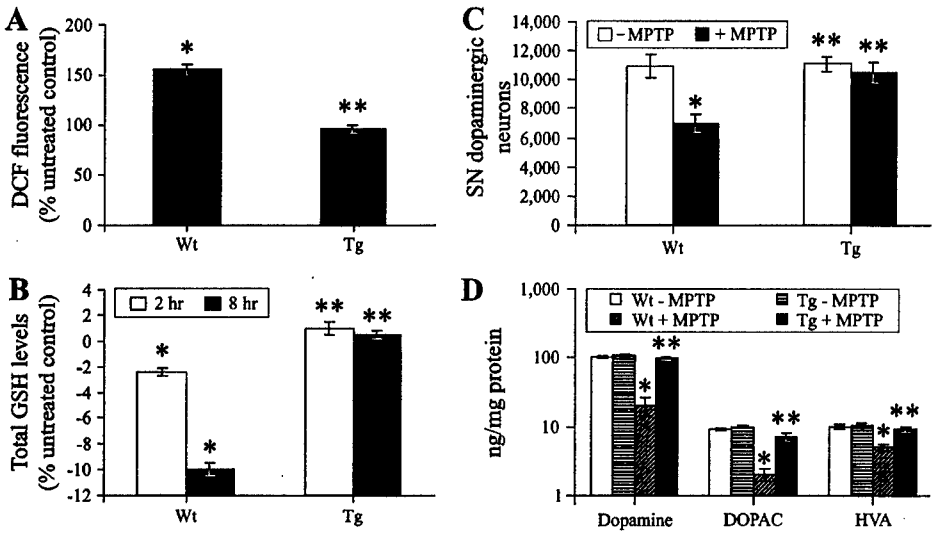


**Figure 3. Effects of Acute MPTP Administration on Levels of Oxidative Stress, Dopaminergic SN Neuronal Cell Number and Striatal (ST) Dopamine and Its Metabolites in pTH-Ferritin Transgenics versus Wild-Type Littermates**

(A) Percentage change in ROS levels in SN tissue 8 hr following acute MPTP administration, *$p < 0.01$, untreated versus MPTP-treated wt; **$p > 0.05$, MPTP-treated Tg versus wt.

(B) Percentage change in GSH levels in SN tissue 2 hr and 8 hr following acute MPTP administration, *$p < 0.01$, untreated versus MPTP-treated wt at 2 and 8 hr; **$p > 0.05$, MPTP-treated Tg versus wt at 2 and 8 hr.

(C) $TH^+$ SN cell counts from transgenics versus nontransgenics 7 days following acute MPTP administration, *$p < 0.01$, MPTP-treated versus untreated wt; **$p > 0.05$; untreated and MPTP-treated Tg versus MPTP-treated wt.

(D) ST DA, DOPAC, and HVA content in ferritin transgenic versus wild-type littermates 7 days following acute MPTP, *$p < 0.01$, untreated versus MPTP-treated wt; **$p > 0.05$, MPTP-treated Tg versus wt.

transgenics (+1.0% ± 0.5% at 2 hr and +0.5% ± 0.3% at 8 hr, respectively, n = 8, **$p > 0.05$).

To assess the effects of ferritin expression on acute MPTP-induced dopaminergic SN cell loss, stereological $TH^+$ cell counts were performed. $TH^+$ cell numbers in the nontransgenic SN were found to decrease by approximately 30% ± 5.2% following acute MPTP administration (Figure 3C; 10,900 ± 800, saline-treated; 7,000 ± 500, MPTP-treated, n = 5, *$p < 0.01$). In contrast, no decrease was noted following acute MPTP administration in the ferritin transgenics (11,100 ± 600, saline-treated; 10,500 ± 700, MPTP-treated, n = 7, **$p > 0.05$). To confirm the protection against $TH^+$ SN cell loss in the ferritin transgenic following acute MPTP administration, levels of striatal dopamine (DA) and its metabolites 3,4-dihydroxyphenylacetic acid (DOPAC) and homovanillic acid (HVA) were measured. Wild-type animals displayed significant depletion of DA, DOPAC, and HVA commensurate with decreased numbers of $TH^+$ SN neurons (Figure 3D; DA, DOPAC, HVA = 100 ± 3.0, 9.0 ± 0.5, 10.0 ± 0.8 ng/mg protein in saline-treated and 20.0 ± 0.6, 2.0 ± 0.4, 5.0 ± 0.6 ng/mg protein in MPTP-treated, n = 4, *$p < 0.01$). These losses were attenuated in the ferritin transgenics (DA, DOPAC, HVA = 105 ± 3.0, 10.0 ± 0.54, 10.5 ± 0.6 ng/mg protein in saline-treated and 95.0 ± 0.8, 7.0 ± 1.0, 9.0 ± 0.7 ng/mg protein in MPTP-treated, n = 5, **$p > 0.05$ compared to wt). The protective effects of the ferritin transgene could not be explained by decreased conversion of MPTP to $MPP^+$ following acute administration (transgenic = 143.04 ± 18.02 ng/mg protein $MPP^+$, wild-type = 109.77 ± 22.03 ng/mg protein $MPP^+$, n = 4, $p > 0.05$).

To test whether pharmacological iron chelation using a reported well-tolerated bioavailable reagent would have similar protective effects afforded by transgenic expression of an iron-chelating molecule, we examined the effects of the metal-chelating agent CQ on susceptibility to acute MPTP administration. Total SN iron levels were found to be reduced approximately 30% in the CQ-fed versus saline-fed animals (Figures 4A and 4B), well within the reported nontoxic range (Yassin et al., 2000). As with the ferritin transgenics, MPTP-mediated increases in SN oxidative stress and decreases in SN GSH were found to be significantly attenuated following CQ pretreatment (Figures 5A–5C). A 20% ± 3% increase in levels of 4-hydroxynonenol (4-HNE)-protein conjugates, a 15% ± 2% increase in protein carbonyl levels, and a 18% ± 3% decrease in GSH were observed in control SN 24 hr following MPTP injection (n = 5 animals per assay, *$p < 0.01$). However, no significant changes in any of these indices of oxidative stress were found in the CQ-pretreated animals (n = 6 animals, **$p > 0.05$ versus wt). To assess the affects of CQ pretreatment on MPTP-induced dopaminergic SN cell loss, measurements of both striatal dopamine levels and stereological $TH^+$ cell numbers were performed following acute treatment with MPTP (Figures 5D and 5E). While reductions in striatal dopamine levels in untreated controls were approximately 80% (121.8 ± 25.6 versus 21.4 ± 4.5 mg/g striatal tissue, *$p < 0.01$ versus untreated control), this loss was only 41% in animals pretreated with CQ (147.2 ± 10.6 versus 60.5 ± 8.8 mg/g striatal tissue, **$p < 0.01$ versus Veh/MPTP). No significant difference in striatal dopamine levels was observed between saline

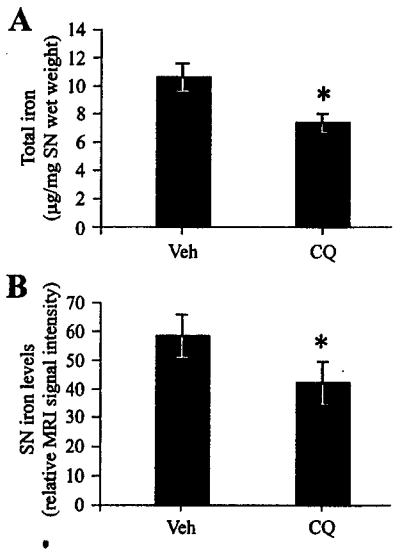


Figure 4. Effects of CQ Pretreatment on Total SN Iron Content
(A) Total SN iron content (μg/mg tissue wet weight) measured via mass spectrometry of vehicle (Veh) versus CQ-fed animals, *$p < 0.01$.
(B) SN iron levels measured via MRI in Veh versus CQ-fed animals, *$p < 0.01$.

versus CQ-fed animals in the absence of MPTP treatment, suggesting that CQ pretreatment alone has no effect (Figure 5D). While SN $TH^+$ cell numbers in untreated animals were decreased by 46% following acute MPTP administration (15,346 ± 1,471, saline-treated; 8,336 ± 1,093, MPTP-treated, n = 5, *$p < 0.01$), only a 25% decrease was noted in the CQ-fed animals (11,462 ± 915, n = 5, **$p < 0.01$ versus MPTP-treated controls). As with transgenic ferritin expression, the protective effects of CQ pretreatment were not explainable by decreased conversion of MPTP to $MPP^+$ (CQ-fed = 134.04 ± 8.70 ng/mg protein $MPP^+$, saline-fed = 138.15 ± 6.63 ng/mg protein $MPP^+$, n = 5, $p > 0.05$).

In order to examine the effects of CQ pretreatment in a different MPTP toxicity paradigm, we also assessed toxin-induced dopaminergic SN cell loss following a chronic regime of MPTP treatment (5 × 20 mg/kg, 24 hr apart; Figure 5F; Vila et al., 2001). Following chronic treatment with MPTP, SN $TH^+$ cell numbers in untreated animals were decreased by 31% (10,143 ± 701, saline-treated; 7,010 ± 238, MPTP-treated, n = 6, *$p > 0.01$), but only by 17% in the CQ-pretreated animals (8449 ± 503, n = 5, **$p > 0.01$ versus MPTP-treated controls). No difference in $TH^+$ cell numbers was observed between vehicle- or CQ-fed animals prior to MPTP treatment (10,143 ± 701, saline-treated; 10,291 ± 660, CQ-fed, n = 6, $p > 0.05$), suggesting the CQ alone had no effect on this parameter.

Finally, we assessed whether either genetic or pharmacological iron chelation provided protection against behavioral motor deficits associated with MPTP treatment (Figure 6). Neither transgenic ferritin expression nor CQ treatment alone was found to result in decreased motor performance as assessed by rotorod (data not shown). However, performance following acute MPTP treatment was found to be decreased, and this MPTP-induced loss in motor activity was significantly attenuated by either transgenic ferritin expression (Figure 6A, 30.86% ± 2.19% decrease in wt; 19.71% ± 1.61% decrease in transgenic versus untreated control, n = 4, $p < 0.01$) or CQ pretreatment (Figure 6B, 36.43% ± 11.7% decrease in vehicle-fed/acute MPTP; 13.55% ± 2.6% decrease in CQ-fed/acute MPTP versus untreated control, n = 4, $p < 0.01$) by 24 hr following the last MPTP dose. In addition, CQ was also found to be protective 96 hr following the chronic MPTP treatment regime (Figure 6C, 24.95% ± 5.97% decrease, vehicle-fed/chronic MPTP; 10.27% ± 3.10% decrease, CQ-fed/chronic MPTP, n = 4, $p < 0.01$).

## Discussion

MPTP-induced neurotoxicity has proven in the past to be an invaluable tool for testing drug therapy in experimental parkinsonism as a model for PD (Sedelis et al., 2001; Beal, 2001). MPTP reproduces virtually all symptoms of the disease, including inhibition of mitochondrial complex I activity, decreased GSH and increased oxidative stress levels in the SN, relatively selective neurodegeneration of the dopaminergic nigrostriatal system, striatal dopamine depletion, and motor control deficits, all of which can be reversed by dopamine substitution therapy, the classic PD drug treatment. Its effects were indeed originally discovered in humans as a consequence of inadvertent injection that resulted in an acute parkinsonism. MPTP does not perfectly model the disorder, particularly in terms of the acute nature of onset using this drug and the absence of inclusion bodies in rodents (Betarbet et al., 2002). However, an animal model does not need to recapitulate every feature of the disease in order to be useful in evaluating the potential therapeutic potential of a particular agent.

Elevated levels of brain iron similar to those reported in PD have been shown to result in significantly higher levels of both oxidative stress and dopaminergic cell loss following MPTP administration in vivo, suggesting that elevated iron can contribute to the toxicity of the compound via an oxidative mechanism (Lan and Jiang, 1997). Redox-available iron has been detected in midbrain Lewy bodies in postmortem parkinsonian brains (Castellani et al., 2000), and the oxidation state of iron has been reported to change from ferrous to ferric within SN $TH^+$ neurons during progression of the disease (Yoshida et al., 2001). Our data demonstrate that chelation of iron via ferritin or CQ in a state that prevents it from participating in oxidative events significantly attenuates toxicity of the parkinsonian-inducing agent MPTP. These results definitively demonstrate the involvement of iron in MPTP-mediated neurodegeneration. These results, in addition, challenge the view that iron accumulation is a late-stage, irreversible event in MPTP toxicity and PD and suggests that iron chelation may be an effective preventative therapy for progressive degeneration associated with the disease.

Transgenic expression of the heavy ferritin subunit was found to prevent dopaminergic SN cell loss associated with MPTP toxicity. The heavy subunit contains catalytic ferroxidase activity, which allows it to detoxify reactive ferrous iron and is the predominant form found

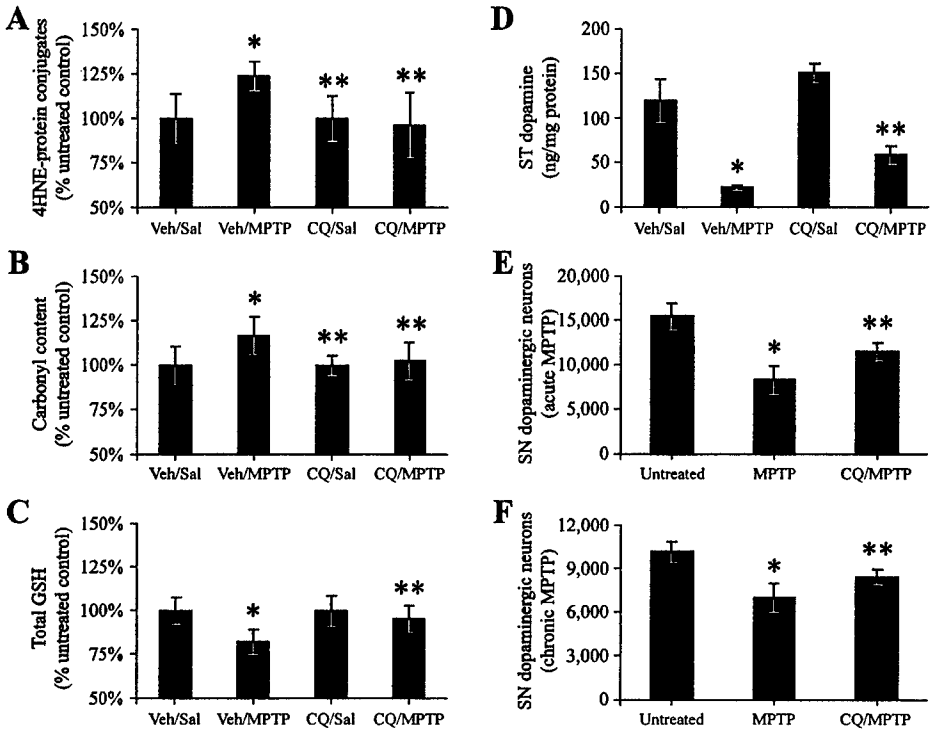


**Figure 5. Protective Effects of CQ Pretreatment against MPTP-Mediated Oxidative Stress and Dopaminergic Cell Loss under Either Acute or Chronic MPTP Dosing Regimes**

(A and B) Levels of 4-HNE-protein conjugates (A) and protein carbonyl content (B) as assessed by slot blot analysis of SN tissue 24 hr following acute MPTP or saline (Sal) administration in the absence or presence of CQ pretreatment, *$p < 0.01$, Veh/MPTP versus Veh/Sal; **$p > 0.05$, CQ/Sal and CQ/MPTP versus Veh/Sal.

(C) Total SN GSH levels 24 hr following acute MPTP or saline administration ± CQ pretreatment, *$p < 0.01$, Veh/MPTP versus Vehl/Sal; **$p > 0.05$, CQ/Sal and CQ/MPTP versus Veh/Sal.

(D) ST DA, DOPAC, and HVA content in saline versus CQ-fed mice 7 days following acute MPTP, *$p < 0.01$, Veh/MPTP versus Veh/Sal; **$p > 0.05$, CQ/Sal and CQ/MPTP versus Veh/Sal.

(E) $TH^+$ SN cell counts from saline versus CQ fed 7 days following acute MPTP administration, *$p < 0.01$, MPTP versus untreated wt; **$p < 0.01$ CQ/MPTP versus MPTP-treated wt.

(F) $TH^+$ SN cell counts from saline versus CQ fed 7 days following chronic MPTP administration, *$p < 0.01$, MPTP versus untreated wt; **$p < 0.01$ CQ/MPTP versus MPTP-treated wt.

in brain neurons (Harrison and Arosio, 1996; Connor et al., 1995; Han et al., 2000). It is rapidly upregulated in response to oxidative stress, and overexpression in vitro results in increased resistance to $H_2O_2$-mediated insult (Orino et al., 2001; Cozzi et al., 2000), suggesting that it may play an important role as a biological antioxidant by sequestering iron that is normally free to participate in oxidative events. Several recent reports have suggested that diseases of iron overload may have their basis in misregulation of iron storage by ferritin. A dominantly inherited iron overload disease in a Japanese pedigree, for example, was recently attributed to a point mutation in the iron response element (IRE) in the H ferritin gene promoter, which leads to increased binding affinity of the iron regulatory protein (IRP), decreasing H ferritin synthesis and resulting in increased cytoplasmic iron levels (Kato et al., 2001). A mutation in the gene encoding the ferritin light subunit has also recently been reported to cause a dominantly inherited adult-onset basal ganglia disease similar to PD due to a change in its conformation that affects its ability to function as a stabilizer of the ferritin-iron core, resulting in increased iron release, suggesting that iron excess can have serious neurological consequences (Curtis et al., 2001; Connor et al., 2001; Thompson et al., 2001).

Like ferritin, CQ also has metal binding properties, although it appears to act via chelation of both ferrous and ferric iron rather than conversion of available ferrous to bound unreactive ferric iron. It is lipophilic and therefore freely crosses the blood-brain barrier. CQ has recently been shown to inhibit plaque formation and accompanying behavioral declines in an AD transgenic mouse model (Cherny et al., 2001; see commentary by Melov, 2002). We found that CQ given at similar concentrations and time periods found to be effective in the AD mouse studies results in significant attenuation of the neurotoxic effects of MPTP. CQ has been shown to reduce bioavailable brain iron in normal control mice with no apparent adverse health or behavioral effects (current study; Yassin et al., 2000). CQ treatment also does not result in depletion in systemic iron levels that could cause adverse physiological effects (Yassin et al., 2000). This is in contrast to other currently used iron chelators administered to patients with iron overload conditions that have been shown to have toxic side effects at the higher dosages needed to overcome the

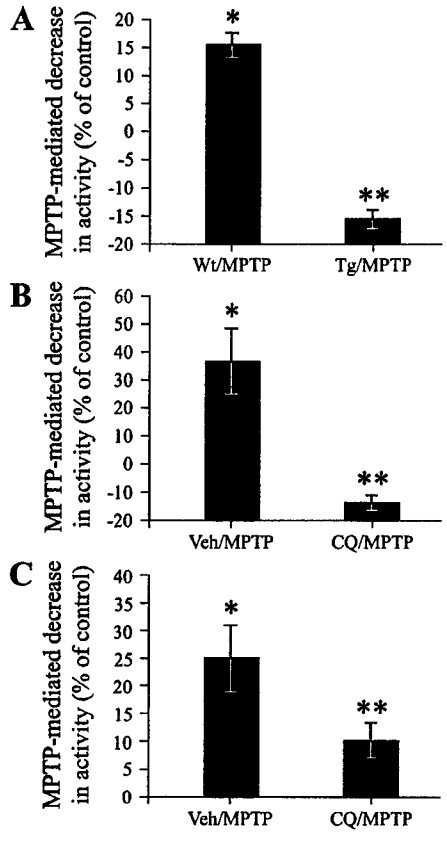


Figure 6. Protective Effects of Transgenic Ferritin Expression and Pharmacological CQ Treatment against Motor Deficits Elicited by Either Acute or Chronic MPTP Treatment

(A) Decreases in motor activity as assessed by rotorod in wt versus ferritin transgenic mice 24 hr following acute MPTP treatment. *$p < 0.01$, MPTP versus untreated wt; **$p > 0.01$, MPTP-treated Tg versus wt.

(B) Decreases in motor activity in Veh versus CQ-fed mice 24 hr following acute MPTP treatment, *$p < 0.01$, MPTP versus saline-treated wt; **$p < 0.01$, MPTP-treated CQ versus wt.

(C) Decreases in motor activity in saline versus CQ-fed mice 96 hr following chronic MPTP mice, *$p < 0.01$, MPTP versus saline-treated wt; **$p < 0.01$, MPTP-treated CQ versus wt.

compounds' low lipid solubility that impair their ability to cross the blood-brain barrier (Porter and Huehns, 1989; Marciani et al., 1991). It should be noted that it cannot be excluded that the protective effects of CQ may be due in part to previously reported CQ-mediated depletions in brain copper levels, as copper can act to facilitate $Fe^{2+}$ toxicity (Cherny et al., 2001); however, copper levels, unlike iron, have not been shown to be elevated in PD. No adverse effects were attributable to CQ administration in our study at a similar dosage (g/kg body weight) to that used in the previous transgenic APP study (Huang et al., 1999; Bush, 2000; Cherny et al., 2001). Results from a recent small two-year double-blind phase II trial assessing the efficacy of CQ as a possible treatment for AD suggest that oral administration of the agent accompanied by B12 supplementation is well tolerated in humans over the period of the trial at similar dosages to those used in both the previous APP transgenic and in our current MPTP study and were, in addition, efficacious in delaying the course of the disease. Acute administration of the compound at significantly higher dosages had previously been associated with a subacute myelo-optic neuropathy (SMON), which was primarily confined to Japan (Masters, 2002; Tsubaki et al., 1971). SMON appears to resemble a subacute accelerated form of B12 deficiency, and CQ has been shown to lower levels of brain and serum vitamin B12 (Yassin et al., 2000). However, a causal relationship between SMON and CQ intake has not been established; for example, CQ was used extensively in Japan for 20 years before the first cases of SMON were reported (Meade, 1975; Nakae et al., 1973; Baumgartner et al., 1979; Clifford Rose and Gawel, 1984). In light of this possibility, the Alzheimer phase II clinical trials (Masters, 2002) were performed with B12 coadministration, and dosages of the drug were kept to a fraction of those dosages used previously that demonstrated neurotoxic effects (e.g., Yoshimura et al., 1992; Tateishi, 2000). The possible toxic effects of chronic CQ administration at these dosages beyond the period of the trial, however, have yet to be assessed.

Increases in reactive brain iron are not specific to PD but are also seen in such diverse neurodegenerative disorders as multiple system atrophy, Huntington's disease, Alzheimer's disease, progressive supranuclear palsy, aceruloplasminemia, and Hallervorden-Spatz (Dexter et al., 1991; Connor et al., 1992; Smith et al., 1997; Gitlin, 1998; Janetzky et al., 1997). Misregulation of iron metabolism resulting in iron accumulation, therefore, may be a general phenomenon contributing to the progression of several neurodegenerative conditions. Brain iron accumulation along with increased ROS production is part of the normal aging process, particularly in the basal ganglia, and this in itself may contribute to the increased age-related susceptibility in a subset of these diseases (Bartzokis et al., 1997; Zecca et al., 2001; Christen, 2000; Thompson et al., 2001). Brain H ferritin levels are known to increase with age, likely as a protective response to increasing iron levels; however, this increase does not appear to occur in either PD or AD brains (Connor et al., 1995; Zecca et al., 2001; Thompson et al., 2001). Although it has been previously speculated that increasing the iron loading of ferritin may increase the risk of free radical damage (Double et al., 1998; Griffiths et al., 1999), our data in contrast suggest that increased ferritin is in fact neuroprotective. Indeed, ferritin has recently been reported to normally be absent in dopaminergic SN neurons, and this may, in combination with other factors such as elevated iron levels, contribute to their susceptibility to oxidative stress (Moos et al., 2000). It is of interest in this regard that SN levels of ferritin in humans have been reported to actually be decreased in PD patients compared to age-matched controls, although this is somewhat controversial (Reiderer et al., 1989; Jellinger et al., 1990; Dexter et al., 1991; Jenner et al., 1992; Mann et al., 1994). Extensive elimination of iron from the brain is not desirable, as it is an abundant brain metal essential for several normal metabolic functions including the synthesis and release of dopamine in the SN (Beard et al., 1993; Glinka et al., 1996; Connor et al., 2001; Thompson et al., 2001). In addition, its deficiency during development has been associated with neurobehavioral dysfunction (Connor et

al., 1995). However, our data suggest that chelators such as ferritin or CQ, which can remove excess iron without apparent interference with its normal functions in the adult nervous system system, may postpone or prevent the progression of such neurological diseases as PD (Gassen and Youdim, 1997).

## Experimental Procedures

### Mouse Studies

Mice were housed according to standard animal care protocols, fed ad libitum, kept on a 12 hr light/dark cycle, and maintained in a pathogen-free environment in the Buck Institute Vivarium. Animals used for studies were young adults (2–6 months of age). Ferritin transgenic mice were generated via injection of an 8.3 kb Hind III DNA fragment containing 4.8 kb of 5′ upstream sequences from the rat TH gene (Banerjee et al., 1992), 2.6 kb of human genomic ferritin DNA encompassing the 4 coding region exons (Hentze et al., 1986), and 3′ SV40 splice and polyadenylation sequences into fertilized B6D2 mouse embryos to create pTH-ferritin transgenic founder animals. For CQ studies, C57Bl mice were obtained from Jackson Labs and randomized for therapy trials. CQ was suspended in saline and delivered via oral gavage at a daily dosage of 30 mg/kg as previously described for a period of 8 weeks (Cherny et al., 2001); controls received vehicle alone. For acute MPTP studies, mice were treated with either 4 × 20 mg/kg, 2 hr apart or 2 × 20 mg/kg, 12 hr apart of the toxin, and SN or ST samples taken at the times specified for various analyses. For chronic MPTP studies, mice were treated with 5 × 20 mg/kg MPTP, 24 hr apart, and samples taken at specified times for analyses.

### Southern Blot Analysis

Genomic DNA from ferritin founders was digested with Xba I, separated on a 1% agarose gel, transferred to Hybond (Amersham), and hybridized with a $^{32}$P-labeled 2.6 kb Xba I-EcoRI ferritin genomic fragment. Founder animals positive for the transgene were bred out to create lines for analysis; nontransgenic littermates were used as negative controls.

### Western/Slot Blot Analyses

SN were dissected and homogenized in 10 mM HEPES-KOH (pH 7.2), 2 mM EDTA, 0.1% CHAPS, 5 mM dithiothreitol (DTT), 1 mM phenylmethylsulfonyl fluoride, 10 μg/ml pepstatin A, 10 μg/ml aprotinin, and 20 μg/ml leupeptin (Nicholson et al., 1995). Fifteen micrograms of total protein from each sample was either run on a 15% SDS-PAGE gel (BioRad) and transferred to nitrocellulose membrane or directly slotted onto membrane. Membranes were incubated with 10–50 μg/ml primary antibody (heavy chain human ferritin monoclonal, Ramco Laboratories; anti-HNE Michaels adduct rabbit polyclonal, Calbiochem; anti-DNP rabbit polyclonal, Intergen), followed by horseradish peroxidase-conjugated secondary antibody (Vector Laboratories). Autoradiography was performed with enhanced chemiluminescence (Amersham Pharmacia). For 4HNE-protein conjugates and protein carbonyls, relative optical band density were quantified using a Chemilmager 5500 (Alpha Innotech Corporation). Reported values are the results of three independent experiments.

### Immunocytochemistry

Animals were cardiac-perfused with phosphate-buffered saline (PBS) followed by 10% formalin, and brains were removed and postfixed for 15 hr followed by 30% sucrose and sectioning at 40 μm on the coronal plane. ICC was performed as previously described (Andersen et al., 1994). Specific primary antibodies were applied and visualized with fluorescence (Streptavidin-Cy3 for red fluorescence and Streptavidin-Cy2 for green fluorescence, Jackson Immunochemicals).

### SN Iron Levels by Magnetic Resonance Imaging (MRI)

MRI studies were performed using a Bruker AMX500 11.7 tesla MRI system as previously described (Gilissen et al., 1998). Brains were fixed as described above and MRI performed in the coronal plane. Comparisons of SN hypointensity (dark area) on T2-weighted MR samples encompassing SNc, SNr, and red nucleus were performed (IPLab Spectrum, Scientific Image Processing from Scanalytics, Inc.; Morgan et al., 1999). Intensity was normalized using cortical white matter as control.

### Spectrophotometric Analysis of Bioavailable Ferrous Iron

Levels of ferrous iron available to bind ferrozine were determined in dissected SN tissue spectrophotometrically at 578 nm as previously described (Agrawal et al., 2001).

### Ferric Iron Histochemistry (Perls)

Coronal sections from brains of adult animals were subjected to formalin fixation and Perls staining using potassium ferrocyanide as previously described (Hill and Switzer, 1984). The percentage area covered by ferric-ferrocyanine product was assessed by Camera Luminace Drawing.

### ROS by DCF Fluorescence

Animals were i.p. injected with either 30 mg/kg body weight MPTP or saline. Eight hours after injection, synaptosomal fractions were prepared from the SN and used for DCF analysis (Ali et al., 1992). Fluorescence was monitored on a Turner spectrofluorometer with an excitation wavelength of 448 mm and an emission wavelength of 525 nm. Protein was normalized by the Bradford method.

### GSH Levels

Following MPTP or saline injection, GSH levels were measured in the SN by the method of Griffith (1980).

### Histology and Neuron Counts

Neuronal counts were performed on TH$^+$-positive SN neurons using the unbiased dissector method (West, 1993). Fixed coronal brain sections (40 μm) were immunostained with TH antibody (1:500 dilution, Chemicon) and coverslipped in aqueous medium, and TH$^+$ cells counted from a total of 15–20 sections in each field per brain (i.e., every second section) at a magnification of 100× using the optical fractionator approach.

### Striatal Dopamine/DOPAC and MPP$^+$ Levels

Animals were injected with either 15 mg/kg body weight MPTP or saline every 2 hr for 4 doses. Dopamine, DOPAC, and HVA or MPP$^+$ from dissected striata were analyzed by HPLC using a 5 μm C-18 reverse phase column and precolumn (Brownlee Labs) followed by electrochemical detection with a glassy carbon electrode (Klivenyi et al., 2000).

### SN Iron Levels by Mass Spectrometry

SN was dissected and snap frozen in liquid nitrogen and the wet weight was determined; then, it was lyophilized and the dry weight/tissue was measured. Preweighed lypholized samples were next taken up in 0.1 ml of concentrated nitric acid (Aristar, BDH) and allowed to digest overnight. The samples were then heated to 80°C for 15 min and cooled, and 0.1 ml 30% hydrogen peroxide added. Samples were heated to 70°C for 15 min, cooled, and diluted 1/40 into 1% $HN0_3$ for analysis by inductively coupled plasma mass spectrometry (ICP-MS) using an Ultramass 700 (Varian) in peak-hopping mode with 0.100 AMU spacing, 1 point per peak, 50 scans per replicate, 3 replicates per sample. Preparation blanks processed in a similar manner were used as controls. Plasma flow was 15 l/min with auxiliary flow of 1.5 l/min, RF power was 1.2 kW, and sample was introduced at a flow rate of 0.88 l/min.

### Rotorod Performance

Motor activity was measured via rotorod performance utilizing an Accelerated Rota-Rod for mice 7650 (UGO Basil, Italy) with a rod diameter of 3 cm according to the manufacturer's instructions. The mice were allowed to acclimatize for 20 s at the lowest speed, i.e., 4 rpm, and then the rotor was allowed to accelerate to 40 rpm during a period of 5 min. Fall of the animal from the rod was taken as the end point of run. Each animal was tested three times on each test day with an hour of rest between consecutive runs. Animals were tested 1, 2, 3, 4, and 7 days post final MPTP treatment.

**Acknowledgments**

This work was funded by NIH R01 grants AG12141 and AG41264 (J.K.A.), the NHMRC (A.I.B. and R.A.C.), the NIA (grant 2RO1AG12686 to A.I.B.), and Prana Biotechnology Ltd (R.A.C.). R.A.C. is a consultant to Prana Biotechnology, and A.I.B. and R.A.C. are minor shareholders in Prana Biotechnology.

Received: November 27, 2001
Revised: February 12, 2003

**References**

Adams, J.D., Jr., and Odunze, I.N. (1991). Oxygen free radicals and Parkinson's disease. Free Radic. Biol. Med. *10*, 161–169.

Agrawal, R., Sharma, P.K., and Rao, G.S. (2001). Release of iron from ferritin by metabolites of benzene and superoxide radical generating agents. Toxicology *168*, 223–230.

Ali, S.F., LeBel, C.P., and Bondy, S.C. (1992). Reactive oxygen species formation as a biomarker of methylmercury and trimethyltin neurotoxicity. Neurotoxicology *13*, 637–648.

Andersen, J.K. (2001). Do alterations in glutathione and iron levels contribute to pathology associated with Parkinson's disease? In Ageing Vulnerability: Causes and Interventions, Novartis Foundation Symposium, Volume 235 (New York: John Wiley and Sons, Inc.), pp. 11–25.

Andersen, J.K., Frim, D.M., Isacson, O., Beal, M.F., and Breakefield, X.O. (1994). Elevation of neuronal MAO-B activity in a transgenic mouse model does not increase sensitivity to the neurotoxin 1-methyl-4-phenyl-1,2,3,6-tetrahydropyridine (MPTP). Brain Res. *656*, 108–114.

Banerjee, S.A., Hoppe, P., Brilliant, M., and Chikaraishi, D.M. (1992). 5′ flanking sequences of the rat tyrosine hydroxylase gene target accurate tissue-specific, developmental, and transsynaptic expression in transgenic mice. J. Neurosci. *12*, 4460–4467.

Bartzokis, G., Beckson, M., Hance, D.B., Marx, P., Foster, J.A., and Marder, S.R. (1997). MR evaluation of age-related increase of brain iron in young adult and older normal males. Magn. Reson. Imaging *15*, 29–35.

Baumgartner, G., Gawel, M.J., Kaeser, H.E., Pallis, C.A., Rose, F.C., Schaumburg, H.H., Thomas, P.K., and Wadia, N.H. (1979). Neurotoxicity of halogenated hydroxyquinolines: clinical analysis of cases reported outside Japan. J. Neurol. Neurosurg. Psychiatry *42*, 1073–1083.

Beal, F. (1992). Does impairment of energy metabolism result in excitotoxic neuronal death in neurodegenerative illnesses? Ann. Neurol. *31*, 119–130.

Beal, M.F. (2001). Experimental models of Parkinson's disease. Nat. Rev. Neurosci. *2*, 325–334.

Beard, J.L., Connor, J.D., and Jones, B.C. (1993). Brain iron: location and function. Prog. Food Nutr. Sci. *17*, 183–221.

Benkovic, S.A., and Connor, J.R. (1993). Ferritin, transferrin, and iron in selected regions of the adult and aged rat brain. J. Comp. Neurol. *338*, 97–113.

Berg, D., Gerlach, M., Youdim, M.B., Double, K.L., Zecca, L., Riederer, P., and Becker, G. (2001). Brain iron pathways and their relevance to Parkinson's disease. J. Neurochem. *79*, 225–236.

Betarbet, R., Sherer, T.B., and Greenamyre, J.T. (2002). Animal models of Parkinson's disease. Bioessays *24*, 308–318.

Bush, A.I. (2000). Metals and neuroscience. Curr. Opin. Chem. Biol. *4*, 184–191.

Cassarino, D.S., Parks, J.K., Parker, W.D., Jr., and Bennett, J.P., Jr. (1999). The parkinsonian neurotoxin MPP+ opens the mitochondrial permeability transition pore and releases cytochrome c in isolated mitochondria via an oxidative mechanism. Biochim. Biophys. Acta *1453*, 49–62.

Castellani, R.J., Siedlak, S.L., Perry, G., and Smith, M.A. (2000). Sequestration of iron by Lewy bodies in Parkinson's disease. Acta Neuropathol. (Berl.) *100*, 111–114.

Caughman, S.W., Hentze, M.W., Rouault, T.A., Hartford, J.B., and Klausner, R.D. (1988). The iron-responsive element is the single element responsible for iron-dependent translational regulation of ferritin biosynthesis. Evidence for function as the binding site for a translational repressor. J. Biol. Chem. *263*, 19048–19052.

Cheepsunthorn, P., Palmer, C., and Connor, J.R. (1998). Cellular distribution of ferritin subunits in postnatal rat brain. J. Comp. Neurol. *400*, 73–86.

Cherny, R.A., Atwood, C.S., Xilinas, M.E., Gray, D.N., Jones, W.D., McLean, C.A., Barnham, K.J., Volitakis, I., Fraser, F.W., Kim, Y., et al. (2001). Treatment with a copper-zinc chelator markedly and rapidly inhibits beta-amyloid accumulation in Alzheimer's disease transgenic mice. Neuron *30*, 665–676.

Chiueh, C.C., and Rauhala, P. (1998). Free radicals and MPTP-induced selective destruction of substantia nigra compacta neurons. Adv. Pharmacol. *42*, 796–800.

Christen, Y. (2000). Oxidative stress and Alzheimer disease. Am. J. Clin. Nutr. *71*, 621S–629S.

Clifford Rose, F., and Gawel, M. (1984). Clioquinol neurotoxicity: an overview. Acta Neurol. Scand. Suppl. *100*, 137–145.

Connor, J.R., Snyder, B.S., Beard, J.L., Fine, R.E., and Mufson, E.J. (1992). Regional distribution of iron and iron-regulatory proteins in the brain in aging and Alzheimer's disease. J. Neurosci. Res. *31*, 327–335.

Connor, J.R., Boeshore, K.L., Benkovic, S.A., and Menzies, S.L. (1994). Isoforms of ferritin have a specific cellular distribution in the brain. J. Neurosci. Res. *37*, 461–465.

Connor, J.R., Snyder, B.S., Arosio, P., Loeffler, D.A., and LeWitt, P. (1995). A quantitative analysis of isoferritins in select regions of aged, Parkinsonian, and Alzheimer's diseased brains. J. Neurochem. *65*, 717–724.

Connor, J.R., Menzies, S.L., Burdo, J.R., and Boyer, P.J. (2001). Iron and iron management proteins in neurobiology. Pediatr. Neurol. *25*, 118–129.

Cozzi, A., Corsi, B., Levi, S., Santambrogio, P., Albertini, A., and Arosio, P. (2000). Overexpression of wild type and mutated human ferritin H-chain in HeLa cells: in vivo role of ferritin ferroxidase activity. J. Biol. Chem. *275*, 25122–25129.

Curtis, A.R., Fey, C., Morris, C.M., Bindoff, L.A., Ince, P.G., Chinnery, P.F., Coulthard, A., Jackson, M.J., Jackson, A.P., McHale, D.P., et al. (2001). Mutation in the gene encoding ferritin light polypeptide causes dominant adult-onset basal ganglia disease. Nat. Genet. *28*, 350–354.

Desole, M.S., Esposito, G., Fresu, L., Migheli, R., Enrico, P., Miele, M., De Natale, G., and Miele, E. (1993). Correlation between 1-methyl-4-phenylpyridinium ion ($MPP^+$) levels, ascorbic acid oxidation and glutathione levels in the striatal synaptosomes of the 1-methyl-4-phenyl-1,2,3,6-tetrahydropyridine (MPTP)-treated rat. Neurosci. Lett. *161*, 121–123.

Dexter, D.T., Wells, F.R., Agid, F., Agid, Y., Lees, A.J., Jenner, P., and Marsden, C.D. (1987). Increased nigral iron content in postmortem parkinsonian brain. Lancet *21*, 1219–1220.

Dexter, D.T., Wells, F.R., Lees, A.J., Agid, F., Agid, Y., Jenner, P., and Marsden, C.D. (1989). Increased nigral iron content and alterations in other metal ions occurring in brain in Parkinson's disease. J. Neurochem. *52*, 1830–1836.

Dexter, D.T., Carayon, A., Javoy-Agid, F., Agid, Y., Wells, F.R., Daniel, S.E., Lees, A.J., Jenner, P., and Marsden, C.D. (1991). Alterations in the levels of iron, ferritin and other trace metals in Parkinson's disease and other neurodegenerative diseases affecting the basal ganglia. Brain *114*, 1953–1975.

Double, K.L., Maywald, M., Schmittel, M., Reiderer, P., and Gerlach, M. (1998). In vitro studies of ferritin iron release and neurotoxicity. J. Neurochem. *70*, 2492–2499.

Du, Y., Ma, Z., Lin, S., Dodel, R.C., Gao, F., Bales, K.R., Triarhou, L.C., Chernet, E., Perry, K.W., Nelson, D.L., et al. (2001). Minocycline prevents nigrostriatal dopaminergic neurodegeneration in the MPTP model of Parkinson's disease. Proc. Natl. Acad. Sci. USA *98*, 14669–14674.

Gassen, M., and Youdim, M.B.H. (1997). The potential role of iron chelators in the treatment of Parkinson's disease and related neurological disorders. Pharmacol. Toxicol. *80*, 159–166.

Gerlach, M., Ben-Shachar, D., Riederer, P., and Youdim, M.B. (1994). Altered brain metabolism of iron as a cause of neurodegenerative diseases? J. Neurochem. *63*, 793–807.

Gillissen, E.P., Ghosh, P., Jacobs, R.E., and Allman, J.M. (1998). Topographical localization of iron in brains of the aged fat-tailed dwarf lemur (*Cheirogaleus medius*) and gray lesser mouse lemur (*Microcebus murinus*). Am. J. Primatol. *45*, 291–299.

Gitlin, J.D. (1998). Aceruloplasminemia. Pediatr. Res. *44*, 271–276.

Glinka, Y., Gassen, M., and Youdim, M.B.H. (1996). The role of iron in Parkinson's disease. In Metals and Oxidative Damage in Neurological Disorders, J.R. Connor, ed. (Boston, MA: Plenium Publishing Corp.), pp. 1–12.

Griffith, O. (1980). Determination of glutathione and glutathione disulfide using glutathione reductase and 2-vinylpyridine. Anal. Biochem. *106*, 207–212.

Griffiths, P.D., Dobson, B.R., Jones, G.R., and Clarke, D.T. (1999). Iron in the basal ganglia in Parkinson's disease. An in vitro study using extended X-ray absorption fine structure and cryo-electron microscopy. Brain *122*, 667–673.

Gutteridge, J.M.C. (1992). Iron and oxygen radicals in brain. Ann. Neurol. *32*, S16–S21.

Han, J., Day, J.R., Thomson, K., Connor, J.R., and Beard, J.L. (2000). Iron deficiency alters H- and L-ferritin expression in rat brain. Cell Mol. Biol. *46*, 517–528.

Harrison, P.M., and Arosio, P. (1996). The ferritins: molecular properties, iron storage function and cellular regulation. Biochim. Biophys. Acta *1275*, 161–203.

Hentze, M.W., Keim, S., Papadopoulos, P., O'Brien, S., Modi, W., Drysdale, J., Leonard, W.J., Harford, J.B., and Klausner, R.D. (1986). Cloning, characterization, expression, and chromosomal localization of a human ferritin heavy-chain gene. Proc. Natl. Acad. Sci. USA *83*, 7226–7230.

Hill, J.M., and Switzer, R.C. (1984). The regional distribution and cellular localization of iron in the rat brain. Neuroscience *11*, 595–603.

Huang, X., Cuajungco, M.P., Atwood, C.S., Hartshorn, M.A., Tyndall, J.D., Hanson, G.R., Stokes, K.C., Leopold, M., Multhaup, G., Goldstein, L.E., et al. (1999). Cu(II) potentiation of Alzheimer α-beta neurotoxicity. Correlation with cell-free hydrogen peroxide production and metal reduction. J. Biol. Chem. *274*, 37111–37116.

Hung, H.-C., and Lee, E.H. (1998). MPTP produces differential oxidative stress and antioxidative responses in the nigrostriatal and mesolimbic dopaminergic pathways. Free Radic. Biol. Med *24*, 76–84.

Janetzky, B., Reichmann, H., Youdim, M.B., and Reiderer, P. (1997). Iron and oxidative damage in neurodegenerative disease. In Mitochondria and Free Radicals in Neurodegenerative Diseases, F. Beal, N. Howell, and I. Bodis-Wollner, eds. (New York: Wiley-Liss Inc), pp. 407–421.

Jellinger, K. (1999). The role of iron in neurodegeneration: prospects for pharmacotherapy of Parkinson's disease. Drugs Aging *14*, 115–140.

Jellinger, K., Paulus, W., Grundke-Iqbal, I., Riederer, P., and Youdim, M.B. (1990). Brain iron and ferritin in Parkinson's and Alzheimer's diseases. J. Neural Transm. Park. Dis. Dement. Sect. *2*, 327–340.

Jenner, P., Schapira, A.H., and Marsden, C.D. (1992). New insights into the cause of Parkinson's disease. Neurology *42*, 2241–2250.

Kato, J., Fujikawa, K., Kanda, M., Fukuda, N., Sasaki, K., Takayama, T., Kobune, M., Takada, K., Takimoto, R., Hamada, H., et al. (2001). A mutation in the iron-responsive element of H-ferritin mRNA causing autosomal dominant iron overload. Am. J. Hum. Genet. *69*, 191–197.

Kidani, Y., Naga, S., and Koike, H. (1974). Mass spectrometry of 5-chloro-7-iodo-8-quinol metal chelates. Jap. Analyst *23*, 1375–1378.

Klivenyi, P., Andreassen, O.A., Ferrante, R.J., Dedeoglu, A., Mueller, G., Lancelot, E., Bogdanov, M., Andersen, J.K., Jiang, D., and Beal, M.F. (2000). Mice deficient in cellular glutathione peroxidase show increased vulnerability to malonate, 3-nitropropionic acid, and 1-methyl-4-phenyl-1,2,5,6-tetrahydropyridine. J. Neurosci. *20*, 1–7.

Lan, J., and Jiang, D.H. (1997). Excessive iron accumulation in the brain: a possible potential risk of neurodegeneration and Parkinson's disease. J. Neural Transm. *104*, 649–660.

Mann, V.M., Cooper, J.M., Danie, S.E., Srai, K., Jenner, P., Marsden, C.D., and Schapira, A.H. (1994). Complex I, iron, and ferritin in Parkinson's disease substantia nigra. Ann. Neurol. *36*, 876–881.

Marciani, M.G., Cianciulli, P., Stefani, N., Stefanini, F., Peroni, L., Sabbadini, M., Maschio, M., Trua, G., and Papa, G. (1991). Toxic effects of high-dose deferoxamine treatment in patients with iron overload: an electrophysiological study of cerebral and visual function. Haematologica *76*, 131–134.

Masters, C. (2002). Alzheimer's disease: modulation of the APP/beta-amyloid pathways toward rational therapeutic intervention. 8th International Conference on Alzheimer's Disease and Related Disorders, Stockholm, Sweden, July 20–25, 2002.

Meade, T.W. (1975). Subacute myelo-optic neuropathy and clioquinol. An epidemiological case-history for diagnosis. Br. J. Prev. Soc. Med. *29*, 157–169.

Melov, S. (2002). And C is for clioquinol—the AβCs of Alzheimer's disease. Trends Neurosci. *25*, 121–123.

Moos, T., Trinder, D., and Morgan, E.H. (2000). Cellular distribution of ferric iron, ferritin, transferrin and divalent metal transporter 1 (DMT1) in substantia nigra and basal ganglia of normal and beta 2-microglobulin deficient mouse brain. Cell Mol. Biol. *46*, 549–561.

Morgan, T.E., Xie, Z., Goldsmith, S., Yoshida, T., Lanzrein, A.S., Stone, D., Rozovsky, I., Perry, G., Smith, M.A., and Finch, C.E. (1999). The mosaic of brain glial hyperactivity during normal ageing and its attenuation by food restriction. Neuroscience *89*, 687–699.

Nakae, K., Yamamoto, S., Shigematsu, I., and Kono, R. (1973). Relation between subacute myelo-optic neuropathy (S.M.O.N.) and clioquinol: nationwide survey. Lancet *1*, 171–173.

Nicholson, D.W., Ali, A., Thornberry, N.A., Vaillancourt, J.P., Ding, C.K., Gallant, M., Gareau, Y., Griffin, P.R., Labelle, M., Lazebnik, Y.A., et al. (1995). Identification and inhibition of the ICE/CED-3 protease necessary for mammalian apoptosis. Nature *376*, 37–43.

Orino, K., Lehman, L., Tsuji, Y., Ayaki, H., Torti, S.V., and Torti, F.M. (2001). Ferritin and the response to oxidative stress. Biochem. J. *357*, 241–247.

Perry, T.L., Godin, D.V., and Hansen, S. (1982). Parkinson's disease: a disorder due to nigral glutathione deficiency? Neurosci. Lett. *33*, 305–310.

Porter, J.B., and Huehns, E.R. (1989). The toxic effects of desferrioxamine. Baillieres Clin. Haematol. *2*, 459–474.

Reiderer, P., Sofic, E., Rausch, W.D., Schmidt, B., Reynolds, G., Jellinger, K., and Youdim, M.B. (1989). Transition metals, ferritin, glutathione, and ascorbic acid in parkinsonian brains. J. Neurochem. *52*, 515–520.

Rucker, P., Torti, F.M., and Torti, S. (1996). Role of H and L subunits in mouse ferritin J. Biol. Chem. *52*, 33352–33357.

Sedelis, M., Schwarting, R.K., and Huston, J.P. (2001). Behavioral phenotyping of the MPTP mouse model of Parkinson's disease. Behav. Brain Res. *125*, 109–125.

Sian, J., Dexter, D.T., Lees, A., Daniel, S., Agid, Y., Javoy-Agid, F., Jenner, P., and Marsden, C.D. (1994). Alterations in glutathione levels in Parkinson's disease and other neurodegenerative disorders affecting basal ganglia. Ann. Neurol. *36*, 348–355.

Smith, M.A., Harris, P.L.R., Sayre, L.M., and Perry, G. (1997). Iron accumulation in Alzheimer disease is a source of redox-generated free radicals. Proc. Natl. Acad. Sci. USA *94*, 9866–9868.

Sofic, E., Riederer, P., Heinsen, H., Beckmann, H., Reynolds, G.P., Hebenstreit, G., and Youdim, M.B. (1988). Increased iron (III) and total iron content in post mortem substantia nigra of parkinsonian brain. J. Neural Transm. *74*, 199–205.

Sofic, E., Paulus, W., Jellinger, K., Riederer, P., and Youdim, M.B. (1991). Selective increase of iron in substantia nigra zona compacta of parkinsonian brains. J. Neurochem. *56*, 978–982.

Tateishi, J. (2000). Subacute myelo-optico-neuropathy: clioquinol

intoxication in humans and animals. Neuropathology. Suppl. *20*, S20–S24.

Tetrud, J.W., and Langston, J.W. (1989). MPTP-induced parkinsonism as a model for Parkinson's disease. Acta. Neuro. Scand. Suppl *126*, 35–40.

Thompson, K.J., Shoham, S., and Connor, J.R. (2001). Iron and neurodegenerative disorders. Brain Res. Bull. *55*, 155–164.

Tsubaki, T., Honma, Y., and Hoshi, M. (1971). Neurological syndrome associated with clioquinol. Lancet *1*, 696–697.

Vila, M., Jackson-Lewis, V., Vukosavic, S., Djaldetti, R., Liberatore, G., Offen, D., Korsmeyer, S.J., and Przedborski, S. (2001). Bax ablation prevents dopaminergic neurodegeneration in the 1-methyl-4-phenyl-1,2,3,6-tetrahydropyridine mouse model of Parkinson's disease. Proc. Natl. Acad. Sci. USA *98*, 2837–2842.

West, M.J. (1993). Regionally specific loss of neurons in the aging human hippocampus. Neurobiol. Aging *14*, 275–285.

Yantiri, F., and Andersen, J.K. (1999). The role of iron in Parkinson disease and 1-methyl-4-phenyl-1,2,3,6-tetrahydropyridine toxicity. IUBMB Life *48*, 1–3.

Yassin, M.S., Ekblom, J., Xilinas, M., Gottfries, C.G., and Oreland, L. (2000). Changes in uptake of vitamin B(12) and trace metals in brains of mice treated with clioquinol. J. Neurol. Sci. *173*, 40–44.

Yong, V.W., Perry, T.L., and Krisman, A.A. (1986). Idiopathic Parkinson's disease, progressive supranuclear palsy and glutathione metabolism in the substantia nigra of patients. Neurosci. Lett. *63*, 56–60.

Yoshida, S., Ektessabi, A., and Fujisawa, S. (2001). XANES spectroscopy of a single neuron from a patient with Parkinson's disease. J. Synchrotron Radiat. *8*, 998–1000.

Yoshimura, S., Imai, K., Saitoh, Y., Yamaguchi, H., and Ohtaki, S. (1992). The same chemicals induce different neurotoxicity when administered in high doses for short term or low doses for long term to rats and dogs. Mol. Chem. Neuropathol. *16*, 59–84.

Youdim, M.B., Ben-Shacher, D., and Reiderer, P. (1993). The possible role of iron in the etiopathology of Parkinson's disease. Mov. Disord. *8*, 1–12.

Zecca, L., Gallorini, M., Schunemann, V., Trautwein, A.X., Gerlach, M., Riederer, P., Vezzoni, P., and Tampellini, D. (2001). Iron, neuromelanin and ferritin content in the substantia nigra of normal subjects at different ages: consequences for iron storage and neurodegenerative processes. J. Neurochem. *76*, 1766–1773.

ELSEVIER

Neurobiology of Disease

www.elsevier.com/locate/ynbdi
Neurobiology of Disease 15 (2004) 610–617

# Neuroprotective mechanisms of creatine occur in the absence of mitochondrial creatine kinase

Peter Klivenyi,[a] Noel Y. Calingasan,[a] Anatoly Starkov,[a] Irina G. Stavrovskaya,[b] Bruce S. Kristal,[a,b,c] Lichuan Yang,[a] Bé Wieringa,[d] and M. Flint Beal[a,*]

[a] *Department of Neurology and Neuroscience, New York-Presbyterian Hospital, Weill Medical College of Cornell University, New York, NY 10021, USA*
[b] *Dementia Research Service, Burke Medical Research Institute, White Plains, NY 10605, USA*
[c] *Department of Biochemistry, Weill Medical College of Cornell University, New York, NY 10021, USA*
[d] *Department of Cell Biology, University Medical Center St. Radboud, NCMLS, University of Nijmegen, Geert Grooteplein 28, 6525 GA, The Netherlands*

Received 27 May 2003; revised 19 December 2003; accepted 23 December 2003

**There is substantial evidence that creatine administration exerts neuroprotective effects both in vitro and in vivo. The precise mechanisms for these neuroprotective effects however are as yet unclear. We investigated whether creatine administration could exert neuroprotective effects in mice deficient in ubiquitous mitochondrial creatine kinase (UbMi-CK). UbMi-CK-deficient mice showed increased sensitivity to 1-methyl-1, 2, 3, 6-tetrahydropyridine (MPTP)-induced dopamine depletion and loss of tyrosine hydroxylase (TH) stained neurons. Isolated mitochondria from these mice showed no alterations in calcium retention, oxygen utilization, membrane potential, or swelling in response to a calcium challenge. Creatine administration significantly increased brain concentrations of both creatine and PCr in the UbMi-CK knockout mice. Creatine administration to the UbMi-CK-deficient mice exerted significant neuroprotective effects against MPTP toxicity that were comparable in magnitude to those seen in wild-type mice. These results suggest that the neuroprotective effects of creatine are not mediated by an effect on UbMi-CK to inhibit the mitochondrial permeability transition, and are more likely to be mediated by maintenance of appropriate ATP/ADP and PCr/Cr levels.**


*Keywords:* Creatine; Creatine kinase; MPTP; Phosphocreatine; Mitochondria

Several isoforms of creatine kinase are compartmentalized within cells to form a buffering system for cellular energy stores, which is thought to be important in tissues with high and fluctuating energy requirements such as brain and muscle. The creatine kinase system can shuttle high-energy phosphates (PCr) to sites of energy usage in the cell, such as ion pumps in organelles in the plasma membranes or dynamic cytoskeletal structures and molecular motors. Creatine may therefore exert neuroprotective effects by increasing PCr levels, and thereby providing extra energy for ion homeostasis and the functional and structural integrity of mitochondria. We and others showed that PCr levels are increased by creatine supplementation both in vitro and in vivo (Brewer and Wallimann, 2000; Ferrante et al., 2000; Holtzman et al., 1998; Matthews et al., 1998). Other neuroprotective effects of creatine may be due to increased glutamate reuptake (Xu et al., 1996), and scavenging of free radicals (Lawler et al., 2002).

Creatine exerts neuroprotective effects in vitro as well as in vivo. Creatine protects against both glutamate and β-amyloid toxicity in rat hippocampal neurons (Brewer and Wallimann, 2000). Creatine also protects against 3-nitropropionic and glutamate neurotoxicity in rat hippocampal and striatal neurons (Brustovetsky et al., 2001). We initially showed that creatine protects against both malonate and 3-nitropropionic acid (3-NP) striatal neurotoxicity in vivo (Matthews et al., 1998). We also found dose-dependent protection against MPTP toxicity (Matthews et al., 1999). Others found protection against traumatic brain injury (Sullivan et al., 2000). More recently, we found that creatine exerts neuroprotective effects in transgenic mouse models of both ALS and Huntington's disease (Andreassen et al., 2001; Ferrante et al., 2000; Klivenyi et al., 1999). Creatine also is protective in the wobbler mouse model of motor neuron disease (Ikeda et al., 2000). Phosphocreatine promotes recovery of ischemic heart tissue in vitro (Sharov et al., 1987), and improves survival of cultured myotubes deficient in dystrophin (Pulido et al., 1998).

A proposed mechanism of neuroprotection is inhibition of activation of the mitochondrial permeability transition pore (mPTP) that is linked to both necrotic and apoptotic cell death (Bernardi et al., 1998). Creatine can stabilize mitochondrial isoform of creatine kinase (Mi-CK) in an octomer that can inhibit activation of the mPTP (O'Gorman et al., 1997). Whether this is an important component of the neuroprotective effects of creatine in vivo however remains controversial (Brustovetsky et al., 2001; Sullivan et al., 2000). To resolve whether inhibition of mPTP plays a role in the neuroprotective effects of creatine, we examined the effects of creatine in ubiquitous mitochondrial creatine kinase (UbMi-CK)-deficient mice. Mice deficient in UbMi-CK are viable

* Corresponding author. Neurology Department, New York Hospital-Cornell Medical Center, 525 East 68th Street, A5, New York, NY 10021. Fax: +1-212-746-8532.
*E-mail address:* fbeal@med.cornell.edu (M.F. Beal).
**Available online on ScienceDirect (www.sciencedirect.com.)**

0969-9961/$ - see front matter © 2004 Published by Elsevier Inc.
doi:10.1016/j.nbd.2003.12.014

and fertile, and show no physical or behavioral deficits (Steeghs et al., 1995). If an interaction of creatine with Mi-CK to stabilize the MPTP plays an important role in the neuroprotective effects of creatine, then creatine feeding should not exert protective effects in UbMi-CK-deficient mice. In the present experiments, we therefore examined whether creatine protects against MPTP neurotoxicity in UbMi-CK-deficient mice.

## Materials and methods

### *Experimental animals*

Our experiments were conducted in accordance with the National Institutes of Health guidelines for the care and use of experimental animals. UbMi-CK knockout mice were generated as described (Steeghs et al., 1995). Briefly, a 7 kbp SstI DNA fragment was isolated from a genomic lambda FIX™ II phage library of mouse F1 hybrid [CBAxC57Bl/6] spleen DNA. The complete 4.8 kbp murine UbCKmit gene is encompassed within this genomic region. Starting from this subclone, a replacement-type vector for homologous recombination was constructed. From this DNA, the 0.6 kbp *Bam*HI–*Bgl*II fragment was deleted and replaced by a 1.1 kbp neomycin resistance ($neo^r$) cassette. This vector was introduced into the wild-type E14 ES cells by electroporation. E14 clones that were positive for homologous recombination were injected into recipient C57Bl/6 blastocysts and transferred into the uterus of pseudopregnant (C57Bl/6xCBA)F1 females. Resulting chimeric males were mated with C57Bl/6 females for 12 generations. Mice heterozygous for mutant UbMi-CK allele were intercrossed and null mutants were obtained. The mice were bred locally.

### *Chemicals*

All chemicals were purchased from Sigma (St. Louis, MO) unless otherwise indicated.

### *Isolated mitochondria measurements*

Nonsynaptic mouse forebrain mitochondria were isolated by the Percoll gradient separation method as described (Sims, 1990). For each experiment, brains of two mice of each type were pooled. The isolation procedure was performed simultaneously and strictly in parallel with both wild-type and UbMi-CK-deficient mouse forebrain tissue. Animals of approximately 12 months of age were used. Membrane potential of isolated mitochondria was estimated using the fluorescence of safranine O (2.5 μM) with excitation and emission wavelengths of 495 and 586 nm, respectively (Starkov et al., 2002). Changes in the extramitochondrial medium-free $Ca^{2+}$ were followed using the fluorescence of Calcium Green 5N ("Molecular Probes", USA) with excitation and emission wavelengths of 506 and 532 nm, respectively. Mitochondrial swelling was estimated by a conventional method, from changes in light scattering of mitochondrial suspension using a fluorimeter set at 660 nm excitation and emission wavelengths with 10:5 nm excitation/emission slits and an 8% transmittance filter set over the photomultiplier window. For all fluorescence measurements, a Hitachi F4500 fluorescent spectrometer equipped with a water-thermostated cuvette holder and a stirrer was utilized.

### *Dopamine measurement*

Control and UbMi-CK knockout mice were fed lab chow diets supplemented with 2% creatine, or a standard unsupplemented diet for 2 weeks before MPTP administration. MPTP (20 mg/kg, 5 ml/kg, i.p.) was administered four times at 2-h intervals to control, heterozygous, and homozygous knockout mice ($n = 12$/group). The animals were killed at 1 week, and both striata were rapidly dissected on a chilled glass plate and frozen at −70°C. The samples were subsequently thawed in 0.4 ml of chilled 0.1 M perchloric acid and sonicated. Aliquots were taken for protein quantification using a spectrophotometric assay. Other aliquots were centrifuged, and dopamine, 3,4-dihydroxyphenylacetic acid (DOPAC), and homovanillic acid (HVA) were measured in supernatants by HPLC with electrochemical detection. Concentrations of dopamine and metabolites were expressed as ng/mg protein (mean ± SEM).

### *$MPP^+$ levels*

To determine whether MPTP uptake or metabolism was altered, MPTP 20 mg/kg was administered intraperitoneally four times, 2 h apart, and mice were killed 90 min after the last injection ($n = 6$/group). $MPP^+$ levels were quantified by HPLC with UV detection at 295 nm. Samples were sonicated in 0.1 M perchloric acid, and an aliquot of supernatant was injected onto a Brownlee aquapore X03-224 cation exchange column (Rainin, Woburn, MA). Samples were eluted isocratically with 90% 0.1 M acetic acid and 75 mM triethylamine HCl, pH 2.3, adjusted with formic acid and 10% acetonitrile.

### *Measurements of creatine, phosphocreatine, and ATP*

Wild-type and homozygous Mi-CK knockout mice (10 mice per group) fed 2% creatine for 2 weeks were killed by the freeze-clamp procedure for measurements of creatine, phosphocreatine, ADP, and ATP in cerebral cortex as previously described (Matthews et al., 1998).

### *Histological analysis*

Control and homozygous UbMi-CK knockout mice were fed lab chow diets supplemented with 2% creatine, or a standard unsupplemented diet for 2 weeks before MPTP administration. MPTP (20 mg/kg, 5 ml/kg, i.p.) was administered three times at 2-h intervals to control, heterozygous, and homozygous knockout mice ($n = 6$/group). After 1 week, the mice were deeply anesthetized with pentobarbital and perfused with ice-cold 0.9% saline followed by 4% paraformaldehyde in 0.1 M sodium phosphate-buffered saline, pH 7.4. Brains were removed, postfixed for 2 h in the same fixative, and then placed in 30% sucrose overnight at 4°C. Serial coronal sections (50 μm) were cut through the substantia nigra. Two sets consisting of eight sections each, 100 μm apart, were prepared. One set of sections was used for Nissl staining (cresyl violet). Another set was processed for tyrosine hydroxylase (TH) immunohistochemistry using avidin–biotin peroxidase technique. Briefly, free-floating sections were pretreated with 3% $H_2O_2$ in PBS for 30 min. The sections were incubated sequentially in (a) 1% bovine serum albumin (BSA)/0.2% Triton X-100 for 30 min, (b) rabbit anti-TH affinity purified antibody (Chemicon, Temecula, CA; 1:2000 in PBS/0.5% BSA) for 18 h, (c)

Table 1
Number of neurons in the substantia nigra pars compacta in mitochondrial creatine kinase knockout and control mice with or without MPTP treatment

| Experimental group | Tyrosine hydroxylase | Nissl |
|---|---|---|
| Control/normal diet/PBS | 9151 ± 460 | 10629 ± 396 |
| Control/normal diet/MPTP | 6326 ± 540** | 6903 ± 265*** |
| Control/creatine/MPTP | 8085 ± 424# | 9639 ± 547### |
| Knockout/normal diet/PBS | 9305 ± 761 | 10848 ± 606 |
| Knockout/normal diet/MPTP | 6285 ± 134xx | 6778 ± 269xxx |
| Knockout/creatine/MPTP | 8052 ± 485+ | 9512 ± 460++ |

Creatine attenuates MPTP-induced neurodegeneration in the SNpc of wild-type controls and Mi-CK knockout mice. Neuronal counts (means ± SEM) were made using the optical fractionator method.
** $P < 0.01$, vs. control/normal diet/PBS.
*** $P < 0.001$, vs. control/normal diet/PBS.
# $P < 0.05$, vs. control/normal diet/MPTP.
### $P < 0.001$, vs. control/normal diet/MPTP.
xx $P < 0.01$, vs. knockout/normal diet/PBS.
xxx $P < 0.001$, vs. knockout/normal diet/PBS.
+ $P < 0.05$, vs. knockout/normal diet/MPTP.
++ $P < 0.01$, vs. knockout/normal diet/MPTP.

biotinylated anti-rabbit IgG (Vector Laboratories, Burlingame, CA; 1:500 in PBS/0.5% BSA) for 1 h, and (d) avidin–biotin–peroxidase complex (Vector; 1:500 in PBS) for 1 h. The immunoreaction was visualized using 3,3-diaminobenzidine tetrahydrochloride dihydrate (DAB) with nickel intensification (Vector) as the chromogen. All incubations and rinses were performed with agitation using an orbital shaker at room temperature. The sections were mounted onto gelatin-coated slides, dehydrated, cleared in xylene, and coverslipped. The numbers of Nissl-stained or TH-immunoreactive cells in the substantia nigra pars compacta (SNpc) were counted using the optical fractionator method in the Stereo Investigator (v. 4.35) software program (Microbrightfield, Burlington, VT).

*Statistical analysis*

Results are expressed as the mean ± SEM. Statistical comparisons were made using one-way ANOVA followed by Newman–Keuls post hoc tests, or two-way ANOVA for the data in Table 1.

## Results

Brain mitochondria isolated from either wild-type or UbMi-CK-deficient mice were incubated in high ionic strength cytosol-mimicking medium and challenged with repeated pulses of 100 μM $Ca^{2+}$, and their responses were compared by several parameters relevant to $Ca^{2+}$-induced damage and the mPTP. Fig. 1A demonstrates that both types of mitochondria possess virtually identical membrane potential. After addition of ADP, the membrane potential transiently decreases in both types of mitochondria indicating the onset of oxidative phosphorylation (state 3). As shown in Fig. 1A, both the amplitude and the duration of the

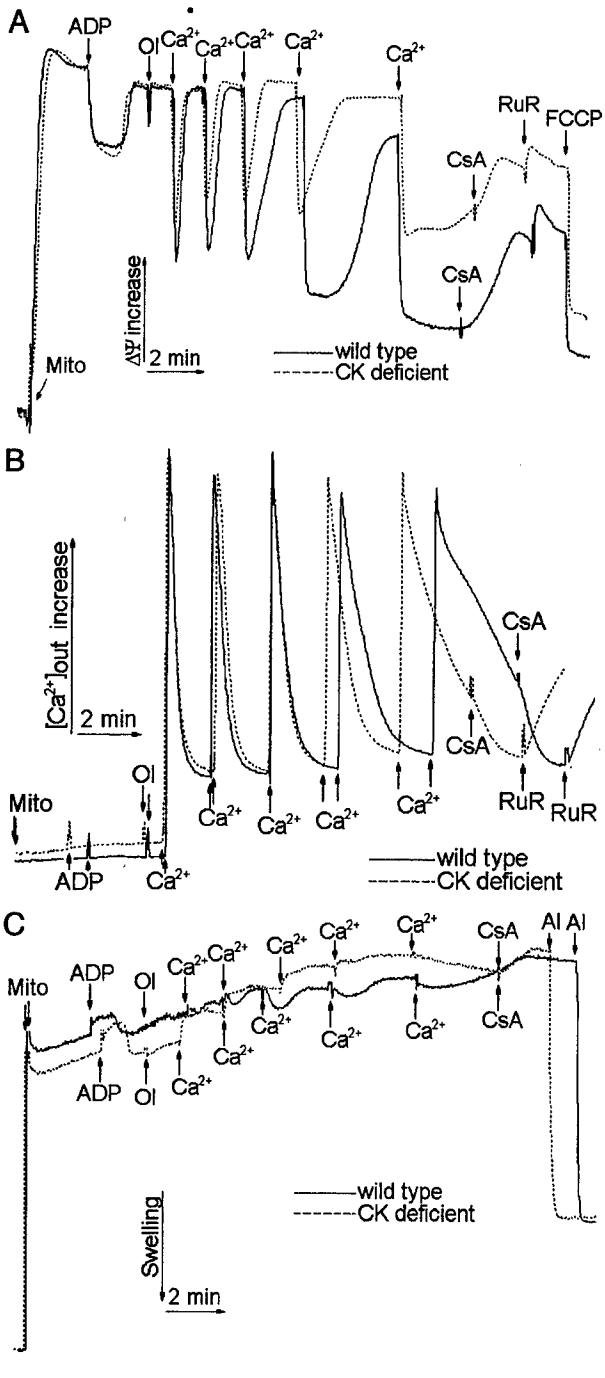


Fig. 1. $Ca^{2+}$-induced changes in membrane potential, $Ca^{2+}$ uptake, and swelling of mouse brain mitochondria. Incubation medium was composed of 125 mM KCl, 2 mM $KH_2PO_4$, 1 mM $MgCl_2$, 13.6 mM NaCl, 20 mM HEPES (pH 7.2), 0.2 mg/ml fatty-acid-free bovine serum albumin, 5 μM EGTA, 10 mM potassium succinate, and 1 μM rotenone; $t = 37°C$. In A, the incubation medium was supplemented with 2.5 μM safranine O. In C, the incubation medium was supplemented with 0.1 μM Calcium Green 5N. Mitochondria were added at 0.125 mg/ml. (A) Membrane potential of mouse brain mitochondria estimated from safranine O fluorescence quenching as described in Materials and methods. Please note that the tracings are inverted upside down for the sake of visual consistency. (B) $Ca^{2+}$ uptake in mitochondria estimated from changes in external $Ca^{2+}$ concentration measured as described in Materials and methods, and (C) the swelling of mitochondria. Additions: Mito, mouse brain mitochondria; ADP, 100 μM ADP; Ol, 1 μg/ml oligomycin; $Ca^{2+}$, 100 μM $CaCl_2$; CsA, 1.1 μM cyclosporine A; RuR, 0.4 μM Ruthenium Red; FCCP, 100 nM FCCP; Al, 80 μg/ml alamethicin A. All tracings were produced in a single experiment representative of five experiments performed.

decrease in membrane potential are virtually identical in both types of mitochondria reflecting an equal efficiency of the oxidative phosphorylation system (mtATPase, ADP/ATP translocator, and Pi transporter) and energy-producing system (substrate transporters and mitochondrial respiratory chain). It is well known that change in the membrane potential is one of the most sensitive parameters reflecting the bioenergetic qualities of mitochondria (Beatrice et al., 1980; Jensen et al., 1986; Petit et al., 1990; Zanotti and Azzone, 1980). Fig. 1A indicates that in the absence of added $Ca^{2+}$, the bioenergetics of UbMi-CK-deficient mitochondria are not different from those of wild-type mitochondria. Addition of $Ca^{2+}$ induced a transient decrease in membrane potential followed by its spontaneous restoration to the initial level reflecting the transport of $Ca^{2+}$ into mitochondria that is an energy-hungry membrane potential dependent process (Gunter and Gunter, 2001; Gunter et al., 1994) (please note that an amplitude of a deflection of tracings immediately after an addition does not bear any relevant information as it merely reflects the insertion and removal of a pipettor's tip into a cuvette). Fig. 1A shows that up to the third addition of $Ca^{2+}$, there was no difference in membrane potential changes in both types of mitochondria. However, after the third $Ca^{2+}$ pulse, a difference became apparent and consisted of a delayed restoration of membrane potential in wild-type mitochondria as compared to UbMi-CK mitochondria. After the fifth $Ca^{2+}$ addition, membrane potential failed to spontaneously restore in wild-type mitochondria whereas the restoration was significantly delayed in UbMi-CK mitochondria. A specific inhibitor of MPTP cyclosporine A (Fournier et al., 1987; Zoratti and Szabo, 1995) promoted a partial restoration of membrane potential in both types of mitochondria indicating an activation of mPTP. The restoration of membrane potential was incomplete and was not further promoted by Ruthenium Red, a specific inhibitor of the mitochondrial $Ca^{2+}$ uniporter (Gunter and Gunter, 2001; Gunter et al., 1994). This indicates that incomplete restoration of the membrane potential was not due to $Ca^{2+}$-induced $Ca^{2+}$-recycling (Gunter and Gunter, 2001; Gunter et al., 1994). Overall, these data imply that there is no significant difference between wild-type and UbMi-CK mitochondria in handling moderate amounts of $Ca^{2+}$ (up to 2400 nmol/mg protein) whereas higher amounts (4000 nmol/mg protein) of $Ca^{2+}$ induced permanent damage to bioenergetics, which was similar in both types of mitochondria (Fig. 1A). However, UbMi-CK mitochondria appear to be slightly more resistant to massive $Ca^{2+}$ loading, since they demonstrate better restoration of membrane potential after the fifth $Ca^{2+}$ addition.

The changes in membrane potential were paralleled by $Ca^{2+}$ fluxes as shown in Fig. 1B. This figure shows that mitochondria efficiently and rapidly remove exogenously added $Ca^{2+}$ upon moderate loading. At higher $Ca^{2+}$ loading, mitochondrial $Ca^{2+}$ uptake became much slower whereas the mPTP inhibitor cyclosporine A promoted the uptake (Fig. 1B). Ruthenium Red stimulated the release of $Ca^{2+}$ back into the incubation medium. Once again, it is clearly seen that UbMi-CK mitochondria exerted relatively better handling of a massive $Ca^{2+}$ load than wild-type mitochondria.

Opening of mPTP is frequently associated with a large amplitude changes in light scattering of a mitochondrial suspension, which is caused by swelling of the mitochondrial matrix, and therefore represents a convenient way of assessing mPTP activation in vitro (Beatrice et al., 1980; Zoratti and Szabo, 1995). Fig. 1C shows that addition of ADP induced a transient increase in light scattering of mitochondria that correlated with changes in the membrane potential (Fig. 1A). These changes are most likely related to the well-known effect of changes in the mitochondrial matrix aggregation state induced by oxidative phosphorylation (so-called "orthodox" to "condensed" state transition) (Hackenbrock, 1981; Mannella et al., 2001). $Ca^{2+}$ additions did not induce any appreciable swelling in either type of mitochondria. Instead, $Ca^{2+}$ caused a moderate increase in light scattering. This is a well-known and frequently observed phenomenon (Andreyev and Fiskum, 1999; Zoratti and Szabo, 1995) that most likely reflects changes in matrix density of mitochondria induced by accumulation of $Ca^{2+}$-phosphate precipitate (Kristian et al., 2002). However, a slow swelling-like response was observed after the fifth $Ca^{2+}$ addition in both types of mitochondria, which was always blocked and reversed by cyclosporin A. Although a similar slow decrease in light scatter-

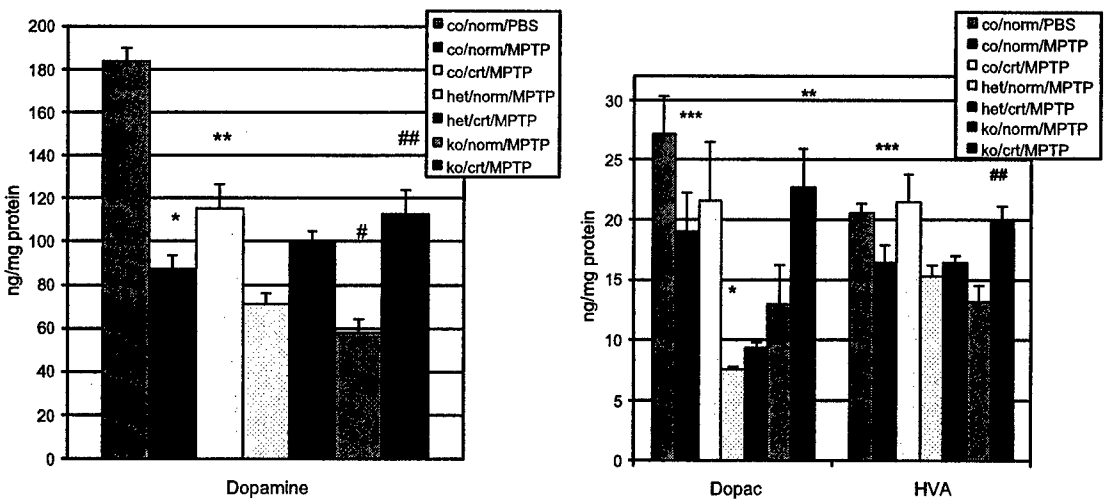


Fig. 2. Effects of MPTP on dopamine, DOPAC, and HVA in wild-type control, UbMi-CK heterozygous knockout, and homozygous knockout mice. *$P <$ 0.001, as compared to PBS-treated animals; **$P < 0.05$, as compared to MPTP-treated wild-type mice, ***$P < 0.05$, as compared to PBS-treated wild-type mice, #$P < 0.05$, as compared to MPTP-treated wild-type mice, ##$P < 0.002$, as compared to MPTP-treated homozygous knockout animals.

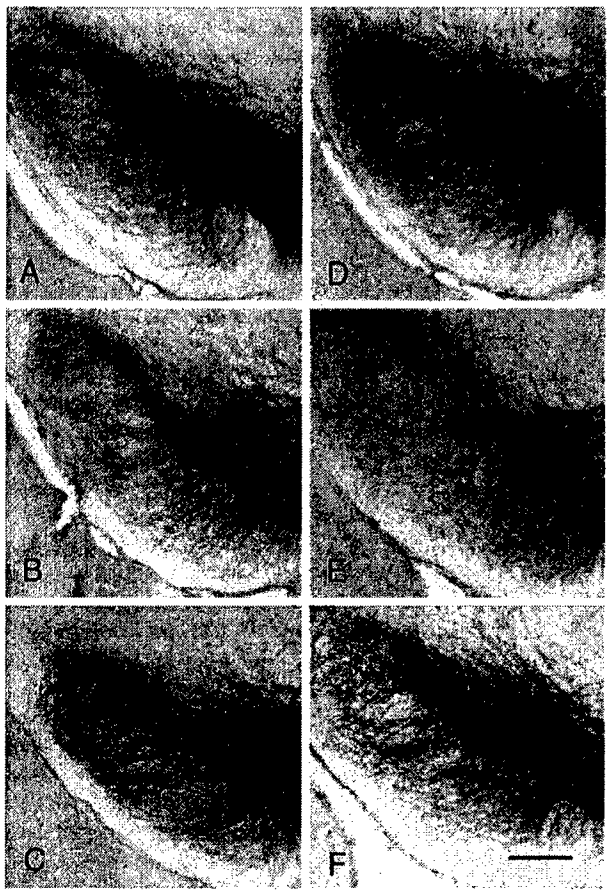


Fig. 3. Photomicrographs of TH-immunostained sections through the substantia nigra pars compacta of wild-type controls (A–C) and UbMi-CK knockout mice (D–F) showing TH-positive neurons following treatment with PBS (A, D), MPTP (B, E), and MPTP and dietary creatine (C, F). Scale bar, 200 μm.

ing was reproducibly observed in all experiments, the amplitude and the velocity of that swelling were inconsistent and varied in both types of mitochondria. As expected, an addition of a pore-forming peptide alamethicin induced similar large amplitude swelling of both types of mitochondria thus indicating their equal ability to swell (Sansom, 1993). Similar findings were made with a four-channel respiration system (Zhu et al., 2002).

The effects of administration of MPTP in wild-type controls and UbMi-CK knockout mice are shown in Fig. 2. The dose of MPTP we used (4 × 20 mg/kg) produced a significant dopamine depletion of 52% in wild-type controls on unsupplemented diet ($P < 0.001$). The same dose of MPTP produced a 61% depletion of dopamine in heterozygous UbMi-CK knockout mice that was not statistically significant as compared to MPTP-treated wild-type mice, and a significant 70% dopamine depletion in homozygous UbMi-CK knockout mice ($P < 0.05$). Supplementation with 2% creatine produced significant protection against MPTP-induced depletion of dopamine both in wild-type mice (38% protection) and in homozygous UbMi-CK knockout mice (98% protection; $P < 0.05$ and $P < 0.001$, respectively). This dose of MPTP produced a significant depletion of HVA in wild-type controls. There was a trend toward decreased levels of HVA in the UbMi-CK knockout mice on an unsupplemented diet, but this did not reach statistical significance. Creatine supplementation produced significant protection against MPTP-induced depletion of HVA in both the wild-type mice as well as in the homozygous UbMi-CK knockout mice ($P < 0.05$ and $P < 0.001$, respectively). The increased sensitivity to MPTP was not caused by an alteration in metabolism of MPTP to $MPP^+$ because striatal $MPP^+$ levels did not significantly differ between the wild-type and the UbMi-CK knockout mice at 90 min after MPTP administration (controls, 96.7 ± 17.1 ng/mg protein; UbMi-CK knockout, 109.6 ± 20.8 ng/mg protein).

Creatine significantly attenuated the MPTP-induced neurodegeneration in both the wild-type controls and UbMi-CK knockout mice. In wild-type controls, MPTP significantly reduced the numbers of TH-immunostained and Nissl-stained neurons in the substantia nigra pars compacta (SNpc) compared with PBS-treated mice by 31% ($P < 0.01$) and 35% ($P < 0.001$), respectively (Table 1, Fig. 3). In UbMi-CK knockout mice, MPTP produced a 32% reduction of TH-positive neurons ($P < 0.01$, vs. PBS) and 38% decrease ($P < 0.001$, vs. PBS) in the number of Nissl-stained neurons in SNpc. In MPTP-treated wild-type controls, 2% dietary creatine treatment significantly increased the numbers of surviving TH-positive neurons ($P < 0.05$) and Nissl-stained cells ($P < 0.001$) compared with the unsupplemented groups. In UbMi-CK knockout mice, creatine

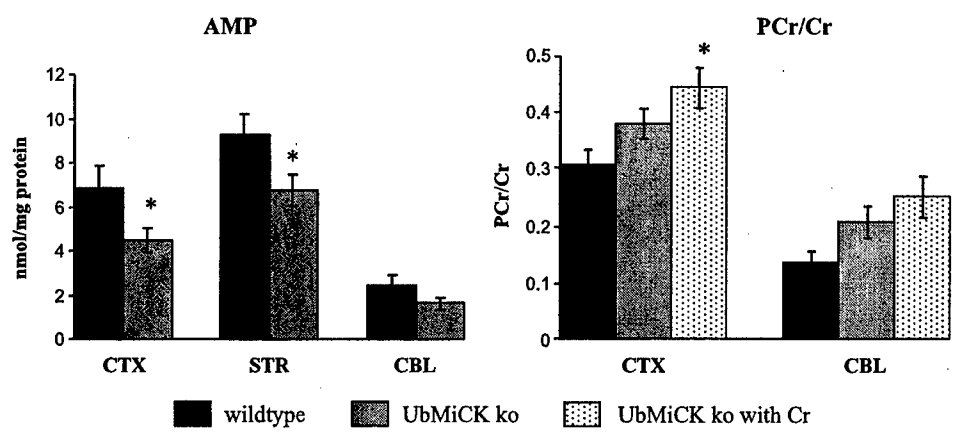


Fig. 4. AMP levels and effects of creatine supplementation for 2 weeks on PCr/Cr concentrations in wild-type (wt) and UbMi-CK-deficient mice. PCr/Cr concentrations were significantly increased in the UbMi-CK mice after creatine supplementation (*$P < 0.001$).

supplementation significantly attenuated the MPTP-induced loss of TH-immunoreactive neurons ($P < 0.05$) and Nissl-stained cells ($P < 0.01$) to a comparable extent.

The effects of creatine supplementation on PCr/Cr levels in cerebral cortex and cerebellum are shown in Fig. 4. There were no significant changes in ADP, ATP in the wild-type mice as compared to UbMi-CK-deficient mice at baseline (data not shown). AMP levels were significantly reduced in both cerebral cortex and striatum of UbMi-CK-deficient mice. Creatine supplementation significantly increased concentrations of creatine and PCr in cerebral cortex of UbMi-CK-deficient mice, and there was a similar trend in cerebellum.

## Discussion

Mi-CK is part of a complex of proteins that form an efficient, tightly coupled multienzyme energy channel, which generates and transports PCr to the cytoplasm. The creatine transporter has recently been localized to the inner mitochondrial membrane and there is evidence that there may be subcellular compartmentalization of Cr/PCr pools that are not fully in equilibrium (Walzel et al., 2002a,b). Substantial evidence supports a direct functional coupling of creatine kinase with $Na^+/K^+$ ATPase, neurotransmitter release, and in maintenance and restoration of ion gradients before and after depolarization (Dunant et al., 1988; Hemmer and Wallimann, 1993). High energy turnover and high creatine kinase concentrations are found in brain regions that are rich in synaptic connections (Kaldis et al., 1996) and creatine kinase flux correlates with brain activity as measured by EEG, as well as the amount of 2-deoxyglucose found in the brain (Sauter and Rudin, 1993). Creatine kinase appears to be coupled directly or indirectly to energetic processes required for calcium homeostasis (de Groof et al., 2002; Steeghs et al., 1997; Wallimann et al., 1992). PCr is essential for normal calcium regulation by the sarcoplasmic reticulum (de Groof et al., 2002; Yang and Steele, 2002). Creatine pretreatment delays increases in intracellular calcium produced by 3-nitropropionic acid (3-NP) in astrocytes in vitro (Deshpande et al., 1997).

There is an extensive literature showing neuroprotective effects of creatine both in vitro and in vivo. Creatine increases PCr levels in cultured neurons and protects against glutamate, 3-NP, and β-amyloid toxicity (Brewer and Wallimann, 2000; Brustovetsky et al., 2001). In hippocampal slices, creatine administration increased PCr levels, delayed synaptic failure, and ameliorated neuronal damage produced by anoxia (Carter et al., 1995; Sharov et al., 1987; Whittingham and Lipton, 1981). Creatine administration to rat pups for 3 days increased brain PCr levels, decreased hypoxia-induced seizures and death, and enhanced PCr and ATP recoveries after hypoxia (Holtzman et al., 1998).

We found that creatine administration increased brain PCr concentrations and produced significant neuroprotection against striatal lesions produced by the mitochondrial toxins 3-nitropropionic acid and malonate (Matthews et al., 1998), and MPTP neurotoxicity (Matthews et al., 1999). Creatine significantly extended survival, improved motor performance, protected against loss of spinal cord motor neurons (Klivenyi et al., 1999), and reductions in Mi-CK activity in a transgenic mouse model of ALS (Wendt et al., 2002).

In two transgenic mouse models of Huntington's disease, creatine administration significantly improved survival, slowed the development of brain atrophy, and delayed the formation of huntingtin-positive aggregates (Andreassen et al., 2001; Ferrante et al., 2000). Using magnetic resonance spectroscopy, we showed that creatine administration increased brain creatine levels 21.3% and delayed decreases in *N*-acetylaspartate concentrations (Andreassen et al., 2001; Ferrante et al., 2000). Creatine administration in a model of traumatic brain injury reduced the extent of cortical damage by 36% in mice and 50% in rats (Sullivan et al., 2000).

A potential neuroprotective mechanism of creatine is to stabilize the mPTP that is linked to both necrotic and apoptotic cell death (Bernardi et al., 1998). The mPTP is a large pore in the inner mitochondrial membrane that is activated by increases in mitochondrial calcium, free radicals, and decreases in reduced pyridine nucleotides. The mitochondrial isoform of creatine kinase (Mi-CK) is located at contact sites between the inner and outer membranes where it is associated with porin (Brdiczka et al., 1998; Schlattner et al., 2001). Mi-CK can convert intramitochondrially produced ATP to PCr directly, which then gets transported to sites of energy consumption. The mitochondrial isoform is also coupled to oxidative phosphorylation via the adenine nucleotide transporter, and creatine stimulates respiration by increasing mitochondrial ADP (Kay et al., 2000). It was suggested that creatine converts UbMi-CK from a dimer to an octomer, which then stabilizes the mPTP (Dolder et al., 2003; O'Gorman et al., 1997). Creatine prevents increases in respiration produced by $Ca^{2+}$ with atractylate, an activator of the mPTP. Furthermore induction of the mPTP was inhibited in cortical mitochondria of rats fed with creatine and then subjected to traumatic brain injury (Sullivan et al., 2000). Studies of isolated brain mitochondria, however, found no effect of creatine on the mPTP, and creatine supplementation for 2 weeks before isolation of brain mitochondria also showed no effect on the MPTP (Brustovetsky et al., 2001).

An important issue therefore is how much of the neuroprotective effects of creatine can be attributed to inhibition of the mPTP, versus maintenance of cellular PCr and ATP levels, which are critical to cellular homeostasis, synaptic transmission, and restoration of ionic gradients. We therefore examined whether creatine could exert neuroprotective effects in mice deficient in UbMi-CK. Mi-CKs are encoded by two nuclear genes. Sarcomeric Mi-CK is expressed in skeletal muscle fibers and cardiac cells, while UbMi-CK is expressed in brain, kidney, intestinal epithelial cells, smooth muscle, and sperm. Mice deficient in either isoform have been generated (Boehm et al., 1996; Steeghs et al., 1995, 1997). Surprisingly, these mice show no overt phenotypic abnormalities.

We found that mice deficient in UbMi-CK have normal ADP and ATP levels at baseline, consistent with studies using phosphorous NMR spectroscopy (Kekelidze et al., 2001). Phosphorous NMR studies showed no differences in brain PCr levels in UbMi-CK knockout mice compared to wild-type mice (Kekelidze et al., 2001). We found that the UbMi-CK mice have reduced AMP levels suggesting that increased adenylate kinase activity may contribute to maintaining ATP levels. The UbMi-CK-deficient mice showed a greater depletion of dopamine than wild-type mice after MPTP administration, suggesting that under conditions that stress mitochondria, compensation is not fully adequate. Similarly, they show greater seizure-induced decreases in PCr and ATP (Kekelidze et al., 2001).

In the present study, isolated brain mitochondria from UbMi-CK-deficient mice did not show any abnormalities in calcium uptake, capacity, and retention, membrane potential, or mitochon-

drial matrix volume changes in response to a calcium challenge. Differences between wild-type and UbMi-CK mitochondria were insignificant and fall within the typical variability of experiments with isolated mitochondria. Overall, these data strongly suggest the absence of any alterations to $Ca^{2+}$-dependent mPTP regulation or elevated sensitivity to $Ca^{2+}$-induced damage inherently present in mitochondria isolated from UbMi-CK-deficient mice.

If the neuroprotective effects of creatine are due to an interaction of creatine with UbMi-CK to prevent the MPTP, one would expect that creatine would not be neuroprotective in the brains of mice deficient in the UbMi-CK. In the present experiments, creatine administration produced significant protection against MPTP neurotoxicity in UbMi-CK-deficient mice as assessed biochemically and histologically. The neuroprotective effects were comparable to those seen in wild-type mice. Furthermore creatine administration significantly increased brain concentrations of both creatine and PCr. These results strongly suggest that the neuroprotective effects of creatine are not mediated by an effect on UbMi-CK to inhibit the mPTP.

Our results are congruent with the recent studies of Brustovetsky et al. (2001) who found that creatine had no significant effects on the mPTP of isolated brain mitochondria, or in brain mitochondria isolated from rats fed with 2% creatine for 2 weeks. These results suggest that the primary neuroprotective effects of creatine are likely to be mediated by maintenance of brain PCr and ATP levels. Creatine administration increases both skeletal muscle and brain PCr levels in man (Dechent et al., 1999; Wiedermann et al., 2001) and it improves exercise performance (Jacobs et al., 2002; Jones et al., 2002). These and other findings suggest that creatine administration is a promising strategy for the treatment of neurodegenerative diseases (Tarnopolsky and Beal, 2001).

## Acknowledgments

The secretarial assistance of Sharon Melanson and Greta Strong is gratefully acknowledged. Dr. Boris Krasnikov is thanked for assistance in analyzing data from the four-channel system. This work was supported by grants from NINDS grant NS39258, NIA grants AG20729 and AG12992, The Department of Defense and The Parkinson's Disease Foundation, The Hereditary Disease Foundation, the Huntington's Disease Society of America, and NIA AG14390 [Director Blass, Projects 2 (PI Kristal) and 5 (PI Beal)].

## References

Andreassen, O.A., Dedeoglu, A., Ferrante, R.J., Jenkins, B.G., Ferrante, K.L., Thomas, M., Friedlich, A., Browne, S.E., Schilling, G., Borchelt, D.R., Hersch, S.M., Ross, C.A., Beal, M.F., 2001. Creatine increase survival and delays motor symptoms in a transgenic animal model of Huntington's disease. Neurobiol. Dis. 8, 479–491.

Andreyev, A., Fiskum, G., 1999. Calcium induced release of mitochondrial cytochrome *c* by different mechanisms selective for brain versus liver. Cell Death Differ. 6 (9), 825–832 (Sep.).

Beatrice, M.C., Palmer, J.W., Pfeiffer, D.R., 1980. The relationship between mitochondrial membrane permeability, membrane potential, and the retention of Ca2+ by mitochondria. J. Biol. Chem. 255 (18), 8663–8671 (Sep. 25).

Bernardi, P., Basso, E., Colonna, R., Costantini, P., Di Lisa, F., Eriksson, O., Fontaine, E., Forte, M., Ichas, F., Massari, S., Nicolli, A., Petronilli, V., Scorrano, L., 1998. Perspectives of the mitochondrial permeability transition. Biochim. Biophys. Acta 1365, 200–206.

Boehm, E.A., Radda, G.K., Tomlin, H., Clark, J.F., 1996. The utilization of creatine and its analogues by cytosolic and mitochondrial creatine kinase. Biochim. Biophys. Acta 1274, 119–128.

Brdiczka, D., Beutner, G., Ruck, A., Dolder, M., Wallimann, T., 1998. The molecular structure of mitochondrial contact sites. Their role in regulation of energy metabolism and permeability transition. BioFactors 8, 235–242.

Brewer, G.J., Wallimann, T.W., 2000. Protective effect of the energy precursor creatine against toxicity of glutamate and β-amyloid in rat hippocampal neurons. J. Neurochem. 74, 1968–1978.

Brustovetsky, N., Brustovetsky, T., Dubinsky, J.M., 2001. On the mechanisms of neuroprotection by creatine and phosphocreatine. J. Neurochem. 76, 425–434.

Carter, A.J., Muller, R.E., Pschorn, U., Stransky, W., 1995. Preincubation with creatine enhances levels of creatine phosphate and prevents anoxic damage in rat hippocampal slices. J. Neurochem. 64, 2691–2699.

Dechent, P., Pouwels, P.J., Wilken, B., Hanefeld, F., Frahm, J., 1999. Increase of total creatine in human brain after oral supplementation of creatine-monohydrate. Am. J. Physiol. 277, R698–R704.

de Groof, A.J.C., Fransen, J.A.M., Errington, R.J., Willems, P.H.G.M., Wieringa, B., Koopman, W.J.H., 2002. The creatine kinase system is essential for optimal refill of the sarcoplasmic reticulum $Ca^{2+}$ store in skeletal muscle. J. Biol. Chem. 277, 5275–5284.

Deshpande, S.B., Fukuda, A., Nishino, H., 1997. 3-Nitropropionic acid increases the intracellular $Ca^{2+}$ in cultured astrocytes by reverse operation of the $Na^{+}$–$Ca^{2+}$ exchanger. Exp. Neurol. 145, 38–45.

Dolder, M., Walzel, B., Speer, O., Schlattner, U., Wallimann, T., 2003. Inhibition of the mitochondrial permeability transition by creatine kinase substrates. J. Biol. Chem. 278, 17760–17766.

Dunant, Y., Loctin, F., Marsal, J., Muller, D., Parducz, A., Rabasseda, X., 1988. Energy metabolism and quantal acetylcholine release: effects of botulinum toxin, 1-fluoro-2,4-dinitrobenzene, and diamide in the *Torpedo* electric organ. J. Neurochem. 50, 431–439.

Ferrante, R.J., Andreassen, O.A., Jenkins, B.G., Dedeoglu, A., Kuemmerle, S., Kubilus, J.K., Kaddurah-Daouk, R., Hersch, S.M., Beal, M.F., 2000. Neuroprotective effects of creatine in a transgenic mouse model of Huntington's disease. J. Neurosci. 20, 4389–4397.

Fournier, N., Ducet, G., Crevat, A., 1987. Action of cyclosporine on mitochondrial calcium fluxes. J. Bioenerg. Biomembr. 19 (3), 297–303 (Jun.).

Gunter, T.E., Gunter, K.K., 2001. Uptake of calcium by mitochondria: transport and possible function. IUBMB Life 52 (3–5), 197–204 (Sep.–Nov.).

Gunter, T.E., Gunter, K.K., Sheu, S.S., Gavin, C.E., 1994. Mitochondrial calcium transport: physiological and pathological relevance. Am. J. Physiol. 267 (2 Pt 1), C313–C339 (Aug.).

Hackenbrock, C.R., 1981. Energy-linked condensed-orthodox ultrastructural transformations in mitochondria. Chemotherapy 27 (Suppl. 2), 21–26.

Hemmer, W., Wallimann, T., 1993. Functional aspects of creatine kinase in brain. Dev. Neurosci. 15, 249–260.

Holtzman, D., Brown, M., O'Gorman, E., Allred, E., Wallimann, T., 1998. Brain ATP metabolism in hypoxia resistant mice fed guanidinopropionic acid. Dev. Neurosci. 20, 469–477.

Ikeda, K., Iwasaki, Y., Kinoshita, M., 2000. Oral administration of creatine monohydrate retards progression of motor neuron disease in the wobbler mouse. Amyotroph. Lateral Scler. Other Mot. Neuron Disord. 1, 207–212.

Jacobs, P.L., Mahoney, E.T., Cohn, K.A., Sheradsky, L.F., Green, B.A., 2002. Oral creatine supplementation enhances upper extremity work capacity in persons with cervical-level spinal cord injury. Arch. Phys. Med. Rehabil. 83, 19–23.

Jensen, B.D., Gunter, K.K., Gunter, T.E., 1986. The efficiencies of the component steps of oxidative phosphorylation: II. Experimental determination of the efficiencies in mitochondria and examination of the

equivalence of membrane potential and pH gradient in phosphorylation. Arch. Biochem. Biophys. 248 (1), 305–323 (Jul.).

Jones, A.M., Carter, H., Pringle, J.S., Campbell, I.T., 2002. Effect of creatine supplementation on oxygen uptake kinetics during submaximal cycle exercise. J. Appl. Physiol. 92, 2571–2577.

Kaldis, P., Hemmer, W., Zanolla, E., Holtzman, D., Wallimann, T., 1996. 'Hot spots' of creatine kinase localization in brain: cerebellum, hippocampus and choroid plexus. Dev. Neurosci. 18, 542–554.

Kay, L., Nicolay, K., Wieringa, B., Saks, V., Wallimann, T., 2000. Direct evidence for the control of mitochondrial respiration by mitochondrial creatine kinase in oxidative muscle cells in situ. J. Biol. Chem. 275, 6937–6944.

Kekelidze, T., Khait, I., Togliatti, A., Benzecry, J.M., Wieringa, B., Holtzman, D., 2001. Altered brain phosphocreatine and ATP regulation when mitochondrial creatine kinase is absent. J. Neurosci. Res. 66, 866–872.

Klivenyi, P., Ferrante, R.J., Matthews, R.T., Bogdanov, M.B., Klein, A.M., Andreassen, O.A., Mueller, G., Wermer, M., Kaddurah-Daouk, R., Beal, M.F., 1999. Neuroprotective effects of creatine in a transgenic animal model of amyotrophic lateral sclerosis. Nat. Med. 5, 347–350.

Kristian, T., Weatherby, T.M., Bates, T.E., Fiskum, G., 2002. Heterogeneity of the calcium-induced permeability transition in isolated non-synaptic brain mitochondria. J. Neurochem. 83 (6), 1297–1308 (Dec.).

Lawler, J.M., Barnes, W.S., Wu, G., Song, W., Demaree, S., 2002. Direct antioxidant properties of creatine. Biochem. Biophys. Res. Commun. 290, 47–52.

Mannella, C.A., Pfeiffer, D.R., Bradshaw, P.C., Moraru I.I., Slepchenko, B., Loew, L.M., Hsieh, C.E., Buttle, K., Marko, M., 2001. Topology of the mitochondrial inner membrane: dynamics and bioenergetic implications. IUBMB Life 52 (3–5), 93–100 (Sep.–Nov.).

Matthews, R.T., Yang, L., Jenkins, B.G., Ferrante, R.J., Rosen, B.R., Kaddurah-Daouk, R., Beal, M.F., 1998. Neuroprotective effects of creatine and cyclocreatine in animal models of Huntington's disease. J. Neurosci. 18, 156–163.

Matthews, R.T., Ferrante, R.J., Klivenyi, P., Yang, L., Klein, A.M., Mueller, G., Kaddurah-Daouk, R., Beal, M.F., 1999. Creatine and cyclocreatine attenuate MPTP neurotoxicity. Exp. Neurol. 157, 142–149.

O'Gorman, E., Beutner, G., Dolder, M., Koretsky, A.P., Brdiczka, D., Wallimann, T., 1997. The role of creatine kinase inhibition of mitochondrial permeability transition. FEBS Lett. 414, 253–257.

Petit, P.X., O'Connor, J.E., Grunwald, D., Brown, S.C., 1990. Analysis of the membrane potential of rat- and mouse-liver mitochondria by flow cytometry and possible applications. Eur. J. Biochem. 194 (2), 389–397 (Dec. 12).

Pulido, S.M., Passaquin, A.C., Leijendekker, W.J., Challet, C., Wallimann, T., Ruegg, U.T., 1998. Creatine supplementation improves intracellular Ca2+ handling and survival in mdx skeletal muscle cells. FEBS Lett. 439, 357–362.

Sansom, M.S., 1993. Alamethicin and related peptaibols—Model ion channels. Eur. Biophys. J. 22 (2), 105–124.

Sauter, A., Rudin, M., 1993. Determination of creatine kinase parameters in rat brain by NMR magnetization transfer: correlation with brain function. J. Biol. Chem. 268, 13166–13171.

Schlattner, U., Dolder, M., Wallimann, T., Tokarska-Schlattner, M., 2001. Mitochondrial creatine kinase and mitochondrial outer membrane porin show a direct interaction that is modulated by calcium. J. Biol. Chem. 276, 48027–48030.

Sharov, V.G., Saks, V.A., Kupriyanov, V.V., Lakomkin, V.L., Kapelko, V.I., Steinschneider, A., Javadov, S.A., 1987. Protection of ischemic myocardium by exogenous phosphocreatine: I. Morphologic and phosphorus 31-nuclear magnetic resonance studies. J. Thorac. Cardiovasc. Surg. 94, 749–761.

Sims, N.R., 1990. Rapid isolation of metabolically active mitochondria from rat brain and subregions using Percoll density gradient centrifugation. J. Neurochem. 55, 698–707.

Starkov, A.A., Polster, B.M., Fiskum, G., 2002. Regulation of hydrogen peroxide production by brain mitochondria by calcium and Bax. J. Neurochem. 83, 220–228.

Steeghs, K., Oerlemans, F., Wieringa, B., 1995. Mice deficient in ubiquitous mitochondrial creatine kinase are viable and fertile. Biochim. Biophys. Acta 1230, 130–138.

Steeghs, K., Benders, A., Oerlemans, F., de Haan, A., Heerschap, A., Ruitenbeek, W., Jost, C., van Deursen, J., Perryman, B., Pette, D., Bruckwilder, M., Koudijs, J., Jap, P., Veerkamp, J., Wieringa, B., 1997. Altered $Ca^{2+}$ responses in muscles with combined mitochondrial and cytosolic creatine kinase deficiencies. Cell 89, 93–103.

Sullivan, P.G., Geiger, J.D., Mattson, M., Scheff, S.W., 2000. Dietary supplement creatine protects against traumatic brain injury. Ann. Neurol. 48, 723–729.

Tarnopolsky, M.A., Beal, M.F., 2001. Potential for creatine and other therapies targeting cellular energy dysfunction in neurological disorders. Ann. Neurol. 49, 561–574.

Wallimann, T., Wyss, M., Brdiczka, D., Nicolay, K., Eppenberger, H.M., 1992. Intracellular compartmentation, structure and function of creatine kinase isoenzymes in tissues with high and fluctuating energy demands: the 'phosphocreatine circuit' for cellular energy homeostasis. Biochem. J. 281, 21–40.

Walzel, B., Speer, O., Boehm, E., Kristiansen, S., Chan, S., Clarke, K., Magyar, J.P., Richter, E.A., Wallimann, T., 2002a. New creatine transporter assay and identification of distinct creatine transporter isoforms in muscle. Am. J. Physiol.: Endocrinol. Metab. 283, E390–E401.

Walzel, B., Speer, O., Zanolla, E., Eriksson, O., Bernardi, P., Wallimann, T., 2002b. Novel mitochondrial creatine transport activity: implications for intracellular creatine compartments and bioenergetics. J. Biol. Chem. 277, 37503–37511.

Wendt, S., Dedeoglu, A., Speer, O., Wallimann, T., Beal, M.F., Andreassen, O.A., 2002. Reduced creatine kinase activity in transgenic amyotrophic lateral sclerosis mice. Free Radical Biol. Med. 32, 920–926.

Whittingham, T.S., Lipton, P., 1981. Cerebral synaptic transmission during anoxia is protected by creatine. J. Neurochem. 37, 1618–1621.

Wiedermann, D., Schneider, J., Fromme, A., Thorwesten, L., Moller, H.E., 2001. Creatine loading and resting skeletal muscle phosphocreatine flux: a saturation-transfer NMR study. MAGMA 13, 118–126.

Xu, C.J., Klunk, W.E., Kanfer, J.N., Xiong, Q., Miller, G., Pettegrew, J.W., 1996. Phosphocreatine-dependent glutamate uptake by synaptic vesicles. J. Biol. Chem. 271, 13435–13440.

Yang, Z., Steele, D.S., 2002. Effects of phosphocreatine on SR Ca(2+) regulation in isolated saponin-permeabilized rat cardiac myocytes. J. Physiol. 539, 767–777.

Zanotti, A., Azzone, G.F., 1980. Safranine as membrane potential probe in rat liver mitochondria. Arch. Biochem. Biophys. 201 (1), 255–265 (Apr. 15).

Zhu, S., Stavrovskaya, I.G., Drozda, M., Kim, B.Y.S., Ona, V., Li, M., Sarang, S., Liu, A.S., Hartley, D.M., Wu, D.C., Gullans, S., Ferrante, R.J., Przedborski, S., Kristal, B.S., Friedlander, R.M., 2002. Minocycline inhibits cytochrome *c* release and delays progression of amyotrophic lateral sclerosis in mice. Nature 417, 74–78.

Zoratti, M., Szabo, I., 1995. The mitochondrial permeability transition. Biochim. Biophys. Acta 1241 (2), 139–176 (Jul. 17).

*Journal of Molecular Neuroscience*

ISSN0895-8696/03/21:191–198/$25.00

ORIGINAL ARTICLE

# Additive Neuroprotective Effects of Creatine and a Cyclooxygenase 2 Inhibitor Against Dopamine Depletion in the 1-Methyl-4-Phenyl-1,2,3,6-Tetrahydropyridine (MPTP) Mouse Model of Parkinson's Disease

***Peter Klivenyi, Gabrielle Gardian, Noel Y. Calingasan, Lichuan Yang, and M. Flint Beal****

*Department of Neurology and Neuroscience, Weill Medical College of Cornell University, New York-Presbyterian Hospital, New York, NY 10021*

Received July 8, 2003; Accepted July 21, 2003

## Abstract

There is evidence that both inflammatory mechanisms and mitochondrial dysfunction contribute to Parkinson's disease (PD) pathogenesis. We investigated whether the cyclooxygenase 2 (COX-2) inhibitor rofecoxib either alone or in combination with creatine could exert neuroprotective effects in the 1-methyl-4-phenyl-1,2,3,6-tetrahydropyridine model of PD in mice. Both rofecoxib and creatine administered alone protected against striatal dopamine depletions and loss of substantia nigra tyrosine hydroxylase immunoreactive neurons. Administration of rofecoxib with creatine produced significant additive neuroprotective effects against dopamine depletions. These results suggest that a combination of a COX-2 inhibitor with creatine might be a useful neuroprotective strategy for PD.

**Index Entries:** Inflammation; free radicals; mitochondria; cyclooxygenase; creatine; Parkinson's disease.

## Introduction

Although a small number of genetic defects are associated with Parkinson's disease (PD), in most patients, the etiology is unknown. There is increasing evidence that both mitochondrial dysfunction and inflammatory mechanisms may contribute to PD pathogenesis. There is an increase in reactive microglia in the striatum and substantia nigra of patients with idiopathic PD (McGeer et al., 1988). Activated microglia are also found in the substantia nigra of humans dying many yr after exposure to 1-methyl-4-phenyl-1,2,3,6-tetrahydropyridine (MPTP) (Langston et al., 1999). Increased interleukin (IL)-1β, IL-6, and tumor necrosis factor (TNF)-α concentrations are reported in the cerebrospinal fluid and striatum of PD patients (Blum-Degen et al., 1995; Mogi et al., 1996; Muller et al., 1998; Mogi et al., 1994a; Mogi et al., 1994b), and an increase in TNF-α and IL-1β immunoreactive glial cells has been reported in the substantia nigra (Hunot et al., 1999). Last, an IL-1β polymorphism was reported to increase the risk of PD (McGeer et al., 2002; Schulte et al., 2002).

Defects in mitochondrial energy metabolism are also implicated in PD pathogenesis. MPTP has been used to model PD both in mice and primates (Beal, 2001). There is substantial evidence that MPTP toxicity involves mitochondrial dysfunction. MPTP is

*Author to whom all correspondence and reprint requests should be addressed: E-mail: fbeal@med.cornell.edu

metabolized to $MPP^+$ by monoamine oxidase B, and is then taken up by the dopamine transporter and accumulates in mitochondria, where it inhibits complex I of the electron transport chain (Gluck et al., 1994; Beal, 2001). Similarly, systemic administration of the complex I inhibitor rotenone produces an animal model of PD (Betarbet et al., 2000).

We previously demonstrated that administration of creatine exerts dose-dependent neuroprotective effects against MPTP neurotoxicity (Matthews et al., 1999). Cyclooxygenase (COX) 2 is induced by cytokines, including IL-1β and TNF-α, and has been implicated in neurodegeneration in a variety of settings (Almer et al., 2001; Iadecola et al., 2001; Hewitt et al., 2000). Cyclooxygenase converts arachidonic acid to PGH2, the precursor of PGE2, and several other prostanoids. COX-1 is expressed constitutively, whereas the expression of COX-2 is induced in inflamed tissue (Smith et al., 2000). Recently it was shown that COX-2 inhibitors exert neuroprotective effects against MPTP toxicity (Teismann et al., 2001; Teismann et al., 2003). In the present experiments, we therefore examined whether creatine could exert additive neuroprotective effects when administered with rofecoxib, one of the two COX-2 inhibitors presently approved for use in man (Fitzgerald and Patrono, 2001).

## Materials and Methods

### *Experimental Animals*

Our experiments were conducted in accordance with the National Institutes of Health guidelines for the care and use of experimental animals. Male 3-mo-old Swiss-Webster mice were fed lab chow diets supplemented with 2% creatine, or 0.005% rofecoxib or their combination for 1 wk before MPTP administration. Standard unsupplemented lab chow diet served as a control. We examined 12 mice in each group for neurochemistry and 10 mice in each group for histology. MPTP (20 mg/kg, 5 mL/kg, intraperitoneally) was administered four times at 2-h intervals to the mice. The animals were killed 1 wk after MPTP treatment, and both striata were rapidly dissected on a chilled glass plate and frozen at –70°C. The samples were subsequently thawed in 0.4 mL of chilled 0.1 *M* perchloric acid and sonicated. Aliquots were taken for protein quantification using a spectrophotometric assay. Other aliquots were centrifuged, and dopamine, 3,4-dihydroxyphenylacetic acid (DOPAC) and homovanillic acid (HVA) were measured in the supernatants by high performance liquid chromatography (HPLC) with electrochemical detection. Concentrations of dopamine and metabolites were expressed as ng/mg of protein (mean ± S.E.M.).

### *$MPP^+$ Levels*

To determine whether MPTP uptake or metabolism was altered, after 1 wk of supplemented or control diets, MPTP 20 mg/kg was administered intraperitoneally four times at 2-h intervals and mice were killed 90 min after the last injection. $MPP^+$ levels were quantified by HPLC with ultraviolet detection at 295 nm. Samples were sonicated in 0.1 *M* perchloric acid and an aliquot of supernatant was injected onto a Brownlee aquapore X03-224 cation exchange column (Rainin, Woburn, MA). Samples were eluted isocratically with 90% 0.1 *M* acetic acid and 75 m*M* triethylamine HCl, pH 2.3, adjusted with formic acid, and 10% acetonitrile (ng/mg protein).

### *Histological Analysis*

Three-month-old Swiss Webster mice were fed a standard lab chow diet (control), or diet containing 2% creatine, 0.005% rofecoxib, or a combination of 2% creatine and 0.005% rofecoxib. After 1 wk, MPTP (20 mg/kg, 5 mL/kg, intraperitoneally) or phosphate-buffered solution (PBS) (5 mL/kg, intraperitoneally) was administered four times at 2-h intervals. One wk after the last MPTP or PBS treatment, mice were deeply anesthetized with sodium pentobarbital (50 mg/kg, intraperitoneally) and perfused transcardially with ice-cold 0.9% NaCl followed by 4% paraformaldehyde in 0.1*M* phosphate buffer, pH 7.4. Brains were removed, postfixed for 2 h in the same fixative, and then cryoprotected in 30% sucrose overnight at 4°C. Serial coronal sections (50 μ m) were cut through the substantia nigra. Three sets consisting of eight sections each, 150 μm apart were prepared for tyrosine hydroxylase (TH), COX-2, or 4-hydroxynonenal immunohistochemistry using the avidin-biotin peroxidase technique. Briefly, free-floating sections were pretreated with 3% $H_2O_2$ in PBS for 30 min. The sections were incubated sequentially in (1) 1% bovine serum albumin (BSA)/0.2% Triton X-100 for 30 min; (2) rabbit anti-TH affinity purified antibody (Chemicon, Temecula, CA; 1:2000), rabbit anti-COX-2 (Cayman Chemical, Ann Arbor, MI; 1:1000), or mouse anti-4-hydroxynonenal (1:1000) diluted in PBS/0.5% BSA) for 18 h; (3) biotinylated anti-rabbit IgG (Vector Laboratories, Burlingame, CA; 1:200 in PBS/0.5% BSA) for 1 h; and (4) avidin-biotin-peroxidase complex

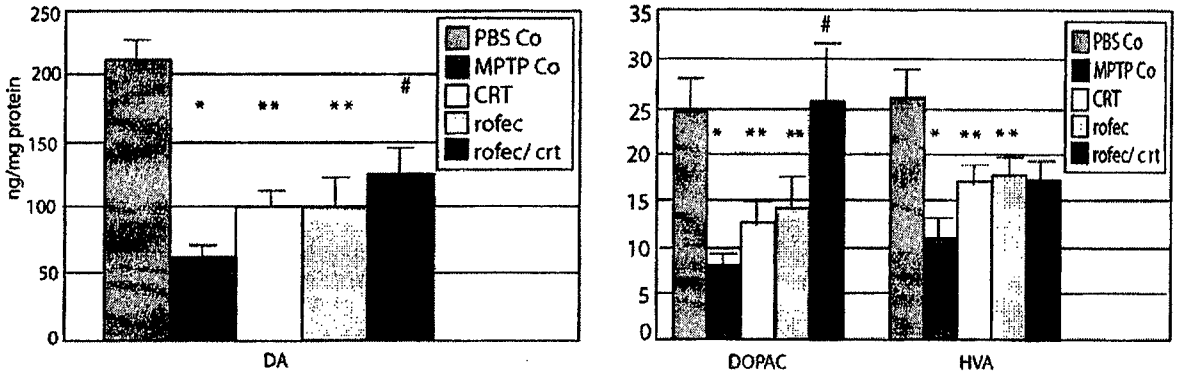


Fig. 1. Effects of MPTP on dopamine, DOPAC, and HVA in mice fed with creatine, rofecoxib, and their combination diet. PBS Co = mice fed with unsupplemented diet and injected with PBS; MPTP Co = mice fed with unsupplemented diet and injected with MPTP; CRT = mice fed with 2% creatine diet; rofec = mice fed with 0.005% rofecoxib; rofec/crt = mice fed with 2% creatine and 0.005% rofecoxib combination diet. *$p < 0.01$, compared with PBS-treated animals on normal diet, **$p < 0.05$ compared with MPTP-treated mice on normal diet. #$p < 0.05$ compared with MPTP treated mice on creatine or rofecoxib diet.

(Vector; 1:200 in PBS) for 1 h. The immunoreaction was visualized using 3,3'-diaminobenzidine tetrahydrochloride dihydrate (DAB) with nickel intensification (Vector) as the chromogen. All incubations and rinses were performed with agitation using an orbital shaker at room temperature. The sections were mounted onto gelatin-coated slides, dehydrated, cleared in xylene, and coverslipped. The numbers of TH-immunoreactive cells in the substantia nigra pars compacta (SNpc) were counted using the optical fractionator method in the Stereo Investigator (v. 4.35) software program (Microbrightfield, Burlington, VT). Results are expressed as the mean ± S.E.M. Statistical comparisons were made using one-way analysis of variance followed by Newman-Keuls *post hoc* tests.

## Results

The effects of administration of MPTP in controls and mice fed with 2% creatine, or 0.005% rofecoxib or their combination are shown in Fig. 1. The dose of MPTP we used (4 × 20 mg/kg), produced significant dopamine depletion of 69% in mice fed with a regular diet ($n$ = 12/group). Either 2% creatine or 0.005% rofecoxib significantly attenuated the dopamine depletion ($p < 0.01$). In mice fed with creatine and rofecoxib combination, there was an additive neuroprotective effect which was significantly better than either creatine or rofecoxib alone ($p < 0.01$). MPTP produced a significant depletion of DOPAC and HVA, which was significantly attenuated in mice fed with either creatine or rofecoxib ($p < 0.05$). In the combined treatment group the DOPAC levels were significantly greater than those in the groups with the creatine or rofecoxib alone. A similar additive effect was not seen with HVA, which may be due to experimental variation. The reduced sensitivity to MPTP was not caused by an alteration in uptake or metabolism of MPTP to $MPP^+$ because striatal $MPP^+$ levels did not significantly differ at 90 min after MPTP administration ($MPP^+$ 30.3 ± 3.5 ng/mg protein in controls, 31.6 ± 3.3 ng/mg protein with creatine, and 38.9 ± 4.2 ng/mg protein with rofecoxib). The combination of creatine with rofecoxib also had no significant effect on MPP+ levels (34.7 ± 3.6 ng/mg protein).

### *Histology*

In mice fed the control diet, MPTP significantly reduced the numbers of TH-immunostained neurons in the substantia nigra pars compacta as compared with PBS-treated mice by 32% ($p < 0.001$ vs PBS, Figs. 2 and 3) ($n$ = 10/group). In MPTP-treated mice, dietary treatment with 2% creatine or 0.005% rofecoxib significantly increased the number of surviving TH-immunoreactive cells as compared with mice that received the control diet ($p < 0.001$ vs control). The combination of creatine and rofecoxib significantly attenuated the TH-immunoreactive neuronal loss ($p < 0.001$ vs control diet/MPTP) although the neuroprotection was not significantly

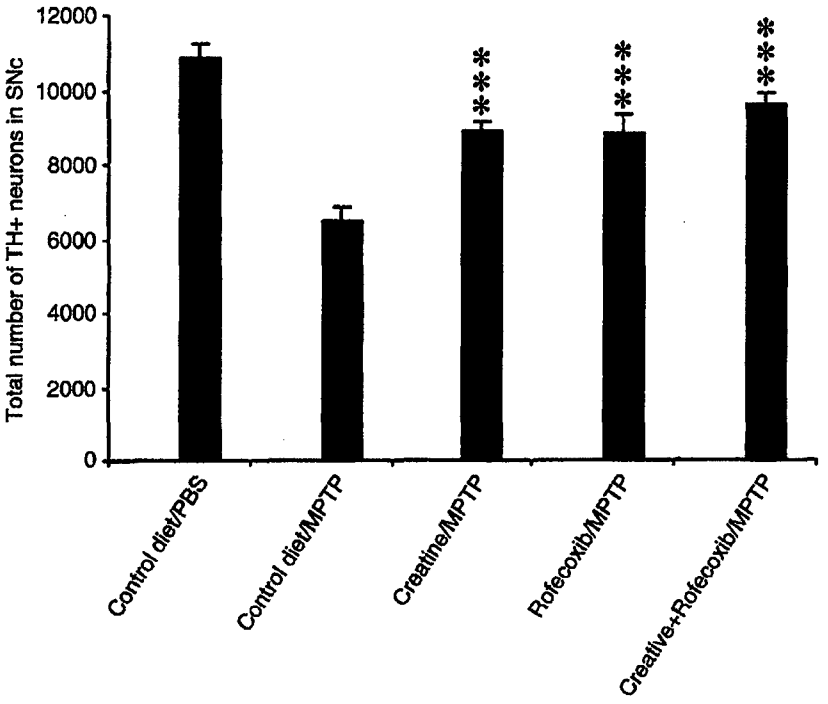


Fig. 2. Effects of creatine and rofecoxib on MPTP-induced loss of TH-immunoreactive neurons in the substantia nigra pars compacta. Cell counts were made using the optical fractionator method. Data are expressed as means ± S.E.M. ($n$ = 10 per group except control diet/PBS, in which $n$ = 8). ***$p < 0.001$ vs control diet/PBS, creatine/MPTP, rofecoxib/MPTP, or creatine+rofecoxib/MPTP.

greater than creatine or rofecoxib alone. This was not the result of downregulation of TH expression because adjacent Nissl sections showed identical changes (data not shown).

The pattern of COX-2 immunoreactivity in MPTP-treated mice that received creatine, rofecoxib or its combination was similar to those treated with control diet (data not shown). 4-Hydroxynonenal immunoreactivity increased in the remaining neurons in the SNpc of control diet/MPTP-treated mice compared with the control diet/PBS group (Fig. 4). Creatine, rofecoxib, or its combination appeared to reduce the intensity of 4-hydroxynonenal immunoreactivity in the substantia nigra (Fig. 4).

## Discussion

There is substantial evidence implicating both mitochondrial dysfunction and inflammatory mechanisms in PD pathogenesis. Evidence for inflammatory mechanisms comes from a number of studies. There is an increase in activated microglia in the substantia nigra of idiopathic PD patients as well as patients previously exposed to MPTP (McGeer et al., 1998; Langston et al., 1999). In PD striatum, messenger RNA for the complement components $C_1Q$ and C9 is increased (McGeer et al., 2001). There is an increase in a number of inflammatory cytokines including TNF-α as well as IL1-β within the substantia nigra of PD patients (Mogi et al., 1994a; Mogi et al., 1994b). After administration of MPTP to mice, there is evidence for a microglial reaction (Kohutnicka et al., 1998; Kurkowska-Jastrzebska et al., 1999), which is associated with an increase in proinflammatory cytokines such as IL-1β (Mogi et al., 1998). Administration of minocycline has neuroprotective effects in the MPTP model, which are associated with a reduction in activated microglia as well as a decrease in mature IL-1β (Du et al., 2001; Wu et al., 2002).

COX-2 is expressed and regulated in glial cells by cytokines including IL-1β and lipopolysaccharide (Cao et al., 1994; O'Banion et al., 1996). Chronic infusion of lipopolysaccharide for 2 wk into the sub-

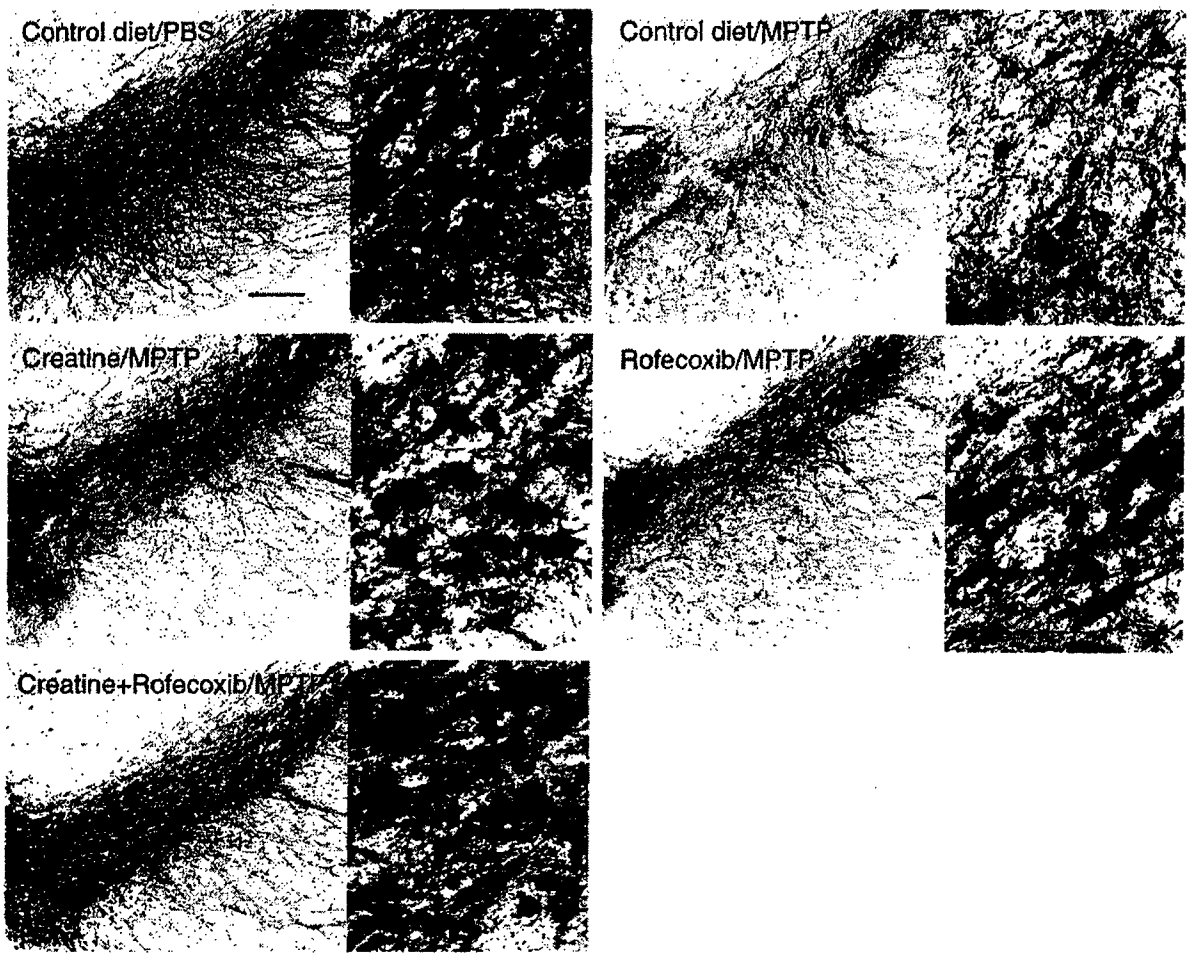


Fig. 3. Low and high magnification photomicrographs of representative TH-immunostained sections through the substantia nigra pars compacta of mice treated with PBS or MPTP that received control diet, creatine, rofecoxib, or a combination of creatine and rofecoxib. A noticeable mitigation of MPTP-induced loss of TH-positive neurons occurred in mice treated with creatine, rofecoxib, or their combination. Scale bar, 200 μ for low magnification photos; 50 μ for high magnification photos.

stantia nigra in rats results in rapid activation of microglia, followed by a delayed and gradual loss of nigral neurons (Gao et al., 2002). COX-2 is also expressed in neurons after excitotoxic lesions, synaptic excitation, cerebral ischemia, and in transgenic mouse models of myotrophic lateral sclerosis (ALS) (Adams et al., 1996; Ho et al., 1998; Planas et al., 1999; Iadecola et al., 2001; Almer et al, 2001). A recent study showed that COX-2 immunoreactivity is expressed in dopaminergic neurons following MPTP as well as in the substantia nigra of PD patients (Teismann et al., 2003). There was no expression in microglia, suggesting that cell autonomous expression of COX-2 may play a role in its toxicity. The enzyme was active both following MPTP and in PD substantia nigra as evidenced by increased PGE2 levels (Teismann et al., 2003).

Several lines of evidence show that COX-2 contributes to neuronal cell death both in vitro and in vivo. Cyclooxygenase catalyzes the formation of prostaglandins, which involves reduction of a hydroperoxide, resulting in the generation of free radicals. Mice overexpressing COX-2 show increased vulnerability to kainic acid and have elevated lipid peroxidation (Kelley et al., 1999). Neuronal death mediated by N-methyl-D-aspartate is diminished in

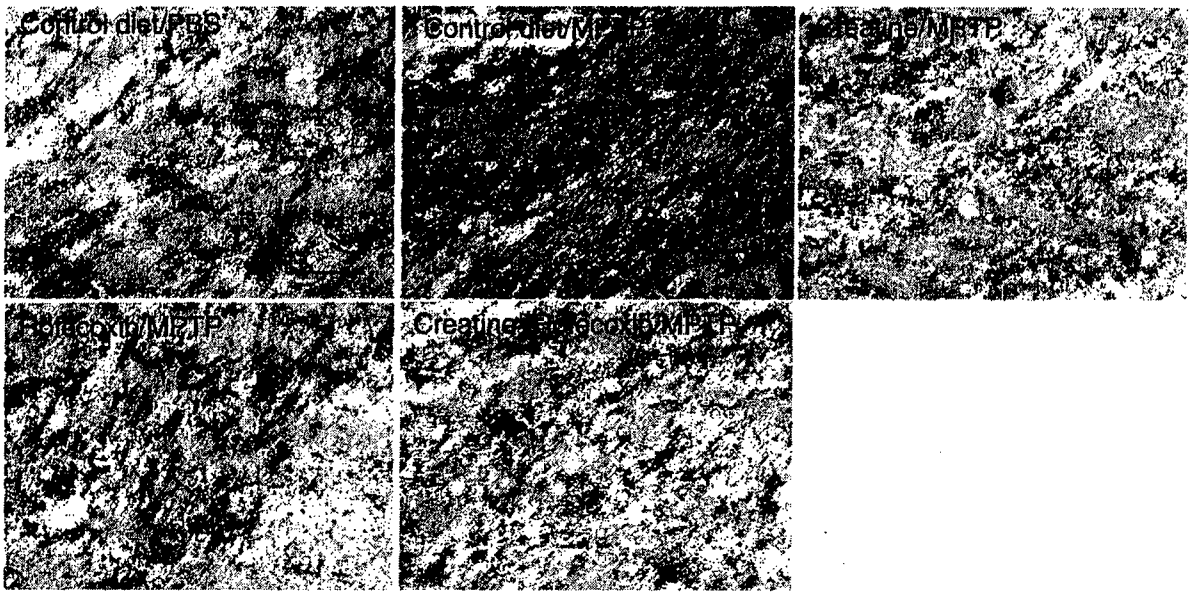

Fig. 4. Photomicrographs of representative 4-hydroxynonenal-immunostained sections through the substantia nigra pars compacta of mice treated with PBS or MPTP, that received control diet, creatine, rofecoxib, or a combination of creatine and rofecoxib. MPTP treatment increased neuronal staining in the substantia nigra pars compacta. Creatine, rofecoxib, or their combination reduced perikaryal HNE immunoreactivity. Scale bar, 50 μ.

a dose-dependent manner by COX-2 inhibitors in primary neuronal cultures (Hewett et al., 2000). Furthermore, transgenic mice that are deficient in COX-2 show reduced susceptibility to N-methyl-D-aspartate-induced excitotoxicity, focal ischemia, and MPTP (Iadecola et al., 2001; Teismann et al., 2003).

We previously showed that mice with a dominant-negative inhibition of interleukin converting enzyme, the known activator of IL-1β, have a marked attenuation of MPTP induced neurodegeneration (Klivenyi et al., 1999). IL-1β is known to induce COX-2, a key enzyme involved in the production of both proinflammatory prostanoids as well as reactive oxygen species (Smith et al., 2000). Furthermore, TNF-α activates COX-2 via the JNK pathway, which has also been implicated in MPTP neurotoxicity (Saporito et al., 1999; Saporito et al., 2000).

In the present experiments we found that the selective COX-2 inhibitor rofecoxib exerted significant neuroprotective effects against the MPTP neurotoxicity. This is consistent with a recent study, which showed that the COX-2 inhibitor meloxicam showed protection against MPTP induced cell loss, and also showed significant protection against impairment of locomotor activity and depletion of striatal dopamine (Teismann et al., 2001). Furthermore, another recent study showed that rofecoxib attenuated MPTP-induced loss of tyrosine hydroxylase immunoreactive neurons as well as fibers in the striatum (Teismann et al., 2003).

We also examined whether administration of creatine either alone or in combination with rofecoxib could exert significant neuroprotective effects. Creatine administration can buffer into cellular energy stores as well as inhibit opening of the mitochondrial permeability transition that is linked to both excitotoxic and apoptotic cell death (O'Gorman et al., 1997). Creatine protects creatine kinase from peroxynitrite mediated damage (Wendt et al., 2002) and contributes to reuptake of glutamate into synaptic vesicles (Xu et al., 1996). We previously demonstrated that creatine produces dose-dependent neuroprotective effects, against MPTP induced striatal dopamine depletion as well as loss of tyrosine hydroxylase positive neurons in the substantia nigra (Matthews et al., 1999) and this was confirmed in the present study. Because the primary neuroprotective effects of COX2 inhibitors are anti-inflammatory and antioxidative, whereas the primary neuroprotective effects of creatine are to buffer intracellular energy stores, and both mechanisms are implicated in MPTP pathogenesis, we examined whether they could exert additive neuroprotective effects. The anti-inflammatory drug

minocycline exerts additive neuroprotective effects with creatine in a transgenic mouse model of amyotrophic lateral sclerosis (Zhu et al., 2003). Furthermore, a combination of minocycline, nimodipine, and riluzole exerted additive neuroprotective effects in a transgenic mouse model of amyotrophic lateral sclerosis (Kriz et al., 2003). We previously showed that the combination of coenzyme Q10 with the N-methyl-D-aspartate antagonist remacemide exerts additive neuroprotective effects in a transgenic mouse model of Huntington's disease (Ferrante et al., 2002). There is, therefore, ample precedent that agents targeting different disease mechanisms may exert additive or synergistic neuroprotective effects.

In the present experiments, creatine exerted significant neuroprotective effects against MPTP, and, when combined with rofecoxib, it produced additive neuroprotective effects. The effects of rofecoxib were associated with a reduction in oxidative damage as assessed by 4-hydroxynonenal immunocytochemistry. This is consistent with a recent report that administration of rofecoxib significantly reduced MPTP induced increases in 5-cysteinyldopamine, a stable adduct produced by COX-related oxidation of dopamine. Both creatine and potent COX-2 inhibitors have been shown to be safe and well tolerated in man and can, therefore, be readily examined in clinical trials. It is, therefore, possible that a combination of creatine with a COX-2 inhibitor might prove to be useful as a strategy for neuroprotective treatment of PD.

## Acknowledgment

Sharon Melanson and Greta Strong are thanked for secretarial assistance. This work was supported by grants from The Department of Defense and the Parkinson's Disease Foundation.

## References

Adams J., Collaco-Moraes Y., and de Belleroche J. (1996) Cyclooxygenase-2 induction in cerebral cortex: an intracellular response to synaptic excitation. *J. Neurochem.* **66,** 6–13.

Almer G., Guegan C., Teismann P., Naini A., Rosoklija G., Hays A. P., et al. (2001) Increased expression of the pro-inflammatory enzyme cyclooxygenase-2 in amyotrophic lateral sclerosis. *Ann. Neurol.* **49,** 176–185.

Bal-Price A., Matthias A., and Brown G. C. (2002) Stimulation of the NADPH oxidase in activated rat microglia removes nitric oxide but induces peroxynitrite production. *J. Neurochem.* **80,** 73–80.

Beal M. F. (2001) Experimental models of Parkinson's disease. *Nat. Rev. Neurosci.* **2,** 325–334.

Betarbet R., Sherer T. B., MacKenzie G., Garcia-Osuna M., Panov A. V., and Greenamyre J. T. (2000) Chronic systemic pesticide exposure reproduces features of Parkinson's Disease. *Nat Neurosci.* **3,** 1301–1306 .

Blum-Degen D., Muller T., Kuhn W., Gerlach M., Przuntek H., and Riederer P. (1995) Interleukin-1 beta and interleukin-6 are elevated in the cerebrospinal fluid of Alzheimer's and de novo Parkinson's disease patients. *Neurosci. Lett.* **202,** 17–20.

Cao X. and Phillis J. (1994) a-Phenyl-tert-butyl nitrone reduced cortical infarct and edema in rats subjected to focal ischemia. *Brain Res.* **644,** 267–272.

Cicchetti F., Brownell A. L., Williams K., Chen Y. I., Livni E., and Isacson O. (2002) Neuroinflammation of the nigrostriatal pathway during progressive 6-OHDA dopamine degeneration in rats monitored by immunohistochemistry and PET imaging. *Eur. J. Neurosci.* **15,** 991–998.

Du Y., Ma Z., Lin S., Dodel R. C., Gao F., Bales K. R., Triarhou L. C., et al. (2001) Minocycline prevents nigrostriatal dopaminergic neurodegeneration in the MPTP model of Parkinson's disease. *Proc. Natl. Acad. Sci. USA* **98,** 14669–14674.

Ferrante R. J., Andreassen O. A., Dedeoglu A., Ferrante K. L., Jenkins B. G., Hersch S. M., et al. (2002) Therapeutic effects of coenzyme Q10 and remacemide in transgenic mouse models of Huntington's disease. *J. Neurosci.* **22,** 1592–1599.

Fitzgerald G. A. and Patrono C. (2001) The coxibs, selective inhibitors of cyclooxygenase-2. *N. Engl. J. Med.* **345,** 433–442.

Gao H. M., Hong J. S., Zhang W., and Liu B. (2002) Distinct role for microglia in rotenone-induced degeneration of dopaminergic neurons. *J. Neurosci.* **22,** 782–790.

Gluck M. R., Youngster S. K., Ramsay R. R., Singer T. P., and Nicklas W. J. (1994) Studies on the characterization of the inhibitory mechanism of 4'-alkylated 1-methyl-4-phenylpyridinium and phenylpyridine analogues in mitochondria and electron transport particles. *J. Neurochem.* **63,** 655–661.

Hewett S. J., Uliasz T. F., Vidwans A. S., and Hewett J. A. (2000) Cyclooxygenase-2 contributes to N-methyl-D-aspartate-mediated neuronal cell death in primary cortical cell culture. *J. Pharmacol. Exp. Ther.* **293,** 417–425.

Ho L., Osaka H., Aisen P. S., and Pasinetti G. M. (1998) Induction of cyclooxygenase (COX)-2 but not COX-1 gene expression in apoptotic cell death. *J. Neuroimmunol.* **89,** 142–149.

Hunot S., Dugas N., Faucheux B., Hartmann A., Tardieu M., Debre P., et al. (1999) FcepsilonRII/CD23 is expressed in Parkinson's disease and induces, in vitro, production of nitric oxide and tumor necrosis factor-alpha in glial cells. *J. Neurosci.* **19,** 3440–3447.

Iadecola C., Niwa K., Nogawa S., Zhao X., Nagayama M., Araki E., et al. (2001) Reduced susceptibility to ischemic brain injury and N-methyl-D-aspartate-mediated neurotoxicity in cyclooxygenase-2-deficient mice. *Proc. Natl. Acad. Sci. USA* **98,** 1294–1299.

Kelley K. A., Ho L., Winger D., Freire-Moar J., Borelli C. B., Aisen P. S., et al. (1999) Potentiation of excitotoxic-

ity in transgenic mice overexpressing neuronal cyclooxygenase-2. *Am. J. Pathol.* **155,** 995–1004.

Klevenyi P., Andreassen O., Ferrante R. J., Schleicher J. R., Jr., Friedlander R. M., and Beal M. F. (1999) Transgenic mice expressing a dominant negative mutant interleukin-1beta converting enzyme show resistance to MPTP neurotoxicity. *Neuroreport.* **10,** 635–638.

Kohutnicka M., Lewandowska E., Kurkowska-Jastrzebska I., Czlonkowski A., and Czlonkowska A. (1998) Microglial and astrocytic involvement in a murine model of Parkinson's disease induced by 1-methyl-4-phenyl-1,2,3,6-tetrahydropyridine (MPTP). *Immunopharmacology* **39,** 167–180.

Kriz J., Gowing C., and Julien JP. (2003) Efficient three-drug cocktail for disease induced by mutant superoxide dismutase. *Ann. Neurol.* **53,** 429–436.

Kurkowska-Jastrzebska I., Wronska A., Kohutnicka M., Czlonkowski A., and Czlonkowska A. (1999) The inflammatory reaction following 1-methyl-4-phenyl-1,2,3,6-tetrahydropyridine intoxication in mouse. *Exp. Neurol.* **156,** 50–61.

Langston J. W., Forno L. S., Tetrud J., Reeves A. G., Kaplan J. A., and Karluk D. (1999) Evidence of active nerve cell degeneration in the substantia nigra of humans yr after 1-methyl-4-phenyl-1,2,3,6-tetrahydropyridine exposure. *Ann. Neurol.* **46,** 598–605.

Matthews R. T., Ferrante R. J., Klivenyi P., Yang L., Klein A. M., Mueller G., et al. (1999) Creatine and cyclocreatine attenuate MPTP neurotoxicity. *Exp. Neurol.* **157,** 142–149.

McGeer P. L., Yasojima K., and McGeer E. G. (2001) Inflammation in Parkinson's disease. *Adv. Neurol.* **86,** 83–89.

McGeer P. L., Yasojima K., and McGeer E. G. (2002) Association of interleukin-1beta polymorphisms with idiopathic Parkinson's disease. *Neurosci. Lett.* **326,** 67–69.

McGeer P. L., Itagaki S., Boyes B. E., and McGeer E. G. (1988) Reactive microglia are positive for HLA-DR in the substantia nigra of Parkinson's and Alzheimer's disease brains. *Neurology.* **38,** 1285–1291.

Mogi M., Harada M., Riederer P., Narabayashi H., Fujita K., and Nagatsu T. (1994b) Tumor necrosis factor-alpha (TNF-alpha) increases both in the brain and in the cerebrospinal fluid from parkinsonian patients. *Neurosci. Lett.* **165,** 208–210.

Mogi M., Harada M., Narabayashi H., Inagaki H., Minami M., and Nagatsu T. (1996) Interleukin (IL)-1 beta, IL-2, IL-4, IL-6 and transforming growth factor-alpha levels are elevated in ventricular cerebrospinal fluid in juvenile parkinsonism and Parkinson's disease. *Neurosci. Lett.* **211,** 13–16.

Mogi M., Harada M., Kondo T., Riederer P., Inagaki H., Minami M., and Nagatsu T. (1994a) Interleukin-1 beta, interleukin-6, epidermal growth factor and transforming growth factor-alpha are elevated in the brain from parkinsonian patients. *Neurosci. Lett.* **180,** 147–150.

Mogi M., Togari A., Ogawa M., Ikeguchi K., Shizuma N., Fan D., et al. (1998) Effects of repeated systemic administration of 1-methyl-4-phenyl-1,2,3,6-tetrahydropyridine (MPTP) to mice on interleukin-1beta and nerve growth factor in the striatum. *Neurosci. Lett.* **250,** 25–28.

Muller T., Blum-Degen D., Przuntek H., and Kuhn W. (1998) Interleukin-6 levels in cerebrospinal fluid inversely correlate to severity of Parkinson's disease. *Acta Neurol. Scand.* **98,** 142–144.

O'Banion M. K., Miller J. C., Chang J. W., Kaplan M. D., and Coleman P. D. (1996) Interleukin-1 beta induces prostaglandin G/H synthase-2 (cyclooxygenase- 2) in primary murine astrocyte cultures. *J. Neurochem.* **66,** 2532–2540.

O'Gorman E., Beutner G., Dolder M., Koretsky A. P., Brdiczka D., and Wallimann T. (1997) The role of creatine kinase inhibition of mitochondrial permeability transition. *FEBS Lett.* **414,** 253–257.

Planas A. M., Soriano M. A., Justicin C., and Rodriguez-Farre E. (1999) Induction of cyclooxygenase-2 in the rat brain after a mild episode of focal ischemia without tissue inflammation or neural cell damage. *Neurosci. Lett.* **275,** 141–144.

Saporito M. S., Thomas B. A., and Scott R. W. (2000) MPTP activates c-Jun NH(2)-terminal kinase (JNK) and its upstream regulatory kinase MKK4 in nigrostriatal neurons in vivo. *J. Neurochem.* **75,** 1200–1208.

Saporito M. S., Brown E. M., Miller M. S., and Carswell S. (1999) CEP-1347/KT-7515, an inhibitor of c-jun N-terminal kinase activation, attenuates the 1-methyl-4-phenyl tetrahydropyridine-mediated loss of nigrostriatal dopaminergic neurons in vivo. *J. Pharmacol. Exp. Ther.* **288,** 421–427.

Schulte T., Schols L., Muller T., Woitalla D., Berger K., and Kruger R. (2002) Polymorphisms in the interleukin-1 alpha and beta genes and the risk for Parkinson's disease. *Neurosci. Lett.* **326,** 70–72.

Smith W. L., DeWitt D. L., and Garavito R. M. (2000) Cyclooxygenases: structural, cellular, and molecular biology. *Annu. Rev. Biochem.* **69,** 145–182.

Teismann P. and Ferger B. (2001) Inhibition of the cyclooxygenase isoenzymes COX-1 and COX-2 provide neuroprotection in the MPTP-mouse model of Parkinson's disease. *Synapse* **39,** 167–174.

Teismann P., Tieu K., Choi D.K., Wu D.C., Naini A., Hunot S., et al. (2003) Cyclooxygenase-2 is instrumental in Parkinson's disease neurodegeneration. *Proc. Natl. Acad. Sci. USA* **100,** 5473–5478.

Wendt S., Dedeoglu A., Speer O., Wallimann T., Beal M. F., and Andreassen O. A. (2002) Reduced creatine kinase activity in transgenic amyotrophic lateral sclerosis mice. *Free Radic. Biol. Med.* **32,** 920–926.

Wu H., Kanatous S. B., Thurmond F. A., Gallardo T., Isotani E., Bassel-Duby R., et al. (2002) Regulation of mitochondrial biogenesis in skeletal muscle by CaMK. *Science* **296,** 349–352.

Xu C. J., Klunk W. E., Kanfer J. N., Xiong Q., Miller G., and Pettegrew J. W. (1996) Phosphocreatine-dependent glutamate uptake by synaptic vesicles. *J. Biol. Chem.* **271,** 13435–13440.

Zhang W., Narayanan M., Friedlander R.M. (2003) Additive neuroprotective effects of minocycline with creatine in a mouse model of ALS. *Ann. Neurol.* **53,** 267–270.

ELSEVIER

Journal of the Neurological Sciences 218 (2004) 39–45

Journal of the Neurological Sciences

www.elsevier.com/locate/jns

# Elevated levels of matrix metalloproteinases-9 and -1 and of tissue inhibitors of MMPs, TIMP-1 and TIMP-2 in postmortem brain tissue of progressive supranuclear palsy

Stefan Lorenzl[a], David S. Albers[a], Jason W. Chirichigno[a], Sarah J. Augood[b], M. Flint Beal[a,*]

[a] *Department of Neurology and Neuroscience, Weill Medical College of Cornell University, Room A-501, New York, NY 10021, USA*
[b] *Neurology Service, Massachusetts General Hospital and Harvard Medical School, Boston, MA, USA*

Received 23 June 2003; received in revised form 14 October 2003; accepted 20 October 2003

**Abstract**

We determined the levels and tissue localization of matrix metalloproteinases (MMPs) as well as their endogenous tissue inhibitors (TIMPs) in postmortem brain tissue from 13 patients with progressive supranuclear palsy (PSP) and 8 age-matched controls. MMP-9 expression was significantly increased in both the frontal cortex ($p=0.002$) and substantia nigra ($p=0.003$) of PSP cases as compared to controls whereas MMP-1 levels were increased in the substantia nigra ($p=0.01$) but unchanged in the frontal cortex ($p=0.41$). Levels of the endogenous tissue inhibitors of MMPs, TIMP-1 and TIMP-2 were significantly elevated in the substantia nigra (TIMP-1: $p=0.004$, TIMP-2: $p=0.01$). Levels of TIMPs were unchanged in PSP frontal cortex as compared to control cases. Together, these data show alterations of MMPs and TIMPs in the substantia nigra as well as in the frontal cortex of PSP, consistent with the possibility that alterations in MMPs/TIMPs may contribute to disease pathogenesis.


*Keywords:* Matrix metalloproteinases; Supranuclear palsy; Substantia nigra

## 1. Introduction

Progressive supranuclear palsy is a rare neurodegenerative disorder, characterized by the appearance of supranuclear gaze palsy in addition to postural instability, dysarthria, truncal dystonia, parkinsonism and dementia. The hallmark pathology is the presence of straight neurofibrillary filaments and tau-positive tangles and extensive neuronal degeneration and gliosis in multiple nuclei located both within the basal ganglia, forebrain and brainstem [1–3].

The etiological basis of PSP is unknown; however, there is a growing body of evidence suggesting a contributory role of mitochondrial dysfunction and oxidative stress in the pathogenesis of PSP [4]. One consequence of increased oxidative stress may be the activation of matrix metalloproteases (MMPs). MMPs are a family of $Zn^{2+}$-endopeptidases that are characterized by their ability to digest components of the extracellular matrix such as collagen, proteoglycan and laminin [5,6]. MMPs in the brain are synthesized primarily by endothelial cells, astrocytes, microglia and neurons [7]. Previous reports have indicated that MMPs are involved in the pathogenesis of neurodegenerative diseases such as Alzheimer's disease (AD) [8–10] and amyotrophic lateral sclerosis (ALS) [11,12], and most recently Parkinson's disease (PD) [13].

Tight regulation of MMP expression occurs physiologically and the major endogenous counter-regulators of MMPs, the tissue inhibitors of the matrix metalloproteinases (TIMPs), are a family of at least four related proteins. In addition to their MMP-inhibitory function, TIMP-1 and TIMP-2 may act as growth factors [14,15].

Based on the hypothesis that the generation of free radicals stimulates the expression/activity of MMPs and that free radical-mediated damage is a key mediator of neuronal damage in PSP, it is tempting to speculate that MMPs may be involved in the pathophysiology of PSP. In the present study, we measured the levels of MMP-2 and MMP-9 via zymography, levels of MMP-1 via western blot analysis, and localized the tissue distribution of MMP-2 and MMP-9 immunohistochemically in frontal cortical areas of PSP from pathologically confirmed cases of PSP and age-matched controls. We quantified the levels of TIMP-1 and TIMP-2 in PSP and control cases using ELISA.

* Corresponding author. Tel.: +1-212-746-6575; fax: +1-212-746-8532.
*E-mail address:* fbeal@med.cornell.edu (M.F. Beal).

0022-510X/$ - see front matter © 2003 Elsevier B.V. All rights reserved.
doi:10.1016/j.jns.2003.10.015

## 2. Materials and methods

### 2.1. Tissue specimens

Tissue from 13 cases with pathologically confirmed PSP (age = 73.23 ± 8.27 years, M/F = 8:7, PMI = 17.31 ± 7.67 h, data are mean ± standard deviation) and 8 control cases (age = 74.38 ± 8.14 years, M/F = 5:3, PMI = 16.50 ± 4.31 h) was provided by the Harvard Brain Tissue Resource Center (Belmont, MA, USA). Cortical tissue was available from all cases; tissue from the substantia nigra was available from eight PSP and five control cases. There was no significant difference in age, PMI or gender between the PSP and control groups. Although there have been few studies, limited evidence suggests that MMPs are stable postmortem [16]. The pathological diagnosis of PSP was made by examination of the contralateral hemisphere using the NINDS pathological criteria [2,3]. In all brains, genotyping and polymorphism analysis was performed to determine *tau* haplotypes as described previously [17]. All PSP cases used in this study had the *tau* H1/H1 genotype [18]. None of the PSP brains examined showed any evidence of a coexisting neurological disorder. The eight control brains examined had no pathological evidence of neurological disease. All tissue samples were stored at −80 °C and processed in parallel.

### 2.2. Extraction of matrix metalloproteinases out of brain tissue

MMP extraction from postmortem brain tissue of PSP cases was performed as previously described [19] with minor modifications. Tissue was homogenized in 10 vol. of cold lysis buffer (50 mM Tris–HCl, 150 mM NaCl, 5 mM $CaCl_2$, 0.05% BRIJ-35, 0.02% $NaN_3$, 1% Triton X-100, pH 7.6). After homogenization, the total protein was measured (BioRad, protein assay). The homogenates were centrifuged at 12,500 × *g* at 4 °C for 5 min. For zymography and Western blot analysis, the supernatants were further incubated with a 1:4 volume of gelatin sepharose 4B (Pharmacia Biotech, Uppsala, Sweden) for 1 h at 4 °C with constant shaking. After centrifugation at 500 × *g* at 4 °C for 5 min, the supernatant was removed and the pellet washed with buffer. After a second centrifugation at 500 × *g* at 4 °C for 5 min, the supernatant was removed and the pellet washed with buffer containing 10% DMSO. The sample was further incubated for 30 min under constant shaking and subjected to zymography. For ELISA of TIMPs, the supernatant after the first centrifugation was used.

### 2.3. Zymography

Gelatinolytic (MMP-2 and MMP-9) activity was measured in postmortem brain tissue samples by zymography as described previously [20]. Briefly, equal amounts of protein from each sample homogenate was mixed with sample buffer (62.5 mM Tris–HCl, 2% SDS, 25% glycerol, 0.01% bromophenol blue) and subjected to SDS-PAGE in 7.5% polyacrylamide gels containing 2 mg/ml gelatine type A (Sigma G 2500). Gels were washed twice for 30 min in 2% Triton X-100 and incubated for 20 h in incubation buffer (50 mM Tris base, 5 mM $CaCl_2$, 1 μM $ZnCl_2$, 0.01% sodium azide, pH 7.5 at 37 °C). After incubation, gels were fixed in 20% trichloroacetic acid (Sigma) for 30 min and stained in 0.5% coomassie brilliant blue (Sigma) for 90 min. After staining, gels were destained in 35% ethanol and 10% acetic acid for 60 min. Gelatinolytic activity was visible as clear bands on a blue background. Standard protein markers (BioRad) and human recombinant MMP-2 and MMP-9 (Oncogene Sciences) were used to size and confirm identity of the gelatinolytic bands on the gels.

### 2.4. Western blot for MMP-1

MMP-1 levels in the frozen postmortem brain tissue were determined via western blot analysis as described previously [21]. Western blot was chosen because for MMP-1 no relevant zymography protocol was available. In brief, equal amounts of protein from each sample were separated via SDS-PAGE on 7.5% polyacrylamide gels. Proteins were transferred to polyvinylidene difluoride (PVDF) membranes and blocked for 1 h in 5% dry milk in TBST (50 mM Tris base, 150 mM NaCl, 0.1% Tween-20, pH 7.4) at room temperature before an overnight incubation at 4 °C with a monoclonal MMP-1 primary antisera (1:200; Oncogene Sciences). After vigorous washes with TBST, the membranes were incubated with horseradish peroxidase-conjugated secondary antisera (Jackson Laboratories) for 1 h at room temperature. Immunoreactive bands were visualized using an enhanced chemiluminescent system (SuperSignal, Pierce, Rockford, IL).

### 2.5. Immunohistochemistry of MMP-2 and MMP-9 in postmortem brain tissue

Ten-micron thick sections of formalin-fixed, paraffin-embedded tissue from nine pathologically confirmed PSP cases and six age-matched control cases were processed for immunohistochemistry using standardized protocols [22]. Various frontal cortical areas were evaluated. Tissue from the substantia nigra was not available for immunohistochemistry. In brief, free-floating tissue sections were pretreated with 30% methanol/$H_2O$ with 0.3% $H_2O_2$ for 30 min to destroy endogenous peroxidase activity, washed in PBS, incubated in blocking buffer and avidin, washed again to remove unbound avidin then incubated in primary antibody (MMP-2 and MMP-9, both 1:50 dilution; Oncogene Sciences) at 4 °C for 24–48 h. GFAP (Sigma) was used to confirm the presence of reactive astrocytes (1:200 dilution). Tissue sections were washed, incubated in biotinylated IgG

for 1 h, washed, incubated in avidin–biotin complex (Vectastain Elite kit) and sites of bound antibody were visualized using $H_2O_2$-activated 3′3-diaminobenzidine (0.5 mg/ml). Sections were rinsed, mounted onto gelatinized slides and counterstained with hematoxylin.

### 2.6. TIMP-1 and TIMP-2 ELISA (Amersham)

Tissue samples were homogenized in cold lysis buffer at 4 °C. The homogenates were centrifuged at 12,000 × *g* for 5 minutes and the protein concentration in the supernatants were determined (BioRad). Equal amounts of protein from each sample were assayed according to manufacturer's instructions. After the incubation period, the developing blue color was stopped using 1 mM sulphuric acid and the yellow colour was read at 450 nm with a spectrophotometer. The following molecular weights derived from the amino acid sequences were used for calculation: 20,695 for TIMP-1 and 21,740 for TIMP-2 [23]. Values were expressed as nanomoles per gram of protein.

### 2.7. Statistical analysis

Statistical analysis of differences in numeric parameters between groups was done using the two-tailed Mann–Whitney *U*-test (InStat; GraphPad, San Diego, CA, USA). Data are expressed as mean ± range. Differences were considered significant at $p < 0.05$.

## 3. Results

### 3.1. Levels of MMP-2, MMP-9 and MMP-1 as well as TIMP-1 and TIMP-2 in frontal cortex and substantia nigra

MMP-9 levels were significantly increased in the frontal cortex ($p = 0.002$) and substantia nigra ($p = 0.003$) from

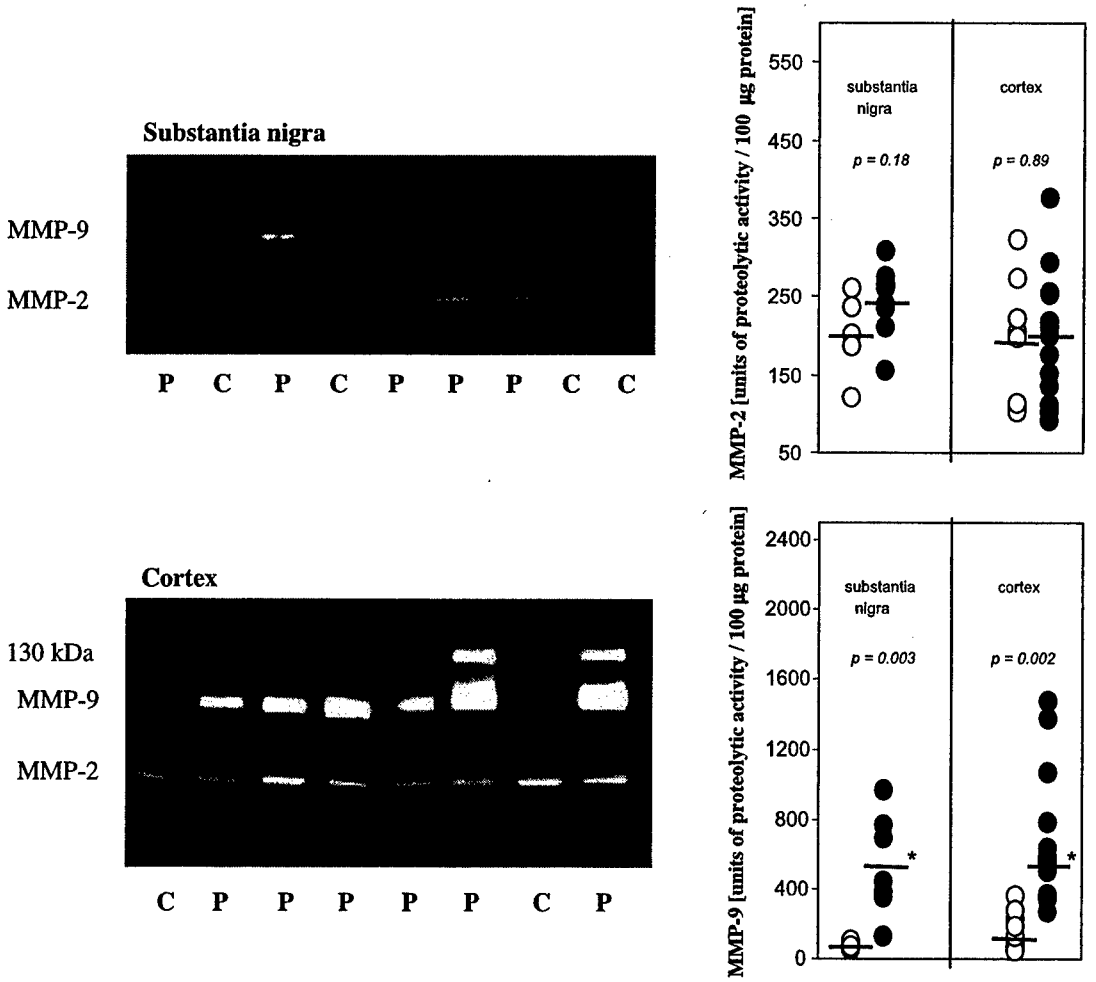


Fig. 1. Shows gelatine zymography of postmortem brain tissue from the substantia nigra from 5 PSP cases (●) and four controls (○) and of postmortem brain tissue from frontal cortex from six PSP cases (●) and two controls (○). The graphs demonstrate the results of quantitative zymography of MMP-2 and MMP-9. On zymography gels, the latent form of MMP-2 and MMP-9 appear. We found a significant increase of MMP-9 in the substantia nigra ($p = 0.003$) and frontal cortex ($p = 0.002$) as compared to controls. Levels of MMP-2 were unchanged.

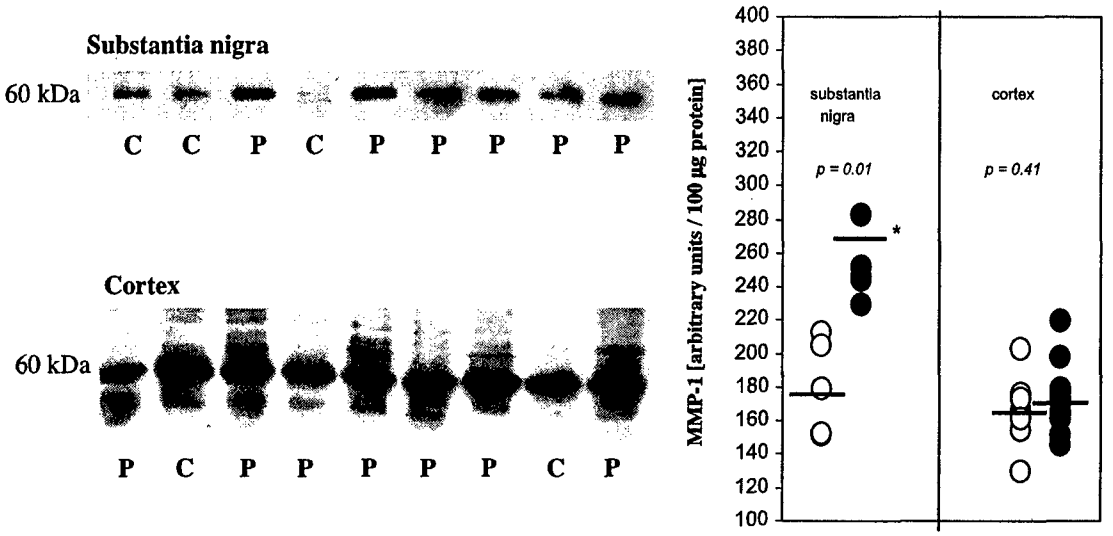


Fig. 2. Shows western blot analysis of postmortem brain tissue from substantia nigra of six PSP cases (●) and three control cases (○) and from frontal cortex tissue of seven PSP cases and two controls as well as the graphs which demonstrate quantitative results of MMP-1. There is a statistically significant ($p=0.01$) upregulation of MMP-1 in the substantia nigra of PSP cases. Levels of MMP-1 were unchanged in the frontal cortex of PSP cases as compared to controls.

PSP cases as compared to cortical and nigral samples from age-matched control cases (Fig. 1). The band at 130 kDa is thought to be a complex of MMP and TIMP1. Nigral levels of MMP-1 were significantly elevated ($p=0.01$), but no differences were observed in the frontal cortex of PSP cases relative to control cases (Fig. 2). Cortical and nigral MMP-2 levels were not different between groups (Fig. 1).

Both TIMP-1 ($p=0.004$) and TIMP-2 ($p=0.01$) levels were significantly higher in PSP substantia nigra. TIMP-1 levels in the frontal cortex were also elevated but the difference was not statistically significant ($p=0.057$). Cortical TIMP-2 levels were not different between groups (Fig. 3).

### *3.2. Immunolocalization of MMPs in postmortem brain tissue from frontal cortex*

Using a monoclonal antibody to MMP-2, we observed labeling of the walls of blood vessels in both control and PSP brain sections. Consistent with our zymographic results, no differences in the intensity of MMP-2 immunostaining between controls and PSP cases were observed (Fig. 4). Also, neither neurons nor glial cells were labeled by the MMP-2 antibody, which is consistent with previously published reports [11,13], and suggests that the endothelium is a likely source of MMP-2 in brain tissue and plasma.

The monoclonal antibody to MMP-9 labeled neurons and some glia in PSP but not in control cases (Fig. 4). The

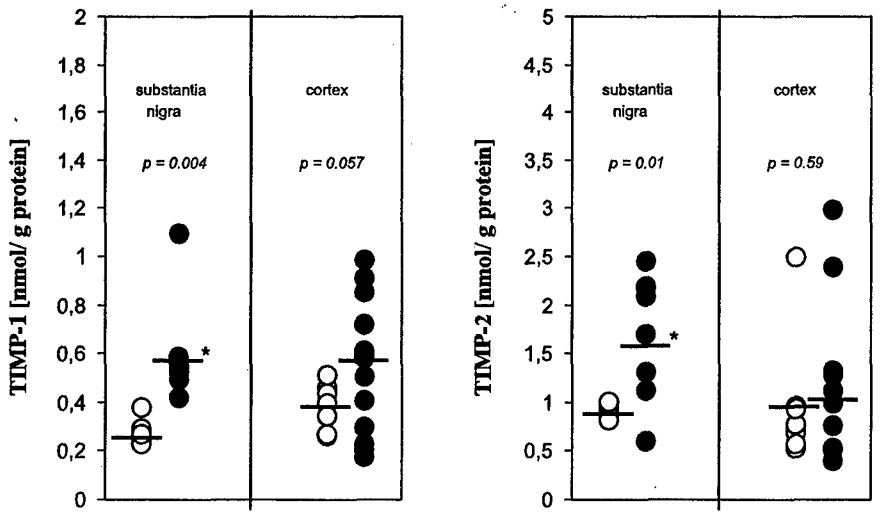


Fig. 3. Graphs demonstrate that levels of TIMP-1 and TIMP-2 are significantly elevated in the substantia nigra of PSP cases (●) but unchanged in the frontal cortex as compared to control cases (○). Levels of TIMPs were measured by ELISA (Amersham). Bars indicate mean values.

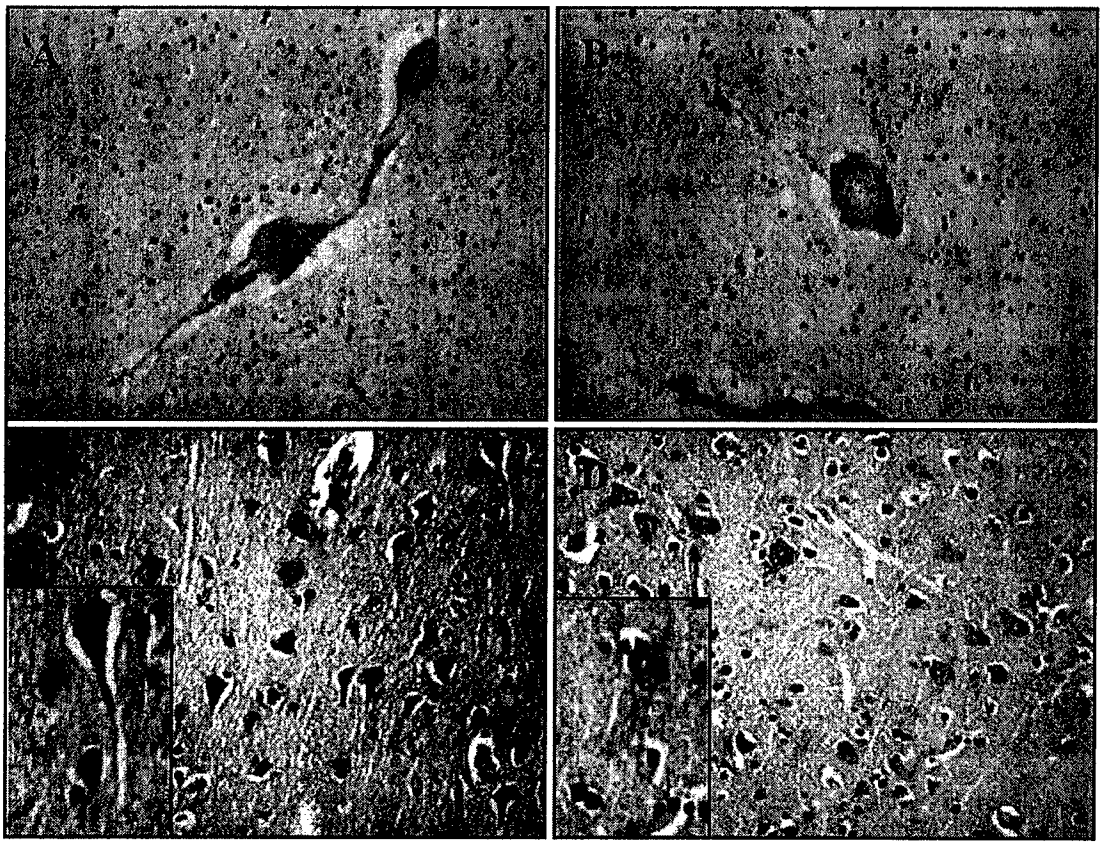


Fig. 4. Immunohistochemical staining was examined in frontal cortex of PSP and control cases. The pictures show staining for MMP-2 of a control (A) and PSP case (B). The MMP-2 antibody labelled vessels but neurons were not stained. Staining for MMP-9 showed increased expression of MMP-9 in neurons and some glia in the frontal cortex of PSP cases (C) but not in controls (D). Neurons in control cases were only weakly labelled. The magnification confirms that predominantly pyramidal neurons were labelled with antibody; however, some glial cells were stained with the MM-9 antibody 600 ×.

pattern of immunoreactivity was predominantly cytoplasmic, with some labeling extending into the dendrites and axons. The nuclei were free of staining. We observed no MMP-9 immunoreactivity in blood vessels in either PSP or control cases.

## 4. Discussion

In the present study, we found increased MMP-1 activity in the substantia nigra of PSP cases as compared to controls as well as increased MMP-9 activity in PSP substantia nigra and frontal cortex. These data coupled with our results showing increased TIMP-1 and TIMP-2 levels in PSP substantia nigra lends credence to the hypothesis that an imbalance in expression/activity of MMPs and TIMPs may contribute to PSP pathophysiology.

Increased expression of MMPs have been reported in postmortem tissue from other neurodegenerative diseases, particularly AD, ALS and PD [11,13,24]. In AD and ALS, increased expression of MMP-9 is found in the cerebral cortex and spinal cord where it is localized primarily to neurons. Significant increases in tissue MMP-9 levels were found in the frontal cortex and substantia nigra in PSP cases.

In postmortem tissue from AD cases, MMP-1 was elevated in frontal, parietal, temporal and occipital cortex [25]. In contrast, in PD cases, MMP-1 in the cortex, hippocampus and substantia nigra were unchanged from controls [13]. Interestingly, in PSP cases, MMP-1 was elevated in the substantia nigra, but not in frontal cortex. The stimulus for elevated MMP-1 and MMP-9 levels in PSP substantia nigra remains unknown. Expression of MMPs may be mediated by the MAP kinase pathway [26] or oxidative stress [27]. We previously showed that mitochondrial dysfunction and increased lipid peroxidation may play a role in PSP [17]. Expression of antioxidant enzymes (SOD1 and SOD2) is also increased in PSP brain [28]. One consequence of oxidative stress in PSP tissue may be the activation of MMPs secondary to oxidative damage. Interestingly, in frontal cortex where MMP-9 was elevated, no significant cell loss has been reported, whereas in the substantia nigra in which there is neuronal loss, MMP-1 and MMP-9 as well as TIMP-1 and TIMP-2 are elevated. It is therefore possible that MMP-1 is involved in cell loss in PSP.

Astrocytes release MMP-1, when stimulated with IL-1β, and active recombinant MMP-1, but not recombinant MMP-9, which is toxic to spinal cord cultures and to human neurons grown in dissociated cultures [29]. Activated microglia may contribute to cell death and elevated MMP production seen in PSP. However, tissue from the substantia nigra was not available for immunohistochemistry for MMP-1.

On our zymography gels only the proform of MMP-9, MMP-2 and on western blot analysis the proform of MMP-1 were detected. This finding may be explained by the fact that MMPs once activated, rapidly degrade in the extracellular space, or are inhibited by local tissue inhibitors of MMPs (TIMPs). TIMP-1 is the endogenous counterregulator for MMP-9 and MMP-1. We found significantly elevated levels of TIMP-1 in the substantia nigra, and attenuated levels of TIMP-1 in the cortex, which may contribute to the absence of activated forms of MMPs in these brain regions.

We observed MMP-2 immunoreactivity to be localized mainly to the basement membranes of blood vessels in PSP and control cases. Zymography analysis revealed no significant difference in MMP-2 expression between PSP and controls in frontal cortex, but it tended to be higher in substantia nigra tissue. Prior studies in man showed that levels of MMP-2 are unchanged in AD hippocampus [10] and in white matter in vascular dementia cases [30] as compared to controls. Increased levels of MMP-2 occur following strokes in human brain tissue [31].

Levels of TIMP-1 and TIMP-2 were both elevated in the substantia nigra, but not in frontal cortex of PSP cases. While TIMP-1 forms strong complexes with MMP-9, MMP-3 and MMP-1, TIMP-2 binds most strongly to MMP-2. Levels of these endogenous counterregulators in the substantia nigra may be increased as a consequence of significantly increased levels of MMP-1 and MMP-9. Although levels of MMP-9 were increased in the frontal cortex, TIMP-1 levels were not different from controls. This may indicate an imbalance in the protease inhibitory system in favor of the proteolytic enzyme, which may contribute to pathological changes. TIMP-positive regions have been localized to neuritic senile plaques and neurofibrillary tangles in AD brains and the pattern was similar to that observed with anti-tau and SP18 antibodies [32].

One unique feature of TIMP-1 and TIMP-2, aside from the classification as an endogenous counterregulator to MMPs, is that they possess mitogenic activity on a number of cell lines which protects them from pro-apoptotic stimuli [14,33]. Neuritic outgrowth of neurons in astrocyte-neuron cocultures is dependent on the MMP-2/TIMP-2 ratio, which promotes laminin stabilization against MMP proteolysis [34]. Laminin bioavailabilty in this experimental paradigm is essential for neurite outgrowth and neuronal migration. Therefore, it is tempting to speculate that increased TIMP-2 levels prevent these events. TIMPs are also able to limit injury-induced matrix proteolysis associated with the remodeling of neuronal circuits after injury—another possible explanation for elevated TIMP levels in PSP substantia nigra.

In summary, we observed differences in the levels of MMPs and TIMPs in postmortem PSP brain tissue as compared to age-matched control brain tissue. The significance of these changes remains uncertain, but suggests that an underlying imbalance in the MMP/TIMP regulatory system may contribute to PSP pathophysiology. The extracellular matrix is an important cell survival factor and changes in the cell–matrix interaction contribute to cell death. MMPs can exert direct neurotoxic effects (e.g. MMP-1) or indirectly cause cell death by degrading extracellular matrix proteins (e.g. MMP-9). The present study must be seen as preliminary, due to the retrospective clinical data and the small number of patients. Nevertheless, we observed a consistent pattern of MMP and TIMP expression, suggesting that these enzymes may play a role in PSP pathophysiology.

## Acknowledgements

This study was supported by the Deutsche Forschungsgemeinschaft (S.L) and the Society for Progressive Supranuclear Palsy (S.L. and D.S.A.), the Department of Defense, NIH, the ALS Association, the Huntington's Disease Society of America and the Hereditary Disease Foundation (M.F.B.).

## References

[1] Steele J, Richardson JC, Olszeewski J. Progressive supranuclear palsy. A heterogeneous degeneration involving the brainstem, basal ganglia and cerebellum with vertical gaze and pseudobulbar palsy, nuchal dystonia and dementia. Arch Neurol 1964;10:333–59.

[2] Hauw JJ, Daniel SE, Dickson D, Horoupian DS, Jellinger K, Lantos PL, et al. Preliminary NINDS neuropathologic criteria for Steele–Richardson–Olszewski syndrome (progressive supranuclear palsy). Neurology 1994;44:2015–9.

[3] Litvan I, Hauw J, Bartko J, Lantos PL, Daniel SE, Horoupian DS, et al. Validity and reliability of the preliminary NINDS neuropathologic criteria for progressive supranuclear palsy and related disorders. J Neuropathol Exp Neurol 1996;55:97–105.

[4] Albers DS, Augood SJ. New insights into progressive supranuclear palsy. Trends Neurosci 2001;24:347–53.

[5] Stetler-Stevenson WG. Dynamics of matrix turnover during pathological remodelling of the extracellular matrix. Am J Pathol 1996; 148:1345–50.

[6] Woessner JF. The family of matrix metalloproteinases. Ann NY Acad Sci 1994;732:11–21.

[7] Gottschall PE, Deb S. Regulation of matrix metalloproteinase expression in astrocytes, microglia and neurons. Neuroimmunomodulation 1996;3:69–75.

[8] Asahina M, Yoshiyama Y, Hattori T. Expression of matrix metalloproteinase-9 and urinary-type plasminogen activator in Alzheimer's disease brain. Clin Neuropathol 2001;20:60–3.

[9] Miyazaki K, Hasegawa M, Funahashi K, Umeda M. A metalloproteinase inhibitor domain in Alzheimer amyloid protein precursor. Nature 1993;362:839–41.

[10] Backstrom JR, Miller CA, Tökés ZA. Characterization of neutral proteinases from Alzheimer-affected and control brain specimens: identification of calcium-dependent metalloproteinases from the hippocampus. J Neurochem 1992;58:983–92.
[11] Lim GP, Backstrom JR, Cullen MJ, Miller CA, Atkinson RD, Tokes ZA. Matrix metalloproteinases in the neocortex and spinal cord of amyotrophic lateral sclerosis patients. J Neurochem 1996;67:251–9.
[12] Beuche W, Yushchenko M, Mader M, Maliszewska M, Felgenhauer K, Weber F. Matrix metalloproteinase-9 is elevated in serum of patients with amyotrophic lateral sclerosis. Neuroreport 2000;11:3419–22.
[13] Lorenzl S, Albers DS, Narr S, Chirichigno J, Beal MF. Expression of MMP-2, MMP-9, and MMP-1 and their endogenous counterregulators TIMP-1 and TIMP-2 in postmortem brain tissue of Parkinson's disease. Exp Neurol 2002;178:13–20.
[14] Hayakawa T, Yamashita K, Ohuchi E, Shinagawa A. Cell growth-promoting activity of tissue inhibitor of metalloproteinases-2 (TIMP-2). J Cell Sci 1994;107:2373–9.
[15] Nemeth JA, Rafe A, Steiner M, Goolsby CL. TIMP-2 growth-stimulatory activity: a concentration- and cell type-specific response in the presence of insulin. Exp Cell Res 1996;224:110–5.
[16] Sylvestre MN, Balcerzak D, Feidt C, Baracos VE, Brun Bellut J. Elevated rate of collagen solubilization and postmortem degradation in muscles of lambs with high growth rates: possible relationship with activity of matrix metalloproteinases. J Anim Sci 2002;80:1871–8.
[17] Baker M, Litvan I, Houlden H, Adamson J, Dickson D, Perez-Tur J, et al. Association of an extended haplotype in the tau gene with progressive supranuclear palsy. Hum Mol Genet 1999;8:711–5.
[18] Albers DS, Augood SJ, Park LC, Browne SE, Martin DM, Adamson J, et al. Frontal lobe dysfunction in progressive supranuclear palsy: evidence for oxidative stress and mitochondrial impairment. J Neurochem 2000;74:878–81.
[19] Zhang JW, Gottschall PE. Zymographic measurement of gelatinase activity in brain tissue after detergent extraction and affinity-support purification. J Neurosci Methods 1997;76:15–20.
[20] Kleiner DE, Stetler-Stevenson WG. Quantitative zymography: detection of picogram quantities of gelatinases. Anal Biochem 1994;34: 217–28.
[21] Dunah AW, Yasuda RP, Wang YH, Luo J, Davila-Garcia M, Gbadegesin M, et al. Regional and ontogenic expression of the NMDA receptor subunit NR2D protein in rat brain using a subunit-specific antibody. J Neurochem 1996;67:2335–45.
[22] Augood SJ, Hollingsworth ZR, Standaert DG, Emson PC, Penney Jr JB. Localization of dopaminergic markers in the human subthalamic nucleus. J Comp Neurol 2000;421:247–55.
[23] Nakamura H, Ueno H, Yamashita K, Shimada T, Yamamoto E, Noguchi M, et al. Enhanced production and activation of progelatinase A mediated by membrane-type 1 matrix metalloproteinase in human papillary thyroid carcinomas. Cancer Res 1999;59:467–73.
[24] Yoshiyama Y, Ashina M, Hattori T. Selective distribution of matrix metalloproteinase-3 (MMP-3) in Alzheimer's disease brain. Acta Neuropathol 2000;99:91–5.
[25] Leake A, Morris CM, Whateley J. Brain matrix metalloproteinase 1 levels are elevated in Alzheimer's disease. Neurosci Lett 2000;291: 201–3.
[26] Wang X, Mori T, Jung JC, Fini ME, Lo EH. Secretion of matrix metallo-proteinase-2 and -9 after mechanical trauma injury in rat cortical cultures and involvement of MAP kinase. J Neurotrauma 2002;19:615–25.
[27] Morita-Fujimura Y, Fujimura M, Gasche Y, Copin J, Chan PH. Overexpression of copper and zinc superoxide dismutase in transgenic mice prevents the induction and activation of matrix metalloproteinases after cold injury induced brain trauma. J Cereb Blood Flow Metab 1999;20:130–8.
[28] Cantuti-Castelvetri I, Keller-McGandy CE, Albers DS, Beal MF, Vonsattel JP, Standaert DG, et al. Expression and activity of antioxidants in the brain in progressive supranuclear palsy. Brain Res 2002;930: 170–81.
[29] Vos CMP, Sjulson L, Nath A, McArthur JC, Pardo CA, Rothstein J, et al. Cytotoxicity by matrix metalloproteinase-1 in organotypic spinal cord and dissociated neuronal cultures. Exp Neurol 2000;163: 324–30.
[30] Rosenberg GA, Sullivan N, Esiri MM. White matter damage is associated with matrix metaloproteinases in vascular dementia. Stroke 2001;32:1162–8.
[31] Clark AW, Krekoski CA, Bou SS, Chapman KR, Edwards DR. Increased gelatinase A (MMP-2) and gelatinase B (MMP-9) activities in human brain after focal ischemia. Neurosci Lett 1997;238:53–6.
[32] Peress N, Perillo E, Zucker S. Localization of tissue inhibitor of matrix metalloproteinases in Alzheimer's disease and normal brain. J Neuropathol Exp Neurol 1995;54:16–22.
[33] Valente P, Fassina G, Melchiori A, Masiello L, Cilli M, Vacca A, et al. TIMP-2 over-expression reduces invasion and angiogenesis and protects B16F10 melanoma cells from apoptosis. Int J Cancer 1998; 75:246–53.
[34] Costa S, Planchenault T, Charriere-Bertrand C, Mouchel Y, Fages C, Juliano S, et al. Astroglial permissivity for neuritic outgrowth in neuron-astrocyte cocultures depends on regulation of laminin bioavailability. Glia 2002;37:105–13.

# Sensitivity to Oxidative Stress in DJ-1-Deficient Dopamine Neurons: An ES-Derived Cell Model of Primary Parkinsonism

**Cecile Martinat[1☯], Shoshana Shendelman[1☯], Alan Jonason[1☯], Thomas Leete[1], M. Flint Beal[2], Lichuan Yang[2], Thomas Floss[3], Asa Abeliovich[1*]**

1 Departments of Pathology and Neurology, Center for Neurobiology and Behavior, and Taub Institute, Columbia University, New York, New York, United States of America, 2 Department of Neurology and Neuroscience, Weill Medical College of Cornell University, New York, New York, United States of America, 3 Institute of Developmental Genetics, GSF-National Research Center for Environment and Health, Neuherberg, Germany

**The hallmark of Parkinson's disease (PD) is the selective loss of dopamine neurons in the ventral midbrain. Although the cause of neurodegeneration in PD is unknown, a Mendelian inheritance pattern is observed in rare cases, indicating a genetic factor. Furthermore, pathological analyses of PD substantia nigra have correlated cellular oxidative stress and altered proteasomal function with PD. Homozygous mutations in *DJ-1* were recently described in two families with autosomal recessive Parkinsonism, one of which is a large deletion that is likely to lead to loss of function. Here we show that embryonic stem cells deficient in DJ-1 display increased sensitivity to oxidative stress and proteasomal inhibition. The accumulation of reactive oxygen species in toxin-treated DJ-1-deficient cells initially appears normal, but these cells are unable to cope with the consequent damage that ultimately leads to apoptotic death. Furthermore, we find that dopamine neurons derived from in vitro–differentiated DJ-1-deficient embryonic stem cells display decreased survival and increased sensitivity to oxidative stress. These data are consistent with a protective role for DJ-1, and demonstrate the utility of genetically modified embryonic stem cell–derived neurons as cellular models of neuronal disorders.**

Citation: Martinat C, Shendelman S, Jonason A, Leete T, Beal MF, et al. (2004) Sensitivity to oxidative stress in DJ-1-deficient dopamine neurons: An ES-derived cell model of primary parkinsonism. PLoS Biol 2(11): e327.

## Introduction

Parkinson's disease (PD) is a progressive neurodegenerative disorder characterized by rigidity, slowed movement, gait difficulty, and tremor at rest (Dauer and Przedborski 2003). The pathological hallmark of PD is the relatively selective loss of dopamine neurons (DNs) in the substantia nigra pars compacta in the ventral midbrain. Although the cause of neurodegeneration in PD is unknown, a Mendelian inheritance pattern is observed in approximately 5% of patients, suggesting a genetic factor. Extremely rare cases of PD have been associated with the toxin 1-methyl-4-phenyl-1,2,3,6-tetrahydropyridine, which is taken up specifically by DNs through the dopamine transporter and is thought to induce cellular oxidative stress. Population-based epidemiological studies have further supported roles for genetic and environmental mechanisms in the etiology of PD (Dauer and Przedborski 2003; Jenner 2003).

The identification of several genes that underlie familial forms of PD has allowed for the molecular dissection of mechanisms of DN survival. Autosomal dominant mutations in *α-synuclein* lead to a rare familial form of PD (Polymeropoulos et al. 1997), and there is evidence that these mutations generate toxic, abnormal protein aggregates (Goldberg and Lansbury 2000) and cause proteasomal dysfunction (Rideout et al. 2001). A majority of patients with sporadic PD harbor prominent intracytoplasmic inclusions, termed Lewy bodies, enriched for α-synuclein (Spillantini et al. 1998), as well as neurofilament protein (Trojanowski and Lee 1998). Mutations in a second gene, *Parkin*, lead to autosomal recessive PD (Hattori et al. 2000). Parkin is a ubiquitin ligase that appears to participate in the proteasome-mediated degradation of several substrates (Staropoli et al. 2003).

Homozygous mutations in a third gene, *DJ-1*, were recently associated with autosomal recessive primary parkinsonism (Bonifati et al. 2003). *DJ-1* encodes a ThiJ domain protein of 189 amino acids that is broadly expressed in mammalian tissues (Nagakubo et al. 1997). Interestingly, DJ-1 was independently identified in a screen for human endothelial cell proteins that are modified with respect to isoelectric point in response to sublethal doses of paraquat (Mitsumoto and Nakagawa 2001; Mitsumoto et al. 2001), a toxin that generates reactive oxygen species (ROS) within cells and has

Received April 28, 2004; Accepted July 29, 2004; Published October 5, 2004
DOI: 10.1371/journal.pbio.0020327



Abbreviations: 6-OHDA, 6-hydroxydopamine; DAT, dopamine transporter; DHR, dihydrorhodamine-123; DIV, d in vitro; DN, dopamine neuron; E[number], embryonic day [number]; ES, embryonic stem; FACS, fluorescence-activated cell sorter; MTT, 3-(4,5-dimethylthiazol-2-yl)-2,5-diphenyltetrazolium bromide; PARP, poly(ADP-ribose)polymerase-1; PI, propidium iodide; PD, Parkinson's disease; RNAi, RNA interference; ROS, reactive oxygen species; SDIA, stromal cell–derived inducing activity; SEM, standard error of the mean; shRNA, short hairpin RNA; TH, tyrosine hydroxylase; WT, wild-type

Academic Editor: Huda Y. Zoghbi, Baylor College of Medicine

*To whom correspondence should be addressed. E-mail: aa900@columbia.edu

☯These authors contributed equally to this work.

been associated with DN toxicity (McCormack et al. 2002). Gene expression of a yeast homolog of DJ-1, YDR533C, is upregulated in response to sorbic acid (de Nobel et al. 2001), an inducer of cellular oxidative stress. These results suggest a causal role for DJ-1 in the cellular oxidative stress response.

Surprisingly, animal models that harbor genetic lesions that mimic inherited forms of human PD, such as homozygous deletions in *Parkin* (Goldberg et al. 2003; Itier et al. 2003) or overexpression of α-synuclein (Masliah et al. 2000; Giasson et al. 2002; Lee et al. 2002), have failed to recapitulate the loss of dopamine cells. An alternative approach, the genetic modification of midbrain DNs in vitro (Staropoli et al. 2003), is potentially useful but limited by the difficulty and variability in culturing primary postmitotic midbrain neurons. Other studies have focused on immortalized tumor cell lines, such as neuroblastoma cells, but these may not accurately model the survival of postmitotic midbrain neurons.

Here we show that DJ-1-deficient cells display increased sensitivity to oxidative stress. DNs appear to be particularly sensitive to the loss of DJ-1. The initial accumulation of ROS is normal in DJ-1-deficient cells, but subsequent cellular defenses to ROS are impaired, leading to increased apoptosis.

## Results

### Generation of DJ-1-Deficient ES Cells

To investigate the normal cellular function of DJ-1 and the pathogenic mechanism of the PD mutations, we generated cells deficient in DJ-1. A murine embryonic stem (ES) cell clone, F063A04, that harbors a retroviral integration at the *DJ-1* locus was obtained through the German Gene Trap Consortium (http://tikus.gsf.de) (Figure 1A; Floss and Wurst 2002). This integration is predicted to disrupt the normal splicing of *DJ-1*, leading to the generation of a truncated protein that lacks the carboxy-terminal domain required for dimerization and stability (unpublished data). Of note, a mutation that encodes a similarly truncated protein (at the human *DJ-1* exon 7 splice acceptor) has been described in a patient with early-onset PD (Hague et al. 2003).

To generate ES cell subclones homozygous for the trapped *DJ-1* allele, clone F063A04 was exposed to a high dose of the antibiotic G418, which selects cells that are homozygous for the neomycin resistance gene insertion (Mizushima et al. 2001). Several homozygous mutant ES cell subclones (that had undergone gene conversion at the *DJ-1* locus) were identified by Southern blotting (Figure 1B). To confirm that the trapped allele leads to the loss of wild-type (WT) DJ-1 protein, cell lysates from homozygous DJ-1-deficient (also termed "knockout" here) ES cell clones as well as the parental heterozygous clone were analyzed by Western blotting using polyclonal antibodies to the amino-terminal region of DJ-1 (amino acids 64–82) or full-length DJ-1 protein (unpublished data). Neither full-length nor truncated DJ-1 protein products were detected in knockout clones (Figure 1C), consistent with instability of the predicted truncated DJ-1 product. In addition, no full-length *DJ-1* RNA was detected in cultures of knockout cells (Figure S1). In contrast, heterozygous and WT ES cells express high levels of DJ-1. Initial phenotypic analysis of knockout subclones indicated that DJ-1 is not essential to the growth rate of ES cells in culture, consistent with the viability of humans homozygous for *DJ-1* mutations.

### DJ-1 Protects Cells from Oxidative Stress and Proteasomal Inhibition

DJ-1 has been hypothesized to function in the cellular response to oxidative stress. To investigate the role of DJ-1 in the oxidative stress response in vivo, DJ-1-deficient knockout and heterozygous ES cell clones were analyzed for cell viability in the context of increasing concentrations of $H_2O_2$. Heterozygous cells were used as controls because the knockout subclones were derived from these. Cell viability was initially determined by MTT assay (which detects reduction of 3-(4,5-dimethylthiazol-2-yl)-2,5-diphenyltetrazolium bromide [MTT] by metabolic enzymes) in triplicate (Fezoui et al. 2000). Exposure to $H_2O_2$ led to significantly greater toxicity in the DJ-1-deficient cells; similar results were obtained with multiple knockout subclones in independent experiments (Figures 1D and 2A). In contrast, in the absence of toxin, heterozygous and knockout cells displayed comparable viability in the MTT assay (Figure S2). Consistent with the MTT assay, fluorescence-activated cell sorting (FACS) analysis of cells stained with annexin V (AV) and propidium iodide (PI) revealed increased death of knockout cells compared to heterozygous cells in the context of $H_2O_2$ exposure (Figure 1E). The increase in AV-positive cells implicated an apoptotic mechanism of cell death (Figure 1F). Furthermore, when exposed to $H_2O_2$, knockout cells displayed potentiated cleavage of poly(ADP-ribose)polymerase-1 (PARP) in a pattern indicative of an apoptotic death program (Gobeil et al. 2001) (Figure 1G).

Additional toxin exposure studies demonstrated that DJ-1-deficient cells were sensitized to the proteasomal inhibitor lactacystin (Figure 2B), as well as to copper (Figure S2), which catalyzes the production of ROS. We did not observe altered sensitivity to several other toxins, including tunicamycin (an inducer of the unfolded protein response in the endoplasmic reticulum; Figure 2C), staurosporine (a general kinase inhibitor that induces apoptosis) (Figure S2), or cycloheximide (an inhibitor of protein translation) (unpublished data).

### WT but Not PD-Associated L166P Mutant DJ-1 Protects Cells from Oxidative Stress

To confirm that altered sensitivity to oxidative stress is a consequence of the loss of DJ-1, we performed rescue experiments by overexpressing WT or mutant human DJ-1 in knockout ES cells. Plasmids encoding human Flag-tagged WT DJ-1, Flag-tagged PD-associated L166P mutant DJ-1, or vector alone, were transiently transfected into DJ-1-deficient clones, and these were subsequently assayed for sensitivity to $H_2O_2$ using the MTT viability assay. DJ-1-deficient cells transfected with a vector encoding Flag-WT human DJ-1 were effectively rescued in terms of viability in the presence of $H_2O_2$ (Figure 2D); Thus, viability in rescued knockout cells mimicked the viability of untransfected heterozygous cells in the context of $H_2O_2$ treatment (Figure 2A and 2D). In contrast, transfection of knockout cells with a vector encoding the PD-associated L166P mutant DJ-1 did not significantly increase the viability of $H_2O_2$-treated knockout cells (Figure 2D). Baseline cell viability in the absence of toxin exposure was not altered by DJ-1 overexpression, and Western blotting of lysates from transfected cells with an antibody specific to human DJ-1 demonstrated that trans-

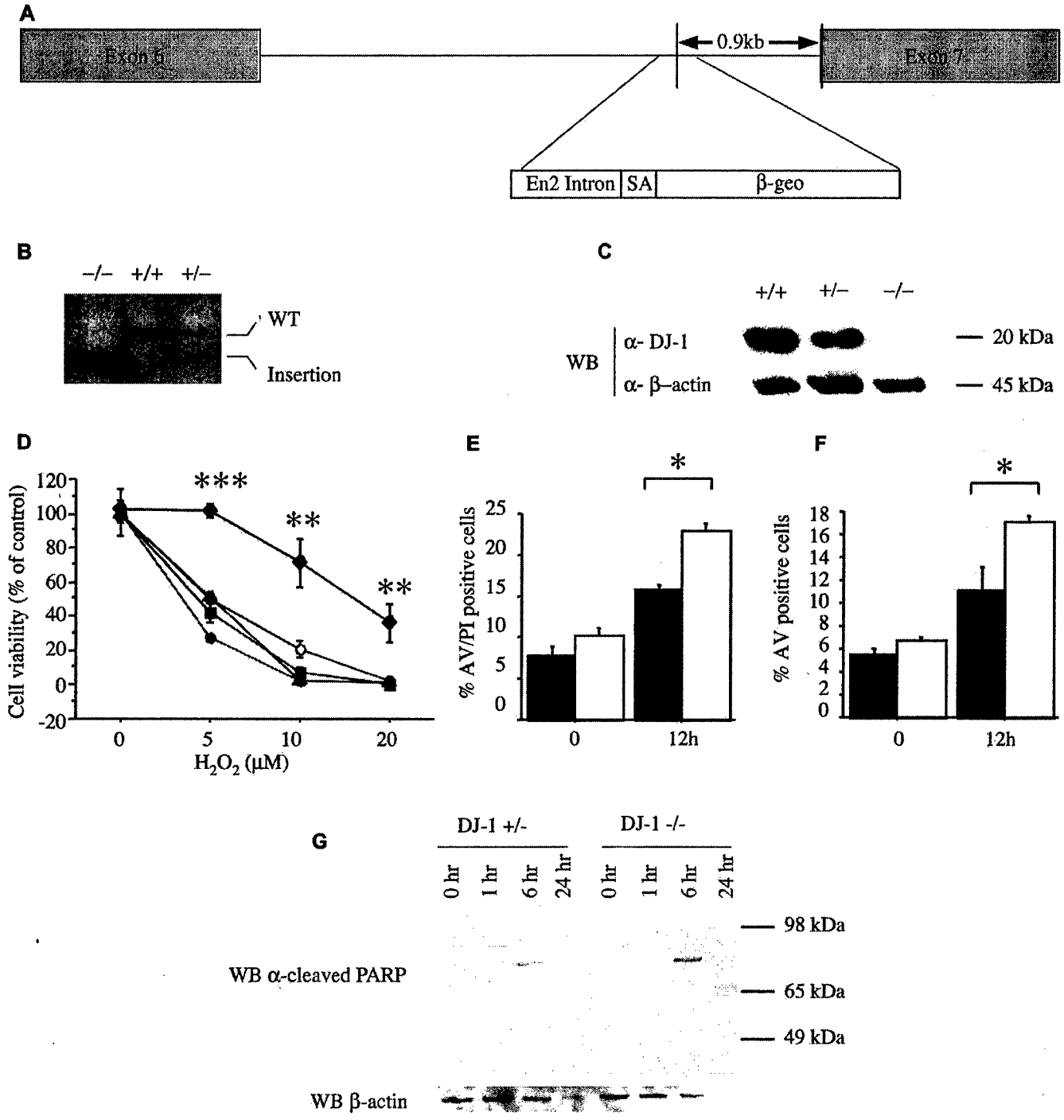


**Figure 1.** DJ-1-Deficient ES Cells Are Sensitized to Oxidative Stress

(A) Schematic map of the murine *DJ-1* gene in clone F063A04. The retroviral insertion places the engrailed-2 (En2) intron, the splice acceptor (SA), and the β-galactosidase/neomycin resistance gene fusion (β-geo) between exons 6 and 7.

(B) Southern blot analysis of KpnI-digested genomic DNA from *DJ-1* homozygous mutant (−/−), WT (+/+), and heterozygous (+/−)cells, probed with murine *DJ-1* cDNA. WT DNA shows a predicted 14-kb band (WT), whereas the mutant allele migrates as a 9-kb band (insertion).

(C) Western blot (WB) of ES cell lysates from WT (+/+), *DJ-1* heterozygous (+/−), and mutant homozygous (−/−) clones with antibodies to murine DJ-1 (α-DJ-1) or β-actin (α-β-actin). DJ-1 migrates at 20 kDa, β-actin at 45 kDa.

(D) ES cells were exposed to 0, 5, 10, and 20 μM $H_2O_2$ for 15 h and viability was assayed by MTT. Responses of *DJ-1* heterozygous cells (diamonds) and *DJ-1* knockout clones 9 (open circles), 16 (solid circles), 23 (squares), and 32 (triangles) are shown. ** $p \leq 0.01$; *** $p \leq 0.0001$.

(E and F) Cell death of *DJ-1* heterozygous and DJ-1-deficient cells (clone 32) after exposure to $H_2O_2$ (10 μM) was quantified by staining with PI and an antibody to AV with subsequent FACS analysis. AV staining marks cells undergoing apoptosis, whereas PI staining indicates dead cells. * $p \leq 0.05$.

(G) *DJ-1* heterozygous (+/−) and knockout (clone 32; −/−) cells were assayed at 1, 6, and 24 h after treatment with 10 μM $H_2O_2$ by Western blotting for cleaved PARP (89 kDa), which indicates apoptosis. No band is seen for cleaved PARP or β-actin for the DJ-1-deficient cells at 24 h due to cell death. Data represent means ± standard error of the mean (SEM) and were analyzed by ANOVA with Fisher's post-hoc test.

DOI: 10.1371/journal.pbio.0020327.g001

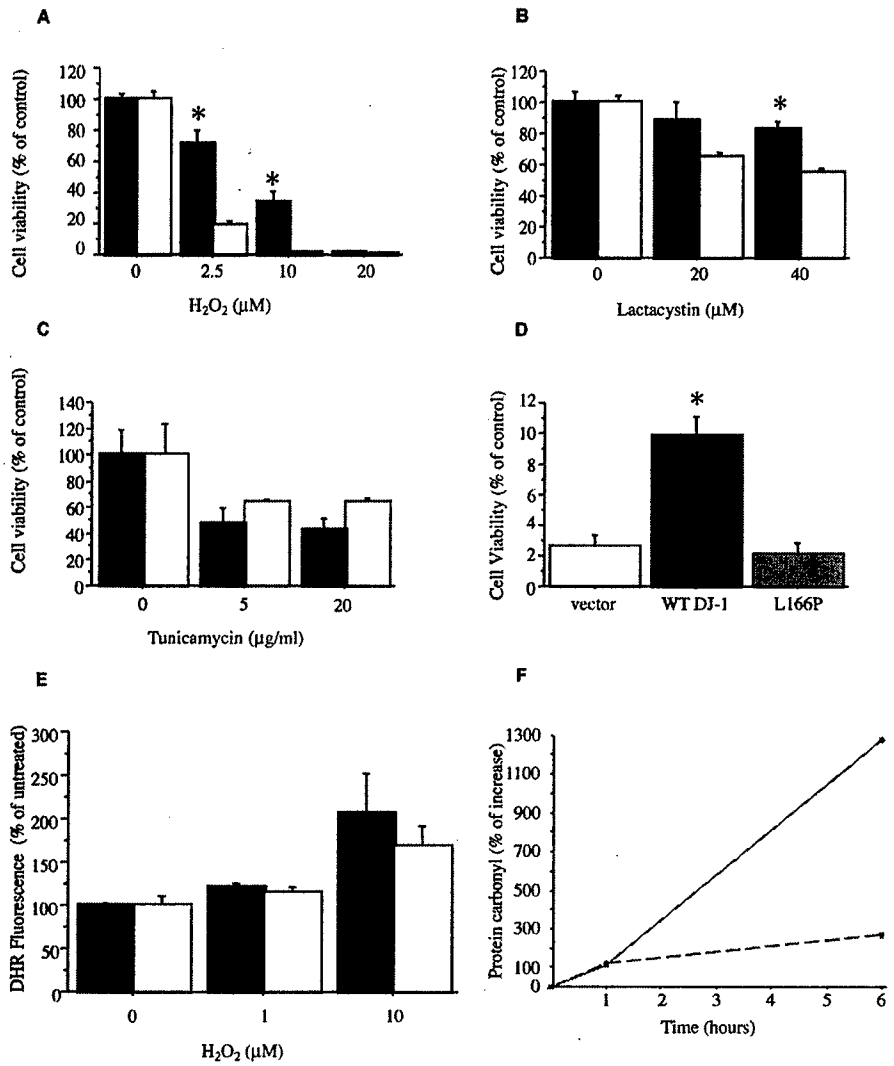


**Figure 2.** Specificity and Mechanism of Altered Toxin Sensitivity in DJ-1-Deficient Cells

(A–C) Cell viability of *DJ-1* heterozygous cells (solid bar) and DJ-1-deficient knockout clone 32 cells (open bar) after 15 h exposure to $H_2O_2$ (A), lactacystin (B), or tunicamycin (C) as assayed by MTT reduction. * $p \leq 0.05$.

(D) DJ-1-deficient knockout cells (clone 32) were transiently transfected with plasmids containing WT human DJ-1 vector (solid bar) and PD-associated L166P mutant DJ-1 vector (gray bar); as a control, knockout cells were also transfected with vector alone (open bar). 48 h after transfection, cells were exposed to 10 μM $H_2O_2$ for 15 h and then assayed by MTT reduction. WT human DJ-1 significantly enhanced survival of the knockout cells, whereas the L166P mutant did not. Similar results were obtained at 20 μM $H_2O_2$ and with a second DJ-1-deficient clone (unpublished data). Transfection efficiency exceeded 90% in all cases and protein expression level was comparable for human WT and L166P mutant DJ-1 as determined by Western blotting (Figure S1). * $p \leq 0.05$.

(E) DJ-1-deficient cells (clone 32; open bar) and control heterozygous cells (solid bar) were assayed for intracellular formation of ROS in response to $H_2O_2$ treatment (15 min, 1 or 10 μM) using DHR and FACS analysis.

(F) Protein carbonyl levels were measured by spectrophotometric analysis of DNP-conjugated lysates from DJ-1-deficient (clone 32; solid red line) and control heterozygous cells (dashed blue line). Data are shown as the mean ± SEM and were analyzed by ANOVA with Fisher's post-hoc test.

DOI: 10.1371/journal.pbio.0020327.g002

fected Flag-WT DJ-1 and Flag-L166P mutant DJ-1 accumulated comparably (Figure S2).

## DJ-1 Deficiency Does Not Alter the $H_2O_2$-Induced Intracellular ROS Burst

We hypothesized that DJ-1 either alters the initial accumulation of intracellular ROS in response to $H_2O_2$ exposure, or that it functions downstream of the ROS burst and protects cells from consequent damage. Therefore, we quantified the accumulation of ROS in response to $H_2O_2$ treatment in knockout and heterozygous cells using the ROS-sensitive fluorescent indicator dye dihydrorhodamine-123 (DHR) and FACS analysis. Initial ROS accumulation (at 15 min after stimulation) appeared unaltered in the DJ-1-deficient cells in comparison to control heterozygous cells (Figure 2E). Consistent with this, accumulation of protein carbonyls, an index of oxidative damage to proteins (Sherer et al. 2002), appeared normal initially (at 1 h after toxin exposure; Figure 2F). However, at 6 h after toxin exposure, a point at which knockout cells already display increased apoptosis (as indicated by PARP cleavage; see Figure 1G), protein carbonyl accumulation was robustly increased in the DJ-1-deficient cells. These data suggest that initial ROS accumulation is not altered by DJ-1 deficiency, but that the mutant cells are unable to appropriately cope with the consequent damage. Consistent with this result, no antioxidant or peroxiredoxin activity with purified DJ-1 protein in vitro was detected (S.S. and A.A., personal communication).

## DJ-1 Is Required for Survival of ES Cell–Derived DNs

Several methods have been established for the differentiation of ES cells into DNs in vitro (Morizane et al. 2002). To extend our analysis of DJ-1 function to DNs, we differentiated DJ-1-deficient ES cells or control heterozygous cells into DNs in vitro by coculture with stromal cell–derived inducing activity (SDIA; Figure 3A) (Morizane et al. 2002; Barberi et al. 2003). DNs were quantified by immunohistochemistry for tyrosine hydroxylase (TH; a marker for DNs and other catecholaminergic cells), or by analysis of dopamine transporter uptake activity (a quantitative DN marker) (Han et al. 2003). Production of DNs appeared to be significantly reduced in knockout ES cell cultures compared to parental heterozygous cultures at 18 days in vitro (DIV) as determined by both dopamine uptake

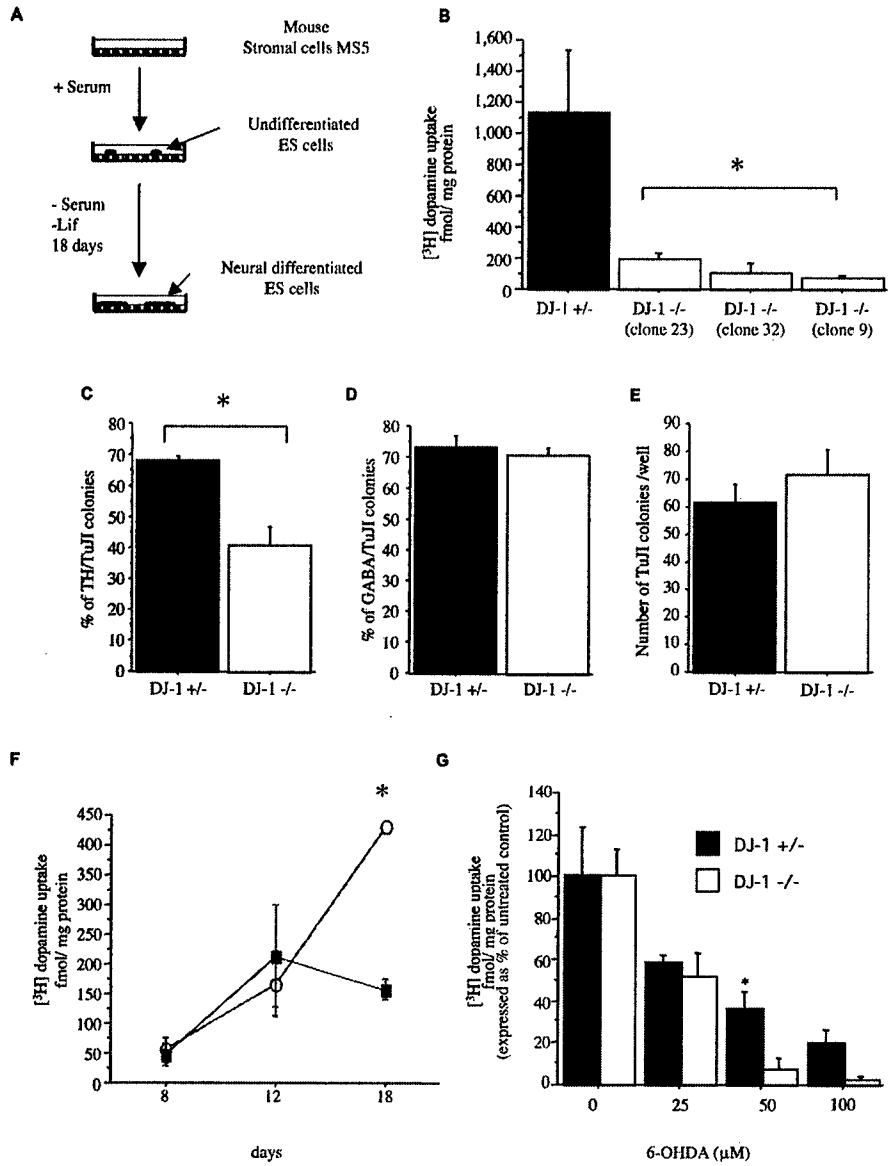


**Figure 3.** DJ-1-Deficient ES Cell Cultures Display Reduced DN Production

(A) The SDIA coculture method. *DJ-1* knockout or control heterozygous ES cells are cocultured with mouse stromal cells (MS5) in the absence of serum and leukemia inhibitory factor for 18 DIV.
(B) DN production was quantified at 18 DIV by $^{3}$H-dopamine uptake assay. DJ-1-deficient ES cell cultures were defective relative to heterozygous control cultures.
(C–D) Neuron production was quantified by immunohistochemical analysis as a percent of TuJ1-positive colonies that express TH (C) or GABA (D). Quantification of TH and GABA immunostaining was performed on all colonies in each of three independent wells. Colonies were scored as positive if any immunostained cells were present. * $p \leq 0.05$.
(E) The absolute number of TuJ1-positive colonies was not significantly different between the two genotypes.
(F) Kinetic analysis of DN differentiation in DJ-1-deficient cultures (clone 32, solid square) and heterozygous controls (open circle) as quantified by $^{3}$H-dopamine uptake assay. * $p \leq 0.05$.
(G) DJ-1-deficient (open bar) and heterozygous control (closed bar) cultures differentiated for 9 DIV and then exposed to 6-OHDA at the indicated dose for 72 h. DNs were quantified by $^{3}$H-dopamine uptake assay. Data represent the means ± SEM and were analyzed by ANOVA followed by Fisher's post-hoc test. * $p \leq 0.05$.
DOI: 10.1371/journal.pbio.0020327.g003

and TH immunoreactivity (Figures 3B and 3C; 4A–4L). In contrast, general neuronal production did not appear altered in this assay in terms of the postmitotic neuronal marker TuJ1 (a monoclonal antibody specific to neuronal, not glial, class III β-tubulin) (Figures 3E and 4A–4L′); other neuronal subtypes also appeared normal, including GABAergic (Figures 3D and 4A′–4L′) and motor neurons (HB9-positive; Figure S3). To investigate whether the reduction in DNs in DJ-1-deficient cultures is due to defective generation or survival, a time course analysis was performed. At early time points (8 and 12 DIV), dopamine uptake activity was comparable in WT and DJ-1-deficient cultures, whereas subsequently the DJ-1-deficient cultures appeared defective (Figure 3F). Consistent with this, intracellular dopamine accumulation (as quantified using high-performance liquid chromatography) was significantly reduced in DJ-1-deficient cultures (6.4 ± 1.5 ng dopamine/mg protein) relative to control heterozygous cultures (66.0 ± 17.4 ng/mg) at 35 DIV. These data strongly suggest that DJ-1 deficiency leads to loss of DNs, rather than simply to downregulation of cell marker expression.

We hypothesized that DJ-1-deficient DNs may be sensitized to oxidative stress, akin to DJ-1-deficient undifferentiated ES cells. To test this, DN cultures from DJ-1-

**Figure 4.** Neuronal Differentiation of DJ-1-Deficient and Control Heterozygous ES Cell Cultures

(A–L) *DJ-1* heterozygous (+/–; A–F) and knockout (–/– [clone 32]; G–L) cultures were differentiated by SDIA for 18 DIV and immunostained with antibodies to TH (green) and TuJ1 (red). Images of both (Merge) are also shown.
(A′–L′) Immunostaining of *DJ-1* heterozygous (+/–, A′–F′) and deficient (–/–, G′–L′) cultures with antibodies for GABA (green) and TuJ1 (red). Scale bar, 50 μm. Images of both (Merge) are also shown.
DOI: 10.1371/journal.pbio.0020327.g004

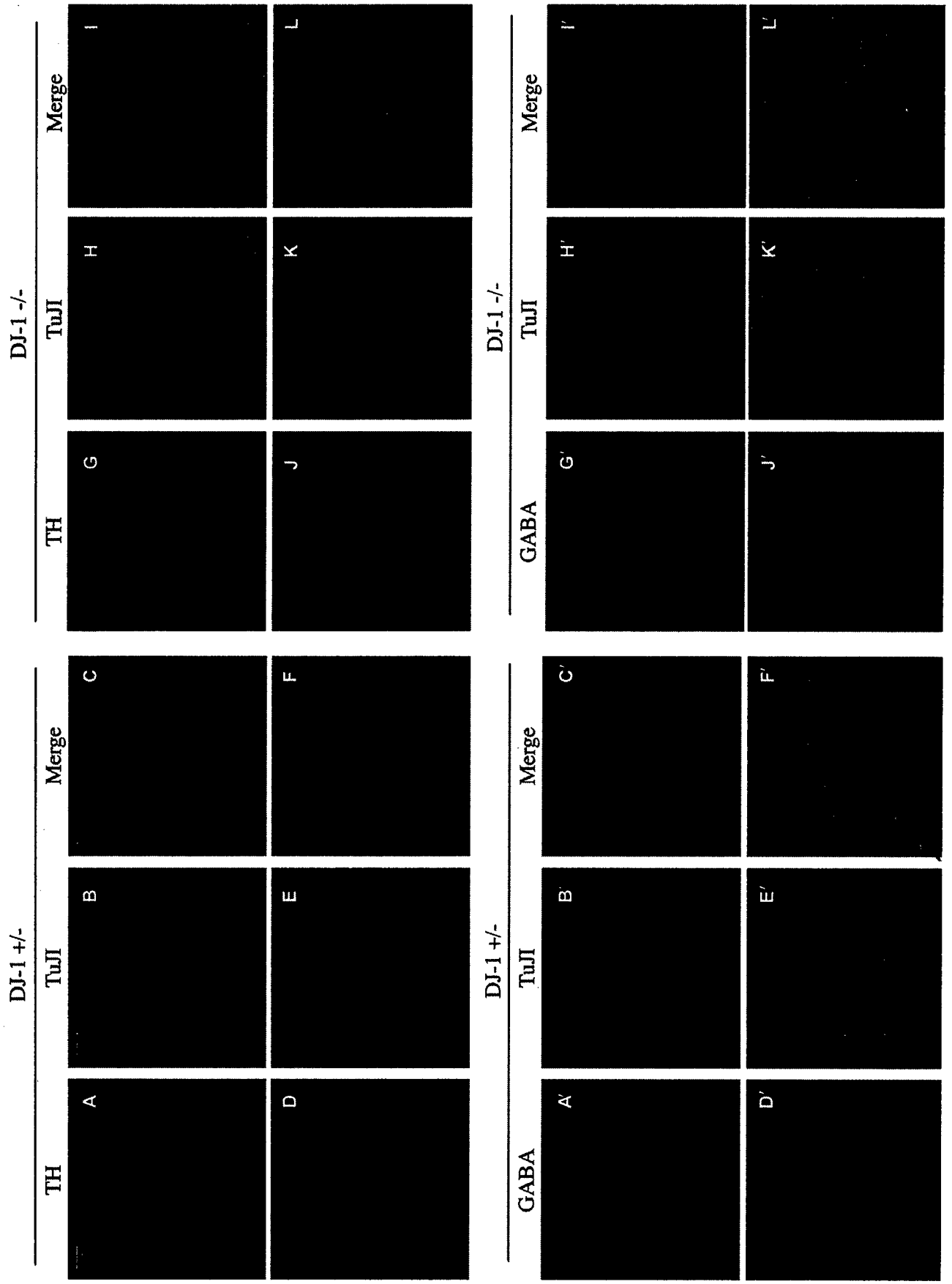
DJ-1 +/-
TH
TuJI
Merge
A
B
C
D
E
F
DJ-1 -/-
TH
TuJI
Merge
G
H
I
J
K
L
DJ-1 +/-
GABA
TuJI
Merge
A'
B'
C'
D'
E'
F'
DJ-1 -/-
GABA
TuJI
Merge
G'
H'
I'
J'
K'
L'

deficient or heterozygous control ES cell cultures at 9 DIV were exposed to oxidative stress in the form of 6-hydroxydopamine (6-OHDA), a DN-specific toxin that enters DNs through the dopamine transporter and leads to oxidative stress and apoptotic death (Dauer and Przedborski 2003). DJ-1-deficient DNs displayed an increased sensitivity to oxidative stress in this assay (Figure 3G). Post-hoc analysis of the data indicates that the difference among genotypes is maximal at an intermediate dose of toxin (50 μM); at the highest dose of 6-OHDA employed (100 μM), the difference is lessened (because the heterozygote is increasingly affected as well), indicating that DJ-1-mediated protection is limited. Although we cannot exclude a role for DJ-1 in the late-stage differentiation of DNs, these data suggest that DJ-1 deficiency leads to reduced DN survival and predisposes these cells to endogenous and exogenous toxic insults.

## RNAi "Knockdown" of DJ-1 in Midbrain Embryonic DNs Leads to Increased Sensitivity to Oxidative Stress

To confirm the role of DJ-1 in primary midbrain DNs, DJ-1 expression was inhibited by RNA interference (RNAi) in embryonic day 13.5 (E13.5) murine primary midbrain cultures by lentiviral transduction of short hairpin RNAs (shRNAs) (Figure 5) (Rubinson et al. 2003). E13.5 midbrain cultures (Staropoli et al. 2003) were transduced with a lentiviral vector that includes a gene encoding the green fluorescent protein marker eGFP, along with shRNAs

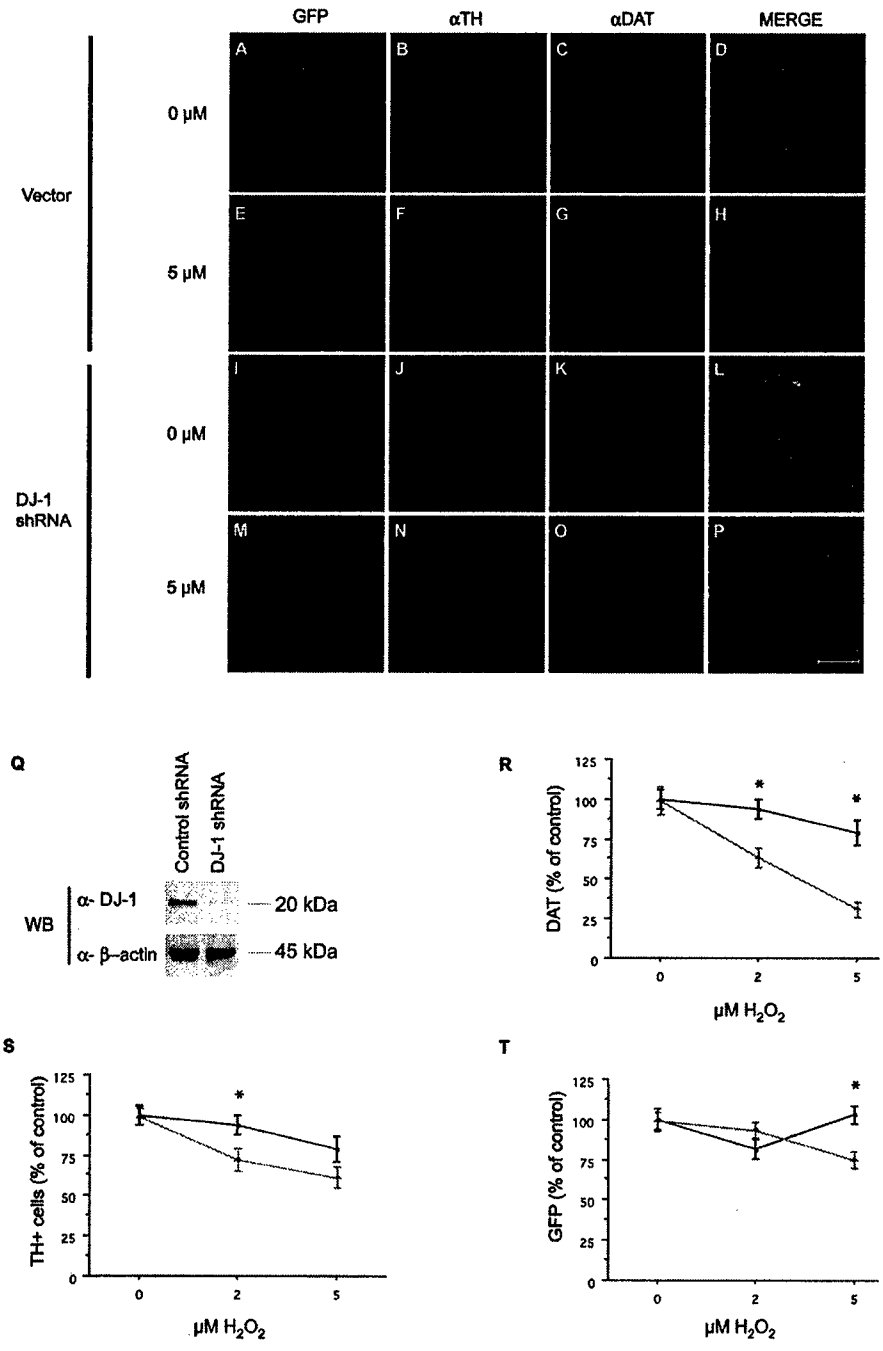


**Figure 5.** RNAi "Knockdown" of *DJ-1* in Primary Embryonic Midbrain DNs Display Increased Sensitivity to Oxidative Stress

(A–P) Primary midbrain cultures from E13.5 embryos were infected with lentiviral vectors encoding *DJ-1* shRNA (or vector alone) under the regulation of the control vector (A–H) or the U6 promoter (I–P). Cells were cultured for 1 wk after infection and then exposed to $H_2O_2$ (5 μM; E–H and M–P) for 24 h. Cultures were immunostained for TH (B, F, J, and N) or DAT (C, G, K, or O) and visualized by confocal microscopy. Images containing all stains are included (Merge; D, H, L, and P). Scale bar, 100 μm.

(Q) Cell lysates prepared from midbrain primary cultures infected with *DJ-1* shRNA lentivirus (or control vector) were analyzed by Western blotting for murine DJ-1 or β-actin.

(R–T) Quantification of TH, DAT, and GFP signal was performed on ten randomly selected fields in each of three wells for each condition. Red triangles, *DJ-1* shRNA treated; black circles, control vector. Data represent the means ± SEM and were analyzed by ANOVA followed by Fisher's post-hoc test. * $p \leq 0.05$.

DOI: 10.1371/journal.pbio.0020327.g005

homologous to murine *DJ-1*. *DJ1*-shRNA virus-infected cells displayed efficient silencing of *DJ-1* gene expression to 10%–20% of control vector-infected cultures (as determined by Western blotting [Figure 5Q]). Transduction efficiency, as assessed by visualization of the fluorescent eGFP marker, exceeded 95% in all cases (Figure 5I and unpublished data). After 7 DIV, cultures were exposed to $H_2O_2$ for 24 h and then evaluated for DN survival as quantified by immunostaining for TH and dopamine transporter (DAT).

Midbrain cultures transduced with *DJ-1* shRNA virus and with control vector displayed similar numbers of TH-positive neurons in the absence of exposure to $H_2O_2$ (Figure 5A–D, 5I–L, and 5R–S). In contrast, in the presence of $H_2O_2$, DJ-1-deficient cultures displayed significantly reduced DN survival as quantified by immunohistochemistry for TH or DAT (Figure 5E–H, 5M–P, 5R–S). These studies were repeated three times with similar results. The reduction in DAT immunoreactivity appears to be more robust than the reduction in TH-positive cell number in the context of $H_2O_2$; this may reflect the differential localization of DAT to DN processes, whereas TH is primarily in the cell body. As we described in a previous manuscript, nondopaminergic cells in the E13.5 primary midbrain cultures are predominantly GABAergic neurons (90%–95%) (Staropoli et al. 2003). Total embryonic midbrain neurons transduced with either *DJ-1* shRNA or vector displayed comparable survival in the context of toxin exposure, suggesting that DJ-1 deficiency leads to a relatively specific alteration in DN survival (Figure 5T). These data are consistent with the analyses of ES cell–derived DNs above and indicate that DJ-1 is required for the normal survival of midbrain DNs in the context of toxin exposure.

## Discussion

In this study we present evidence that DJ-1 is an essential component of the oxidative stress response of DNs. DJ-1-deficient cells display an apparently normal initial burst of ROS in response to $H_2O_2$, but they are unable to cope with the consequent toxicity, culminating in apoptosis. Additionally, we find that DJ-1 deficiency sensitizes cells to the proteasomal inhibitor lactacystin but not other toxic stimuli such as tunicamycin. Proteasomal inhibition induces the accumulation of short-lived and misfolded cytoplasmic proteins, leading to oxidative stress and apoptosis (Demasi and Davies 2003). ROS and proteasomal inhibition have previously been correlated with PD pathology (Dauer and Przedborski 2003), and it is therefore tempting to hypothesize that *DJ-1* mutations lead to PD because of an increased sensitivity to such stressors.

The apparent cell-type specificity of DN impairment in patients with the Parkinsonism-associated *DJ-1* mutation is not predicted by the ubiquitous expression of DJ-1 (Nagakubo et al. 1997). In this study, we find that DJ-1 protects both dopaminergic and nondopaminergic cells from oxidative insult. However, DJ-1-deficient DNs appear to be especially sensitive to oxidative insult, suggesting relative cell-type specificity to the consequences of DJ-1 deficiency. Similar results are observed in DJ-1-knockout ES cell–derived DNs (which are devoid of any detectable DJ-1) and in primary DNs with DJ-1 levels reduced by RNAi "knockdown." However, we find that even in the absence of exogenous toxin exposure, the knockout ES cell–derived DNs display reduced survival, whereas survival of the primary embryonic midbrain RNAi knockdown DNs appears to be similar to WT cells. We hypothesize that this discrepancy reflects the activity of residual DJ-1 (approximately 10%–20%) in the RNAi knockdown cultures. Alternatively, the knockout ES cell–derived DNs may be exposed to a greater degree of oxidative stress in vitro than are the knockdown-derived DNs even in the absence of added toxin. The mechanism by which DNs are preferentially targeted for destruction in the absence of DJ-1 is unclear. It has been proposed that DNs are subject to high levels of endogenous oxidative stress that may relate to dopamine metabolism (Jenner and Olanow 1998).

DJ-1 is structurally modified in the context of cellular oxidative stress (Mitsumoto and Nakagawa 2001), suggesting a possible function. Two recent studies (Yokota et al. 2003; Taira et al. 2004) investigated the role of DJ-1 in the oxidative stress response of neuroblastoma tumor cells. Both studies used RNAi to perturb the expression of DJ-1 in neuroblastoma tumor cell lines, and suggested that DJ-1 deficiency sensitizes cells to oxidative stress; these results are consistent with our data. Taira et al. (2004) further reported that overexpression of DJ-1 in neuroblastoma cells leads to a reduction in ROS accumulation and hypothesized that DJ-1 may harbor antioxidant activity in vivo. In contrast, we find that ES cells that are deficient in DJ-1 display a normal initial burst of ROS in the context of $H_2O_2$. Consistent with this, we fail to detect DJ-1 antioxidant activity in vitro (Shendelman et al. 2004).

Finally, this study presents a novel, ES cell-based genetic approach to the study of neurodegenerative disorders. Mouse genetic models of disease are often limited by the inherent variability of animal experiments, the limited mouse life span, and the difficulties in manipulating whole animals. For instance, genetic rescue experiments and toxicological dose-response studies are impractical in whole animals. Furthermore, genetic cell models are more readily amenable to molecular dissection of disease mechanisms than are whole animals. Thus, genetically altered, ES cell–derived neurons are likely to be generally useful as cellular models of neurodegenerative disorders. Future studies may also utilize available human ES cells to investigate species differences.

## Materials and Methods

**Cell culture.** Undifferentiated ES cells were cultured using standard techniques (Abeliovich et al. 2000). SDIA differentiation of ES cell cultures to DNs was performed as described in Kawasaki et al. (2000), except that ES cells were plated at a density of 500 cells/cm$^2$ rather than approximatively 1,000 cells/cm$^2$, and were cocultured with the MS5 mouse stromal cell line (Barberi et al. 2003). For rescue experiments, cells were plated at a cell density of $1.4 \times 10^6$ cells/well. Transfections with plasmids encoding human Flag-WT DJ-1, PD-associated L166P mutant DJ-1, or vector alone, were performed using Lipofectamine 2000 (Life Technologies) for 18–36 h according to the manufacturer's instructions (Staropoli et al. 2003). 24 hours post-transfection, cells were split into 96-well plates and treated as described below. Primary cultures and lentiviral transductions were performed as described in Staropoli et al. (2003).

**Generation of knockout ES cell clones.** The pT1ATGβgeo gene trap vector, which includes βgeo, a fusion of the genes for β-galactosidase and neomycin resistance, is present between exons 6 and 7 of the murine *DJ-1* gene, as determined by cDNA sequencing of trapped transcripts and genomic analysis (Figure 1A). To select for ES cell subclones homozygous for the trapped *DJ-1* allele, we treated clone F063A04 with 4 mg/ml G418. Several subclones that were homozygous for the mutant *DJ-1* allele were identified by Southern blotting (see Figure 1B), and three were chosen for further experimentation:

clones 9, 23, and 32. To confirm that the trapped allele leads to the loss of wild-type (WT) DJ-1 protein, cell lysates from these clones, as well as from the parental heterozygous clone, were analyzed by Western blotting using polyclonal antibodies to the amino-terminal region of DJ-1 or the full-length DJ-1 protein. For Western blotting, cells were resuspended in 50 mM Tris-HCl (pH 7.4), 150 mM NaCl, and 0.2% Triton X-100, and incubated at 4 °C, rotating for 20 min. Cleared lysate was prepared by centrifuging the lysate at 13,000 rpm for 10 min at 4 °C.

**Antibodies.** A rabbit polyclonal antibody to DJ-1 was generated against the synthetic polypeptide QNLSESPMVKEILKEQESR, which corresponds to amino acids 64–82 of the mouse DJ-1 protein. Antiserum was produced by the Polyquick polyclonal antibody production service of Zymed Laboratories (South San Francisco, California, United States). The antiserum was affinity-purified on a peptide-coupled Sulfolink column (Pierce Biotechnology, Rockford, Illinois, United States) according to the manufacturer's instructions. Antibody was used at a dilution of 1:200 for immunohistochemistry and Western blotting as described (Staropoli et al. 2003). Immunohistochemistry was performed with a rabbit polyclonal antibody to TH (PelFreez, Rogers, Arizona, United States; dilution 1:1000), the mouse monoclonal antibody to neuronal class III β-tubulin TuJ1 (Covance, Princeton, New Jersey, United States; dilution 1:500), and a rabbit polyclonal antibody to GABA (Sigma, St. Louis, Missouri, United States; dilution 1:1000). Western blotting was performed using a polyclonal antibody to cleaved PARP (Cell Signaling Technology, Beverly, Massachusetts, United States; dilution 1:500), a monoclonal antibody to DJ-1 (Stressgen Biotechnologies, San Diego, California, United States; dilution 1:1000), and a mouse monoclonal antibody to β-actin (Sigma, 1:500).

**In vivo assays.** ES cells plated in 96-well format ($2.3 \times 10^4$ cells/well) were treated for 15 h with $H_2O_2$ in ES cell medium deficient in β-mercaptoethanol (Abeliovich et al. 2000). Cell viability (as a percent of untreated control) was determined by MTT assay in triplicate (Fezoui et al. 2000). AV/PI (Molecular Probes, Eugene, Oregon, United States) staining was performed according to the manufacturer's instructions. For DHR staining (Molecular Probes) (Walrand et al. 2003), cells were preincubated for 30 min with DHR (5 μM), washed with PBS, then treated with $H_2O_2$ in ES cell medium deficient in β-mercaptoethanol for 15 min at 37 °C. The FACS analysis was performed using a FACSTAR sorter (Becton-Dickinson, Palo Alto, California, United States). Dopamine uptake assays were performed as described (Farrer et al. 1998). Reported values represent specific uptake from which nonspecific uptake, determined in the presence of mazindol, was subtracted. Uptake values were normalized for protein content with the BCA kit (Pierce).

For 6- hydroxydopamine (6-OHDA, Sigma) treatment, the drug was diluted in the differentiation medium (Kawasaki et al. 2000) and medium was changed every day for 72 h.

Primary midbrain embryonic cultures were prepared and transduced with lentiviral vectors as described in Staropoli et al. (2003). The *DJ-1* shRNA vector was generated by insertion of annealed oligonucleotides 5′-TGTCACTGTTGCAGGCTTGGTTCAAGAGACCAAGCCTGCAACAGTGACTTTTTTC-3′ and 5′-ACAGTGACAACGTCCGAACCAAGTTCTCTGGTTCGGACGTTGTCACTGAAAAAAGAGCT-3′ into the LentiLox vector (Rubinson et al. 2003). For cellular dopamine quantification, cultures were incubated in standard differentiation medium supplemented with L-DOPA (50 μM) for 1 h to amplify dopamine production, as described in Pothos et al. (1996). Subsequently, cells were washed in PBS and then lysed in 0.2 M perchloric acid. Dopamine levels were quantified by HPLC (Yang et al. 1998) and normalized for protein content as above.

**Expression vectors.** The cDNA for human *DJ-1* was PCR-amplified from a human liver cDNA library (Clontech, Palo Alto, California, United States). For expression of DJ-1 in ES cell rescue experiments, *DJ-1* was cloned into the expression vector pcDNA3.1 (Invitrogen, Carlsbad, California, United States) containing a Flag peptide sequence at the N-terminus using standard cloning techniques. Flag-L166P *DJ-1* (pcDNA3) was generated by PCR-mediated mutagenesis.

**Protein carbonyl analysis.** For protein carbonyl quantitation (Bian et al. 2003), cells were plated ($1.4 \times 10^5$ cells per well), grown for 24 h, and then treated with 10 μM $H_2O_2$ as indicated. Cells were lysed in 200 μl lysis buffer and cleared lysate was prepared as described above. An aliquot of 40 μl from each time point was added to 2 M HCl (120 μl) with or without 10 μM 2,4-dinitrophenyl-hydrazine and incubated for 1 h at 24 °C with shaking. Proteins were then TCA-precipitated and resuspended in 200 μl of 6 M guanidinium chloride. Absorbance was measured at 360 nm, and DNP-conjugated samples were normalized for protein concentration with the underivitized control samples.

## Supporting Information

**Figure S1.** Quantitative Real-Time PCR for *DJ-1* Gene Expression

(A) Real-time PCR analyses of *DJ-1* cDNA in WT (+/+), heterozygous (+/−), and knockout (−/−) cultures. Each expression value was normalized to that of β-actin and expressed relative to the respective value of the WT (+/+) control. These gene expression patterns were replicated in at least three independent PCR experiments. Total RNA from ES cells differentiated with the SDIA method for 18 days was isolated using the Absolutely RNA Miniprep kit (Stratagene, La Jolla, California, United States). Synthesis of cDNA was performed using the SuperScript first strand synthesis system for RT-PCR (Invitrogen). Real-time PCR reactions were optimized to determine the linear amplification range. Quantitative real-time RT-PCRs were performed (Stratagene MX3000P) using the QuantiTect SYBR Green PCR Master Mix (Qiagen, Valencia, California, United States) according to the manufacturer's instructions. *DJ-1* primer sequences were 5′-CGAAGAAATTCGATGGCTTCCAAAAGAGCTCTGGT-3′ and 5′-CAGACTCGAGCTGCTTCACATACTACTGCTGAGGT-3′; primers used for β-actin were 5′-TTTTGGATGCAAGGTCACAA-3′ and 5′-CTCCACAATGGCTAGTGCAA-3′. For quantitative analyses, PCR product levels were measured in real time during the annealing step, and values were normalized to those of β-actin.

(B) Ethidium bromide staining of the PCR products obtained after 29 cycles for *DJ-1* (625 bp) and *β-actin* (350 bp).

Found at DOI: 10.1371/journal.pbio.0020327.sg001 (704 KB EPS).

**Figure S2.** Analysis of DJ-1-Deficient ES Cells

(A and B) Cell viability of *DJ-1* heterozygous cells (solid bar) and DJ-1-deficient knockout clone 32 (open bar) after exposure to $CuCl_2$ or staurosporine at the doses indicated.

(C) MTT values of untreated DJ-1-deficient ES cell clones and the control heterozygous cells. Assays were performed exactly as in Figure 2, but in the absence of toxin.

(D) MTT values of untreated DJ-1-deficient ES cells transfected with vector alone or various DJ-1-encoding plasmids. Transfection and expression of WT DJ-1 or mutant forms of DJ-1 does not alter the basal metabolic activity or viability of the cells.

(E) Western blotting of extracts from ES cells transfected with vectors harboring WT human *DJ-1* or the L166P mutant.

Found at DOI: 10.1371/journal.pbio.0020327.sg002 (545 KB EPS).

**Figure S3.** Immunocytochemistry for HB9 and GABA Neurons in DJ-1-Deficient and Control Heterozygous ES Cells

Both cell cultures were differentiated by SDIA for 18 DIV. Cells were fixed with 4% paraformaldehyde and stained with mouse monoclonal antibodies against HB9 (gift from T. Jessell, dilution 1:50) and rabbit polyclonal antibodies against GABA (Sigma, dilution 1:1000) as in Figure 5. Scale bar, 50 μM.

Found at DOI: 10.1371/journal.pbio.0020327.sg003 (5.5 MB TIF).

### Accession Numbers

The GenBank (http://www.ncbi.nlm.nih.gov/) accession numbers of the genes discussed in this paper are *α-synuclein* (NM_000345), *Parkin* (AB009973), and *DJ-1* (AB073864).

## Acknowledgments

We thank O. Hobert and L. Clark for critical reading of the manuscript. SS is funded by the Integrated Graduate Program Training Grant (National Institutes of Health); CM is funded by the American Parkinson's Disease Association; AA receives funding from the Spitzer, Rockefeller Brothers, Taub and M. J. Fox Foundations, National Institute of Neurological Disorder and Stroke (NINDS) and National Institute of Aging (NIA), and is a Culpeper and Beeson scholar.

**Conflicts of interest.** The authors have declared that no conflicts of interest exist.

**Author contributions.** CM, SS, and AA conceived and designed the experiments. CM, SS, AJ, TL, and AA performed the experiments. CM, SS, AJ, and AA analyzed the data. CM, SS, AJ, MFB, LY, TF, and AA contributed reagents/materials/analysis tools. CM, SS, and AA wrote the paper.

**References**


Abeliovich A, Schmitz Y, Farinas I, Choi-Lundberg D, Ho WH, et al. (2000) Mice lacking α-synuclein display functional deficits in the nigrostriatal dopamine system. Neuron 25: 239–252.

Barberi T, Klivenyi P, Calingasan NY, Lee H, Kawamata H, et al. (2003) Neural subtype specification of fertilization and nuclear transfer embryonic stem cells and application in parkinsonian mice. Nat Biotechnol 21: 1200–1207.

Bian K, Gao Z, Weisbrodt N, Murad F (2003) The nature of heme/iron-induced protein tyrosine nitration. Proc Natl Acad Sci U S A 100: 5712–5717.

Bonifati V, Rizzu P, van Baren MJ, Schaap O, Breedveld GJ, et al. (2003) Mutations in the DJ-1 gene associated with autosomal recessive early-onset parkinsonism. Science 299: 256–259.

Dauer W, Przedborski S (2003) Parkinson's disease: Mechanisms and models. Neuron 39: 889–909.

Demasi M, Davies KJ (2003) Proteasome inhibitors induce intracellular protein aggregation and cell death by an oxygen-dependent mechanism. FEBS Lett 542: 89–94.

de Nobel H, Lawrie L, Brul S, Klis F, Davis M, et al. (2001) Parallel and comparative analysis of the proteome and transcriptome of sorbic acid-stressed *Saccharomyces cerevisiae*. Yeast 18: 1413–1428.

Farrer M, Wavrant-De Vrieze F, Crook R, Boles L, Perez-Tur J, et al. (1998) Low frequency of α-synuclein mutations in familial Parkinson's disease. Ann Neurol 43: 394–397.

Fezoui Y, Hartley DM, Walsh DM, Selkoe DJ, Osterhout JJ, et al. (2000) A de novo designed helix-turn-helix peptide forms nontoxic amyloid fibrils. Nat Struct Biol 7: 1095–1099.

Floss T, Wurst W (2002) Functional genomics by gene-trapping in embryonic stem cells. Methods Mol Biol 185: 347–379.

Giasson BI, Duda JE, Quinn SM, Zhang B, Trojanowski JQ, et al. (2002) Neuronal α-synucleinopathy with severe movement disorder in mice expressing A53T human α-synuclein. Neuron 34: 521–533.

Gobeil S, Boucher CC, Nadeau D, Poirier GG (2001) Characterization of the necrotic cleavage of poly(ADP-ribose) polymerase (PARP-1): Implication of lysosomal proteases. Cell Death Differ 8: 588–594.

Goldberg MS, Lansbury PT, Jr. (2000) Is there a cause-and-effect relationship between α-synuclein fibrillization and Parkinson's disease? Nat Cell Biol 2: E115–119.

Goldberg MS, Fleming SM, Palacino JJ, Cepeda C, Lam HA, et al. (2003) Parkin-deficient mice exhibit nigrostriatal deficits but not loss of dopaminergic neurons. J Biol Chem 278: 43628–43635.

Hague S, Rogaeva E, Hernandez D, Gulick C, Singleton A, et al. (2003) Early-onset Parkinson's disease caused by a compound heterozygous DJ-1 mutation. Ann Neurol 54: 271–274.

Han BS, Hong HS, Choi WS, Markelonis GJ, Oh TH, et al. (2003) Caspase-dependent and -independent cell death pathways in primary cultures of mesencephalic dopaminergic neurons after neurotoxin treatment. J Neurosci 23: 5069–5078.

Hattori N, Shimura H, Kubo S, Kitada T, Wang M, et al. (2000) Autosomal recessive juvenile parkinsonism: A key to understanding nigral degeneration in sporadic Parkinson's disease. Neuropathology 20 (Suppl): 85–90.

Itier JM, Ibanez P, Mena MA, Abbas N, Cohen-Salmon C, et al. (2003) Parkin gene inactivation alters behaviour and dopamine neurotransmission in the mouse. Hum Mol Genet 12: 2277–2291.

Jenner P (2003) Oxidative stress in Parkinson's disease. Ann Neurol 53 (Suppl 3): 26–38.

Jenner P, Olanow CW (1998) Understanding cell death in Parkinson's disease. Ann Neurol 44 (Suppl 1): 72–84.

Kawasaki H, Mizuseki K, Nishikawa S, Kaneko S, Kuwana Y, et al. (2000) Induction of midbrain dopaminergic neurons from ES cells by stromal cell-derived inducing activity. Neuron 28: 31–40.

Lee MK, Stirling W, Xu Y, Xu X, Qui D, et al. (2002) Human α-synuclein-harboring familial Parkinson's disease-linked Ala-53 → Thr mutation causes neurodegenerative disease with α-synuclein aggregation in transgenic mice. Proc Natl Acad Sci U S A 99: 8968–8973.

Masliah E, Rockenstein E, Veinbergs I, Mallory M, Hashimoto M, et al. (2000) Dopaminergic loss and inclusion body formation in α-synuclein mice: Implications for neurodegenerative disorders. Science 287: 1265–1269.

McCormack AL, Thiruchelvam M, Manning-Bog AB, Thiffault C, Langston JW, et al. (2002) Environmental risk factors and Parkinson's disease: Selective degeneration of nigral dopaminergic neurons caused by the herbicide paraquat. Neurobiol Dis 10: 119–127.

Mitsumoto A, Nakagawa Y (2001) DJ-1 is an indicator for endogenous reactive oxygen species elicited by endotoxin. Free Radic Res 35: 885–893.

Mitsumoto A, Nakagawa Y, Takeuchi A, Okawa K, Iwamatsu A, et al. (2001) Oxidized forms of peroxiredoxins and DJ-1 on two-dimensional gels increased in response to sublethal levels of paraquat. Free Radic Res 35: 301–310.

Mizushima N, Yamamoto A, Hatano M, Kobayashi Y, Kabeya Y, et al. (2001) Dissection of autophagosome formation using Apg5-deficient mouse embryonic stem cells. J Cell Biol 152: 657–668.

Morizane A, Takahashi J, Takagi Y, Sasai Y, Hashimoto N (2002) Optimal conditions for in vivo induction of dopaminergic neurons from embryonic stem cells through stromal cell-derived inducing activity. J Neurosci Res 69: 934–939.

Nagakubo D, Taira T, Kitaura H, Ikeda M, Tamai K, et al. (1997) DJ-1, a novel oncogene which transforms mouse NIH3T3 cells in cooperation with ras. Biochem Biophys Res Commun 231: 509–513.

Polymeropoulos MH, Lavedan C, Leroy E, Ide SE, Dehejia A, et al. (1997) Mutation in the α-synuclein gene identified in families with Parkinson's disease. Science 276: 2045–2047.

Pothos E, Desmond M, Sulzer D (1996) L-3,4-dihydroxyphenylalanine increases the quantal size of exocytotic dopamine release in vitro. J Neurochem 66: 629–636.

Rideout HJ, Larsen KE, Sulzer D, Stefanis L (2001) Proteasomal inhibition leads to formation of ubiquitin/α-synuclein-immunoreactive inclusions in PC12 cells. J Neurochem 78: 899–908.

Rubinson DA, Dillon CP, Kwiatkowski AV, Sievers C, Yang L, et al. (2003) A lentivirus-based system to functionally silence genes in primary mammalian cells, stem cells and transgenic mice by RNA interference. Nat Genet 33: 401–406.

Shendelman S, Jonason A, Martinat C, Leete T, Abeliovich A (2004) DJ-1 is a redox-dependent molecular chaperone that inhibits α-synuclein aggregation formation. PLoS Biol 2(11): e362.

Sherer TB, Betarbet R, Stout AK, Lund S, Baptista M, et al. (2002) An in vitro model of Parkinson's disease: Linking mitochondrial impairment to altered α-synuclein metabolism and oxidative damage. J Neurosci 22: 7006–7015.

Spillantini MG, Crowther RA, Jakes R, Cairns NJ, Lantos PL, et al. (1998) Filamentous α-synuclein inclusions link multiple system atrophy with Parkinson's disease and dementia with Lewy bodies. Neurosci Lett 251: 205–208.

Staropoli JF, McDermott C, Martinat C, Schulman B, Demireva E, et al. (2003) Parkin is a component of an SCF-like ubiquitin ligase complex and protects postmitotic neurons from kainate excitotoxicity. Neuron 37: 735–749.

Taira T, Saito Y, Niki T, Iguchi-Ariga SM, Takahashi K, et al. (2004) DJ-1 has a role in antioxidative stress to prevent cell death. EMBO Rep 5: 213–218.

Trojanowski JQ, Lee VM (1998) Aggregation of neurofilament and α-synuclein proteins in Lewy bodies: implications for the pathogenesis of Parkinson disease and Lewy body dementia. Arch Neurol 55: 151–152.

Walrand S, Valeix S, Rodriguez C, Ligot P, Chassagne J, et al. (2003) Flow cytometry study of polymorphonuclear neutrophil oxidative burst: A comparison of three fluorescent probes. Clin Chim Acta 331: 103–110.

Yang L, Matthews RT, Schulz JB, Klockgether T, Liao AW, et al. (1998) 1-Methyl-4-phenyl-1,2,3,6-tetrahydropyride neurotoxicity is attenuated in mice overexpressing Bcl-2. J Neurosci 18: 8145–8152.

Yokota T, Sugawara K, Ito K, Takahashi R, Ariga H, et al. (2003) Down regulation of DJ-1 enhances cell death by oxidative stress, ER stress, and proteasome inhibition. Biochem Biophys Res Commun 312: 1342–1348.

Available online at www.sciencedirect.com

SCIENCE DIRECT

Experimental Neurology 191 (2005) 86–93

Experimental Neurology

www.elsevier.com/locate/yexnr

# A novel azulenyl nitrone antioxidant protects against MPTP and 3-nitropropionic acid neurotoxicities

Lichuan Yang[a], Noel Y. Calingasan[a], Junyu Chen[a], James J. Ley[b], David A. Becker[b], M. Flint Beal[a,*]

[a]*Department of Neurology and Neuroscience, Weill Medical College of Cornell University, New York, NY 10021, USA*
[b]*Department of Chemistry, Florida International University, Miami, FL 33199, USA*

Received 16 March 2004; revised 7 July 2004; accepted 12 July 2004
Available online 21 November 2004

**Abstract**

Oxidative stress plays an important role in neuronal death in neurodegenerative disorders such as Parkinson's disease (PD) and Huntington's disease (HD). Animal models of PD or HD, produced by administration of the mitochondrial toxins 1-methyl-4-phenyl-1,2,3,6-tetrahydropyridine (MPTP) or 3-nitropropionic acid (3NP), respectively, show increased free radical generation. Free radicals generated in biological systems can react with spin-trapping compounds, such as nitrones, to form stable adducts. In recent years, the utility of nitrones has moved beyond analytical applications and into the realm of neuroprotection as antioxidants in both brain ischemia and models of neurodegenerative diseases. In the present study, we administered a new nitrone antioxidant, stilbazulenyl nitrone (STAZN), with either MPTP or 3NP. STAZN attenuated MPTP-induced striatal dopamine depletion by 40% and showed a tendency to dose-dependent neuroprotection. STAZN dose-dependently protected against loss of tyrosine hydroxylase immunoreactive neurons in the substantia nigra pars compacta. STAZN reduced the striatal lesion volume caused by systemic 3NP administration from 44 ± 9 to 20 ± 6 $mm^3$. The lipid peroxidation marker, malondialdehyde(MDA), was significantly increased in the striatum, cortex, and cerebellum of rats after administration of 3NP. These increases were blocked by co-injection of STAZN. Our data provide further evidence that STAZN is a neuroprotective free radical spin trap, and suggest that the development of new antioxidants will broaden our therapeutic strategies for neurodegenerative diseases.


*Keywords:* Free radicals; Spin trapping; Parkinson's disease; Huntington's disease

## Introduction

The neurotoxin 1-methyl-4-phenyl-1,2,3,6-tetrahydropyridine (MPTP) causes a parkinsonian syndrome in man and monkey (Bloem et al., 1990). Its mechanism of neurotoxicity involves conversion by monoamine oxidase B into an active toxic metabolite, 1-methyl-4-phenylpyridinium (MPP+) (Tipton and Singer, 1993). MPP+ rapidly accumulates in dopaminergic neurons via the plasma membrane dopamine transporter. Once inside cells, MPP+ accumulates in mitochondria where it inhibits complex I of the mitochondrial electron transport chain. This leads to impairment of energy production and increased free radical generation, and eventually causes dopaminergic neuron death. There is substantial evidence in vivo that MPTP or MPP+ causes increased free radical production and lipid peroxidation in brain (Alcaraz-Zubeldia et al., 2001; Chiueh et al., 1992; Rojas and Rios, 1993; Thomas et al., 2000). Furthermore, MPTP neurotoxicity is attenuated in mice by a variety of anitioxidative strategies, such as overexpression of Cu, Zn superoxide dismutase, Mn superoxide dismutase, or treatment with copper sulfate (Alcaraz-Zubeldia et al., 2001; Klivenyi et al., 1998a,b; Przedborski et al., 1992).

The use of the mitochondrial inhibitor 3-nitropropionic acid (3-NP) to produce animal models of Huntington's

* Corresponding author. Department of Neurology and Neuroscience, Weill Medical College at Cornell University, Room F 610, 525 East 68th Street, New York, NY 10021. Fax: +1 212 746 8532.
*E-mail address:* fbeal@med.cornell.edu (M.F. Beal).

0014-4886/$ - see front matter © 2004 Elsevier Inc. All rights reserved.
doi:10.1016/j.expneurol.2004.07.012

disease has been shown to lead to pathology similar to that of HD (Brouillet et al., 1995). Oxidative stress and excitotoxicity have been implicated in the selective striatal vulnerability caused by 3-NP (Bogdanov et al., 1998; Kim et al., 2000; Schulz et al., 1996). Oxidative stress induced by 3-NP also extends to the cerebral cortex, an area where little neuron loss occurs (La Fontaine et al., 2000). Antioxidative strategies, including administration of antioxidants (taurine) (Rivas-Arancibia et al., 2001) as well as overexpression of genes involved in attenuating oxidative stress, showed significant neuroprotection against 3-NP toxicity (Beal et al., 1995). In contrast, animals with deficiencies of antioxidative enzymes, such as manganese superoxide dismutase (Andreassen et al., 2001) and glutathione peroxidase (Klivenyi et al., 2000), showed significantly increased vulnerability to 3-NP toxicity. Furthermore, the transgenic mouse model of HD, which overexpresses the human huntingtin gene with lengthened CAG repeat, also showed increased vulnerability to 3-NP toxicity as well as increased generation of free radicals induced by 3-NP (Bogdanov et al., 1998).

Free radicals formed in vivo can be trapped by spin-trapping compounds to form their stable adducts, which can be detected by electron spin resonance in organic extracts and provide evidence of in vivo free radical formation. Spin traps commonly used in biological system are nitroso compounds or nitrones and their radical adducts are all nitroxide free radicals. Nitrone spin traps are more stable than those of nitroso compounds (Knecht and Mason, 1993). In recent years, the utility of nitrones has moved beyond analytical application and into the realm of neuroprotection. The nitrone spin trap *N-tert*-butyl-α-phenyl nitrone (PBN) delivered to mice in a single dose before MPTP or subchronically following MPTP injections showed protective effects against both the functional changes and striatal dopamine depletion caused by MPTP, possibly through its free radical spin-trapping mechanism (Fredriksson et al., 1997). In an earlier study, we found *N-tert*-butyl-α-(2-sulfophenyl) nitrone (S-PBN), a derivative of PBN with a lower oxidation potential that is more potent in trapping free radicals, produced significant protection against a MPTP dosing regimen resulting in a mild to moderate depletion of dopamine, but not against more severe depletion (Schulz et al., 1995). Another cyclic nitrone free radical spin trap, called MDL 101,002, also produced dose-dependent neuroprotection against malonate-induced striatal lesions, and significant protection against MPTP-induced depletions of dopamine and its metabolites (Matthews et al., 1999).

Azulenyl nitrones are a unique class of free radical spin-trapping compounds. These compounds possess many theoretical advantages over conventional spin traps like PBN. Azulenyl nitrone (AZN) is synthesized from the natural product guaiazulene, which itself has been used in several medical applications. Althaus et al. (1998) synthesized AZN, assessed the effect of AZN on the formation of free radicals in bilateral carotid ischemia/reperfusion animal models, and demonstrated neuroprotective effects in preserving the hippocampal CA1 pyramidal cells against the ischemia/reperfusion. In a parallel study, both water-soluble and lipid-soluble AZN compounds produced significant neuroprotection against MPTP-induced depletion of dopamine and its metabolites in mouse striatum (Klivenyi et al., 1998a,b).

Stilbazulenyl nitrone (STAZN) is an azulenyl nitrone derivative that bears some structural resemblance to stilbene (Fig. 1) (Becker et al., 2002). The oxidation potential of STAZN has been determined to be 0.33 V, which is almost half a volt lower than AZN (0.84 V) and more than a full volt lower than PBN (1.47 V) and S-PBN (1.34 V). Among common aromatic carbocyclic and heterocyclic nitrone-based free radical spin traps, STAZN possesses an oxidation potential that remains exceptionally lower by comparison. Furthermore, azulene-based spin traps also possess lipophilicity. Therefore, STAZN may exhibit improved antioxidant properties and may more readily penetrate the blood–brain barrier. We tested STAZN for neuroprotective effects against MPTP and 3-NP toxicity in our present study.

## Materials and methods

### *Animals and materials*

Male C57 black mice (3-month old, 25–30 g) and male Lewis rats (3-month old, 300–350 g) were obtained from the Jackson Laboratory (Bar Harbor, ME, USA). Neurotoxin compounds of MPTP, 3NP, and standard compounds of dopamine, 3,4-dihydroxyphenylacetic acid (DOPAC), homovanillic acid (HVA), and malondialdehyde were all bought from Sigma (St. Louis, MO, USA). The STAZN spin trap was a gift from Dr. David A. Becker in Florida International University. All animal experimental procedures were in strict accordance with protocols approved by the Weill Cornell Medical College Animal Care Committee.

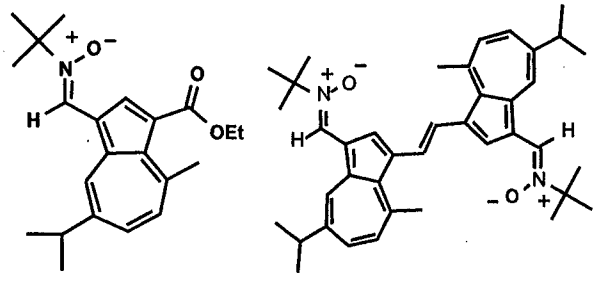


AZN STAZN

Fig. 1. Comparison between the two chemical structures of azulenyl nitrone (AZN) and its new derivant stilbazulenyl nitrone (STAZN). The latter was used in the present experiment.

MPTP and 3-NP manipulations were carried out in a special animal room restricted for neurotoxin manipulation.

*Animal models and STAZN treatment*

STAZN is highly lipophilic and has limited aqueous solubility. It is soluble in both peanut oil and in dimethyl sulfoxide (DMSO). Instead of choosing DMSO, we used peanut oil as our vehicle for STAZN administration because DMSO is recognized to have a potential antioxidant action that might contribute to neuroprotection (Chiueh et al., 1994; Repine et al., 1981; Shimizu et al., 1997). The STAZN was obtained as dark green solid granules and kept at −20°C for stability. The compound stays yellow-brown when suspended and dissolved in peanut oil but can be oxidized by peroxyl radicals leading to the formation of its aldehyde adducts (Becker, 1996, 1999; Becker et al., 2002). Therefore, a fresh peanut oil preparation of STAZN was made just at the time of injections. Controls received the peanut oil vehicle.

MPTP, prepared 2 mg/ml in phosphate-buffered saline (PBS), was injected intraperitoneally to C57 black mice 10 mg/kg for four times with an interval of 2 h. STAZN (10 or 20 mg/kg), or the same volume of peanut oil vehicle, was administered intraperitoneally 30 min before each MPTP dose and 3, 12, and 24 h after the last dose of MPTP. Mice were sacrificed 7 days after MPTP injection and fresh striata were dissected for catecholamine analysis.

3-NP, prepared at 80 mg/ml in $H_2O$ and adjusted with 10 N NaOH to pH 7.4, was injected subcutaneously to Lewis rats at a dose of 20 mg/kg twice a day for 5 days. Intraperitoneal administration of STAZN (10 mg/kg, twice a day), or the same volume peanut oil vehicle was started 1 day before the start of the 3-NP injections and ended 1 day after the end of 3-NP injection. Animals were sacrificed following the last STAZN injection and brains were fixed in 4% paraformaldehyde for 5 days, cryoprotected in 30% sucrose for 1 day, and sectioned in cryostat for cresyl-violet staining. Another group of rats were subcutaneously dosed with 3-NP at 25 mg/kg twice a day for 2 days and intraperitoneally injected STAZN 10 mg/kg or vehicle 30 min before each 3-NP dosing. Animals were sacrificed 4 h after the last dose of 3-NP and cortex, striatum, and cerebellum were dissected out and kept in freezer for malondialdehyde analysis.

*HPLC assay for catecholamines*

Dissected striata were sonicated and centrifuged in chilled 0.1 M perchloric acid (PCA, about 100 μl/mg tissue). The supernatants were taken for measurements of dopamine and its metabolites 3,4-dihydroxyphenylacetic acid (DOPAC), and homovanillic acid (HVA) by HPLC as modified from our previously described method (Beal et al., 1990, 1992). Briefly, 10 μl supernatant was isocratically eluted through an 80 × 4.6-mm C18 column (ESA, Inc., Chelmsford, MA) with a mobile phase containing 0.1 M $Li_3PO_4$, 0.85 mM 1-octanesulfonic acid, and 10% (v/v) methanol, and detected by a 2-channel Coulochem II electrochemical detector (ESA, Inc.). Concentrations of dopamine and its metabolites are expressed as nanograms per milligram protein. The protein concentrations of tissue homogenates were measured with the Bio-Rad protein analyze protocol (Bio-Rad Laboratories, Hercules, CA) and Perkin Elmer Bio Assay Reader (Norwalk, CT).

*HPLC assay for malondialdehyde*

The determination of MDA by HPLC was carried out according to a recent report (Agarwal and Chase, 2002). Briefly, tissues were homogenized in 40% ethanol solution. Sample derivatization was carried out in 2-ml-capacity plastic centrifuge tubes fitted with screw-on caps. To a 50-μl aliquot of sample or MDA standard, 50 μl of 0.05% butylated hydroxytoluene (BHT), 400 μl of 0.44 M $H_3PO_4$, and 100 μl of 0.42 mM 2-thiobarbituric acid (TBA) were added. Sample tubes were capped tightly, vortex mixed, then heated for 1 h on a 100°C dry bath incubator. Following heat derivatization, samples were placed on an ice-water (0°C) bath for 5 min to cool, with 250 μl *n*-butanol subsequently added to each vial for extraction of the MDA–TBA complex. Tubes were vortex mixed 5 min then centrifuged 3 min at 14000 rpm to separate the two phases. Aliquots of 100 μl were removed from the *n*-butanol layer of each sample and placed in HPLC vials for analysis without evaporation. The HPLC system consisted of a Waters 717plus autosampler, 515 pump, and 470 scanning fluorescence detector (Waters, Milford, MA). The pump flow-rate was 1.0 ml/min with mobile phase comprised of acetonitrile–buffer (20:80, v/v). The buffer was 50 mM potassium monobasic phosphate (anhydrous) with an adjusted pH of 6.8 using 5 M potassium hydroxide. The fluorescence detector was set at an excitation wavelength of 515 nm and emission wavelength of 553 nm. The column was an ESA 150 × 3-mm C18 column with particle size of 3 μm (ESA, Inc.) and placed in a column warmer set to 30°C. Peak heights were integrated by an ESA 501 chromatography data system (ESA, Inc.). The concentration of MDA is expressed as nanomoles per milligram protein. Tissue protein concentrations were measured by using the Bio-Rad protein analyses protocol (Bio-Rad Laboratories) and Perkin Elmer Bio Assay Reader.

*Substantia nigra histological analysis*

Tissues for histological analysis were fixed with 4% paraformaldehyde in 0.1 M phosphate buffer (pH 7.4) by immersion for 48 h at 4°C, and then cryoprotected in 30% sucrose overnight at 4°C. Serial coronal sections (50 μm) were cut through the substantia nigra using a cryostat. Two sets of sections were prepared with each set consisting of seven to eight sections, 100-μm apart. One set of sections was used for Nissl staining (cresyl violet). Another set was

processed for tyrosine hydroxylase (TH) immunohistochemistry using avidin–biotin peroxidase technique. Briefly, free-floating sections were pretreated with 3% $H_2O_2$ in PBS for 30 min. The sections were incubated sequentially in (a) 1% bovine serum albumin (BSA)/0.2% Triton X-100 for 30 min, (b) rabbit anti-TH affinity purified antibody (Chemicon, Temecula, CA; 1:4000 in PBS/0.5% BSA) for 18 h (c) biotinylated anti-rabbit IgG (Vector Laboratories, Burlingame, CA; 1:500 in PBS/0.5%BSA) for 1 h, and (d) avidin–biotin–peroxidase complex (Vector; 1:500 in PBS) for 1 h. The immunoreaction was visualized using 3,3′-diaminobenzidine tetrahydrochloride dihydrate (DAB) with nickel intensification (Vector) as the chromogen. All incubations and rinses were performed with agitation using an orbital shaker at room temperature. The sections were mounted onto gelatin-coated slides, dehydrated, cleared in xylene, and coverslipped. The numbers of Nissl-stained or TH-immunoreactive cells in the substantia nigra pars compacta (SNpc) were counted using the optical fractionator method in the Stereo Investigator (v. 4.35) software program (Microbrightfield, Burlington, VT).

*3NP lesion volume measurement*

Fifty-micrometer sections were collected at every 500-μm interval and stained for Nissl substance using 0.2% cresyl violet. All samples were blindly coded and the lesion area was measured using a microcomputer image device (MCID, Imaging Research Inc., St. Catharine, Ont. Canada). The lesion volume (expressed by $mm^3$) was calculated by multiplying the lesion areas by thickness of all sections.

*Statistical analysis*

Results were expressed as means ± standard error of means (SEM). Differences between STAZN-treated and control groups were assessed by ANOVA, followed by Tukey–Kramer test for comparison among different means. Value $P < 0.05$ was taken as being statistically significant.

## Results

*STAZN attenuates MPTP-induced striatal dopamine depletion*

Fig. 2 shows that STAZN provided significant protection against dopamine, DOPAC, and HVA depletion in the striatum of mice treated by MPTP. There is a tendency to dose-dependent protection by STAZN. STAZN protected about 40% of dopamine and its metabolites from MPTP-induced depletion. Both 10 and 20 mg/kg doses of STAZN showed significant protection.

MPTP significantly reduced the numbers of TH-immunoreactive or Nissl-stained neurons in the substantia nigra pars compacta (SNpc) compared with vehicle-treated controls by 64% ($P < 0.001$) and 65% ($P < 0.001$), respectively (Figs. 3 and 4). STAZN significantly increased the numbers of TH-positive or Nissl-stained neurons in the SNpc compared with the MPTP-lesioned mice that did not receive STAZN ($P < 0.05$).

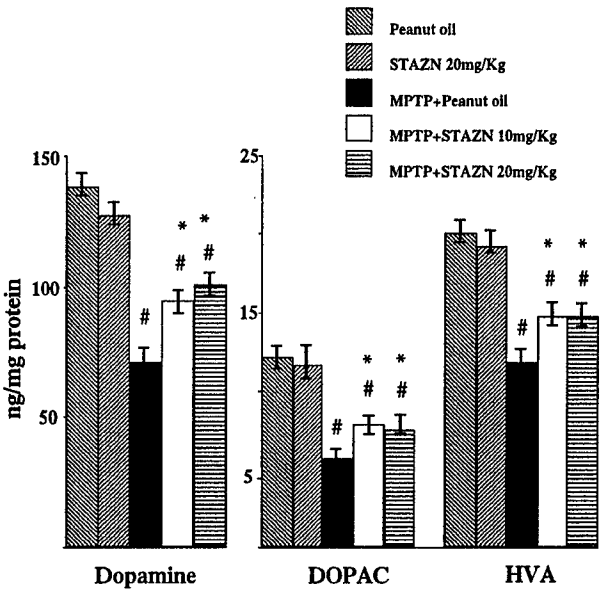


Fig. 2. Effects of administration of STAZN on MPTP-induced depletion of dopamine and its metabolites DOPAC and HVA in mouse striatum. #, $P < 0.05$ when compared with peanut oil or STAZN alone controls. *, $P < 0.05$ when compared with MPTP + peanut oil.

*STAZN reduces 3-NP-induced striatal lesions and 3-NP-induced lipid peroxidation*

Bilateral striatal damage was found in all rats after the systemic delivery of 3-NP for 5 days (Fig. 5A). However, the lesion volume was reduced more than 50% when STAZN was administered (Fig. 5B). To verify the antioxidative effect of STAZN on our 3-NP model, we measured the lipid peroxidation product malondialdehyde levels in brain tissues. The elevation of MDA production induced by 3-NP involved not just the striatum but also the cerebral cortex and cerebellum, meaning that oxidative stress induced by 3-NP extends broadly in the brain even to the areas where little neuron loss occurs. STAZN significantly reduced the MDA levels down to the baseline levels in all the three brain areas, implying it works as an antioxidant in its neuroprotective effects (Fig. 6).

## Discussion

There is substantial evidence that oxidative damage contributes to the pathogenesis of several neurodegenerative diseases including Huntington's and Parkinson's diseases. There is evidence for increased oxidative damage in HD postmortem brain tissue (Browne et al., 1999). In Parkin-

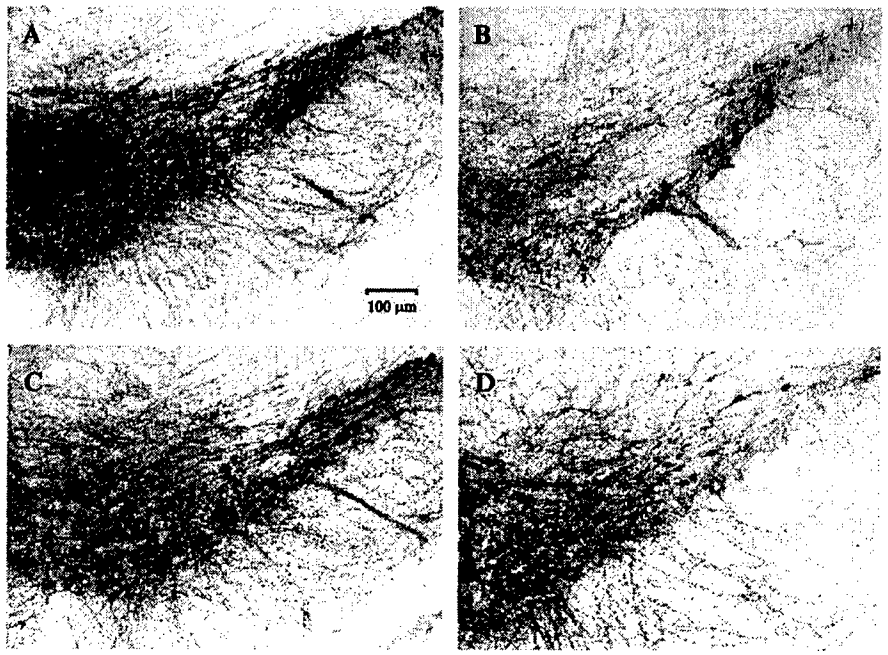


Fig. 3. Photomicrographs of tyrosine hydroxylase (TH)-immunostained sections through the substantia nigra pars compacta (SNpc) of vehicle-treated controls (A) and mice treated with MPTP + peanut oil (B), MPTP + STAZN 10 mg/kg (C), or MPTP + STAZN 20 mg/kg (D), showing a significant attenuation of MPTP-induced neuronal loss after STAZN treatment.

son's disease (PD), there is evidence of increased lipid peroxidation, increased protein carbonyls, and increases in 8-hydorxy-2-deoxyguanosine (Alam et al., 1997; Dexter et al., 1994; Sanchez-Ramos et al., 1994). There is also a reduction in glutathione levels in both patients with PD as well as individuals with incidental Lewy Body disease, which may be a presymptomatic stage of PD (Dexter et al., 1994; Sofic et al., 1992). Immunocytochemistry has also shown oxidative damage to DNA and RNA as well as increases in 3-nitrotyrosine (Zhang et al., 1999; Good et al., 1998). The latter finding was confirmed with antibodies specific for nitrated α-synuclein (Giasson et al., 2000).

In recent years, nitrone-based agents have emerged as promising therapeutic agents for pathological conditions involving free radical driven oxidative damage. Nitrones react with free radicals to make stable adducts. Nitrone spin

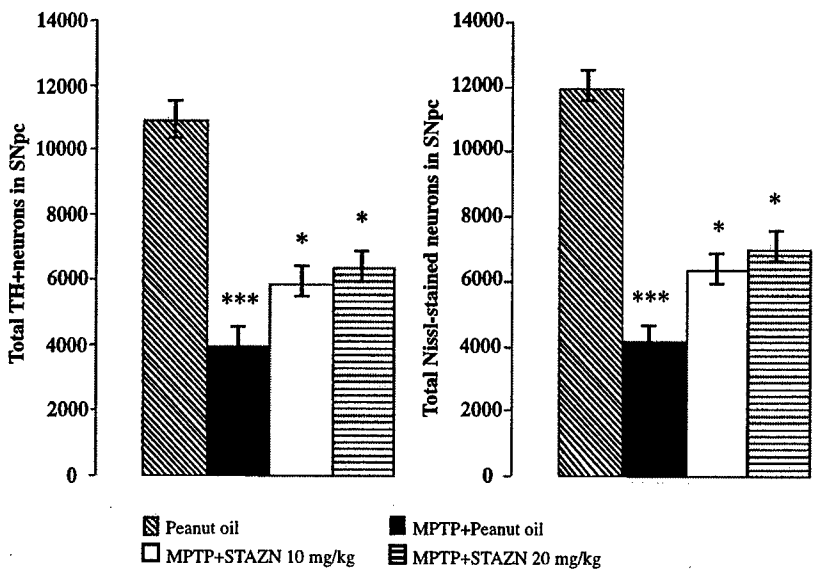


Fig. 4. Effect of STAZN on MPTP-induced neuronal loss determined by stereological analysis of TH-immunoreactive (top) or Nissl-stained (bottom) neurons in the substantia nigra pars compacta (SNpc). Neuronal counts (means ± SEM) were determined using the optical fractionator method. ***$P < 0.001$, vs. peanut oil; *$P < 0.05$, vs. MPTP + peanut oil.

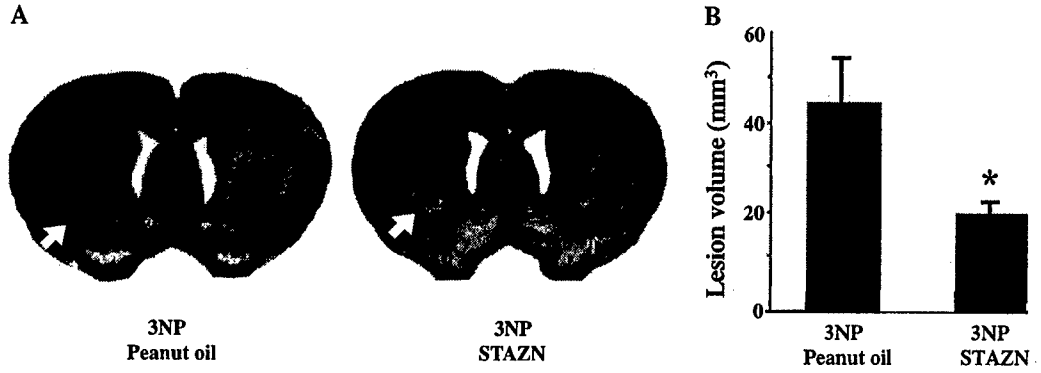


Fig. 5. Cresyl violet staining showing the striatal lesions (see arrows) caused by subcutaneous 3-NP injection (A). The bar graph shows the administration of STAZN significantly reduces striatal lesion volumes caused by 3-NP. * means $P < 0.05$.

traps, chiefly the α-phenyl nitrones, such as α-phenyl-*N*-*tert*-butyl-nitrone (PBN), and its 2,4-bis sodium sulfonate derivative known as NXY-059, have been widely tested as antioxidant therapies to counter free-radical-mediated damage. Becker first synthesized a novel class of nitrones, the azulenyl nitrones, and noted that they were sensitive colorimetric detectors of oxyradical end products (Becker, 1996). The azulenyl-based chain-breaking antioxidants have low oxidation potentials and they tend to be highly lipophilic, a property that would favor their blood–brain barrier permeability.

Recently, a new class of azulenyl nitones has been synthesized (Becker et al., 2002). Stilbazulenyl nitrone (STAZN) has been reported to be an improved antioxidant as compared to other members of its class. Antioxidant assays based on the oxidation of cumene to cumene hydroperoxide by atmospheric oxygen in the presence of a free radical initiator showed that STAZN possesses remarkable potency as a chain-breaking antioxidant. It markedly outperformed PBN in concentrations lower by 2–3 orders of magnitude. It was more than 300 times more potent than NXY-059 in suppressing free-radical-driven peroxidation of cumene. In more polar solutions, STAZN rivaled the antioxidant efficacy of vitamin E. The oxidation potential of STAZN is more than a full volt lower than PBN as well as NXY-059, which helps to account for its superior antioxidant function.

We previously demonstrated that several free radical spin traps can protect against MPTP and 3-nitropropionic acid (3-NP) neurotoxicity (Matthews et al., 1999; Schulz et al., 1996). Both MPTP and 3-NP toxicity have been shown to be associated with the generation of free radicals as well as peroxynitrite as assessed by 3-nitrotyrosine concentrations. We studied the first-generation azulenyl nitrone spin traps and showed that they dose-dependently protected against MPTP toxicity with increased efficacy as compared to S-PBN (Klivenyi et al., 1998a,b). In the present study, we examined the efficacy of STAZN to prevent toxicity of both MPTP and 3-NP. STAZN produced dose-dependent significant protection against MPTP-induced depletion of both striatal dopamine and tyrosine hydroxylase immunoreactive neurons in the substantia nigra pars compacta. It significantly reduced the lesion volume produced by 3-NP by

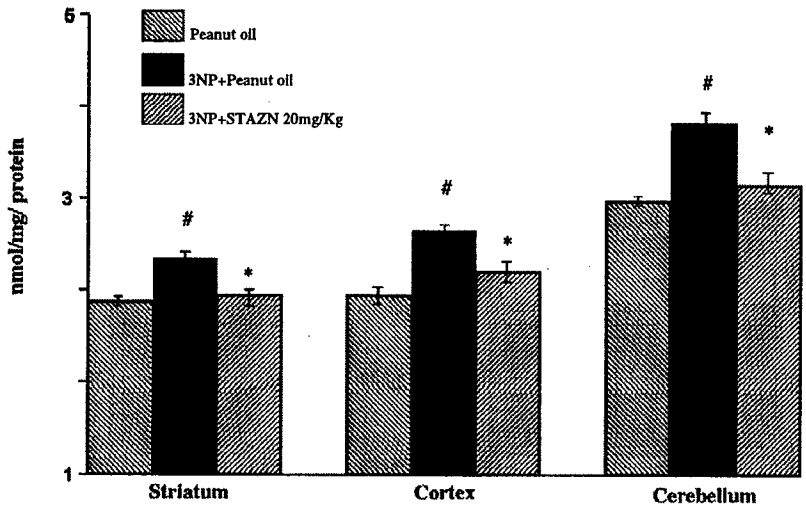


Fig. 6. The production of malondialdehyde was elevated in striatum, cortex, and cerebellum by subcutaneous 3-NP injection, #, $P < 0.05$ when compared with corresponding areas of peanut oil controls. The administration of STAZN significantly reduced the 3-NP-induced malondialdehyde increment back to the control's levels. *, $P < 0.05$ when compared with 3-NP + peanut oil.

approximately 50%. Lastly, it significantly inhibited lipid peroxidation in the striatum, cerebral cortex, and cerebellum produced by systemic administration of 3-NP. This provides further evidence that it is indeed a potent antioxidant that inhibits lipid peroxidation in vivo. It appears to be more potent than the first-generation azulenyl nitrone (AZN), as its protective effects were only significant at a dose of 20 mg/kg (Klivenyi et al., 1998a,b).

Recent studies have shown that STAZN is effective in a model of traumatic brain injury in rats (Belayev et al., 2002). It significantly improved neurologic deficits and reduced contusion size. Furthermore, it was recently shown to be extremely effective in a model of focal ischemia in rats (Ginsberg et al., 2003). In three independent studies, STAZN produced significant improvement in behavior as well as a reduced mean cortical infarct volume of 64–97% and total infarct volume of 42–72%. In over one half of the STAZN treated animals, the cortical infarct was virtually abolished.

STAZN therefore appears to be an extremely promising antioxidant that may have widespread applications for the treatment of neurological disorders including stroke. Results with the neurotoxins MPTP and 3-NP suggest that it may also be a useful antioxidant for the treatment of Parkinson's and Huntington's diseases.

## Acknowledgments

The secretarial assistance of Greta Strong is gratefully acknowledged. This work was supported by the Department of Defense and The Parkinson's Disease Foundation.

## References

Agarwal, R., Chase, S.D., 2002. Rapid, fluorimetric-liquid chromatographic determination of malondialdehyde in biological samples. J. Chromatogr., B, Analyt. Technol. Biomed. Life Sci. 775, 121–126.

Alam, Z.I., Daniel, S.E., Lees, A.J., Marsden, D.C., Jenner, P., Halliwell, B., 1997. A generalized increase in protein carbonyl in the brain in Parkinson's but not incidental Lewy body disease. J. Neurochem. 69, 1326–1329.

Alcaraz-Zubeldia, M., Rojas, P., Boll, C., Rios, C., 2001. Neuroprotective effect of acute and chronic administration of copper (II) sulfate against MPP+ neurotoxicity in mice. Neurochem. Res. 26, 59–64.

Althaus, J.S., Fleck, T.J., Becker, D.A., Hall, E.D., Vonvoigtlander, P.F., 1998. Azulenyl nitrones: colorimetric detection of oxyradical end products and neuroprotection in the gerbil transient forebrain ischemia/reperfusion model. Free Radical Biol. Med. 24, 738–744.

Andreassen, O.A., Ferrante, R.J., Dedeoglu, A., Albers, D.W., Klivenyi, P., Carlson, E.J., Epstein, C.J., Beal, M.F., 2001. Mice with a partial deficiency of manganese superoxide dismutase show increased vulnerability to the mitochondrial toxins malonate, 3-nitropropionic acid, and MPTP. Exp. Neurol. 167, 189–195.

Beal, M.F., Matson, W.R., Swartz, K.J., Gamache, P.H., Bird, E.D., 1990. Kynurenine pathway measurements in Huntington's disease striatum: evidence for reduced formation of kynurenic acid. J. Neurochem. 55, 1327–1339.

Beal, M.F., Matson, W.R., Storey, E., Milbury, P., Ryan, E.A., Ogawa, T., Bird, E.D., 1992. Kynurenic acid concentrations are reduced in Huntington's disease cerebral cortex. J. Neurol. Sci. 108, 80–87.

Beal, M.F., Ferrante, R.J., Henshaw, R., Matthews, R.T., Chan, P.H., Kowall, N.W., Epstein, C.J., Schulz, J.B., 1995. 3-Nitropropionic acid neurotoxicity is attenuated in copper/zinc superoxide dismutase transgenic mice. J. Neurochem. 65, 919–922.

Becker, D.A., 1996. Highly sensitive colorimetric detection and facile isolation of diamagnetic free radical adducts of novel chromotropic nitrone spin trapping agents readily derived from guaiazulene. J. Am. Chem. Soc. 118, 905–906.

Becker, D.A., 1999. Diagnostic and therapeutic applications of azulenyl nitrone spin traps. Cell. Mol. Life Sci. 56, 626–633.

Becker, D.A., Ley, J.J., Echegoyen, L., Alvarado, R., 2002. Stilbazulenyl nitrone (STAZN): a nitronyl-substituted hydrocarbon with the potency of classical phenolic chain-breaking antioxidants. J. Am. Chem. Soc. 124, 4678–4684.

Belayev, L., Becker, D.A., Alonso, O.F., Liu, Y., Busto, R., Ley, J.J., Ginsberg, M.D., 2002. Stilbazulenyl nitrone, a novel azulenyl nitrone antioxidant: improved neurological deficit and reduced contusion size after traumatic brain injury in rats. J. Neurosurg. 96, 1077–1083.

Bloem, B.R., Irwin, I., Buruma, O.J., Haan, J., Roos, R.A., Tetrud, J.W., Langston, J.W., 1990. The MPTP model: versatile contributions to the treatment of idiopathic Parkinson's disease. J. Neurol. Sci. 97, 273–293.

Bogdanov, M.B., Ferrante, R.J., Kuemmerle, S., Klivenyi, P., Beal, M.F., 1998. Increased vulnerability to 3-nitropropionic acid in an animal model of Huntington's disease. J. Neurochem. 71, 2642–2644.

Brouillet, E., Hantraye, P., Ferrante, R.J., Dolan, R., Leroy-Willig, A., Kowall, N.W., Beal, M.F., 1995. Chronic mitochondrial energy impairment produces selective striatal degeneration and abnormal choreiform movements in primates. Proc. Natl. Acad. Sci. U. S. A. 92, 7105–7109.

Browne, S.E., Ferrante, R.J., Beal, M.F., 1999. Oxidative stress in Huntington's disease. Brain Pathol. 9, 147–163.

Chiueh, C.C., Krishna, G., Tulsi, P., Obata, T., Lang, K., Huang, S.J., Murphy, D.L., 1992. Intracranial microdialysis of salicylic acid to detect hydroxyl radical generation through dopamine autooxidation in the caudate nucleus: effects of MPP+. Free Radical Biol. Med. 13, 581–583.

Chiueh, C.C., Wu, R.M., Mohanakumar, K.P., Sternberger, L.M., Krishna, G., Obata, T., Murphy, D.L., 1994. In vivo generation of hydroxyl radicals and MPTP-induced dopaminergic toxicity in the basal ganglia. Ann. N. Y. Acad. Sci. 738, 25–36.

Dexter, D.T., Holley, A.E., Flitter, W.D., Slater, T.F., Wells, F.R., Daniel, S.E., Jenner, P., Marsden, C.D., 1994. Increased levels of lipid hydroperoxides in the parkinsonian substantia nigra: an HPLC and ESR study. Mov. Disord. 9, 92–97.

Fredriksson, A., Eriksson, P., Archer, T., 1997. MPTP-induced deficits in motor activity: neuroprotective effects of the spintrapping agent, alpha-phenyl-*tert*-butyl-nitrone (PBN). J. Neural Transm. 104, 579–592.

Giasson, B.I., Duda, J.E., Murray, I.V.J., Chen, Q., Souza, J.M., Hurtig, H.I., Ischiropoulos, H., Trojanowski, J.Q., Lee, V.M.-Y., 2000. Oxidative damage linked to neurodegeneration by selective a-Synuclein nitration in synucleinopathy lesions. Sci. Mag. 290, 985–989.

Ginsberg, M.D., Becker, D.A., Buston, R., Belayev, A., Zhang, Y., Khoutorova, L., Ley, J.J., Zhao, W., Belayev, L., 2003. Stilbazulenyl nitrone, a novel antioxidant, is highly neuroprotective in focal ischemia. Ann. Neurol. 54, 330–342.

Good, P.F., Hsu, A., Werner, P., Perl, D.P., Olanow, C.W., 1998. Protein nitration in Parkinson's disease. J. Neuropathol. Exp. Neurol. 57, 338–342.

Kim, G.W., Copin, J.C., Kawase, M., Chen, S.F., Sato, S., Gobbel, G.T., Chan, P.H., 2000. Excitotoxicity is required for induction of oxidative stress and apoptosis in mouse striatum by the mitochondrial toxin, 3-nitropropionic acid. J. Cereb. Blood Flow Metab. 20, 119–129.

Klivenyi, P., Matthews, R.T., Wermer, M., Yang, L., MacGarvey, U., Becker, D.A., Natero, R., Beal, M.F., 1998. Azulenyl nitrone spin traps protect against MPTP neurotoxicity. Exp. Neurol. 152, 163–166.

Klivenyi, P., St. Clair, D., Wermer, M., Yen, H.-C., Oberley, T., Yang, L., Beal, M.F., 1998. Manganese superoxide dismutase overexpression attenuates MPTP toxicity. Neurobiol. Dis. 5, 253–258.

Klivenyi, P., Andreassen, O.A., Ferrante, R.J., Dedeoglu, A., Mueller, G., Lancelot, E., Bogdanov, M., Andersen, J.K., Jiang, D., Beal, M.F., 2000. Mice deficient in cellular glutathione peroxidase show increased vulnerability to malonate, 3-nitropropionic acid, and 1-methyl-4-phenyl-1,2,5,6-tetrahydropyridine. J. Neurosci. 20, 1–7.

Knecht, K.T., Mason, R.P., 1993. In vivo spin trapping of xenobiotic free radical metabolites. Arch. Biochem. Biophys. 303, 185–194.

La Fontaine, M.A., Geddes, J.W., Banks, A., Butterfield, D.A., 2000. 3-nitropropionic acid induced in vivo protein oxidation in striatal and cortical synaptosomes: insights into Huntington's disease. Brain Res. 858, 356–362.

Matthews, R.T., Klivenyi, P., Mueller, G., Yang, L., Wermer, M., Thomas, C.E., Beal, M.F., 1999. Novel free radical spin traps protect against malonate and MPTP neurotoxicity. Exp. Neurol. 157, 120–126.

Przedborski, S., Kostic, V., Jackson-Lewis, V., Naini, A.B., Simonetti, S., Fahn, S., Carlson, E., Epstein, C.J., Cadet, J.L., 1992. Transgenic mice with increased Cu/Zn-superoxide dismutase activity are resistant to *N*-methyl-4-phenyl-1,2,3,6-tetrahydropyridine-induced neurotoxicity. J. Neurosci. 12, 1658–1667.

Repine, J.E., Pfenninger, O.W., Talmage, D.W., Berger, E.M., Pettijohn, D.E., 1981. Dimethyl sulfoxide prevents DNA nicking mediated by ionizing radiation or iron/hydrogen peroxide-generated hydroxyl radical. Proc. Natl. Acad. Sci. U. S. A. 78, 1001–1003.

Rivas-Arancibia, S., R., A.I., Zigova, T., Willing, A.E., Brown, W.D., Cahill, D.W., Sanberg, P.R., 2001. Taurine increases rat survival and reduces striatal damage caused by 3-nitropropionic acid. Int. J. Neurosci. 108, 55–67.

Rojas, P., Rios, C., 1993. Increased striatal lipid peroxidation after intracerebroventricular MPP+ administration to mice. Pharmacol. Toxicol. 72, 364–368.

Sanchez-Ramos, J.R., Overvik, E., Ames, B.N., 1994. A marker of oxyradical-mediated DNA damage (8-hydroxy-2′deoyguanosine) is increased in nigro-striatum of Parkinson's disease brain. Neurodegeneration 3, 197–204.

Schulz, J.B., Henshaw, D.R., Matthews, R.T., Beal, M.F., 1995. Coenzyme Q10 and nicotinamide and a free radical spin trap protect against MPTP neurotoxicity. Exp. Neurol. 132, 279–283.

Schulz, J.B., Henshaw, D.R., MacGarvey, U., Beal, M.F., 1996. Involvement of oxidative stress in 3-nitropropionic acid neurotoxicity. Neurochem. Int. 29, 167–171.

Shimizu, S., Simon, R.P., Graham, S.H., 1997. Dimethylsulfoxide (DMSO) treatment reduces infarction volume after permanent focal cerebral ischemia in rats. Neurosci. Lett. 239, 125–127.

Sofic, E., Lange, K.W., Jellinger, K., Riederer, P., 1992. Reduced and oxidized glutathione in the substantia nigra of patients with Parkinson's disease. Neurosci. Lett. 142, 128–130.

Thomas, B., Muralikrishnan, D., Mohanakumar, K.P., 2000. In vivo hydroxyl radical generation in the striatum following systemic administration of 1-methyl-4-phenyl-1,2,3,6-tetrahydropyridine in mice. Brain Res. 852, 221–224.

Tipton, K.F., Singer, T.P., 1993. Advances in our understanding of the mechanisms of the neurotoxicity of MPTP and related compounds. J. Neurochem. 61, 1191–1206.

Zhang, J., Perry, G., Smith, M.A., Robertson, D., Olson, S.J., Graham, D.G., Montine, T.J., 1999. Parkinson's disease is associated with oxidative damage to cytoplasmic DNA and RNA in substantia nigra neurons. Am. J. Pathol. 154, 1423–1429.

ELSEVIER

Neurobiology of Disease

www.elsevier.com/locate/ynbdi
Neurobiology of Disease 17 (2004) 250–259

# A novel systemically active caspase inhibitor attenuates the toxicities of MPTP, malonate, and 3NP in vivo

Lichuan Yang,[a] Shuei Sugama,[b] Ronald P. Mischak,[c] Mahmoud Kiaei,[a] Nicolas Bizat,[d] Emmanuel Brouillet,[d] Tong H. Joh,[b] and M. Flint Beal[a,*]

[a]*Department of Neurology and Neuroscience, Weill Medical College of Cornell University, New York, NY 10021, USA*
[b]*Burke Medical Research Institute, White Plains, NY 10605, USA*
[c]*Enzyme Systems Products, Inc., Livermore, CA 94550, USA*
[d]*URA-CEA-CNRS 2210, Service Hospitalier Frédéric Joliot, DRM, DSV, CEA, Orsay 91401 Cedex, France*

Received 22 December 2003; revised 26 July 2004; accepted 28 July 2004

**Molecular machinery involved in apoptosis plays a role in neuronal death in neurodegenerative disorders such as Parkinson's disease (PD) and Huntington's disease (HD). Several caspase inhibitors, such as the well-known peptidyl inhibitor carbobenzoxy-Val-Ala-Asp-fluoromethylketone (zVADfmk), can protect neurons from apoptotic death caused by mitochondrial toxins. However, the poor penetrability of zVADfmk into brain and toxicity limits its use therapeutically. In the present study, a novel peptidyl broad-spectrum caspase inhibitor, Q-VD-OPH, which offers improvements in potency, stability, and toxicity over zVADfmk, showed significant protection against 1-methyl-4-phenyl-1,2,3,6-tetrahydropyridine (MPTP), 3-nitropropionic acid (3NP), and malonate toxicities. Q-VD-OPH significantly reduced dopamine depletion in striatum produced by MPTP administration and prevented MPTP-induced loss of dopaminergic neurons in the substantia nigra. It significantly reduced the size of striatal lesions produced by intrastriatal malonate injections and systemic administration of 3NP. Western blots performed on tissues from the midbrain following administration of MPTP or the striatum in 3NP-treated animals showed increases of the active forms of caspase-9 and caspase-8, as well as the caspase-8-mediated proapoptotic protein Bid, which were inhibited Q-VD-OPH treatment. These findings suggest that systematically active broad-spectrum caspase inhibitors maybe useful in the treatment of neurodegenerative diseases such as PD and HD.**


*Keywords:* Caspase inhibitor; Calpain; Parkinson's disease; Huntington's disease; ALS

## Introduction

There is substantial evidence implicating apoptosis and caspase activation in neurodegenerative diseases as well as in animal models of neurodegenerative diseases. Mitochondrial injury, which is implicated in these diseases, leads to release of cytochrome *c* into the cytoplasm where it can initiate the cascade of caspase activation by triggering the activation of caspase-9, which elicits the activation of capsase-3, leading to the morphologic changes associated with apoptosis (Friedlander, 2003). Alternatively, activation of death receptors (FADD or TRADD) leads to activation of caspase-8, which can truncate Bid, which translocates to mitochondria, leading to cytochrome *c* release and ultimately to caspase-3 activation.

The development of systemically active caspase inhibitor may therefore prove useful for treatment of neurodegenerative diseases. A number of mitochondrial toxins have been used to model neurodegenerative diseases. These include 1-methyl-4-phenyl-1,2,3,6-tetrahydropyridine (MPTP) to model Parkinson's disease (PD) and 3-nitropropionic acid (3NP) and malonate to model Huntington's disease (HD). As yet, no systemically available caspase inhibitors have been reported, which show efficacy in the central nervous system. Recently, a broad-spectrum caspase inhibitor was developed in which a carboxy terminal phenoxy group was conjugated to amino acids valine and aspartate (Q-VD-OPH). This compound is significantly more effective than the widely used inhibitors zVAD-Fmk and Boc-D-Fmk in preventing apoptosis in vitro (Caserta et al., 2003). It is equally effective in preventing apoptosis mediated by the three major apoptotic pathways: caspase-9/3, caspase-8/10, and caspase-12. It is not toxic to cells even at extremely high concentrations. In the present study, we therefore examined the efficacy of Q-VD-OPH against MPTP, malonate, and 3NP neurotoxicity. We also examined the effects of Q-VD-OPH on MPTP- and 3NP-induced activation of caspase-8, caspase-9, Bid truncation, and calpain activation.

* Corresponding author. Department of Neurology and Neuroscience, Weill Medical College of Cornell University, Room F610, 525 East 68th Street, New York, NY 10021. Fax: +1 212 746 8532.
*E-mail address:* fbeal@med.cornell.edu (M.F. Beal).
**Available online on ScienceDirect (www.sciencedirect.com.)**

0969-9961/$ - see front matter © 2004 Elsevier Inc. All rights reserved.
doi:10.1016/j.nbd.2004.07.021

## Materials and methods

### *Animals and materials*

Male Swiss–Webster mice (3 months old, 30–35 g), male Lewis rats (3 months old, 300–350 g), and male Sprague–Dawley (SD) rats (350–400 g) were obtained from the Jackson Laboratory (Bar Harbor, ME, USA). MPTP, 3NP, and malonic acid were bought from Sigma (St. Louis, MO, USA). The caspase inhibitor Q-VD-OPH was a gift from Enzyme Systems (Livermore, CA, USA). All animal experimental procedures were in strict accordance with the regulations of the Weill Cornell Medical College and in accordance with the NIH Guide for the Care and Use of Laboratory Animals.

### *Animal models and Q-VD-OPH treatment*

Q-VD-OPH was dissolved in 100% dimethyl sulfoxide (DMSO) and was administered intraperitoneally at a dose of 20 mg $kg^{-1}$ $day^{-1}$ in all experiments. An equal volume of DMSO was given to controls. Q-VD-OPH and DMSO administrations were started 12 h before the injections of the mitochondrial toxins and continued for 3 days in the malonate model, 4 days in the acute MPTP model, and 7 days in the 3NP and the chronic MPTP model.

We examined both acute and chronic regimens of MPTP administration. In the acute regimen, MPTP in phosphate-buffered saline (PBS) was injected intraperitoneally to Swiss–Webster mice at doses of 10, 15, or 20 mg/kg, four times at intervals of 2 h. For each dose, 8–14 mice were examined. Mice were sacrificed 7 days after the MPTP injections, and the striata were dissected for catecholamine analysis. The mesencephalons were fixed in 4% paraformaldehyde for 5 days for tyrosine hydroxylase (TH) immunostaining. Fresh striatal and mesencephalic tissues taken 1 day after MPTP injection were prepared for assessment of caspase activation by Western blot analysis. The brains were sliced at 1 mm intervals and the striatum and ventral midbrain including the substantia nigra were dissected. The chronic regimen consisted of MPTP 15, 20, or 30 mg/kg, once a day for 5 days in Swiss–Webster mice. Animals were sacrificed 7 days after the last dose of MPTP and fresh tissues were dissected for measurements, dopamine, and numbers of TH immunoreactive neurons, as described above.

For the 3NP experiments, 100 mg/ml of 3NP stock solution was made in 1 N NaOH and adjusted to pH 7.4. The stock solution was diluted according to the initial weight of individual Lewis rats and a dose of 56 mg $kg^{-1}$ $day^{-1}$ and was delivered by subcutaneous infusion using Alzet osmotic minipumps (Durect Corporation, Cupertino, CA, USA, model 2ML1, 10 μl/h for 7 days), which were implanted beneath the skin between the scapulae under pentobarbital anesthesia. Signs of dystonia including limb dragging, wobbling gait, and recumbency were seen from the 3rd day onwards of the 3NP infusions in both Q-VD-OPH- or DMSO-treated groups (15 rats in each group). All animals were sacrificed on the 7th day of the 3NP infusion, and brains were rapidly removed and placed in cold saline for 10 min before being processed for 2,3,5-triphenyltetrazolium chloride monohydrate staining (TTC; Sigma). Another set of 3NP and Q-VD-OPH- or DMSO-cotreated animals had their striata dissected at 1, 3, and 5 days after the 3NP infusion for measurements of active caspases by Western blot (five animals per group).

In the malonate experiments, SD rats pretreated with Q-VD-OPH or DMSO (eight animals per group) were anesthetized with pentobarbital and positioned on a David Kopf stereotaxic instrument (Tujunga, CA, USA) with the incisor bar at 3.3 mm below the interaural line. A volume of 1.5 μl of 2 M malonic acid (3 μmol in amount) in $H_2O$, pH 7.4 with HCl, was injected into left striatum with a 10-μl Hamilton syringe (Reno, NE, USA) at the coordinates 1 mm anterior to the bregma, 2.6 mm lateral to the midline, and 5 mm ventral to the dura. All injections were made over 2 min and the needle was left in the striatum for an additional 2 min before being slowly withdrawn. Animals were sacrificed 1 week after the surgery and brain slices were examined using TTC staining.

### *TTC staining and lesion volume measurement*

Two percent TTC solution was made with distilled water and kept in brown bottles at 4°C until use. One-millimeter-thick fresh brain slices were cut with a rat brain matrix (Harvard Apparatus, Holliston, MA, USA) and promptly dipped in dishes with 2% TTC for 30 min in a dark cabinet until the intact tissue of the slice was stained to deep purple and the lesioned area was noted by pale staining. Stained slices were then kept in 4% paraformaldehyde in the dark at 4°C not more than 2 weeks before analysis. All samples were blindly coded and the lesion area was measured on both the anterior and posterior sides of each slice using a microcomputer imaging device (MCID; Imaging Research Inc., St. Catharine, Ont. Canada). The lesion volume (expressed in $mm^3$) was calculated by averaging the lesion area of each section, multiplying it with the section thickness, and summing the values of all the lesioned sections. We previously demonstrated that TTC measurements directly correlate with measurements made on adjacent Nissl-stained sections (Schulz et al., 1995).

### *HPLC assay for catecholamines*

Dissected striata were sonicated and centrifuged in chilled 0.1 M perchloric acid (PCA; 100 μl/mg tissue). The supernatants were used for measurements of dopamine and its metabolites 3,4-dihydroxyphenylacetic acid (DOPAC) and homovanillic acid (HVA) by HPLC as modified from our previously described method (Beal et al., 1990). Briefly, 10 μl supernatant was isocratically eluated through a 80 × 4.6 mm C18 column (ESA, Inc. Chelmsford, MA) with a mobile phase containing 0.1 M, $Li_3PO_4$, 0.85 mM 1-octanesulfonic acid, and 10% (v/v) methanol and detected by a 2-channel Coulochem II electrochemical detector (ESA, Inc.). Concentrations of dopamine and its metabolites are expressed as nanogram per milligram protein. The protein concentration were measured using the Bio-Rad protein analyze protocol (Bio-Rad Laboratories, Hercules, CA) and Perkin Elmer Bio Assay Reader (Norwalk, CT).

### *Immunostaining for tyrosine hydroxylase-positive neurons*

Midbrains from MPTP-treated mice that were also treated with either Q-VD-OPH or vehicle were postfixed in 4% paraformaldehyde for 5 days and cryoprotected in 30% sucrose overnight. Sections (40 μm) through both the left and right substantia nigra pars compacta (SNpc) were washed for 30 min in PBS, incubated with 1% bovine serum albumin (BSA) and 0.2% Triton X-100 in 0.1 M PBS for 1 h, washed in PBS containing 0.5% BSA for 30 min, then incubated overnight in blocking solution containing antibody to tyrosine hydroxylase (TH, 1:25,000; Incstar, Stillwater, MN). Sections were washed in PBS-BSA, incubated for 1 h with

biotinylated secondary anti-rabbit antibody (1:200, Vector Laboratories, Burlingame, CA), and visualized by reaction with 3,3′-diaminobenzidin-terahydrochloride (DAB, 0.05%) as a chromogen and hydrogen peroxide (0.003%) for 5 min. Sections were mounted on gelatin-coated slides, dehydrated through graded ethanols, and cleared in xylene before being coverslipped with Permount. TH-positive neurons in the outlined SNpc were counted under 100× oil magnification as they appeared within a counting frame created by KS 400 software (Zeiss, Thornwood, NY). These counts were within a homogenous structure, thus allowing for valid stereological measurements.

*Western blot for analyzing caspase-8, caspase-9, and Bid cleavages*

Brain tissues were sonicated briefly in 200 μl of lysis buffer containing 250 mM sucrose, 10 mM KCl, 1.5 mM MgCl2, 2 mM EDTA pH 6.8, 20 mM HEPES, and protease inhibitor (Complete, Roche, Basel, Switzerland), centrifuged at 9000 × *g* for 20 min at 4°C, and the supernatants were collected. Protein concentrations were measured using the Bio-Rad protein assay. Supernatants were loaded with 60 μg protein in each lane on a precast 4–20% Tris–HCl gel (Bio-Rad) and the separated proteins were blotted on a PVDF membrane (NOVEX, San Diego, CA). Primary antibodies applied to the blots were 1:1000 dilutions of polyclonal anti-human/mouse Bid (R&D Systems, Minneapolis, MN), polyclonal anti-mouse/rat caspase-8 (Pharmingen, San Diego, CA), and polyclonal anti-mouse/rat caspase-9 (Stressgen, Victoria, BC, Canada), followed by incubation with horseradish peroxidase-conjugated secondary antibody (Zymed Lab, San Francisco, CA), and peroxidase activity was detected using enhanced chemiluminescence (ECL; Amersham Pharmacia Biotech, Arlington Heights, IL).

The optical density of Western blot bands measured with the density analysis software installed in the microcomputer imaging device (MCID; Imaging Research Inc.). A density step wedge (Kodak, NY) was used to establish the calibration curve and all the density values read from the blot bands were in the liner range of calibration without reaching the saturation limits. A rectangular measuring cursor was sized in the center of the bands and the same size was fixed to measure all the bands on the same film. Density reading from the film background was subtracted from the band density readings. Five animals were examined for each Western blot.

*Proteolytic activity assay using fluorogenic substrates for calpain and caspase-8*

The fluorescent assays of calpain or caspase-8 activities are based on the cleavage of 7-amino-4-methyl-coumarin (AMC) or 7-amino-4-trifluoro-methyl-coumarin (AFC) dyes from the C-terminus of the peptide substrates. Calpain activity was determined using *N*-succinyl-Leu-Tyr-(*N*-succinyl-LY)-AMC, a substrate preferentially cleaved by μ- or m-calpain (McDonald et al., 2001). Calpain activity ($Ca^{2+}$-dependent cleavage of *N*-succinyl-LY-AMC) present in brain sample supernatants (approximately 10 μl containing about 30 μg of protein) was determined as the difference between the calcium- and the non-calcium-dependent fluorescence. The calcium-dependent fluorescence released was measured after a 30-min incubation at 37°C in buffer A containing 63 mM imidazole–HCl, pH 7.3, 10 mM β-mercaptoethanol, and 5 mM $CaCl_2$ and is due to the cleavage of 150 μM *N*-succinyl-LY-AMC. The non-calcium-dependent fluorescence was measured under the same conditions using buffer A without added calcium and containing 1 mM EDTA and 1 mM EGTA. To determine whether Q-VD-OPH inhibits calpain activity in vitro, 10 μl of inhibitor solution (from 10 nM to 1 mM) was incubated in 90 μl of calpain assay buffer containing purified μ-calpain (0.2 units; Calbiochem, San Diego, CA, USA). Caspase-8 activity was tested on peptidic substrates (Biomol) using *N*-acetyl-Ile-Glu-Thr-Asp-AFC (IETD-AFC). Soluble fractions (30 μg of protein) were incubated at 37°C for 45 min in a caspase buffer B (20 mM HEPES, pH 7.4, 50 mM NaCl, 0.2 mM EDTA, 4 mM DTT) with 40 μM of the appropriate substrate. The nonspecific activity was considered as the activity remaining in the presence of the fluorogenic substrate and 10 μM of the appropriate caspase inhibitor, that is, the C-terminal aldehyde form (CHO) of the substrate (IETD-CHO). Fluorescence (excitation/emission: 400/505 nm for AFC and 380/460 nm for AMC) was measured in 96-well plates using a "Fusion" fluorimeter (Packard Bioscience, Rungis, France). Enzyme activity was calculated using standard curves of AFC or AMC and expressed as pmol AFC or AMC released min/mg of protein.

*Statistical analysis*

Results were expressed as means ± standard error of the mean (SEM). Differences between Q-VD-OPH-treated and control groups were assessed by ANOVA, followed by Tukey–Kramer test for comparison among different means. The value $P < 0.05$ was taken as being statistically significant.

## Results

*Q-VD-OPH protects mice from MPTP dopaminergic toxicity*

Transgenic animals overexpressing the apoptosis inhibitors p35 or Bcl-2 are resistant to neurotoxicity produced MPTP (Viswanath et al., 2001; Yang et al., 1998). In line with this, activation of caspases has been reported in MPTP-treated mice (Turmel et al., 2001; Viswanath et al., 2001). In the present study, we examined whether administration of the caspase inhibitor peptide Q-VD-OPH could block MPTP-induced neurodegeneration. As shown in Table 1, Q-VD-OPH attenuates the depletion of dopamine and its metabolites in striatum caused by acute MPTP toxicity (Table 1). Three different MPTP doses were examined in our acute MPTP toxicity regime. MPTP (10 mg/kg ip, four times a day) depleted striatal dopamine levels to 30% of vehicle-injected controls, whereas coinjection of Q-VD-OPH, 20 mg/kg daily, resulted in striatal dopamine levels that were 59% of control levels. When the MPTP dose was increased to 15 mg/kg four times a day, the striatal dopamine depletion with Q-VD-OPH was 43% of controls. This dose alone reduced striatal dopamine to 24% of controls. Increasing the MPTP dosage further to 20 mg/kg completely abolished the protective effect of Q-VD-OPH against MPTP-induced striatal dopamine depletion. The dopamine levels in the MPTP alone and MPTP with Q-VD-OPH-treated groups were both reduced to 14% of controls, consistent with a "floor effect" in which the toxicity associated with this dose of MPTP was too severe to be prevented by Q-VD-OPH. It is also likely that necrotic cell death may be predominate with severe toxic insults. The dopamine metabolites DOPAC and HVA showed similar patterns to dopamine. Q-VD-OPH itself did not influence catecholamine

Table 1
Q-VD-OPH attenuate striatal DA, DOPAC, and HVA depletion caused by acute MPTP toxicity but not that caused by chronic MPTP toxicity

| MPTP | DMSO (μl) | Q-VD in DMSO (mg/kg) | *n* | DA | DOPAC | HVA |
|---|---|---|---|---|---|---|
| 0 | 50 | | 13 | 116.9 ± 2.8 | 10.3 ± 0.5 | 14.2 ± 0.6 |
| 0 | | 20 | 13 | 115.9 ± 4.3 | 10.6 ± 0.8 | 12.7 ± 0.7 |
| Acute regime (mg/kg) | | | | | | |
| 10 | 50 | | 14 | 34.9 ± 4.2[a] | 4.4 ± 0.3[a] | 7.3 ± 0.4[a] |
| | | 20 | 14 | 68.3 ± 7.5[a,b] | 7.8 ± 0.6[a,b] | 10.7 ± 0.6[a,b] |
| 15 | 50 | | 10 | 28.4 ± 5.6[a] | 2.3 ± 0.4[a] | 5.7 ± 0.7[a] |
| | | 20 | 8 | 49.8 ± 5.5[a,b] | 4.0 ± 0.4[a,b] | 9.0 ± 1.8[a,b] |
| 20 | 50 | | 11 | 17.1 ± 3.0[a] | 1.5 ± 0.1[a] | 4.5 ± 0.3[a] |
| | | 20 | 11 | 17.1 ± 1.5[a] | 1.6 ± 0.1[a] | 4.5 ± 0.2[a] |
| Chronic regime (mg/kg) | | | | | | |
| 15 | 50 | | 13 | 51.7 ± 4.6[a] | 6.3 ± 0.6[a] | 8.4 ± 0.6[a] |
| | | 20 | 14 | 57.2 ± 2.6[a] | 7.5 ± 0.3[a] | 9.7 ± 0.4[a] |
| 20 | 50 | | 14 | 37.1 ± 2.1[a] | 3.7 ± 0.3[a] | 7.2 ± 0.3[a] |
| | | 20 | 12 | 42.1 ± 3.2[a] | 3.7 ± 0.2[a] | 8.1 ± 0.4[a] |
| 30 | 50 | | 13 | 30.3 ± 3.7[a] | 2.8 ± 0.3[a] | 7.3 ± 0.8[a] |
| | | 20 | 13 | 41.1 ± 4.8[a] | 3.6 ± 0.5[a] | 8.5 ± 0.7[a] |

Values expressed as ng/mg protein; data expressed as mean ± SEM. Acute regime, MPTP dosed every 2 h for four times in total; chronic regime, MPTP dosed once a day for 5 days. DA, Dopamine; DOPAC, 3,4-dihydroxyphenylacetic acid; HVA, homovanillic acid.
[a] Statistically significant from DMSO- or Q-VD-treated controls.
[b] Statistically significant from correspondent MPTP dosing mice.

metabolism in the striatum (data not shown). The protective property of Q-VD-OPH against acute MPTP toxicity was confirmed by preservation of TH-immunoreactive neurons in the SNpc. Administration of MPTP, 10 mg/kg, four times in a day, caused 30% cell loss in SNc as compared to controls, whereas coinjection with 20 mg/kg Q-VD-OPH showed 15% cell loss (Figs. 1 A, C, and E), achieving a 50% protective effect, which matches well with its 50% protection effect against striatal dopamine depletion.

We did not see a protective effect of Q-VD-OPH against depletion of striatal dopamine and its metabolites in our chronic MPTP toxicity dosing regimen, even though the severity of the dopamine depletion caused by the three MPTP doses chosen in this regimen, 15, 20, or 30 mg/kg, once a day for 5 days, was milder than that seen in our acute regime (Table 1). However, a significant preservation of TH-immunoreactive neurons in the SNpc by Q-VD-OPH (17% cell loss) was observed with chronic MPTP toxicity administered at 20 mg/kg, once a day for 5 days, which caused a 38% of TH-immunoreactive cell loss as compared to controls (Figs. 1B, D, and F). It is possible that with more chronic dosing, activation of calpain may play a more critical role in MPTP toxicity as recently shown by other authors (Crocker et al., 2003).

*Q-VD-OPH reduces both malonate- and 3NP-caused striatal lesions*

Malonate is a reversible inhibitor of the mitochondrial enzyme succinate dehydrogenase and is used to model HD (Beal et al., 1993). Intrastriatal injection of malonate induces caspase cleavage and apoptotic cell death, which is reduced by the caspase inhibitor *N*-benzyloxycarbonyl-Val-Ala-Asp-fluoromethylketon (zVAD-fmk) delivered into the brain by intraventricular injection (Schulz et al., 1998). Q-VD-OPH administration significantly reduced striatal lesions produced by intrastriatal injection of malonate. The lesion volume in the striatum of rats treated with vehicle was 27.3 ± 2.0 $mm^3$. Q-VD-OPH significantly ($P < 0.05$) reduced the striatal lesion volume by 30% to 19.3 ± 2.6 $mm^3$ (Fig. 2A).

The 3NP irreversibly blocks the mitochondrial enzyme succinate dehydrogenase. Systemic administration of 3NP by either intraperitoneal injection or subcutaneous pump implantation produces striatal lesions, which mimic the histopathology of HD (Brouillet et al., 1999). The 3NP-induced cell death involves caspase activation (Bizat et al., 2003; Duan et al., 2000). Therefore, we studied whether the caspase inhibitor Q-VD-OPH could reduce 3NP-induced striatal lesions. The 3NP was delivered subcutaneously via osmotic pumps for 7 days in Lewis rats. Lewis rats were chosen in our study because they have a less individual variability in their vulnerability to 3NP toxicity than Sprague–Dawley rats (Ouary et al., 2000). The lesion volume of the striata of rats treated with vehicle was 28.8 ± 7 $mm^3$ and the lesion volume was reduced to less than 50% of the vehicle controls in rats treated with Q-VD-OPH (12.4 ± 4 $mm^3$, $P < 0.05$) (Fig. 2B).

*Q-VD-OPH inhibits MPTP- or 3NP-induced cleavage of caspase-8, caspase-9, and Bid and reduces caspase-8 activity induced by 3NP*

Caspase-3 activation can elicit the activation of caspase-8, which can truncate Bid, and cause caspase-8-mediated mitochondrial damage and cell death (Tang et al., 2000; Viswanath et al., 2001). Bid is a member of the Bcl-2 family, and truncated Bid translocates from the cytoplasm to mitochondria, where it appears to interact with and antagonize the actions of antiapoptotic members of the Bcl-2 family, thereby causing an efflux of cytochrome *c* from the mitochondria (Li et al., 1998). The possibility that Q-VD-OPH blocks caspase activation is suggested by its neuroprotective effects in our MPTP, malonate, and 3NP animal models. We performed Western blots to investigate changes in cleaved fragments of caspase-9, caspase-8, and Bid in our MPTP and 3NP animal models with or without Q-VD-OPH treatment. We found that Q-VD-OPH inhibits MPTP- or 3NP-induced cleavage of these two caspases as well as Bid. Animals treated with an acute MPTP (15 mg/kg) regimen manifested significant elevations in cleaved caspase-9, caspase-8, and Bid in midbrains, whereas these elevations were diminished to control levels in animals cotreated

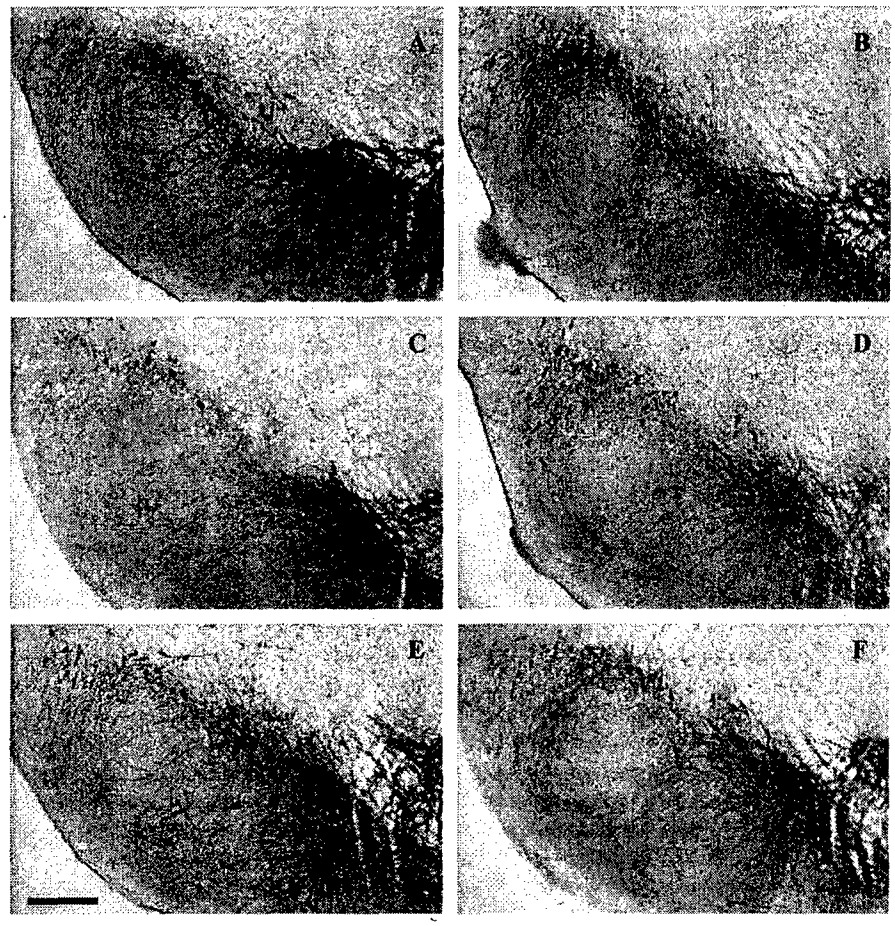


Fig. 1. Immunostaining for tyrosine hydroxylase-positive neurons in substantia nigra pars compacta in mice treated with just vehicle DMSO (A and B), acute MPTP dose regime alone (C) and with Q-VD-OPH (E), chronic MPTP dose regime alone (D) and with Q-VD-OPH (F). As shown in the figure, both MPTP dose regimes significantly reduce the number of TH-immunoreactive-positive neurons and Q-VD-OPH treatment significantly preserves the loss of neurons. All the representative pictures were taken from midbrain sections −3.52 mm away from bregma. Scale bar = 200 μm.

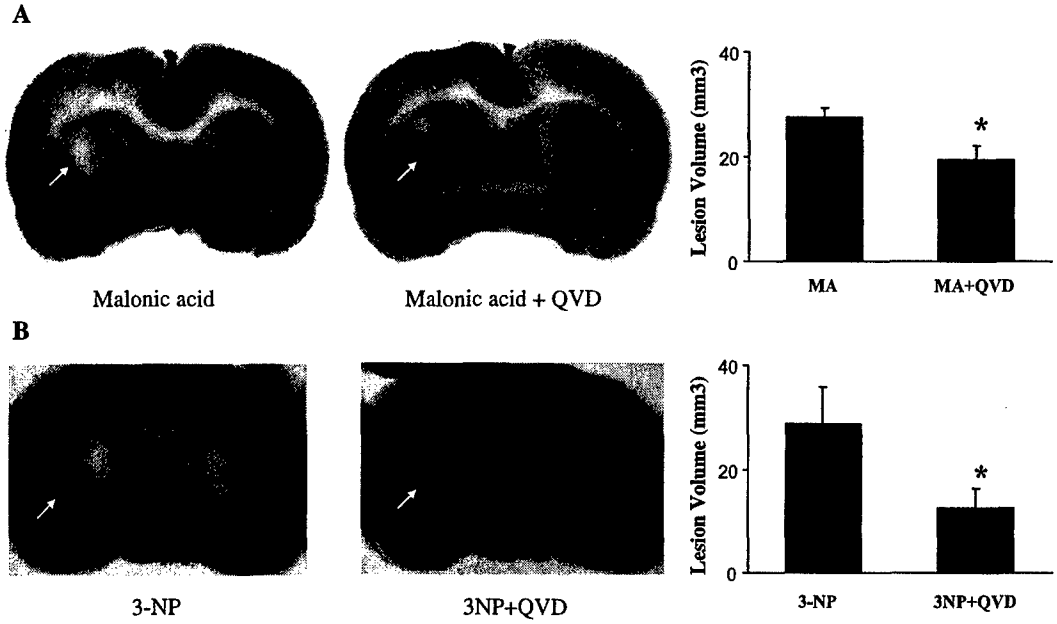


Fig. 2. TTC staining showing striatal lesions (see arrows) caused by intrastriatal malonic acid (MA) injection (A) and subcutaneous 3NP infusion (B). Q-VD-OPH significantly reduced striatal lesion volumes caused by these two toxins. Bar graphs show the comparison between groups; $^{*}P < 0.05$.

with Q-VD-OPH (Fig. 3). MPTP also induced a significant increase of procaspase-9 and procaspase-8 in these brain regions; however, Q-VD-OPH did not block the increases of procaspases indicating that it is specifically targeting caspase cleavage. Following systemic delivery of 3NP to rats by subcutaneously installed osmotic minipumps, we found that both pro- and cleaved forms of caspase-9 and caspase-8 increased in the striatum at 1, 3, and 5 days. Q-VD-OPH significantly inhibited 3NP-induced increments in the cleaved fragments of these two caspases. The cleaved fragment of Bid in the striatum was significantly increased from the 3rd day on following 3NP administration, and Q-VD-OPH reduced the cleaved Bid fragments to the control levels on the 5th day following 3NP delivery. The lag in Bid cleavage shown in our Western blots is probably due to its property as a specific substrate of active caspase-8 (Fig. 4). In our enzyme activity assays, caspase-8 activity was significantly increased on the 3rd day following 3NP delivery and was reduced by Q-VD-OPH to a level that was not significantly different from the control levels (Fig. 5).

*Q-VD-OPH does not inhibit increased calpain activity induced in vivo by 3NP*

Calpains (μ calpain and m-calpain) belong to a family of cysteine proteases, which are different from caspases. Calpains are present in the cell cytosol as heterodimers consisting of a catalytic 80-kDa subunit and a regulatory 30-kDa subunit. They are activated by increases in calcium concentration leading to autolytic processing (Chan and Mattson, 1999; Wang, 2000). Once activated by micromolar concentrations of $Ca^{2+}$, μ-calpain can itself activate m-calpain through a "heterolytic" processing (Tompa et al., 1996). In the brain, calpain participates in $Ca^{2+}$-dependent events such as synaptic plasticity. Many protein substrates of calpain have been identified such as intracellular signaling kinases, cytoskeleton components, neurotransmitter membrane receptors, and transcription factors (Chan and Mattson, 1999). Activation of calpain plays an important role in cell death induced by excitotoxicity and hypoxia or ischemia, which are associated with calcium dysregulation. It was recently shown that calpain plays a role in striatal degeneration in vivo in a chronic model of 3NP administration (Bizat et al., 2003). Since there exists a crosstalk between calpain and caspase pathways and calpain may down-regulate the caspase-9 or caspase-3 pathway, we examined whether Q-VD-OPH interacted with calpain (Bizat et al., 2003). We found a fivefold increase in calpain activity in the striatum on the 5th day following systemic 3NP administration. Administration of the caspase inhibitor Q-VD-OPH slightly reduced 3NP-induced activation of calpain, but this was not statistically significant, and in vitro Q-VD-OPH demonstrated no inhibitory effect on μ-calpain activity (Fig. 6B).

## Discussion

In the present study, we examined the efficacy of a novel systemically active caspase inhibitor against lesions produced by mitochondrial toxins, which have been used to model human neurodegenerative diseases. We examined the effects of the novel peptidyl broad-spectrum caspase inhibitor Q-VD-OPH. This compound is a new generation broad-spectrum caspase inhibitor that offers improvements in potency, stability, and toxicity over the benchmark caspase inhibitor z-VAD-Fmk (Caserta et al., 2003). The improvements derive from significant changes in its structural design that include replacement of the carbobenzoxy blocking group (Z) with a quinoline derivative (Q), modification of the tripeptide sequence from VAD to VD, and replacement of the toxic fluoromethyl ketone (FMK) with the nontoxic 2,6-difluorophenol leaving group. The mechanism of action involves the formation of an irreversible thioether bond between the aspartic acid derivative

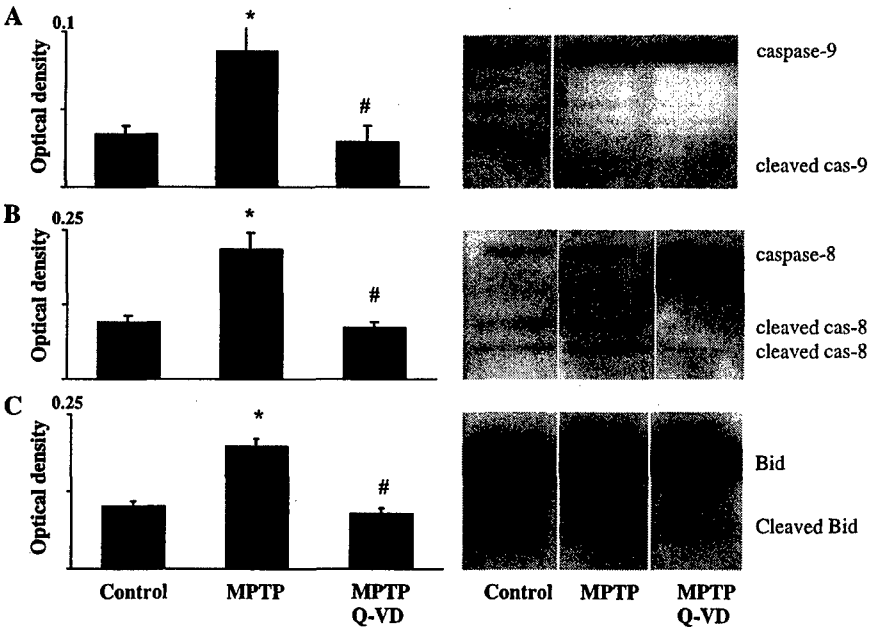


Fig. 3. Western blots showing accumulations of caspase-9 (A), caspase-8 (B), and Bid (C) in midbrains in mice treated with vehicle (control), MPTP alone, and MPTP with Q-VD-OPH (Q-VD). MPTP induces significant increases in cleaved caspase-9, caspase-8, and Bid fragments and Q-VD-OPH significantly inhibits these MPTP-induced increases. Bar graphs show the comparison among groups; *statistically significant from controls; #statistically significant from MPTP alone group. Gel graphs also show that the production of procaspase-9 and procaspase-8 was markedly induced by MPTP and is not inhibited by Q-VD-OPH.

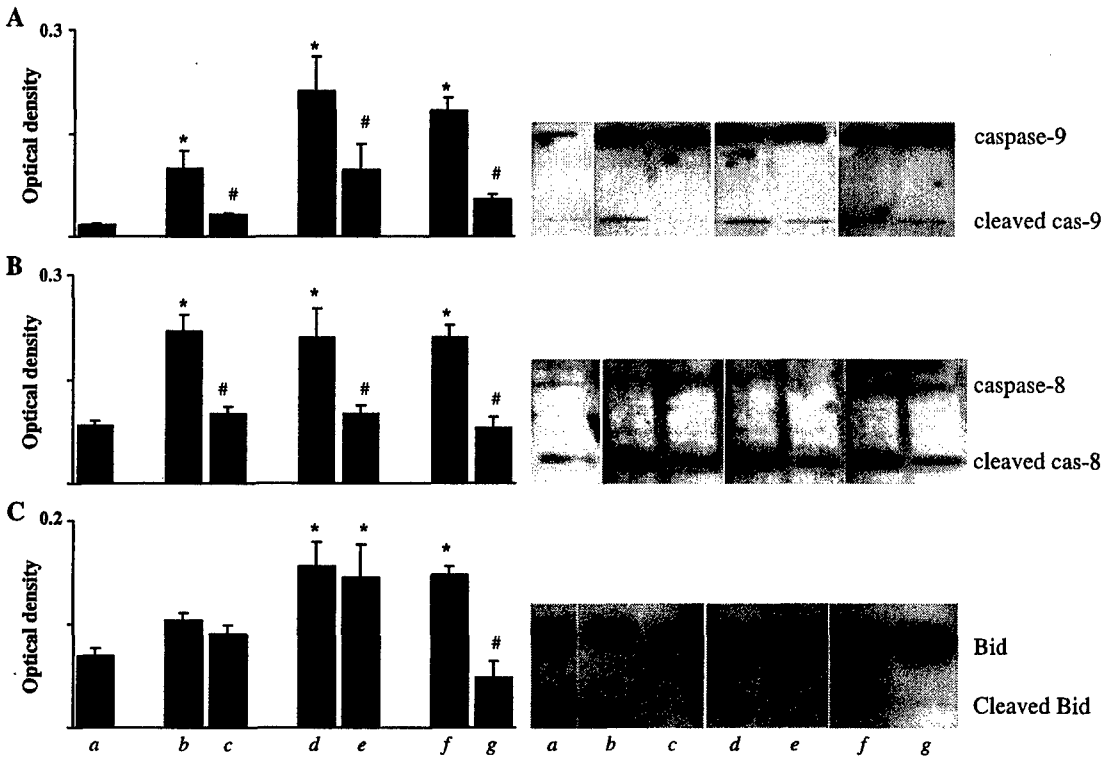


Fig. 4. Western blots showing accumulations of caspase-9 (A), caspase-8 (B), and Bid (C) in the striatum of rats treated with vehicle (*a*), 3NP alone (*b*, *d*, and *f*), and 3NP with Q-VD-OPH (*c*, *e*, and *g*) at day 1 (*b* and *c*), day 3 (*d* and *e*), and day 5 (*f* and *g*) following 3NP subcutaneous infusion. 3NP induces significant increases in cleaved caspase-9 and caspase-8 fragments in the striatum at all time points, and Q-VD-OPH significantly inhibited these 3NP-induced increases. The accumulation of cleaved Bid fragments was significantly increased by 3NP from the 3rd day onward and was significantly reduced by Q-VD-OPH at 5th day following 3NP infusion. Bar graphs show the comparison among groups; *statistically significant from vehicle controls; #statistically significant from 3NP alone group. Gel graphs also show the production of procaspase-9, and procaspase-8 was markedly induced by 3NP and was not inhibited by Q-VD-OPH.

in the inhibitor and the active site cysteine of the caspase, with displacement of the 2,6-difluorophenol leaving group. In vitro studies show that Q-VD-OPH inhibits caspases-1, -3, -8, and -9 with IC 50 values of 25–400 nM (Enzyme Systems, unpublished data). It is much more potent than zVAD-Fmk in inhibiting apoptosis in vitro and it blocks apoptosis mediated by the three major apoptotic pathways: caspase-9/3, caspase-8/10, and caspase-12 (Caserta et al., 2003).

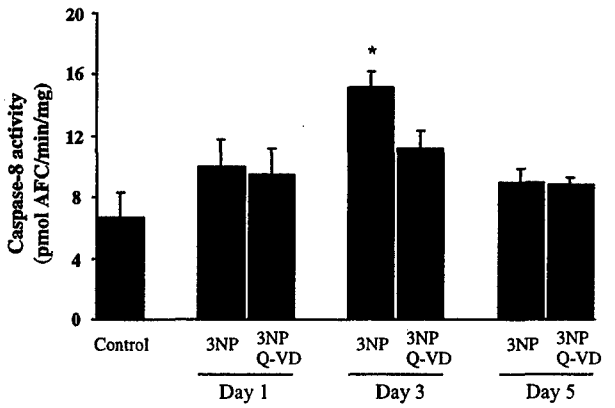


Fig. 5. Proteolytic activity of active caspase-8 from the striatal tissues in rats treated with vehicle (control), 3NP alone, and 3NP with Q-VD-OPH (Q-VD) at days 1, 3, and 5 following 3NP subcutaneous infusion. Caspase-8 activity increased significantly at the 3rd day following 3NP infusion and was reduced by coinjecting Q-VD-OPH, but the reduction failed to reach statistical significance. *Statistically significant from the vehicle control.

In the present studies, we found that Q-VD-OPH produced significant protection against an acute regimen of MPTP-induced dopamine depletion with moderate dosing (70% and 76% depletions), whereas it had no protective effect with a more severe regimen producing a dopamine depletion of 86%. This may reflect a greater involvement of necrosis when MPTP is administered at higher doses. The protective effect of Q-VD-OPH was confirmed by protection of TH immunoreactive neurons in the SNc.

We also utilized a subacute dosing regimen of MPTP at 30 mg daily for 5 days, which was shown to induce cell death by apoptosis as assessed by terminal deoxynucleotidyl transferase labeling (TUNEL), and acridine orange to visualize clumped chromation (Tatton and Kish, 1997). Following administration of MPTP, there is evidence for apoptotic cell death as well as activation of caspase-9, caspase-3, caspase-8, and Bid cleavage (Hartmann et al., 2000; Tatton and Kish, 1997; Turmel et al., 2001; Viswanath et al., 2001). With a chronic dosing regimen of MPTP 30 mg/kg once a day for 5 days, there was no protection against dopamine depletion. However, there was a significant protection against loss of TH immunoreactive neurons in the SNpc when MPTP was administered at a lower dose of 20 mg/kg once a day for 5 days.

Interestingly, we observed a similar improved preservation of dopamine following acute MPTP administration, as compared to chronic MPTP administration, in transgenic mice overexpressing the antiapoptotic protein Bcl2.

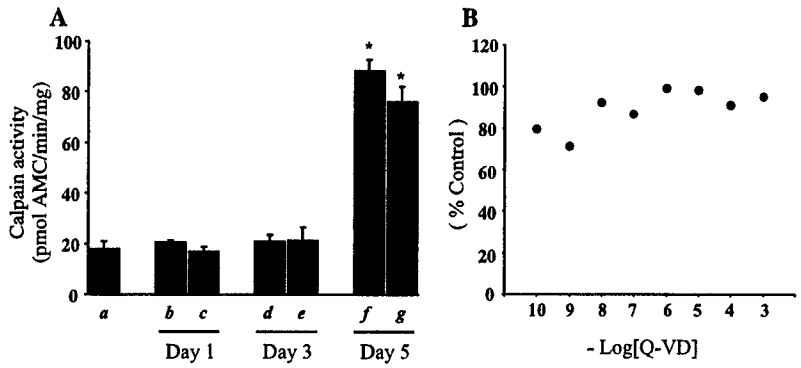


Fig. 6. (A) Proteolytic activity of calpain in striatal tissues of rats treated with vehicle (*a*), 3NP alone (*b*, *d*, and *f*), and 3NP with Q-VD-OPH (*c*, *e*, and *g*) at days 1, 3, and 5 following 3NP subcutaneous infusion. Calpain activity increased more than fourfold at the 5th day following 3NP infusion (*$P < 0.0001$ when compared to vehicle controls). Q-VD-OPH had no effect on the in vivo calpain activity alteration. (B) In vitro dose–response inhibition results, showing that Q-VD-OPH has no effect on inhibiting calpain activity.

Adenovirus administration of a protein caspase inhibitor, x-linked inhibitor of apoptosis protein (XIAP), protects dopamine cell bodies but does not protect terminals (Xia et al., 2001), similar to the effects we observed with Q-VD-OPD treatment with MPTP administration at 20 mg/d for 5 days. The reason for this protection of cell bodies in preference to axons is unclear. It has been demonstrated that apoptotic cell death programs are present in axon terminals and that activation of them may precede activation of apoptosis in cell bodies (Mattson and Duan, 1999). Furthermore, it has been demonstrated that Bcl-2 overexpression protects against motor neuron cell body loss but not axonal degeneration in the progressive motor neuropathy mouse (Sagot et al., 1995). An analogous situation may occur with chronic MPTP administration.

Mice with a dominant-negative inhibition of caspase-1 and mice deficient in the proapoptotic protein Bax are also resistant to MPTP toxicity (Klivenyi et al., 1999; Vila et al., 2001). A deficiency of p53, overexpression of p35 (a broad-spectrum viral caspase inhibitor), transgenic mice overexpressing XIAP, and pharmacologic inhibition of the proapoptotic c-Jun NH2-terminal kinase (JNK) pathway also protect (Crocker et al., 2003; Eberhardt et al., 2000; Offen et al., 1998; Saporito et al., 2000; Trimmer et al., 1996; Viswanath et al., 2001; Yang et al., 1998).

We found that Q-VD-OPH significantly reduced striatal lesions produced by the reversible and irreversible succinate dehydrogenase inhibitors malonate and 3NP. Both of these compounds have been used to mimic the histopathologic and phenotypical features of Huntington's disease (Brouillet et al., 1999, 2000). Intrastriatal injection of malonate results in TUNEL-positive neurons and induces cleavage of caspase-2 beginning at 6 h and caspase-3-like activity at 12 h (Schulz et al., 1998). Malonate lesions are attenuated in transgenic mice expressing a dominant-negative inhibitor of caspase-1, as well as by intrastriatal injection of the broad-spectrum caspase inhibitor zVAD-Fmk (Andreassen et al., 2000; Schulz et al., 1998).

There is also substantial evidence that at least part of the molecular machinery involved in apoptosis may be involved in 3NP toxicity (Alexi et al., 1998; Behrens et al., 1995; Duan et al., 2000; Garcia et al., 2002; Kim et al., 2000; Sugino et al., 1997). Treatment of cultured hippocampal neurons with 3NP results in either necrotic or apoptotic cell death (Pang and Geddes, 1997), and cycloheximide prevents the apoptotic cell death. The 3NP induces apoptosis in the striatum of rats as detected by TUNEL staining and internucleosomal DNA fragmentation (Sato et al., 1998). We found that 3NP lesions were attenuated in transgenic mice overexpressing the antiapoptotic protein Bcl2 or a dominant-negative inhibitor of caspase-1 (Andreassen et al., 2000; Bogdanov et al., 1999).

In the present study, the broad-spectrum caspase inhibitor Q-VD-OPH significantly reduced striatal lesions produced by either malonate or 3NP. We also studied the mechanism of Q-VD-OPH by investigating changes in cleaved fragments of caspase-9 and caspase-8 as well as Bid following either MPTP or 3NP administration. We found that MPTP administration induced significant increases in cleaved caspase-9, caspase-8, and Bid in the midbrain and striata, which were blocked in mice treated with Q-VD-OPH. Similarly, following administration of 3NP to rats, there were increases in cleaved caspase-9, caspase-8, and Bid in the striatum at 1, 3, and 5 days, which were significantly inhibited by Q-VD-OPH administration. We also investigated whether Q-VD-OPH could inhibit calpain activity following administration of 3NP. An in vitro dose–response study showed that Q-VD-OPH had no effect on calpain activity, and it had no significant effect on blocking 3NP induced increases in calpain activity in vivo.

A role for caspase activation in the pathogenesis of neurodegenerative diseases has been established on the basis of studies in both postmortem brain tissue as well as animal models of neurodegenerative diseases (Mattson, 2000; Friedlander, 2003). In postmortem spinal cord tissue of ALS patients, there is activation of caspase-1 and caspase-3, as well as morphologic evidence of apoptosis (Li et al., 2000; Martin, 1999). A dominant-negative inhibitor of caspase-1 and intracerebroventricular administration of zVAD-Fmk significantly prolong survival in ALS-transgenic mice (Friedlander et al., 1997; Li et al., 2000). In ALS-transgenic mice, there is early caspase-1 activation followed by caspase-3 activation (Li et al., 2000; Pasinelli et al., 2000; Vukosavic et al., 1999; Vukosavic et al., 2000). Caspase-9 activation and cleaved Bid are seen early in symptomatic G93A SOD1-transgenic ALS mice, whereas activation of caspase-8 occurs in end-stage mice (Guégan et al., 2002). A recent study, however, showed that although caspase-11 deficiency blocked increases in caspase-1 and caspase-3 activity in a transgenic mouse model of ALS, there was no effect on disease onset and progression (Kang et al., 2003).

In PD substantia nigra, there is evidence for TUNEL staining, ultrastructural changes of apoptosis, and evidence of chromatin condensation using a fluorescent dye that binds to DNA (Anglade et al., 1997; Mochizuki et al., 1995; Tatton et al., 1998). The number of neurons immunoreactive for activated caspase-3 was increased from

3.9% in controls to 6.5% in PD SNc (Hartmann et al., 2000). Parkin, which is implicated in early onset PD, may play a role since it binds to mitochondria, and overexpression blocks mitochondrial swelling and cytochrome *c* release (Darios et al., 2003).

In HD, we found increased neuronal cytochrome *c* immunoreactivity with increased neuropathologic severity (Kiechle et al., 2002). There is also evidence of increases in activated, caspase-1, caspase-9, caspase-3, and caspase-8, (Kiechle et al., 2002; Ona et al., 1999; Sanchez et al., 1999). In transgenic mouse models of HD, a dominant-negative inhibitor of caspase-1 and intracerebroventricular administration of zVAD-Fmk, and as well as administration of minocycline, which indirectly inhibits caspase-1 and caspase-3, improves survival (Chen et al., 2000; Ona et al., 1999). Caspases may also play a role in processing of huntingtin (Wellington et al., 2002).

Caspase activation may therefore play a critical role in the pathogenesis of neurodegenerative diseases. Our present findings show that Q-VD-OPH is neuroprotective in mitochondrial toxin models of PD and HD and that it blocks activation of caspase-9 and caspase-8, as well as cleavage of Bid. We do not yet know the long-term effects of Q-VD-OPH but we have administered it over several months in transgenic mice without evidence of toxicity. In summary, Q-VD-OPH appears to be a novel systemically active broad-spectrum caspase inhibitor, which has the potential to exert therapeutic effects in a broad-spectrum of neurodegenerative diseases.

## Acknowledgments

The secretarial assistance of Greta Strong and Connie Boyd is gratefully acknowledged. This work was supported by NINDS grant 39258, The Department of Defense, The Hereditary Disease Foundation, and The Huntington's Disease Society of America.

## References

Alexi, T., Hughes, P.E., Knusel, B., Tobin, A.J., 1998. Metabolic compromise with systemic 3-nitropropionic acid produces striatal apoptosis in Sprague-Dawley rats but not in BALB/c ByJ mice. Exp. Neurol. 153, 74–93.

Andreassen, O.A., Ferrante, R.J., Hughes, D.B., Klivenyi, P., Dedeoglu, A., Ona, V.O., Friedlander, R.M., Beal, M.F., 2000. Malonate and 3-nitropropionic acid neurotoxicity are reduced in transgenic mice expressing a caspase-1 dominant-negative mutant. J. Neurochem. 75, 847–852.

Anglade, P., Vyas, S., Javoy-Agid, F., Herrero, M.T., Michel, P.P., Marquez, J., Mouatt-Prigent, A., Ruberg, M., Hirsch, E.C., Agid, Y., 1997. Apoptosis and autophagy in nigral neurons of patients with Parkinson's disease. Histol. Histopathol. 12, 25–31.

Beal, M.F., Matson, W.R., Swartz, K.J., Gamache, P.H., Bird, E.D., 1990. Kynurenine pathway measurements in Huntington's disease striatum, evidence for reduced formation of kynurenic acid. J. Neurochem. 55, 1327–1339.

Beal, M.F., Brouillet, E., Jenkins, B.G., Ferrante, R.J., Kowall, N.W., Miller, J.M., Storey, E., Srivastava, R., Rosen, B.R., Hyman, B.T., 1993. Neurochemical and histologic characterization of striatal excitotoxic lesions produced by the mitochondria toxin 3-nitropropionic acid. J. Neurosci. 13, 4181–4192.

Behrens, M.I., Koh, J., Canzoniero, L.M., Sensi, S.L., Csernansky, C.A., Choi, D.W., 1995. 3-Nitropropionic acid induces apoptosis in cultures striatal and cortical neurons. Neuroreport 6, 545–548.

Bizat, N., Hermel, J.M., Boyer, F., Jacquard, C., Creminon, C., Ouary, S., Escartin, C., Hantraye, P., Krajewski, S., Brouillet, E., 2003. Calpain is a major cell death effector in selective striatal degeneration induced in vivo by 3-nitropropionate. Implication for Huntington's disease. J. Neurosci. 23, 5020–5030.

Bogdanov, M.B., Ferrante, R.J., Mueller, G., Ramos, L.E., Martinou, J.C., Beal, M.F., 1999. Oxidative stress is attenuated in mice overexpressing BCL-2. Neurosci. Lett. 262, 33–36.

Brouillet, E., 2000. Animal models of Huntington's disease, from basic research on neuronal death to assessment of new therapeutic strategies. Funct. Neurol. 15, 239–251.

Brouillet, E., Conde, F., Beal, M.F., Hantraye, P., 1999. Replicating Huntington's disease phenotype in experimental animals. Prog. Neurobiol. 59, 427–468.

Caserta, T.M., Smith, A.N., Gultice, A.D., Reedy, M.A., Brown, T.L., 2003. Q-VD-Oph, a broad spectrum caspase inhibitor with potent antiapoptotic properties. Apoptosis 8, 345–352.

Chan, S.L., Mattson, M.P., 1999. Caspase and calpain substrates, roles in synaptic plasticity and cell death. J. Neurosci. Res. 58, 167–190.

Chen, M., Ona, V.O., Li, M., Ferrante, R.J., Fink, K.B., Zhu, S., Bian, J., Guo, L., Farrell, L.A., Hersch, S.M., Hobbs, W., Vonsattel, J.P., Cha, J.H., Friedlander, R.M., 2000. Minocycline inhibits caspase-1 and caspase-3 expression and delays mortality in a transgenic mouse model of Huntington's disease. Nat. Med. 6, 797–801.

Crocker, S.J., Liston, P., Anisman, H., Lee, C.J., Smith, P.D., Earl, N., Thompson, C.S., Park, D.S., Korneluk, R.G., Robertson, G.S., 2003. Attenuation of MPTP-induced neurotoxicity and behavioral impairment in NSE-XIAP transgenic mice. Neurobiol. Dis. 12, 150–161.

Darios, F., Corti, O., Lucking, C.B., Hampe, C., Muriel, M.P., Abbas, N., Gu, W.J., Hirsch, E.C., Rooney, T., Ruberg, M., Brice, A., 2003. Parkin prevents mitochondrial swelling and cytochrome *c* release in mitochondria-dependent cell death. Hum. Mol. Genet. 12, 517–526.

Duan, W., Zhiong, G., Mattson, M., 2000. Participation of Par- in the degeneration of striatal neurons induced by metabolic compromise with 3-nitropropionic acid. Exp. Neurol. 165, 1–11.

Eberhardt, O., Coelln, R.V., Kugler, S., Lindenau, J., Rathke-Hartlieb, S., Gerhardt, E., Haid, S., Isenmann, S., Gravel, C., Srinivasan, A., Bahr, M., Weller, M., Dichgans, J., Schulz, J.B., 2000. Protection by synergistic effects of adenovirus-mediated X-chromosome-linked inhibitor of apoptosis and glial cell line-derived neurotrophic factor gene transfer in the 1-methyl-4-phenyl-1,2,3,6-tetrahydropyridine model of Parkinson's disease. J. Neurosci. 20, 9126–9134.

Friedlander, R.M., 2003. Apoptosis and caspases in neurodegenerative diseases. N. Engl. J. Med. 348, 1365–1375.

Friedlander, R.M., Brown, R.H., Gagliardini, V., Wang, J., Yuan, J., 1997. Inhibition of ICE slows ALS in mice. Nature 388, 31.

Garcia, M., Vanhoutte, P., Pages, C., Besson, M.J., Brouillet, E., Caboche, J., 2002. The mitochondrial toxin 3-nitropropionic acid induces striatal neurodegeneration via a c-Jun N-terminal kinase/c-Jun module. J. Neurosci. 22, 2174–2184.

Guégan, C., Vila, M., Teissman, P., Chen, C., Onténiente, B., Li, M., Friedlander, R.M., Przedborski, S., 2002. Instrumental activation of Bid by caspase-1 in a transgenic mouse model of ALS. Mol. Cell. Neurosci. 20, 553–562.

Hartmann, A., Hunot, S., Michel, P.P., Muriel, M.-P., Vyas, S., Faucheux, B.A., Mouatt-Prigent, A., Turnel, H., Srinivasan, A., Ruberg, M., Evan, G.I., Agid, Y., Hirsch, E.C., 2000. Caspase-3, A vulnerability factor and final effector in apoptotic death of dopaminergic neurons in Parkinson's disease. Proc. Natl. Acad. Sci. U. S. A. 97, 2875–2880.

Kang, S.J., Sanchez, I., Jing, N., Yuan, J., 2003. Dissociation between neurodegeneration and caspase-11-mediated activation of caspase-1 and caspase-3 in a mouse model of amyotrophic lateral sclerosis. J. Neurosci. 23, 5455–5460.

Kiechle, T., Dedeoglu, A., Kubilus, J., Kowall, N.W., Beal, M.F., Friedlander, R.M., Hersch, S.M., Ferrante, R.J., 2002. Cytochrome *c* and caspase 9 expression in Huntington's disease. NeuroMol. Med. 1, 183–195.

Kim, G.W., Copin, J.C., Kawase, M., Chen, S.F., Sato, S., Gobbel, G.T., Chan, P.H., 2000. Excitotoxicity is required for induction of oxidative

stress and apoptosis in mouse striatum by the mitochondrial toxin 3-nitropropionic acid. J. Cereb. Blood Flow Metab. 20, 119–129.

Klivenyi, P., Andreassen, O., Ferrante, R.J., Schleicher Jr., J.R., Friedlander, R.M., Beal, M.F., 1999. Transgenic mice expressing a dominant negative mutant interleukin-1beta converting enzyme show resistance to MPTP neurotoxicity. NeuroReport 10, 635–638.

Li, H., Zhu, H., Xu, C.J., Yuan, J., 1998. Cleavage of BID by caspase 8 mediates the mitochondrial damage in the Fas pathway of apoptosis. Cell 94, 491–501.

Li, M., Ona, V.O., Guegan, C., Chen, M., Jackson-Lewis, V., Andrews, L.J., Olszewski, A.J., Stieg, P.E., Lee, J.P., Przedborski, S., Friedlander, R.M., 2000. Functional role of capsase-1 and caspase-3 in an ALS transgenic mouse model. Science 288, 335–339.

Martin, L.J., 1999. Neuronal death in amyotrophic lateral sclerosis is apoptosis, possible contribution of a programmed cell death mechanism. J. Neuropathol. Exp. Neurol. 58, 459–471.

Mattson, M.P., 2000. Apoptosis in neurodegenerative disorders. Nat. Rev., Mol. Cell Biol. 1, 120–129.

Mattson, M.P., Duan, W., 1999. Apoptotic biochemical cascades in synaptic compartments: roles in adaptive plasticity and neurodegenerative disorders. J. Neurosci. Res. 58, 152–166.

McDonald, M.C., Mota-Filipe, H., Paul, A., Cuzzocrea, S., Abdelrahman, M., Harwood, S., Pelvin, R., Chatterjee, P.K., Yaqoob, M.M., Thiemermann, C., 2001. Calpain inhibitor I reduces the activation of nuclear factor-kappa B and organ injury/dysfunction in hemorrhagic shock. FASEB J. 15, 171–186.

Mochizuki, H., Goto, K., Mori, H., Mizuno, Y., 1995. Histochemical detection of apoptosis in Parkinson's disease. J. Neurol. Sci. 137, 120–123.

Offen, D., Beart, P.M., Cheung, N.S., Pascoe, C.J., Hochman, A., Gorodin, S., Melamed, E., Bernard, R., Bernard, O., 1998. Transgenic mice expressing human Bcl-2 in their neurons are resistant to 6-hydroxydopamine and 1-methyl-4-phenyl-1,2,3,6-tetrahydropyridine neurotoxicity. Proc. Natl. Acad. Sci. U. S. A. 95, 5789–5794.

Ona, V.O., Li, M., Vonsattel, J.P., Andrews, L.J., Khan, S.Q., Chung, W.M., Frey, A.S., Menon, A.S., Li, X.J., Stieg, P.E., Yuan, J., Penney, J.B., Young, A.B., Cha, J.H., Friedlander, R.M., 1999. Inhibition of caspase-1 slows disease progression in a mouse model of Huntington's disease. Nature 399, 263–267.

Ouary, S., Bizat, N., Altairac, S., Menetrat, H., Mittoux, V., Conde, F., Hantraye, P., Brouillet, E., 2000. Major strain differences in response to chronic systemic administration of the mitochondrial toxin 3-nitropropionic acid in rats, implications for neuroprotection studies. Neuroscience 97, 521–530.

Pang, Z., Geddes, J.W., 1997. Mechanisms of cell death induced by the mitochondrial toxin 3-nitropropionic acid: acute excitotoxic necrosis and delayed apoptosis. J. Neurosci. 17, 3064–3073.

Pasinelli, P., Houseweart, M.K., Brown Jr., R.H., Cleveland, D.W., 2000. Caspase-1 and -3 are sequentially activated in motor neuron death in Cu, Zn superoxide dismutase-mediated familial amyotrophic lateral sclerosis. Proc. Natl. Acad. Sci. U. S. A. 97, 13901–13906.

Sagot, Y., Dubois-Dauphin, M., Tan, S.A., deBilbao, F., Aebischer, P., Martinou, J.C., Kato, C., 1995. Bcl-2 overexpression prevents motorneuron cell body loss but not axonal degeneration in a mouse model of a neurodegenerative disease. J. Neurosci. 15, 7727–7733.

Sanchez, I., Xu, C.J., Juo, P., Kakizaka, A., Blenis, J., Yuan, J., 1999. Caspase-8 is required for cell death induced by expanded polyglutamine repeats. Neuron 22, 623–633.

Saporito, M.S., Thomas, B.A., Scott, R.W., 2000. MPTP activates c-Jun NH (2)-terminal kinase (JNK) and its upstream regulatory kinase MKK4 in nigrostriatal neurons in vivo. J. Neurochem. 75, 1200–1208.

Sato, S., Gobbel, G.T., Honkaniemi, J., Li, Y., Kondo, T., Murakami, K., Sato, M., Copin, J.C., Sharp, F.R., Chan, P.H., 1998. Decreased expression of bcl-2 and bcl-x mRNA coincides with apoptosis following intracerebral administration of 3-nitropropionic acid. Brain Res. 808, 56–64.

Schulz, J.B., Henshaw, D.R., Siwek, D., Jenkins, B.G., Ferrante, R.J., Cipolloni, P.B., Kowall, N.W., Rosen, B.R., Beal, M.F., 1995. Involvement of free radicals in excitotoxicity in vivo. J. Neurochem. 64, 2239–2247.

Schulz, J.B., Weller, M., Matthews, R.T., Heneka, M.T., Groscurth, P., Martinou, J.C., Lommatzsch, J., von Coelln, R., Wullner, U., Loschmann, P.A., Beal, M.F., Dichgans, J., Klockgether, T., 1998. Extended therapeutic window for caspase inhibition and synergy with MK-801 in the treatment of cerebral histotoxic hypoxia. Cell Death Differ. 5, 847–857.

Sugino, T., Nozaki, K., Tokime, T., Hashimoto, N., Kikuchi, H., 1997. 3-nitropropionic Oacid induces poly (ADP-ribosylation) and apoptosis related gene expression in the striatum in vivo. Neurosci. Lett. 237, 121–124.

Tang, D., Lahti, J.M., Kidd, V.J., 2000. Caspase-8 activation and bid cleavage contribute to MCF7 cellular execution in a caspase-3-dependent manner during staurosporine-mediated apoptosis. J. Biol. Chem. 275, 9303–9307.

Tatton, N.A., Kish, S.J., 1997. In situ detection of apoptotic nuclei in the substantia nigra compacta of 1-methyl-4-phenyl-1,2,3,6-tetrahydropyridine-treated mice using terminal deoxynucleotidyl transferase labelling and acridine orange staining. Neuroscience 77, 1037–1048.

Tatton, N.A., Maclean-Fraser, A., Tatton, W.G., Perl, D.P., Olanow, C.W., 1998. A fluorescent double-labeling method to detect and confirm apoptotic nuclei in Parkinson's disease. Ann. Neurol. 44, S142–S148.

Tompa, P., Baki, A., Schad, E., Friedrich, P., 1996. The calpain cascade. Mu-calpain activates m-calpain. J. Biol. Chem. 271, 33161–33164.

Trimmer, P.A., Smith, T.S., Jung, A.B., Bennett Jr., J.P., 1996. Dopamine neurons from transgenic mice with a knockout of the p53 gene resist MPTP neurotoxicity. Neurodegeneration 5, 233–239.

Turmel, H., Hartmann, A., Parain, K., Douhou, A., Srinivasan, A., Agid, Y., Hirsch, E.C., 2001. Caspase-3 activation in 1-methyl-4-phenyl-1,2,3,6-tetrahydropyridine (MPTP)-treated mice. Mov. Disord. 16, 185–189.

Vila, M., Jackson-Lewis, V., Vukosavic, S., Djaldetti, R., Liberatore, G., Offen, D., Korsmeyer, S.J., Przedborski, S., 2001. Bax ablation prevents dopaminergic neurodegeneration in the 1-methyl-4-phenyl-1,2,3,6-tetrahydropyridine mouse model of Parkinson's disease. Proc. Natl. Acad. Sci. USA 98, 2837–2842.

Viswanath, V., Wu, Y., Boonplueang, R., Chen, S., Stevenson, F.F., Yantiri, F., Yang, L., Beal, M.F., Andersen, J.K., 2001. Caspase-9 activation results in downstream caspase-8 activation and bid cleavage in 1-methyl-4-phenyl-1,2,3,6-tetrahydropyridine-induced Parkinson's disease. J. Neurosci. 21, 9519–9528.

Vukosavic, S., Dubois-Dauphin, M., Romero, N., Przedborski, S., 1999. Bax and Bcl-2 interaction in a transgenic mouse model of familial amyotrophic lateral sclerosis. J. Neurochem. 73, 2460–2468.

Vukosavic, S., Stefanis, L., Jackson-Lewis, V., Guegan, C., Romero, N., Chen, C., Dubois-Dauphin, M., Prsedborski, S., 2000. Delaying caspase activation by Bcl-2, A clue to disease retardation in a transgenic mouse model of amyotrophic lateral sclerosis. J. Neurosci. 20, 9119–9125.

Wang, K.K., 2000. Calpain and caspase, can you tell the difference? Trends Neurosci. 23, 20–26.

Wellington, C.L., Ellerby, L.M., Gutckunst, C.A., Rogers, D., Warby, S., Graham, R.K., Loubser, O., van Raamsdonk, J., Singaraja, R., Yang, Y.Z., Gafni, J., Bredesen, D., Hersch, S.M., Leavitt, B.R., Roy, S., Nicholson, D.W., Hayden, M.R., 2002. Caspase cleavage of mutant huntingtin precedes neurodegeneration in Huntington's disease. J. Neurosci. 22, 7862–7872.

Xia, G., Harding, T., Weller, M., Beineman, A., Uney, J.B., Schulz, J.B., 2001. Gene transfer of the JNK interacting protein-1 protects dopaminergic neurons in the MPTP model of Parkinson's disease. Proc. Natl. Acad. Sci. U. S. A. 98, 10433–10438.

Yang, L., Matthews, R.T., Schulz, J.B., Klockgether, T., Liao, A.W., Martinou, J.C., Penney Jr., J.B., Hyman, B.T., Beal, M.F., 1998. 1-Methyl-4-phenyl-1,2,3,6-tetrahydropyride neurotoxicity is attenuated in mice overexpressing Bcl-2. J. Neurosci. 18, 8145–8152.

Journal of Neuroscience Research 74:278–285 (2003)

# Minocycline Enhances MPTP Toxicity to Dopaminergic Neurons

**Lichuan Yang,[1] Shuei Sugama,[2] Jason W. Chirichigno,[1] Jason Gregorio,[1] Stefan Lorenzl,[1] Dong H. Shin,[2] Susan E. Browne,[1] Yoshinori Shimizu,[2] Tong H. Joh,[2] M. Flint Beal,[1] and David S. Albers[1]**

[1]Neurochemistry and Neurodegenerative Disease Laboratory, Weill Medical College at Cornell University, New York, New York

[2]Burke Medical Research Institute, Department of Neurology and Neuroscience, Weill Medical College at Cornell University, New York, New York

Minocycline has been shown previously to have beneficial effects against ischemia in rats as well as neuroprotective properties against excitotoxic damage in vitro, nigral cell loss via 6-hydroxydopamine, and to prolong the life-span of transgenic mouse models of Huntington's disease (HD) and amyotrophic lateral sclerosis (ALS). We investigated whether minocycline would protect against toxic effects of 1-methyl-4-phenyl-1,2,3,6-tetrahydropyridine (MPTP), a toxin that selectively destroys nigrostriatal dopaminergic (DA) neurons and produces a clinical state similar to Parkinson's disease (PD) in rodents and primates. We found that although minocycline inhibited microglial activation, it significantly exacerbated MPTP-induced damage to DA neurons. We present evidence suggesting that this effect may be due to inhibition of DA and 1-methyl-4-phenylpridium ($MPP^+$) uptake into striatal vesicles. 

**Key words:** inflammation; Parkinson's disease; vesicles; tetracycline; doxycycline

Parkinson's disease (PD) is a neurodegenerative disorder of unknown etiology characterized by the loss of dopaminergic neurons (DA) in the substantia nigra pars compacta (SNpc). The clinical features of PD include a resting tremor, bradykinesia, stooped posture, shuffling gait, difficulty swallowing, and rigidity in the extremities accompanied by a loss in control of fine movements. A pivotal event in PD research was the demonstration of the toxicity of 1-methyl-4-phenyl-1,2,3,6-tetrahydropyridine (MPTP) to DA neurons. Systemic administration of MPTP produces DA cell loss and a clinical state similar to idiopathic PD in both humans and experimental animals (Langston et al., 1983; Heikkila et al., 1984). MPTP is converted to its toxic metabolite 1-methyl-4-phenylpyridium ($MPP^+$) by monoamine oxidase B (Chiba et al., 1984). $MPP^+$ is accumulated actively in DA neurons by the high-affinity DA transporter (Javitch et al., 1985) and exerts its toxic effects by inhibiting complex I of the mitochondrial electron transport chain (Nicklas et al., 1985) leading to many deleterious consequences, including increased free radical production, resulting ultimately in cell death.

There is accumulating evidence that suggests the involvement of specific immune reactions in pathogenesis of several neurodegenerative disorders, including PD (McGeer et al., 1993). These include studies demonstrating the presence of microglia, T-lymphocytes, and inducible nitric oxide synthase (iNOS) in PD SNpc as well as increased expression of inflammatory cytokines in the striatum from parkinsonian brains (for review, see Nagatsu et al., 2000). Further, microglial and astrocytic proliferation have been described in damaged regions after MPTP administration (Kurkowska-Jastrzebska et al., 1999). These results, coupled with the observation that tyrosine-hydroxylase (TH)-immunoreactive SNpc cell bodies in mice lacking the iNOS gene are relatively resistant to MPTP toxicity (Liberatore et al., 1999), suggest that glial activation and the subsequent release of nitric oxide (NO) may contribute to MPTP toxicity.

Minocycline, a second-generation tetracycline, has anti-inflammatory properties independent of its antimicrobial effects. Minocycline has been reported to have beneficial effects against both focal and global ischemia in rats (Yrjanheikki et al., 1998, 1999) as well as neuroprotective properties against excitotoxic damage in vitro and nigral cell loss via 6-hydroxydopamine in mice (He et al., 2001; Tikka et al., 2001). It has been reported to delay disease progression and prolong the life-span of transgenic

Contract grant sponsor: USAMRC; Contract grant sponsor: The Parkinson's Disease Foundation; Contract grant sponsor: National Institute of Neurological Disorders and Stroke (NINDS).

*Corresponding author: M. Flint Beal, MD, Department of Neurology and Neuroscience, Weill Medical College at Cornell University, Room F 610, 525 East 68th Street, New York, NY 10021.
E-mail: fbeal@med.cornell.edu

Received 22 April 2003; Revised 16 May 2003; Accepted 20 May 2003

mouse models of Huntington's disease (HD) and amyotrophic lateral sclerosis (ALS) (Chen et al., 2000; Zhu et al., 2002). Several mechanisms have been suggested to explain these neuroprotective properties of minocycline, including inhibition of caspase-1, caspase-3, inducible nitric oxide synthase (iNOS) expression, and the mitochondrial permeability transition (Amin et al., 1996; Yrjanheikki et al., 1998, 1999; Chen et al., 2000; Du et al., 2001; He et al., 2001; Tikka et al., 2001; Zhu et al., 2002). We investigated whether minocycline would protect against toxic effects of MPTP. A recent report showed that minocycline blocked MPTP-induced microglial activation and toxicity to DA neurons (Wu et al., 2002). Using a different dosing regimen, we found that minocycline blocked MPTP-induced microglial activation, but in contrast we found that MPTP toxicity to DA neurons was exacerbated.

## MATERIALS AND METHODS

MPTP, tetracycline, doxycycline, minocycline, amphetamine, and creatine were obtained from Sigma (St. Louis, MO). Minocycline (0.005%), creatine (2%), and the combined minocycline (0.005%)/creatine (2%) test diets were manufactured by Purina Test Diet, Inc. (Richmond, IN). All drugs were dissolved in phosphate-buffered saline (PBS; pH 7.4).

### Animals and Drug Administration

All experiments were conducted in either young (2–3 month) or old (8 month) male C57BL mice (Jackson Labs, Bar Harbor, ME) in accordance with the NIH Guide for the Care and Use of Laboratory Animals, and all procedures were approved by a local Animal Care and Use Committee. Mice were group-housed at 20–22°C and maintained on a 12-hr light-dark cycle with food and water available ad lib.

Mice received four intraperitoneal (i.p.) injections of MPTP (5, 10, 15, or 20 mg/kg) or PBS vehicle at 2-hr intervals, as described previously (Sonsalla et al., 1992). Mice were pretreated 1 day before MPTP administration with minocycline, doxycycline, tetracycline (2× 45 mg/kg or 60 mg/kg i.p.), or PBS vehicle at 12-hr intervals. Mice were again treated with PBS or minocycline, doxycycline, or tetracycline (2× 45mg/kg or 60 mg/kg at 12-hr intervals) on the day of MPTP administration and post-treated for 1 day with a reduced dose (2× 22.5 mg/kg or 30 mg/kg at 12-hr intervals). We also tested effects on MPTP toxicity of minocycline administered orally, either by gavage or in the diet. Mice were pretreated 2 days before MPTP administration with PBS or minocycline (1× 90 or 120 mg/kg/day, orally by gavage) and for 7 days after MPTP treatment. In another experimental group, mice were fed for 2 weeks before and during MPTP administration (4× 10 mg/kg at 2-hr intervals) with diets containing minocycline (0.005%), creatine (2%), or combined minocycline (0.005%)/creatine (2%). Control animals were fed unsupplemented diet. In these studies, animals were fed the special diets throughout the study period until the day of sacrifice. In all MPTP experiments, mice were sacrificed 7 days after MPTP treatment. Both neostriata were dissected, frozen rapidly and stored at −80°C until assayed.

### Neurochemical Measurements

Striatal levels of DA and its metabolites were measured by high-pressure liquid chromatography (HPLC) with electrochemical detection, and TH activity by a radioenzymatic technique as described previously (Albers et al., 1996; Yang et al., 1998). Striatal $MPP^+$ levels were measured by HPLC with UV detection as described previously (Matthews et al., 1999). All samples were normalized for protein content, which was determined spectrophotometrically using the Bio-Rad protein assay kit (Bio-Rad, Hercules, CA).

### HPLC Assay for Minocycline and Tetracycline

For HPLC determinations of minocycline and tetracycline levels, 4 animals were examined from each group (minocycline or tetracycline alone and minocycline or tetracycline with co-injection of MPTP). Minocycline or tetracycline were administered at 45 mg/kg i.p. twice per day, starting 12 hr before administration of MPTP, which was administered at 10 mg/kg i.p. every 2 hr, for 4 doses. At 2 hr after the last MPTP dose and 1 hr after the last minocycline or tetracycline dose, animals were perfused intracardially with PBS to wash out blood from the brain, and perfused brain tissues were taken for HPLC assay.

Dissected striata were sonicated and centrifuged (14,000 × *g*, 2× 10 min) in chilled 0.05 M perchloric acid, and 50 μl of supernatant was isocratically eluted through a 250 × 4.6 mm × 5 μm C18 column (Tosoh Biosep, Japan) with a mobile phase containing 200 mM $NaH_2PO_4$, 1 mM 1-octanesulfonic acid, and 25% (v/v) acetonitrile, and detected at 354 nm wavelength by a Waters 490 UV detector (Sharon, MA). Concentrations of minocycline and tetracycline are expressed as pg/mg protein. Protein concentration was determined by using the Bio-Rad method and Perkin Elmer Bio Assay Reader (Norwalk, CT).

### Vesicle Preparation

Vesicles were prepared as described previously (Staal and Sonsalla, 2000). Striata from mice (total of 120–150 mg wet weight tissue) were homogenized in 0.32 M sucrose and subjected to a number of centrifugation steps. At the end of the last centrifugation, the pellet was resuspended in vesicle assay buffer (VAB, pH 7.4): 25 mM HEPES, 100 mM potassium tartrate, 0.5 mM EDTA, 0.05 mM EGTA, 2 mM ATP-$Mg^{2+}$, 1.7 mM ascorbic acid and 4 mM KCl, pH 7.4). The final vesicle suspension was used for [$^3$H]-DA and [$^3$H]-$MPP^+$ uptake and protein determination.

### Vesicular [$^3$H]-DA and [$^3$H]-$MPP^+$ Uptake

Vesicle suspensions (5 μg protein) were incubated with buffers containing [$^3$H]-DA and cold DA or [$^3$H]-$MPP^+$ and cold MPP for 2 min at 37°C and uptake terminated by the addition of ice-cold VAB (no ascorbate or ATP-$Mg^{2+}$) as described previously (Del Zompo et al., 1993; Staal et al., 2000). Vesicles were collected on Whatman F filters washed with 0.5% polyethylenenine to prevent $MPP^+$ sticking to glass filters, washed with ice-cold VAB, and immersed in ethanol to extract the [$^3$H]-DA or [$^3$H]-$MPP^+$. Radioactivity was determined by scintillation spectroscopy. Nonspecific uptake was determined as

**TABLE I. Neurochemical Effects of MPTP and Minocycline in Young and Old C57BL Mice†**

| Treatment | *n* | DA (ng/mg protein) | DOPAC (ng/mg protein) | DOPAC/DA ratio | HVA (ng/mg protein) | TH activity (nmol/g/hr) |
|---|---|---|---|---|---|---|
| Young mice (2–3 months old) | | | | | | |
| PBS | 26 | 124 ± 7.7 | 10.4 ± 0.8 | 0.10 ± 0.01 | 14.4 ± 0.5 | 519 ± 26 |
| Minocycline (2 × 45 mg/kg, ip) | 22 | 130 ± 9.2 | 12.4 ± 1.2 | 0.12 ± 0.02 | 16.3 ± 0.7 | 588 ± 64 |
| MPTP (4 × 10 mg/kg) | 33 | 66 ± 3.8* | 7.9 ± 1.0* | 0.10 ± 0.01 | 10.4 ± 0.4* | 260 ± 27* |
| + Minocycline (2 × 45 mg/kg, ip) | 20 | 36 ± 3.6** | 7.2 ± 1.2* | 0.18 ± 0.02** | 8.2 ± 0.4** | 130 ± 18** |
| + Minocycline (2 × 60 mg/kg, ip) | 10 | 43 ± 4.2** | 13.5 ± 1.0** | 0.18 ± 0.01** | 9.2 ± 0.4** | ND |
| + Minocycline (1 × 90 mg/kg, po) | 9 | 49 ± 5.2** | 16.6 ± 1.3** | 0.20 ± 0.01** | 9.8 ± 0.4* | ND |
| + Minocycline (1 × 120 mg/kg, po) | 11 | 53 ± 4.6** | 16.3 ± 1.2** | 0.18 ± 0.01** | 10.1 ± 0.3* | ND |
| MPTP (4 × 15 mg/kg) | 32 | 36 ± 3.3* | 2.6 ± 0.2* | 0.09 ± 0.002 | 6.5 ± 0.3* | ND |
| + Minocycline (2 × 45 mg/kg, ip) | 31 | 19 ± 1.8** | 1.7 ± 0.1** | 0.12 ± 0.04** | 5.3 ± 0.2** | ND |
| MPTP (4 × 20 mg/kg) | 10 | 24 ± 2.4* | 2.3 ± 0.2* | 0.10 ± 0.01 | 5.7 ± 0.4* | ND |
| + Minocycline (2 × 45 mg/kg, ip) | 10 | 16 ± 3.9** | 1.5 ± 0.2** | 0.14 ± 0.01** | 4.4 ± 0.4** | ND |
| Old mice (8 months old) | | | | | | |
| PBS | 7 | 80 ± 4.7 | 14.7 ± 3.3 | 0.19 ± 0.05 | 9.4 ± 0.4 | 340 ± 34 |
| Minocycline (2 × 45 mg/kg, ip) | 8 | 82 ± 1.6 | 16.0 ± 3.0 | 0.20 ± 0.03 | 10.5 ± 0.4 | 370 ± 22 |
| MPTP (4 × 5 mg/kg) | 10 | 33 ± 6.4* | 12 ± 1.9 | 0.38 ± 0.03* | 6.7 ± 0.6* | 222 ± 38* |
| MPTP + minocycline | 9 | 16 ± 3.9** | 7.6 ± 1.3** | 0.52 ± 0.05** | 5.4 ± 0.5* | 104 ± 16** |

†Data expressed as mean ± SEM. ND, not determined. DA, dopamine; DOPAC, 3,4-dihydroxyphenylacetic acid; HVA, homovanillic acid; TH, tyrosine hydroxlase.
*Significantly different from PBS-treated controls ($P < 0.05$).
**Significantly different from MPTP-treated mice ($P < 0.05$).

**TABLE II. TH-Immunopositive and Cresyl Violet-Stained Cell Counts in SNpc 7 days After Minocycline and MPTP Treatment†**

| Treatment | *n* | TH-immunopositive neurons | Cresyl violet-stained neurons |
|---|---|---|---|
| PBS | 4 | 10,320 ± 303 | 13,016 ± 494 |
| Minocycline alone (2 × 45 mg/kg, ip) | 4 | 10,658 ± 160 | 13,160 ± 450 |
| MPTP alone (4 × 10 mg/kg, ip) | 4 | 9,286 ± 186* | 11,416 ± 284* |
| Minocycline + MPTP | 4 | 3,720 ± 792** | 4,816 ± 304** |

†Data expressed as mean ± SEM. TH, tyrosine hydroxylase.
*Statistically different from PBS alone ($P < 0.05$).
**Statistically different from MPTP alone ($P < 0.05$).

[$^3$H]-DA or [$^3$H]-MPP$^+$ uptake in samples incubated on ice, and by the effects of amphetamine.

### Immunostaining for Tyrosine Hydroxylase and Microglia

Hindbrains from mice were fixed in 4% paraformaldehyde for 24 hr and cryoprotected in 30% sucrose overnight. Sections (40 μm) were washed for 30 min in PBS, incubated with 1% bovine serum albumin (BSA) and 0.2% Triton X-100 in 0.1 M PBS for 1 hr, washed in PBS containing 0.5% BSA for 30 min, then incubated overnight in blocking solution containing antibodies to either TH (1:25,000; Weiser et al., 1993) or CD11b (1:1,000: Serotec, UK). CD11b reacts with the mouse complement type 3 receptor (CR3). Sections were washed in PBS-BSA, incubated for 1 hr with biotinylated secondary anti-rabbit or anti-rat antibodies (Vector Laboratories, Burlingame, CA) and visualized by reaction with 3,3′-diaminobenzidine-tetrahydrochloride (DAB; 0.05%) as a chromagen and hydrogen peroxide (0.003%) for 5 min. Sections were mounted on gelatin-coated slides, dehydrated through graded ethanols, and cleared in xylene before being coverslipped with Permount.

### Cresyl Violet Staining

Midbrain sections containing SNpc were stained with cresyl violet. Sections were then mounted on gelatinized slides, left to dry overnight, dehydrated in increasing alcohol concentrations, and coverslipped with Permount.

### Cell Counting

The total number of TH-immunoreactive cell bodies and cresyl violet-stained SNpc neurons were counted in 4 mice per group using the optical dissector technique, as published previously (Coggeshall, 1992; Gundersen, 1992; DeGiorgio et al., 1998; Volpe et al., 1998) with minor modifications. In brief, serial midbrain sections containing SNpc were stained for TH and cresyl violet. Digital images of TH-immunoreactive SNpc neurons were acquired at 30× magnifications on a Zeiss Axiophot microscope fitted with an Axiocam video camera. A counting frame (100 μm × 100 μm) created by KS 400 image analysis software (Zeiss, Thornwood, NY) was systematically passed over the outlined SNpc by a motorized stage. Neurons were counted under 100× oil magnification as they appeared within the counting frame (50 μm × 50 μm). This procedure

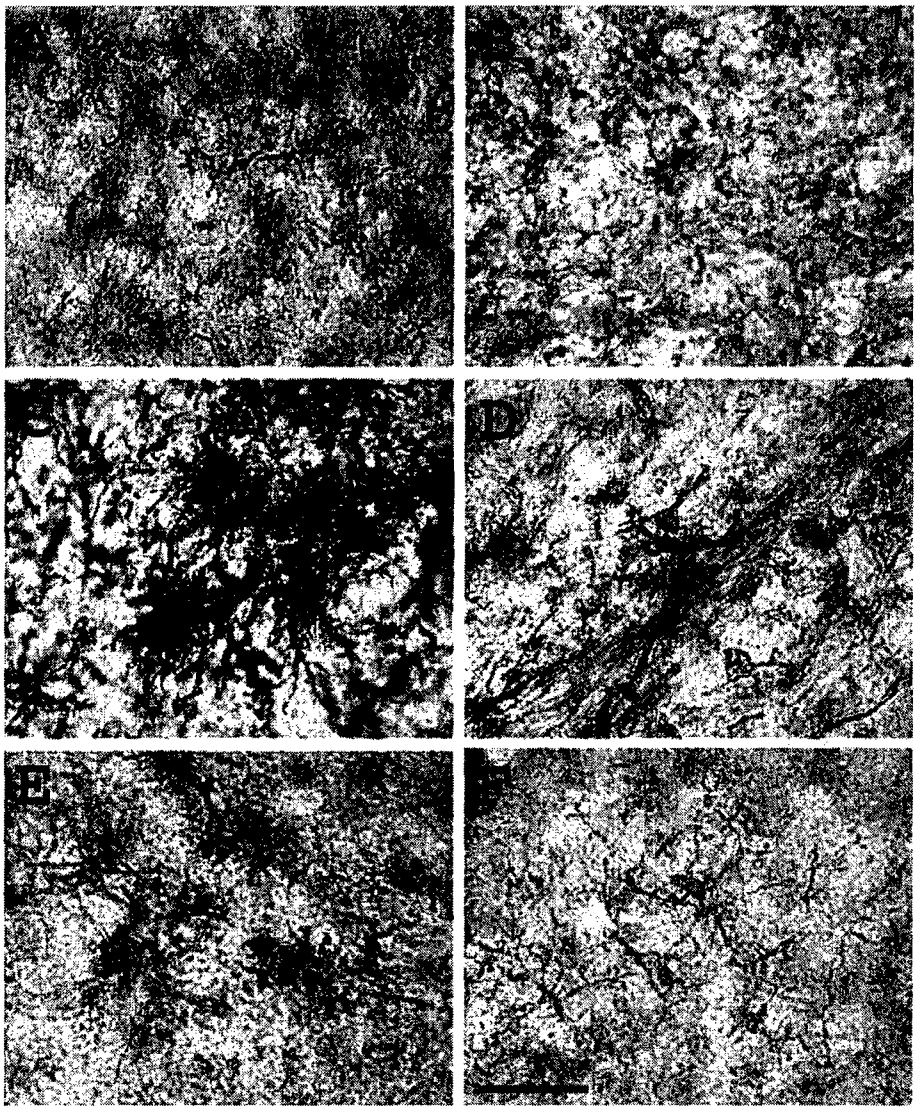


Fig. 1. Microglial staining in SNpc (**A,C,E**) and SNpr (**B,D,F**) in 8-month-old mice treated with PBS (A,B), MPTP alone (C,D), and MPTP+ minocycline. (E,F). As expected, there is robust microglial activation after MPTP treatment in the SNpc and SNpr (C,D), which is blocked by concurrent administration of minocycline (E,F). Scale bar = 20 μm.

was carried out on four sections at a periodicity of 160 μm in the SNpc. All TH- or cresyl violet-stained neurons were counted. An average neuron density was obtained by summing the number of neuron profiles divided by the calculated volume. The total number of neurons was calculated as the product of the neuron density and the volume of SNpc as described previously (Volpe et al., 1995; DeGiorgio et al., 1998).

### Statistical Analysis

Values of neurochemical measurements are expressed as the mean ± SEM. Results were analyzed by non-parametric Mann-Whitney *U*-test or one-way analysis of variance (ANOVA) followed by Newman-Keuls test (Instat, San Diego, CA). Differences were considered significant at $P < 0.05$.

## RESULTS AND DISCUSSION

The MPTP dosing regimens employed in these studies have been characterized previously (Sonsalla et al., 1992) and shown to result in moderate DA depletion within the adult mouse striatum. Seven days after MPTP treatment, striatal DA, its metabolites 3,4-dihydroxyphenylacetic acid (DOPAC) and homovanillic acid (HVA), as well as tyrosine hydroxylase (TH) activity were decreased in a dose-dependent manner (Table I). Using an

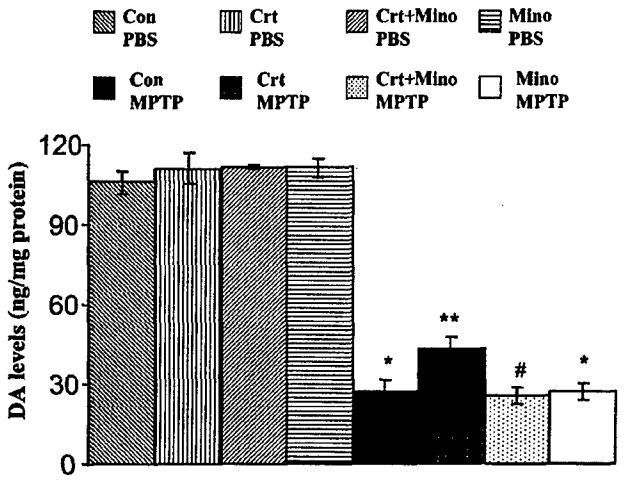


Fig. 2. Effects of 0.005% minocycline supplementation on MPTP toxicity. Mice were fed control, minocycline (mino)-containing, 2% creatine (crt)-containing, or minocycline and creatine (crt+mino)-containing mouse feed for 2 weeks before MPTP administration. Data are expressed as the mean ± SEM of 10 mice per group. Minocycline supplementation did not have any effect whereas creatine supplementation reversed the effects of MPTP toxicity as compared to MPTP-treated mice on control diet. The mixed diet produced the same level of DA depletion as MPTP-treated mice on control diet, suggesting minocycline reversed the creatine effect. *Significantly different from PBS-treated animals, $P < 0.05$; **Significantly different from MPTP-treated animals, $P < 0.05$; #Significantly different from CRT + MPTP-treated animals, $P < 0.05$.

intraperitoneal dosing paradigm for minocycline shown previously to be neuroprotective (Yrjanheikki et al., 1998, 1999), we observed a significant reduction ($P < 0.05$) in striatal DA levels and TH activities in young (2–3 month) mice treated with MPTP and minocycline, as compared to mice treated with MPTP alone, for all doses of MPTP tested (Table I). Minocycline alone did not have any effect on striatal DA levels or TH activity 7 days after administration.

Striatal $MPP^+$ levels measured 2 hr after the last MPTP injection (4× 10 mg/kg) in young mice were not different in animals treated with MPTP alone, or MPTP and minocycline (686 ± 149 and 675 ± 111 ng/mg protein, respectively; $P > 0.05$). Of note, a significant reduction in body weight (from 25.7 ± 0.1 to 24.3 ± 0.1 g; $P < 0.001$) was observed in minocycline-treated mice after pretreatment; this reduction was not observed in PBS-injected control mice in this same period. After MPTP injections, both minocycline-injected mice and PBS-treated controls showed similar weight losses (24.3 ± 0.1 to 23.0 ± 0.2 g, $P < 0.01$; and 25.8 ± 0.2 to 24.5 ± 0.3 g, $P < 0.01$, respectively). Further, there was an accompanying 10% loss of TH-immunopositive cell bodies in the substantia nigra pars compacta (SNpc) in MPTP-treated mice (4× 10 mg/kg; Table II). This loss of TH-immunopositive neurons was exacerbated significantly (−65%) in mice co-treated with minocycline (Table II). We stained serial sections with cresyl violet to determine whether this loss of immunostaining was due to loss of TH-positive neurons, or a downregulation of TH. The reductions in cresyl violet-stained cells were similar to those found via TH immunohistochemistry, confirming the loss of TH-immunopositive cells (Table II). It is noteworthy that the mean number of SNpc neurons in our analysis is comparable to previously published reports (German and Manaye, 1993; Volpe et al., 1995).

It has been suggested that neuroprotective effects of minocycline are due to inhibition of microglial activation (Yrjanheikki et al., 1998, 1999; Chen et al., 2000; Du et al., 2001; He et al., 2001; Tikka et al., 2001; Wu et al., 2002). To examine effects of minocycline treatment on microglial activation in our dosing paradigm, we conducted studies in older mice (8 months), where a robust MPTP-induced microglial activation can been observed as early as 12 hrs post-MPTP and remains elevated for up to 14 days (Kurkowska-Jastrzebska et al., 1999). A lower dose of MPTP (4× 5 mg/kg, i.p.) was administered due to the age-dependency of MPTP toxicity in older mice (Sonsalla et al., 1992). In agreement with our studies in young animals, a significant exacerbation in striatal DA depletion and decreased TH activity was measured in minocycline-treated MPTP mice (see Table I). The MPTP treatment induced robust microglial activation in the SNpc and substantia nigra pars reticulata (SNpr) of these animals, whereas the microglial staining pattern was less much intense in mice treated with minocycline and MPTP (Fig. 1), consistent with previous reports showing inhibition of microglial activation via minocycline (Yrjanheikki et al., 1998, 1999; Chen et al., 2000; He et al., 2001; Tikka et al., 2001; Wu et al., 2002).

It is clear from our studies that minocycline is not neuroprotective with the present dosing regimens of MPTP. Indeed, a range of doses of minocycline, as well as different routes of administration, all produced a consistent potentiation of MPTP-induced striatal damage. It is important to note that neither systemic minocycline alone nor minocycline via oral administration had any effect on basal striatal DA levels (Table I). In MPTP-treated mice (4× 10 mg/kg) fed mouse chow containing 0.005% minocycline, striatal DA levels were similar to MPTP-treated mice fed control diet (Fig. 2). Further, no apparent weight reduction was observed in the minocycline-fed mice (data not shown). Given the marked exacerbation of MPTP toxicity after intraperitoneal minocycline administration, these results suggest that the minocycline dose in the diet may be too low to exacerbate MPTP toxicity. Dietary supplementation of 0.005% minocycline, however, reversed the neuroprotective effects of 2% creatine (Matthews et al., 1999), suggesting that this dose of minocycline had a deleterious effect (Fig. 2).

We also examined the effects of tetracycline and doxycycline against MPTP toxicity in young mice. Consistent with our findings with minocycline, combined treatments of doxycycline with MPTP or tetracycline with MPTP produced greater reductions in striatal DA levels (Table III) as compared to mice treated with MPTP alone (4× 10 mg/kg). The results with tetracycline were unex-

**TABLE III. Minocycline, Doxycycline, and Tetracycline in the Presence and Absence of MPTP in Two- to Three-Month-Old C57BL Mice†**

| Treatment | *n* | Striatal DA (ng/mg protein) | Striatal TH activity (nmol/g/hr) |
|---|---|---|---|
| PBS | 9 | 123 ± 5.5 | 534 ± 31 |
| Minocycline alone (2 × 45 mg/kg, ip) | 5 | 132 ± 3.3 | 588 ± 68 |
| Doxycycline alone (2 × 45 mg/kg, ip) | 5 | 131 ± 11 | 590 ± 20 |
| Tetracycline alone (2 × 45 mg/kg, ip) | 5 | 140 ± 5.6 | 634 ± 38 |
| MPTP alone (4 × 10 mg/kg) | 20 | 73 ± 8.1* | 268 ± 17* |
| Minocycline + MPTP | 11 | 38 ± 7.2** | 130 ± 18** |
| Doxycycline + MPTP | 10 | 32 ± 4.8** | 194 ± 15** |
| Tetracycline + MPTP | 11 | 43 ± 8.7** | 135 ± 20** |

†Data expressed as mean ± SEM. DA, dopamine; TH, tyrosine hydroxylase.
*Significantly different from PBS-treated controls ($P < 0.05$).
**Significantly different from MPTP-treated mice ($P < 0.05$).

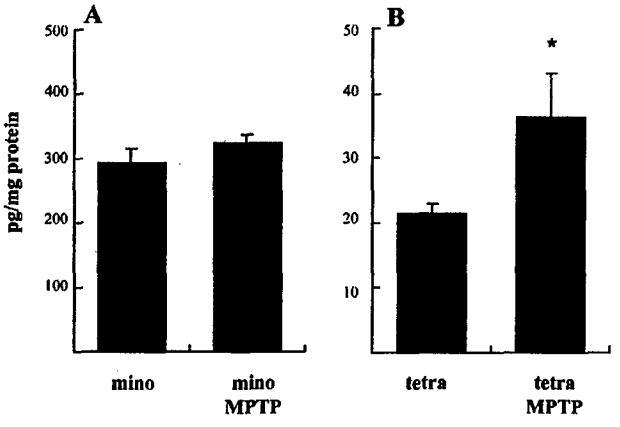


Fig. 3. Minocycline and tetracycline brain levels before and after MPTP administration. Data are mean ± SEM. *Significantly different from tetracycline alone ($P < 0.05$).

pected due to its low brain penetration. We therefore measured brain minocycline and tetracycline levels after administration of the compounds both alone and with MPTP (15 mg/kg × 4 doses). We found that brain concentrations of minocycline were approximately 10-fold greater than those of tetracycline; however, tetracycline did accumulate in brain, and levels were almost doubled after MPTP administration (Fig. 3).

The exacerbation of MPTP-induced damage by minocycline is strikingly similar to the neurochemical deficits observed by two independent groups in MPTP-treated VMAT2 knockout mice (Takahashi et al., 1997; Gainetdinov et al., 1998). Furthermore, pharmacologic inhibition of VMAT2 exacerbates MPTP toxicity (German et al., 2000). Thus, we investigated whether minocycline had a direct effect on VMAT2 function, in particular reducing the sequestration of DA into vesicles. In vesicular preparations from C57BL/6 mouse striata, we observed $V_{max}$ values for [$^3$H]-DA uptake consistent with those reported previously (Del Zompo et al., 1993; Staal and Sonsalla, 2000). Moreover, [$^3$H]-DA uptake was blocked by amphetamine (1 and 10 μM) by 44 and 80%, respectively (data not shown), consistent with a previous study (Del Zompo et al., 1993), which demonstrates the integrity of our vesicular preparations. In these preparations, the addition of minocycline (0.1, 1, and 10 μM) decreased $V_{max}$ values for [$^3$H]-DA uptake (Fig. 4) by 23, 30, and 40% (1 and 10 μM were significant; $P < 0.05$), respectively, compared to vehicle-treated controls. We also found that minocycline significantly inhibited vesicular uptake of $MPP^+$. As shown in Table I, the DOPAC/DA ratio was increased consistently in mice treated with minocycline and MPTP, consistent with an effect on VMAT2, because this increases dopamine in the cytoplasm, allowing more to be metabolized to DOPAC.

Our studies therefore demonstrate that minocycline exacerbates MPTP-induced damage to DA neurons by interfering acutely with VMAT2 function (i.e., sequestration of $MPP^+$, DA, or both). It is well established that vesicular uptake of $MPP^+$ reduces its toxicity (Liu et al., 1992; Staal and Sonsalla, 2000). This seems to account for the resistance of rats to MPTP (Staal et al., 2000). Thus, perturbation in intracellular sequestration of $MPP^+$, via pharmacologic or genetic manipulation, results in increased concentrations of free $MPP^+$, resulting in increased mitochondrial accumulation and more extensive damage to DA neurons. Further, compromised VMAT2 function can lead to increased free DA within the presynaptic nerve terminal, which in turn can lead to the formation DA metabolites (increased DOPAC/DA ratios; Table I) as we observed. DA quinones and reactive oxygen species can modify protein function directly by oxidative modifications (Berman and Hastings, 1999; Kristal et al., 2001). The present data coupled with a recent report describing the destruction of synaptic vesicles by protofibrillar α-synuclein (Volles et al., 2001), highlights the vulnerability of DA neurons to pharmacologic, environmental, or genetic insults that affect specific vesicular properties. Furthermore, DA neurons are selectively vulnerable to toxic effects of overexpression of α-synuclein in vitro (Xu et al., 2002).

Previous studies have suggested the suppression of microglial activation by minocycline accounts for the ob-

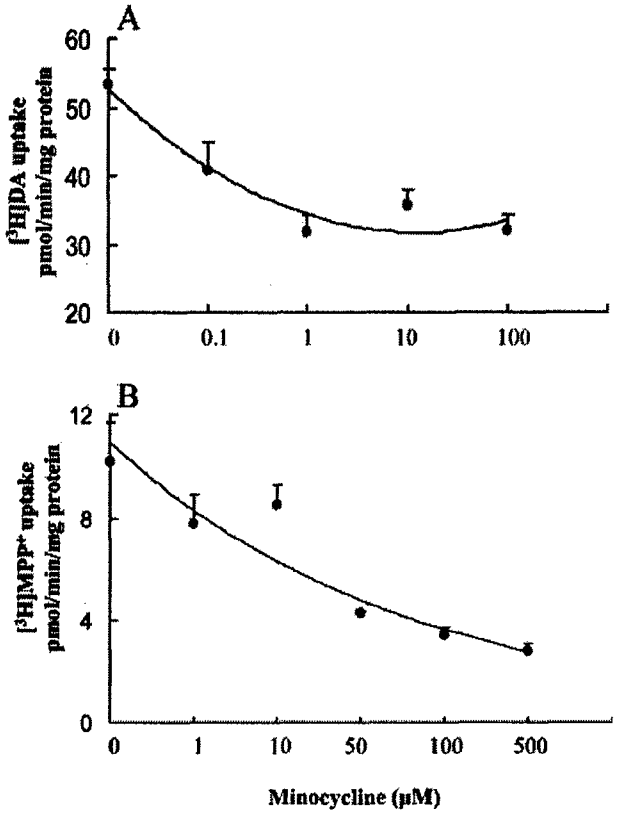


Fig. 4. Effects of minocycline on [$^3$H]-DA or [$^3$H]-MPP$^+$ uptake into vesicular preparations. Uptake of [$^3$H]-DA into vesicles isolated from C57BL/6 mouse striata was inhibited by the addition minocycline (0.1–10 μM) in a dose-dependent manner as compared to vehicle controls. Data are expressed as mean ± SEM of four separate experiments. *Significantly different from vehicle-containing controls.($P < 0.05$).

served neuroprotection (Amin et al., 1996; Yrjanheikki et al., 1998, 1999; Chen et al., 2000; Du et al., 2001; He et al., 2001; Tikka et al., 2001; Wu et al., 2002), although the mechanisms by which microglia become activated remain unknown. One consequence of a microglial response is the recruitment of other components of an immune response such as cytokines including IL-1β, IL-6, TNF-α, and IFN-γ, which may be part of a repair and protect response. Thus, it is tempting to speculate that another mechanism to explain the effect of minocycline on MPTP-induced toxicity is that minocycline suppresses the ability of microglia to supply these cytokines needed for neuronal survival; however, microglia also produce proinflammatory cytokines and oxygen-derived reactive species, namely nitric oxide (NO) from iNOS, which have been demonstrated to play a role in MPTP-mediated neuronal injury (Liberatore et al., 1999). Inhibiting inflammation may not always be beneficial, because recent work showed MPTP-induced dopamine depletion was exacerbated in IL-6-deficient mice as well as mice deficient in TNFα receptors (Bolin et al., 2002; Rousselet et al., 2002).

A recent study by Du et al. (2001) reported neuroprotective effects of minocycline in the MPTP-treated mouse model. In their study, the observed neuroprotection by minocycline was associated with its ability to suppress the MPTP-induced increases in iNOS and caspase-1 expression in the midbrain. They administered minocycline by gavage in sucrose. Similarly, the recent study of Wu et al. (2002) showed neuroprotective effects of minocycline against MPTP-induced damage to TH neurons, which was attributed to inhibition of microglia. In this study, protection was seen with MPTP administered 4 times at 16 mg/kg but not at 18 mg/kg. This dosing regimen differed from ours. We administered minocycline every 12 hr for 3 days starting 1 day before the first MPTP dose, whereas they administered minocycline i.p. starting 30 min. after the first MPTP dose and then for an additional 4 days. Another group reported that minocycline blocked the microglial response in the nigra and did not affect striatal DA depletion induced by MPTP (Ghulam et al., 2001).

We observed robust nigral microglial activation after MPTP administration that was reversed by minocycline, consistent with previous reports. Nevertheless, relative to levels in vehicle-treated mice, there was increased striatal DA depletion in mice treated with minocycline and MPTP, as compared to MPTP-treated mice. These studies clearly demonstrate the ability of minocycline to block inflammatory responses resulting from MPTP treatment, yet it is perplexing that the results on dopaminergic markers vary between laboratories. It is possible that differences in routes of administration, dosing intervals, or drug concentrations could account for such differences. The present data show that minocycline significantly exacerbates MPTP-induced damage to DA neurons and inhibits VMAT2 function of striatal vesicles, which is a novel mechanism of action. The results suggest that although minocycline is a promising neuroprotective agent for the treatment of neurodegenerative disease, some caution in its administration may be warranted.

## REFERENCES

Albers DS, Zeevalk GD, Sonsalla PK. 1996. Damage to dopaminergic nerve terminals in mice by combined treatment of intrastriatal malonate with systemic methamphetamine or MPTP. Brain Res 718:217–220.

Amin AR, Thakker GD, Patel PD, Vyas PR, Patel RN, Patel IR, Abramson SB. 1996. A novel mechanism of action of tetracyclines: effects on nitric oxide synthases. Proc Natl Acad Sci USA 93:14014–14019.

Berman SB, Hastings TG. 1999. Dopamine oxidation alters mitochondrial respiration and induces permeability transition in brain mitochondria: implications for Parkinson's disease. J Neurochem 73:1127–1137.

Bolin LM, Strycharska-Orczyk I, Murray R, Langston JW, DiMonte D. 2002. Increased vulnerability of dopaminergic neurons in MPTP-lesioned interleukin-6 deficient mice. J Neurochem 83:167–175.

Chen MO, Li M, Ferrante RJ, Fink KB, Zhu S, Bian J, Guo L, Farrell LA, Hersch SM, Hobbs W, Vonsattel JP, Cha JH, Friedlander RM. 2000. Minocycline inhibits caspase-1 and caspase-3 expression and delays mortality in a transgenic mouse model of Huntington disease. Nat Med 6:797–801.

Chiba K, Trevor A, Castagnoli N Jr. 1984. Metabolism of the neurotoxic tertiary amine, MPTP, by brain monoamine oxidase. Biochem Biophys Res Commun 120:574–578.

Coggeshall R. 1992. A consideration of neural counting methods. Trends Neurosci 15:9–12.

DeGiorgio LA, Dibinis C, Milner TA, Saji M, Volpe BT. 1998. Histological and temporal characteristics of nigral transneuronal degeneration after striatal injury. Brain Res 795:1–9.

Del Zompo M, Piccardi MP, Ruiu S, Quartu M, Gessa GL, Vaccari A. 1993. Selective MPP+ uptake into synaptic dopamine vesicles: possible involvement in MPTP neurotoxicity. Br J Pharmacol 109:411–414.

Du Y, Ma Z, Lin S, Dodel RC, Gao F, Bales KR, Triarhou LC, Chernet E, Perry KW, Nelson DL, Luecke S, Phebus LA, Bymaster FP, Paul SM. 2001. Minocycline prevents nigrostriatal dopaminergic neurodegeneration in the MPTP model of Parkinson's Disease. Proc Natl Acad Sci USA 98:14669–14674.

Gainetdinov RR, Fumagalli F, Wang YM, Jones SR, Levey AI, Miller GW, Caron MG. 1998. Increased MPTP neurotoxicity in vesicular monoamine transporter 2 heterozygote knockout mice. J Neurochem 70:1973–1978.

German DC, Liang CL, Manaye KF, Lane K, Sonsalla PK. 2000. Pharmacological inactivation of the vesicular monoamine transporter can enhance 1-methyl-4-phenyl-1,2,3,6-tetrahydropyridine-induced neurodegeneration of midbrain dopaminergic neurons, but not locus coeruleus noradrenergic neurons. Neuroscience 101:1063–1069.

German DC, Manaye KE. 1993. Midbrain dopaminergic neurons (Nuclei A9 and A10). J Comp Neurol 331:297–309.

Ghulam N, Sager T, Laursen H, Vaudano E. 2001. Minocycline reduces microglia activation in the chronic MPTP mouse model of Parkinson's Disease. Soc Neurosci 27:887–888.

Gundersen HJ. 1992. Stereology: the fast lane between neuroanatomy and brain function—or still only a tightrope? Acta Neurol Scand 137:8–13.

He Y, Appel S, Le W. 2001. Minocycline inhibits microglial activation and protects nigral cells after 6-hydroxydopamine injection into mouse striatum. Brain Res 909:187–193.

Heikkila RE, Hess A, Duvoisin RC. 1984. Dopaminergic neurotoxicity of 1-methyl-4-phenyl-1,2,3,6-tetrahydropyridine mice. Science 224:1451–1453.

Javitch JA, D'Amato RJ, Strittmatter SM, Snyder SH. 1985. Parkinsonism-inducing neurotoxin, N-methyl-4-phenyl-1,2,3,6-tetrahydropyridine: uptake of the metabolite N-methyl-4-phenylpyridinium by dopamine neurons explains selective toxicity. Proc Natl Acad Sci USA 82:2173–2177.

Kristal BS, Conway AD, Brown AM, Jain JC, Ulluci PA, Li SW, Burke WJ. 2001. Selective dopaminergic vulnerability: 3,4-dihydroxy-phenylacetaldehyde targets mitochondria. Free Rad Biol Med 30:924–931.

Kurkowska-Jastrzebska I, Wronska A, Kohutnicka M, Czlonkowska A, Czlonkowska A. 1999. The inflammatory reaction following 1-methyl-4-phenyl-1,2,3,6-tetrahydropyridine intoxication in mouse. Exp Neurol 156:50–61.

Langston JW, Ballard P, Tetrud JW, Irwin I. 1983. Chronic parkinsonism in humans due to a product of meperidine-analog synthesis. Science 219:979–980.

Liberatore GT, Vukosavic S, Mandir AS, Vila M, McAuliffe WG, Dawson VL, Dawson TM, Przedborski S. 1999. Inducible nitric oxide synthase stimulates dopaminergic neurodegeneration in the MPTP model of Parkinson's disease. Nat Med 5:1403–1409.

Liu Y, Peter D, Roghani A, Schuldiner S, Prive GG, Eisenberg D, Brecha N, Edwards RH. 1992. A cDNA that suppresses MPP+ toxicity encodes a vesicular amine transporter. Cell 70:539–551.

Matthews RT, Klivenyi P, Yang L, Klein AM, Mueller G, Kaddurah-Daouk R, Beal MF. 1999. Creatine and cyclocreatine attenuate MPTP neurotoxicity. Exp Neurol 157:142–149.

McGeer PL, Kawamata T, Walker DG, Akiyama H, Tooyama I, McGeer EG. 1993. Microglia in degenerative neurological disease. Glia 7:84–92.

Nagatsu T, Mogi M, Ichinose H, Togari A. 2000. Changes in cytokines and neurotrophins in Parkinson's disease .J Neural Transm Suppl 60:277–920.

Nicklas WJ, Vyas I, Heikkila RE. 1985. Inhibition of NADH-linked oxidation by brain mitochondria by 1-methyl-4-phenylpyridine, a metabolite of the neurotoxin, 1-methyl-4-phenyl-1,2,3,6-tetrahydropyridine. Life Sci 36:2503–2508.

Rousselet E, Callebert J, Parain K, Joubert C, Hunot S, Hartmann A, Jacque C, Perez-Diaz F, Cohen-Salmon C, Launay J-M, Hirsch EC. 2002. Role of TNFalpha receptors in mice intoxicated with the parkinsonian toxin MPTP. Exp Neurol 17:183–192.

Sonsalla PK, Giovanni A, Sieber BA, Donne KD, Manzino L. 1992. Characteristics of dopaminergic neurotoxicity produced by MPTP and methamphetamine. Ann N Y Acad Sci 648:229–238.

Staal RG, Hogan KA, Liang C-L, German DC, Sonsalla PK. 2000. In vitro studies of striatal vesicles containing the vesicular monoamine transporter (VMAT2): Rat versus mouse differences in sequestration of 1-methyl-4-phenylpyridinium. J Pharmacol Exp Ther 293:329–335.

Staal RG, Sonsalla PK. 2000. Inhibition of brain vesicular monoamine transporter (VMAT2) enhances 1-methyl-4-phenylpyridium in vivo in rat striata. J Pharmacol Exp Ther 293:336–342.

Takahashi N, Miner LL, Sora I, Ujike H, Revay RS, Kostic V, Jackson-Lewis V, Przedborski S, Uhl GR. 1997. VMAT2 knockout mice: heterozygotes display reduced amphetamine-conditioned reward, enhanced amphetamine locomotion, and enhanced MPTP toxicity. Proc Natl Acad Sci USA 94:9938–9943.

Tikka T, Fiebich BL, Goldsteins G, Keinanen R, Koistinaho J. 2001. Minocycline, a tetracycline derivative, is neuroprotective against excitotoxicity by inhibiting activation and proliferation of microglia. J Neurosci 21:2580–2588.

Volles MJ, Lee SJ, Rochet JC, Shtilerman MD, Ding TT, Kessler JC, Lansbury PT Jr. 2001. Vesicle permeabilization by protofibrillar alpha-synuclein: implications for the pathogenesis and treatment of Parkinson's disease. Biochemistry 40:7812–7819.

Volpe BT, Blau AD, Wessel TC, Saji M. 1995. Delayed histopathological neuronal damage in the substantia nigra compacta (nucleus A9) after transient forebrain ischaemia. Neurobiol Dis 2:119–127.

Volpe BT, Wildmann J, Altar CA. 1998. Brain-derived neurotrophic factor prevents the loss of nigral neurons induced by excitotoxic striatal-pallidal lesions. Neuroscience 83:741–748.

Weiser M, Baker H, Wessel TC, Joh TH. 1993. Differential spatial and temporal gene expression in response to axotomy and deafferentation following transection of the medial forebrain bundle. J Neurosci 13:3472–3484.

Wu DC, Jackson-Lewis V, Vila M, Tieu K, Teismann P, Vadseth C, Choi D-K, Ischiropoulos H, Przedborski S. 2002. Blockade of microglial activation is neuroprotective in the 1-methyl-4-phenyl-1,2,3,6-tetrahydropyridine mouse model of Parkinson's disease. J Neurosci 22:1763–1771.

Xu J, Kao SY, Lee FJ, Song W, Jin LW, Yankner BA. 2002. Dopamine-dependent neurotoxicity of alpha-synuclein: a mechanism for selective neurodegeneration in Parkinson disease. Nat Med 8:600–606.

Yang L, Schulz JB, Klockgether T, Liao AW, Martinou JC, Penney JB Jr, Hyman BT, Beal MF. 1998. 1-Methyl-4-phenyl-1,2,3,6-tetrahydropyridine neurotoxicity is attenuated in mice overexpressing Bcl-2. J Neurosci 18:8145–8152.

Yrjanheikki J, Keinanen R, Goldsteins G, Chan PH, Koistinaho J. 1999. A tetracycline derivative, minocycline, reduces inflammation and protects against focal cerebral ischemia with a wide therapeutic window. Proc Natl Acad Sci USA 96:13496–13500.

Yrjanheikki J, Pellikka M, Hokfelt T, Koistinaho J. 1998. Tetracyclines inhibit microglial activation and are neuroprotective in global brain ischemia. Proc Natl Acad Sci USA 95:15769–15774.

Zhu S, Stavrovskaya IG, Drozda M, Kim BY, Ona V, Li M, Sarang S, Liu AS, Hartley DM, Wu du C, Gullans S, Ferrante RJ, Przedborski S, Kristal BS, Friedlander RM. 2002. Minocycline inhibits cytochrome c release and delays progression of amyotrophic lateral sclerosis in mice. Nature 417:74–78.